Maike Christina Rentel

New College

Signal transduction in response to active oxygen species in *Arabidopsis thaliana*

Department of Plant Sciences

University of Oxford

Submitted for the Degree of Doctor of Philosophy

Michaelmas, 2002

Signal transduction in response to active oxygen species in *Arabidopsis thaliana*

Maike Christina Rentel, New College
Submitted for the degree of Doctor of Philosophy, Michaelmas, 2002

Many environmental stresses result in increased generation of active oxygen species (AOS) in plant cells, leading to the induction of protective mechanisms. In this study, signalling components linking AOS perception to downstream responses were examined, with particular emphasis on H_2O_2 signalling.

All AOS investigated had an early $[Ca^{2+}]_{cyt}$ peak in common, but differed in other aspects of their Ca^{2+} signatures, indicating that the plant is able to discriminate between different types of AOS. An early event in AOS signal transduction may involve changes in the cellular redox balance as reduction of glutathione levels prior to stress application increased the height of the first $[Ca^{2+}]_{cyt}$ peak. Inhibiting or enhancing the height of the H_2O_2-triggered Ca^{2+} signature lead to inhibition or enhancement of *GST1* and *APX1* induction, respectively, demonstrating that the Ca^{2+} signature is required for induction of genes encoding antioxidant enzymes.

OX1, encoding a putative ser/thr kinase, was shown to be involved in signal transduction in response to H_2O_2-generating stresses. Transcript levels of *OX1* were increased upon treatment with H_2O_2 and a range of abiotic and biotic stresses as well as ABA, all of which have been shown to result in H_2O_2 accumulation. Inhibition of stress-induced $[Ca^{2+}]_{cyt}$ elevations inhibited *OX1* induction, placing the OX1 kinase downstream of Ca^{2+} in the signalling chain. *OX1* is required for full activation of AtMPK3 and AtMPK6 in response to ozone fumigation, indicating that OX1 functions upstream of these MAP kinases. An *ox1* null-mutant displayed enhanced susceptibility to infection with a virulent *Peronospora parasitica* isolate as well as reduced induction of several defence genes. In addition, the *ox1* mutant exhibited shorter root hairs and an early flowering phenotype.

AOS treatment induced several genes encoding *AtERF* transcription factors, but did not have an effect on other members of this family. Induction occurred in an ethylene-independent but Ca^{2+}-dependent manner.

Acknowledgements

I would like to thank all the people who have made this thesis and the work behind it not only possible but also enjoyable. First and foremost, Marc Knight for excellent supervision, both in terms of intellectual input and emotional support. My second supervisor Jane Langdale, and my assessment committee, Chris Leaver and Nick Kruger, for useful discussions about the project. Joy Boyce, Richard Capper, Nicola Evans, Heather Knight, Jane Larkindale, Catherine Moore, Haruko Okamoto, Andrew Parsons, Lindsay Petersen, Sarah Scrase-Field and Helen Townley for invaluable help with experimental techniques as well as invaluable company and entertainment. We will always be the Smug Lab. Also many thanks to Vakkas Tekin and Pauline White for keeping the lab running smoothly.

I would like to thank the Gatsby Charitable Foundation for funding this work and for the opportunities it has given me to meet other Plant Scientists through the Plant Science Network.

Finally, I would like to thank the many teachers and lecturers and, most of all, my parents who have over many years helped me channel my curiosity through a huge range of exciting pursuits, and I'm still not bored.....

'The cure for boredom is curiosity. There is no cure for curiosity.'

Ellen Parr

'Wenn die Neugier sich auf ernsthafte Dinge richtet, dann nennt man sie Wissensdrang.'
(*When curiosity turns to serious matters, it's called research.*)

Aphorismen, Marie Freiin von Ebner-Eschenbach, 1830 – 1916

Table of Contents

Chapter 2 Materials and Methods

Abbreviations

A	
A. thaliana	*Arabidopsis thaliana*
A. tumefaciens	*Agrobacterium tumefaciens*
ABA	abscisic acid
ACC	1-aminocyclopropane-1-carboxylic acid
ACX1	*ACYL-CoA OXIDASE1*
ADP	adenosine diposphate
AOS	active oxygen species
AOS	*ALLENE OXIDE SYNTHASE*
APX1	*ASCORBATE PEROXIDASE1*
ATP	adenosine trisphosphate
B	
BAPTA	1,2-bis(2-aminophenoxy)ethane-N,N,N',N'-tetraacetic acid
BLAST	Basic Local Alignment Search Tool
BSO	L-buthionine-[S,R]-sulfoximine
bp	basepairs
C	
°C	degrees celsius
$[Ca^{2+}]_{cyt}$	cytosolic calcium concentration
cADPR	cyclic ADP-ribose
CaMV	cauliflower mosaic virus
CAT3	*CATALASE3*
Col-0	Columbia-0
D	
DHA	dihydroascorbate
DHAR	dihydroascorbate reductase
DMF	dimethylfluoride
DMSO	dimethylsulfoxide
DNA	deoxyribonucleic acid
DNase	deoxyribonuclease
DPI	diphenyleneiodonium chloride
E	
E. coli	**Escherichia coli**
eds1	**enhanced disease susceptibility1**
EDTA	ethylenediaminetetraacetic acid
EGTA	ethylene glycol-bis(β-aminoethyl ether) N,N,N',N'-tetraacetic acid
ER	endoplasmic reticulum
ERF	ethylene responsive element binding factor
EST	expressed sequence tag
F	
FLC	*FLOWERING LOCUS C*
for	forward
G	
g	gravitational force

GR	glutathione reductase
GSH	glutathione
GSSG	glutathione disulfide
GST1	*GLUTATHIONE-S-TRANSFERASE1*
GUS	glucuronidase
H	
h	hours
H_2O_2	hydrogen peroxide
HR	hypersensitive response
I	
INA	2,6 – dichloroisonicotinic acid
IP_3	inositol trisphosphate
J	
JA	jasmonic acid
K	
KAc	potassium acetate
kDa	kilo Dalton
L	
$LaCl_3$	lanthanum chloride
LB	Luria-Bertani
LUC	luciferase
M	
µM	micromolar
MAPK	mitogen-activated protein kinase
min	minutes
M	molar
mM	millimolar
MS medium	Murashige and Skoog medium
N	
NAA	2-napthalene acetic acid
NaAc	sodium acetate
nM	nanomolar
NO	nitric oxide
NTP	nucleotide trisphosphate
O	
O_3	ozone
$^{\bullet}O_2^-$	superoxide
OX1	*OXIDATIVE STRESS-INDUCBILE1*
OX2	*OXIDATIVE STRESS-INDUCBILE2*
P	
P. parasitica	**Peronospora parasitica**
P. syringae	**Pseudomonas syringae**
PCR	polymerase chain reaction
P_i	orthophosphate
ppb	parts per billion
PR-1	*PATHOGENESIS-RELATED PROTEIN1*
psi	pounds per square inch
R	

RBOH	respiratory burst oxidase homolog
rev	reverse
RLK	receptor-like kinase
RNA	ribonucleic acid
RNase	ribonuclease
rpm	revolutions per minute
RR	ruthenium red
RT-PCR	reverse transcription PCR
S	
s	seconds
SA	salicylic acid
SAR	systemic acquired resistance
ser	serine
SIPK	SA-induced kinase
SOD	superoxide dismutase
T	
THI2.2	*THIONIN2.2*
thr	threonine
TMV	tobacco mosaic virus
TUB	*β-TUBULIN*
tyr	tyrosine
U	
UBC8	*UBIQUITIN LIGASE8*
UTR	untranslated region
UV	ultra-violet
V	
(v/v)	volume per volume
W	
(w/v)	weight per volume
WIPK	wound-induced kinase
WS-2	Wassiliewskija-2
X	
X-gal	5-bromo-4-chloro-3-indolyl-β-D-galactoside
X-gluc	5-bromo-4-chloro-3-indolyl-β-D-glucuronide, CHA salt

1. Introduction

1.1. AOS production and oxidative stress

Many stresses have been shown to result in increased generation of active oxygen species (AOS). This group of molecules includes superoxide ($O_2^{\bullet -}$), hydrogen peroxide (H_2O_2) and hydroxyl radicals ($OH^{\bullet}$), produced by successive one-electron reduction of atmospheric oxygen, as well as singlet oxygen ($^1O_2$), formed by transfer of energy from a light-excited molecule (such as chlorophyll) to ground state O_2 (McKersie, 1996) (Figure 1.1).

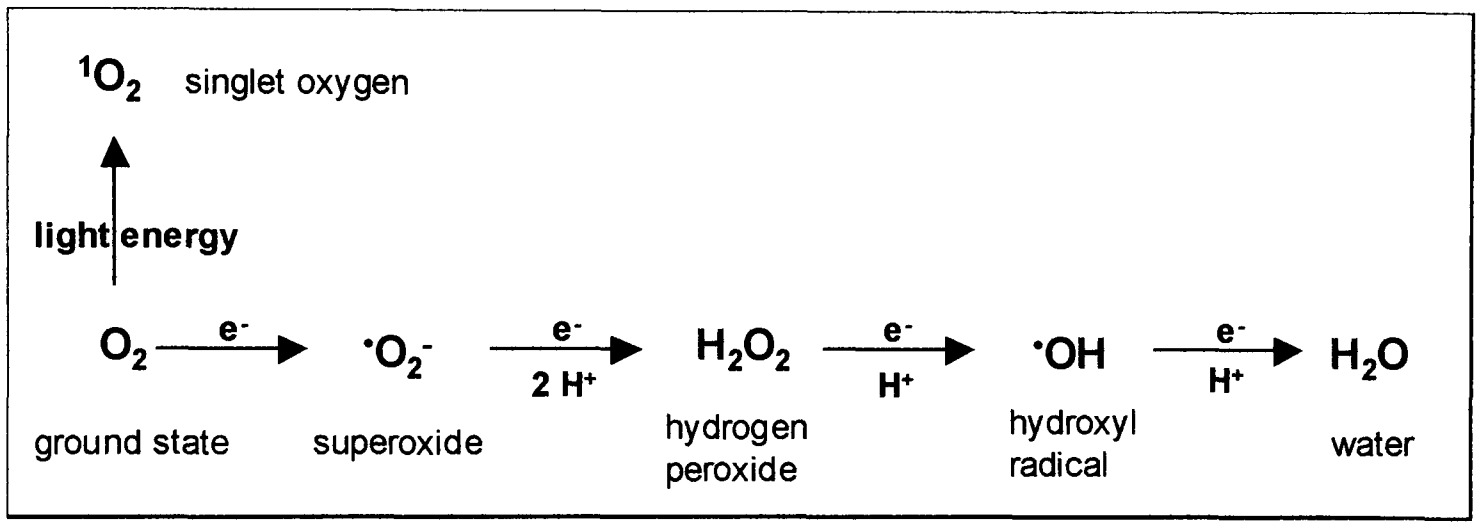

Figure 1.1: Generation of AOS from O_2 (adapted from Wojtaszek, 1997)
Singlet oxygen is generated by absorption of light energy whereas the other AOS are generated by stepwise monovalent reduction. The first step, forming superoxide, is endothermic but subsequent reductions are exothermic (McKersie, 1996)

In plants, AOS may be produced either directly through ozone pollution or indirectly, as a result of abiotic stresses (*e.g.* cold, drought or high light intensity) leading to perturbations in cellular O_2 processing (Vranová *et al.*, 2002). Even during regular metabolism, AOS are generated as a side product in electron transport processes, such as photosynthesis and respiration. The plant experiences oxidative stress only once a serious imbalance between the production of AOS and antioxidant defences has occurred (Moller, 2001). Oxidative stress can therefore be defined as a

disruption of the cellular redox balance. The main sites for AOS production in the plant cell during abiotic stress are organelles with highly oxidising metabolic activities or with intense electron flows: chloroplasts, mitochondria, and microbodies (Dat *et al.*, 2000; Vranová *et al.*, 2002). For example, in situations where limited CO_2 fixation is possible, $NADP^+$ regeneration by the Calvin cycle is significantly reduced, leading to overreduction of the photosynthetic electron transport chain and hence formation of $^{\bullet}O_2^-$ and $^1O_2$ in the chloroplasts (Vranová *et al.*, 2002).

AOS have traditionally been considered to be toxic by-products of aerobic metabolism. However, in recent years, it has become apparent that plant cells generate low levels of AOS endogenously in response to a number of biotic and abiotic stresses (see section 1.2), such as pathogenic elicitors and ozone (Lamb and Dixon, 1997; Wohlgemut *et al.*, 2002). The paradox of 'self-imposed' stress points to a role of AOS in signalling, where increased accumulation of H_2O_2 and changes in redox status alerts the plant cell to environmental change. Thus, the task of the plant's defence 'arsenal' described below may not be elimination of AOS but adjustment of the cellular redox status in order to enable redox signalling (see section 1.1.3) (Noctor and Foyer, 1998).

1.1.1. The chemistry of AOS

The three AOS generated by step-wise one-electron reductions of O_2 have different properties concerning reactivity and membrane permeability.

Superoxide ($^{\bullet}O_2^-$) is formed by a one-electron reduction of ground state oxygen and can act as either an oxidant or a reductant: it can oxidise ascorbic acid or NADPH but reduce metal ions or cytochrome C (McKersie, 1996). A dismutation reaction

leading to the formation of H_2O_2 and O_2 can occur spontaneously, or is catalysed by the enzyme superoxide dismutase (SOD) (see section 1.1.2). The univalent reduction of $^{\bullet}O_2^-$ produces **hydrogen peroxide (H_2O_2)**, which is not a free radical as all of its electrons are paired. H_2O_2 rapidly oxidises thiol groups in proteins, but has otherwise relatively low reactivity in the absence of metal ions (Halliwell and Gutteridge, 1999). Unlike other AOS, H_2O_2 permeates membranes (through aquaporins (Henzier and Steudle, 2000)) and is therefore not compartmentalised within the cell. Most damage inflicted by addition of H_2O_2 is mediated by the **hydroxyl radical ($^{\bullet}OH$),** which is formed from H_2O_2 in the Fenton reaction (Reaction 1) by donation of an electron from a reduced metal ion. This radical is the strongest oxidising agent known and reacts with organic molecules at diffusion-limited rates (Halliwell and Gutteridge, 1999).

$Fe^{2+} + H_2O_2 \rightarrow Fe^{3+} + {}^{\bullet}OH + OH^-$ Reaction 1 (Fenton reaction)

In the plant cell, the availability of reduced metal ions (*e.g.* ferrous or cuprous ions) limits the rate of reaction. However, the metal can be recycled from the oxidised to the reduced form by a reducing agent which thereby maintains an ongoing Fenton reaction, leading to the generation of hydroxyl radicals. One suitable reducing agent is $^{\bullet}O_2^-$ which participates in the overall reaction 2 as two half reactions (2a and 2b) (McKersie, 1996).

$^{\bullet}O_2^- + H_2O_2 \rightarrow O_2 + OH + OH^-$ Reaction 2 (Haber-Weiss reaction)

$Fe^{2+} + H_2O_2 \rightarrow Fe^{3+} + OH + OH^-$ Reaction 2a

$^{\bullet}O_2^- + Fe^{3+} \rightarrow O_2 + Fe^{2+}$ Reaction 2b

Ozone (O_3) is produced by the photodissociation of molecular O_2 into oxygen atoms, which then react with O_2 molecules to from O_3 (Halliwell and Gutteridge, 1999). Ozone is a powerful oxidising agent, adding across double bonds to form ozonides which decompose to yield organic radicals and H_2O_2 (Halliwell and Gutteridge, 1999). Ozone enters the intercellular leaf space through stomata and decomposes in the aqueous solution of the apoplast, forming $^{\bullet}O_2^-$ and subsequently H_2O_2 and $^{\bullet}OH$ (Rao *et al.*, 2000).

Most damage caused by AOS in the cell is mediated through formation of the hydroxyl radical. Oxidation of organic substances by $^{\bullet}OH$ proceeds by either addition of OH to the organic molecule, or abstraction of a hydrogen atom from it, followed by radical chain reactions with other organic molecules (Halliwell and Gutteridge, 1999). Abstraction reactions are responsible for lipid peroxidation in cell membranes, with severe damage resulting from relatively low hydroxyl radical concentrations due to its self-propagating nature. The chain reactions are terminated by cross-linking of two organic radicals (McKersie, 1996). AOS thus cause cellular damage by reacting with lipids, proteins and DNA. An example of oxidative damage is seen in plants exposed to ozone. Acute dosages (>150 ppb) cause severe physiological alterations, such as leaf lesions, accelerated organ senescence and reduced shoot and root growth. Chronic O_3 stress through long

term exposure of low concentrations does not produce visible injury, but both the photosynthetic rate and plant productivity are reduced (Pasqualini *et al.*, 2001) and lipid peroxidation is increased (Pell *et al.*, 1997).

1.1.2. Plant defence mechansims

Plants have evolved a number of mechansims to protect themselves from AOS-mediated damage. The term 'antioxidant' can be considered to describe any compound capable of quenching AOS without itself undergoing conversion to a destructive radical (Noctor and Foyer, 1998; Dröge, 2002). Antioxidant enzymes catalyse such reactions, or are involved in the direct processing of AOS. Superoxide dismutase (SOD), which is found in most cellular compartments, catalyses the dismutation of superoxide to H_2O_2 and oxygen (Kliebenstein *et al.*, 1998). The H_2O_2 generated is subsequently degraded by catalase (CAT) or peroxidases. CAT, a peroxisomal enzyme, converts H_2O_2 to H_2O and O_2 (Noctor and Foyer, 1998). An alternative mode of H_2O_2 destruction is via peroxidases, which are found throughout the cell and have a much higher affinity for H_2O_2 (Noctor and Foyer, 1998). Unlike CAT, peroxidases require a reductant. In plant cells, the most important reducing substrate for H_2O_2 detoxification is ascorbate, *e.g.* in the ascorbate-gluathione cycle (see Figure 1.2). Ascorbate peroxidases (APXs) have high affinity for H_2O_2 and are present in most compartments, indicating a role in fine-tuning the level of AOS in different locations (Mittler, 2002).

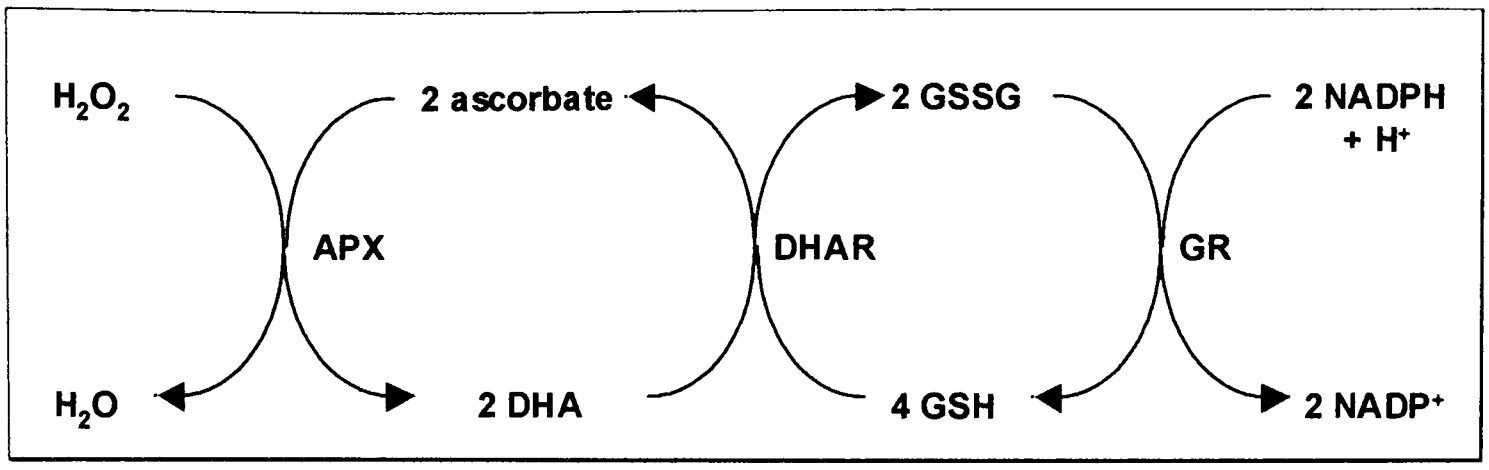

Figure 1.2: The ascorbate – glutathione cycle (adapted from Noctor and Foyer, 1998)
Ascorbate peroxidase (APX) uses two molecules of ascorbate to reduce H_2O_2 to water, generating dehydroascorbate (DHA). DHA is reduced back to ascorbate by the action of DHA reductase (DHAR), using glutathione (GSH) as the reducing substrate. The glutathione disulphide (GSSG) is generated, which in turn is re-reduced to GSH by NADPH in a reaction catalysed by GSH reductase (GR). Ascorbate and gluathione are not consumed in this pathway but participate in a cyclic transfer of reducing equivalents. Components of this cycle are present in chloroplasts, the cytosol and mitochondria (Smirnoff, 1995)

Induction and activation of individual antioxidant enzymes as a result of oxidative stress have been reported (Bowler *et al.*, 1992; Conklin and Last, 1995), but can be extremely variable and, in many cases, relatively minor (reviewed in Noctor and Foyer, 1998). Variation may reflect the importance of compartment-specific changes, as most measurements were made in whole tissue. Suppression of *APX* or *CAT* (by antisense) induces increased production of other antioxidant genes, probably to compensate for the loss of APX and CAT activity, indicating significant flexibility in the antioxidant system (Mittler, 2002).

In addition to antioxidant enzymes, non-enzymatic free radical scavengers also protect the plant cell from oxidative damage. These include carotenoids, tocopherols, which trap singlet oxygen and peroxyl radicals, respectively, and ascorbate, which can also react non-enzymatically with AOS (McKersie, 1996).

Another class of detoxifiying enzymes is constituted by the glutathione-*S*-transferases (GSTs). These enzymes catalyse the conjugation of glutathione to a

variety of hydrophobic, electrophilic, and usually cytotoxic substrates and their role in detoxifying electrophilic herbicides is well known (Marrs, 1996). However, the endogenous role of GSTs is less clear, despite numerous reports of increases in GST levels during plant development and after exposure to pathogens and abiotic stresses (Edwards *et al.*, 2000). GSTs with high affinity for auxins and cytokinin have been suggested to play a role in hormone homeostasis. Their role in protection against oxidative damage may lie in conjugation (and thus detoxification) of metabolites arising from oxidative damage, *e.g.* lipid peroxidation or oxidative DNA degradation products (Marrs, 1996).

1.1.3. Redox signalling

In order to activate protective antioxidant mechanisms, cells have to be able to sense reactive oxygen species. This process of redox regulation requires the presence of redox-sensitive proteins that can undergo reversible oxidation/reduction and are thereby activated or de-activated. Redox-sensitive proteins can be oxidised directly by AOS, or indirectly through the cellular redox state (Vranová *et al.*, 2002). The mechanisms by which prokaryotic cells sense AOS are relatively well understood, and involve redox-sensitive transcription factors. In *E. coli*, antioxidant genes are induced by the OxyR regulon, which senses excess H_2O_2 through oxidative modification of cysteine residues, and the SoxR regulon, which senses $^{\bullet}O_2^-$ through redox active [2Fe-2S] clusters (Demple, 1996; Zheng and Storz, 2000; Kim *et al.*, 2002). In yeast, the Yap1 transcription factor senses AOS in a similar fashion to the OxyR protein (Delaunay *et al.*, 2000). In animal cells, the cellular redox balance plays a role in the activation of transcription factor NF-κB by

triggering degradation of the inhibitory subunit IκB (Schoonbroodt and Piette, 2000). Other transcription factors are regulated in their DNA-binding capacity by oxidation of cysteines (Schoonbroodt and Piette, 2000). In addition, tyrosine phosphatases, which have an essential cysteine in their catalytic site, may also be inactivated by oxidation (Haring *et al.*, 1995; Herrlich and Bohmer, 2000). This could account for oxidative stress-mediated activation of tyrosine kinases, such as the platelet-derived growth factor receptor by H_2O_2 (Herrlich and Bohmer, 2000), linking 'traditional' phosphorylation based signalling and redox sensing.

An example of redox sensing in plants is the dissociation of the light-harvesting complex from photosystem II in response to excess light. Reduction of the plastoquinone pool causes a structural change of an Fe-S protein associated with the cytochrome *bf* complex. As a consequence, a kinase is activated and causes dissociation by phosphorylation (Vener *et al.*, 1998). Recently, thiol modification by H_2O_2 was implicated in inactivation of the ABA-insensitive1 (ABI1) and ABI2 phosphatases, providing an example for direct redox regulation of enzymatic activity in plants (Meinhard and Grill, 2001; Meinhard *et al.*, 2002).

1.2. H_2O_2 as a mobile signalling molecule

Among the AOS, H_2O_2 is the only uncharged species. This property, together with its relative stability, allows H_2O_2 to cross membranes and reach neighbouring cells. Intercellular movement of H_2O_2 has been demonstrated in tobacco epidermal peels across 5 – 6 cell layers (Allan and Fluhr, 1997). Hence, H_2O_2 may function as a local signalling molecule. Indeed, H_2O_2 has been implicated in signal transduction mediating a variety of responses (reviewed in Neill *et al.*, 2002). For example, high

light irradiation causes induction of APX both locally and in adjacent (shaded) leaves, which was correlated with increases in H_2O_2 levels and could be inhibited by infiltration with CAT (but not SOD) (Karpinski *et al.*, 1999). Acclimation of chilling-sensitive maize seedlings to cold (4 °C) by pre-exposure to 14 °C was accompanied by increases in H_2O_2 levels and could be induced at room temperature by application of H_2O_2 or menadione (Prasad *et al.*, 1994). Similarly, pre-treatment of rice seedlings with H_2O_2 increased salt and heat tolerance (Uchida *et al.*, 2002). Curiously, processes that do not involve H_2O_2 accumulation due to environmental stress conditions, such as stomatal closure in response to ABA treatment (Guan *et al.*, 2000; Pei *et al.*, 2000) and the root gravitropism response (Joo *et al.*, 2001) also require H_2O_2. Active generation of H_2O_2 in plant cells, in a process termed the oxidative burst, has been demonstrated in response to a wide variety of stresses, *e.g.* pathogen attack (Doke, 1983), wounding (Doke, 1997; Orozco-Cadenas and Ryan, 1999), ozone fumigation (Wohlgemut *et al.*, 2002), irradiation with UV-B (Rao *et al.*, 1996; Allan and Fluhr, 1997), application of abscisic acid (ABA) (Pei *et al.*, 2000), hyperosmotic shock (Coelho *et al.*, 2002) and auxin (Joo *et al.*, 2001). Plant responses after pathogen attack and wounding stress are outlined in sections 1.4 and 1.5, followed by a more detailed discussion of the oxidative burst itself (section 1.7).

1.3. Signal transduction

As sessile organisms, plants need to be able to respond to changing environmental conditions by induction of various protective mechanisms. Among the components in the signal transduction chain linking perception of a stress to activation of cellular defences are increases in cytosolic calcium concentrations ($[Ca^{2+}]_{cyt}$) and modulation of protein activity through phosphorylation catalysed by kinases. In addition, the plant produces 'stress' hormones such as ethylene, jasmonic acid (JA) and salicylic acid (SA), which have been shown to play roles in wounding and resistance to pathogens (Reymond and Farmer, 1998; Thomma *et al.*, 2001a; Wang *et al.*, 2002). Changes in gene induction are ultimately effected by activation of transcription factors.

1.3.1. The calcium signal

The requirement of orthophosphate (P_i) and phosphorylated organic compounds, together with the low solubility product of Ca^{2+} with P_i, necessitated the evolution of mechanisms able to sustain low cytosolic calcium concentrations ($[Ca^{2+}]_{cyt}$) within the cell. Thus, the basal level of $[Ca^{2+}]_{cyt}$ is typically maintained at ~ 100 nM whereas $[Ca^{2+}]$ in the apoplast and the vacuole are estimated at 100 µM – 1 mM and 1 mM, respectively (Bush, 1995). The ER, plastids and mitochondria are also believed to sequester Ca^{2+} (Sanders *et al.*, 2002). In addition, the cytosol is strongly buffered against high concentrations of Ca^{2+} by a range of Ca^{2+}-binding proteins such that, in mammalian cells, Ca^{2+} ions were estimated to diffuse no more than 100 – 500 nm (Clapham, 1995). The large concentration gradient between cytosol and apoplast / organelles together with the restricted movement of the ion enabled

cells to utilize Ca^{2+} influx as a fast and localised signal in development and in response to external stimuli (reviewed in Malhó *et al.*, 1998). Thus, increases in intracellular Ca^{2+} have been measured in response to a wide range of abiotic and biotic stresses. Upon stimulation, Ca^{2+} ions flow down the concentration gradient into the cytosol via Ca^{2+}-permeable ion channels either in the plasma membrane or in organelles (reviewed in Sanders *et al.*, 2002). Ca^{2+} currents have been detected across the plasma membrane in response to depolarisation and hyperpolarisation. In *A. thaliana*, a putative depolarisation-activated channel, *TPC1*, as well as several members of the cyclic nucleotide-gated channel (CNGC) family, have been identified on the basis of their sequence homology to mammalian Ca^{2+} channels. In addition, two voltage-gated (hyper- and de-polarisation) and two ligand-gated (inositol trisphosphate (IP_3) and cyclic ADP-ribose (cADPR)) Ca^{2+} release channels have been reported to reside in the vacuolar membrane. The ER membrane also contains two voltage-dependent, as well as putative IP_3- and cADPR-gated, channels. Ca^{2+} release in response to nicotinic acid adenine dinucleotide phosphate (NAADP) indicates the presence of a third ligand-gated pathway in this membrane (Sanders *et al.*, 2002).

As a result of channel activation, $[Ca^{2+}]_{cyt}$ is elevated transiently and mediates an array of downstream processes through Ca^{2+}-dependent proteins. This involves binding of Ca^{2+}-ions, generally to protein domains containing EF-hand motifs (Ikura, 1996), followed by a conformational change which either affects the protein's affinity for downstream signalling components, or directly changes enzyme activity. A common 'interpreter' of Ca^{2+} elevations is calmodulin, a relatively small molecule with four EF-hands, which relays the Ca^{2+} signal by associating with downstream

proteins in its Ca^{2+}-bound form (Snedden and Fromm, 2001). Among proteins directly activated through Ca^{2+}-binding are the calcium-dependent protein kinases (CDPKs), which contain a calmodulin-like domain (see section 1.3.2.1) (Harmon *et al.*, 2001). Basal $[Ca^{2+}]_{cyt}$ levels are re-established by Ca^{2+} pumps or H^+/Ca^{2+} antiporters present in all membrane systems analysed so far (for reviews, see Poovaiah and Reddy, 1993; Bush, 1995; Sanders *et al.*, 1999; Sanders *et al.*, 2002).

1.3.2. Protein kinases in stress signalling

Protein kinases catalyse phosphorylation of target proteins in response to numerous stimuli. In this manner, kinases amplify stimulus perception and mediate stimulus-specific responses through activation of appropriate downstream signalling cascades.

Protein kinases are classified into two groups according to their side chain specificities of target proteins: serine/threonine (ser/thr) kinases and tyrosine (tyr) kinases. A few of these proteins, termed dual-specificity kinases, are capable of phosphorylating serine, threonine and tyrosine (Hardie, 1999). Classically, a protein kinase possesses a catalytic domain of approximately 200 – 300 amino acids, which is composed of 12 conserved subdomains that are highly conserved between kinases (Hanks and Quinn, 1991). A 'non-conventional' kinase group is constituted by the histidine (his) kinases, which autophosphorylate on an active site histidine residue before transfer of the phosphate to an aspartate residue in a 'response regulator' domain (Satterlee and Sussman, 1998).

Plant ser/thr kinases can be divided into 14 subfamilies, including the calcium-dependent protein kinases (CDPKs), the receptor-like kinases (RLKs) and the

kinases of the mitogen-activated protein kinase (MAPK) cascades (Hardie, 2000). The CDPK family, as well as kinases of MAPK cascades, have been studied most intensively and are discussed in more detail below.

1.3.2.1. Calcium-dependent protein kinases (CDPKs)

Unlike calcium/calmodulin-dependent kinases (CaMKs), which are well studied in animal systems and require binding of a Ca^{2+}-calmodulin complex for activation, the members of the CDPK family are directly activated by Ca^{2+} ions (Satterlee and Sussman, 1998; Hrabak, 2000). This difference was explained after the first CDPK gene was cloned (Harper *et al.*, 1991). CDPKs consist of an N-terminal protein kinase catalytic domain followed by an autoregulatory domain and a C-terminal domain with 39 % identity to calmodulin. In most CDPKs identified to date, the four defining 'EF-hand' Ca^{2+}-binding motifs are conserved within this domain (Hrabak, 2000). It was suggested that, upon binding Ca^{2+} via the calmodulin-like domain, the autoinhibitory domain dissociates from the catalytic site of the kinase domain, thus activating the enzyme. This model is supported by the observation that deletion of only the calmodulin-like domain generates an inactive enzyme unable to respond to Ca^{2+}; whereas, deletion of both the autoinhibitory and calmodulin-like domains generates a constitutively active, Ca^{2+}-insensitive enzyme (Sheen, 1996).

Analysis of the genome sequence of *A. thaliana* indicates the presence of 34 CDPK genes (Harmon *et al.*, 2001; Cheng *et al.*, 2002). Due to their Ca^{2+} dependence, CDPKs are likely candidates for translating information encoded in a stimulus-triggered Ca^{2+} signature. Differences in localisation and Ca^{2+}-binding properties may determine which CDPK isoform is activated in response to a specific Ca^{2+}-transient

(Sheen, 1996). Specificity in CDPK signalling properties may lie with differences in downstream targets, as well as modulation of activity, *e.g.* by phosphorylation. In addition, spatiotemporal regulation of CDPK gene expression may play a role (Cheng *et al.*, 2002).

1.3.2.2. Mitogen-activated protein kinase (MAPK) signalling cascades

Studies in yeast and mammalian cells have identified MAPK cascades as major components downstream of receptors or sensors that transduce extracellular stimuli into intracellular responses (Cohen, 1997). MAPK cascades have been studied extensively in yeast (*e.g.* the HOG pathway in response to high osmolarity (O'Rourke *et al.*, 2002)) as well as mammalian cells (*e.g.* the stress-activated protein kinase (SAPK) and p38 pathways in response to UV radiation and osmotic shock (Toone and Jones, 1998; Kyriakis and Avruch, 2001)). The basic MAPK cascade module consists of a MAPK kinase kinase (MAPKKK), which phosphorylates a MAPK kinase (MAPKK), which in turn phosphorylates a MAPK on thr and tyr residues (Toone and Jones, 1998). Specificity of signalling appears partially mediated by the formation of protein complexes through assembly of signalling molecules on scaffolding, anchoring and adaptor proteins (Madhani and Fink, 1998). Following activation, MAPKs phosphorylate a range of target proteins on ser or thr residues, including enzymes, cytoskeletal substrates, nuclear proteins and other signalling molecules (Jouannic *et al.*, 2000). MAPKs are de-activated by dual-specificity phosphatases which are able to dephosphorylate both phospho-tyr and phospho-ser/thr residues (Keyse, 2000).

As MAPK signalling pathways are conserved across kingdoms (see above), plant cells may employ a similar system. Indeed, approximately 20 MAPKs have been identified in the *A. thaliana* genome, along with 10 MAPKKs and 60 MAPKKKs (Jonak *et al.*, 2002); whereas, yeast has only 6 MAPKs (Madhani and Fink, 1998). The task of assigning this large number of kinases to specific signalling modules has only just been begun. However, the complexitiy of the system has already become apparent. Unlike their counterparts in other eukaryotes, a given plant MAPKK can interact with and activate more than one MAPK (Jonak *et al.*, 2002). Thus, transient transfection studies of protoplasts showed that two *A. thaliana* MAPKKs, AtMKK4 and AtMKK5, can activate both AtMPK3 and AtMPK6 (Asai *et al.*, 2002). Similary, two alfalfa MAPKKs were shown to activate up to three different types of MAPKs, depending on the stimulus (Cardinale *et al.*, 2002).

Several MAPKs are activated in response to wounding, pathogen attack, some plant hormones, and various abiotic stresses (Jonak *et al.*, 2002). A plant MAPK signalling module involved in the response to the bacterial elicitor flagellin was recently identified (Asai *et al.*, 2002). Together, these findings predict a role for MAPK cascades in plant stress signalling (see section 4.1). Signalling specificity may be determined by which MAPKs are activated following stimulation. For example, four alfalfa MAPKs were activated to different degrees and with different kinetics depending on the applied elicitor (Cardinale *et al.*, 2000). De-activation of MAPKs, like in other eukaryotes, appears to be mediated by dual-specificity phosphatases. For example, a dual-specificity phosphatase able to de-activate AtMPK4 was recently identified in *A. thaliana* (Gupta *et al.*, 1998).

1.3.3. Plant hormones

1.3.3.1. Ethylene

The gaseous plant hormone ethylene is involved in many aspects of the plant life cycle, including germination, root hair development, senescence and fruit ripening. In addition, ethylene is implicated in responses to environmental stresses, such as elevated ozone levels (Overmyer *et al.*, 2000) and pathogen attack (Thomma *et al.*, 2001a; Kunkel and Brooks, 2002).

Ethylene is synthesised from *S*-adenosyl-L-methionine via 1-aminocyclopropane-1-carboxylic acid (ACC) by the enzymes ACC synthase and ACC oxidase (reviewed in Bleecker and Kende, 2000; Wang *et al.*, 2002). Mutant analysis led to the proposal of a model for the ethylene signal transduction pathway. According to this model, the released ethylene molecule is perceived by a family of receptors with similarity to bacterial two-component histidine kinase receptors (Chang and Stadler, 2001). These receptors are negative regulators of the ethylene response pathway, repressing ethylene responses in the absence of the ethylene signal (Hua and Meyerowitz, 1998). Binding of ethylene inactivates its receptor and relieves the inhibition on the ethylene signalling cascade. The next known downstream component is the protein kinase CONSTITUTIVE TRIPLE RESPONSE1 (CTR1) which exhibits similarity to the Raf family of MAPKKKs (Kieber, 1997). Loss-of-function *ctr1* mutants exhibit a constitutive triple response, identifying this kinase as a negative regulator of ethylene responses. Signal transduction from CTR1 to the nucleus requires ETHYLENE-INSENSITIVE2 (EIN2) which contains twelve putative trans-membrane domains and displays similarity to the Nramp family of metal ion carriers (Alonso *et al.*, 1999). Cloning of the *ein3* mutant gene provided a direct link

to ethylene-induced changes in gene expression. *EIN3* encodes a nuclear-localised protein which was shown to bind an element in the promoter of the *ETHYLENE-RESPONSIVE ELEMENT BINDING FACTOR* (*ERF1*) gene and activate its transcription (Solano *et al.*, 1998). The ERFs have been implicated in transcription of ethylene-induced genes (see section 5.1) (Ohme-Takagi and Shinshi, 1990; Solano *et al.*, 1998).

1.3.3.2. Jasmonic acid

Jasmonic acid and its derivatives (here all termed JA) are involved in a range of developmental processes such as fruit ripening, production of viable pollen, root growth and tendril coiling (reviewed in Creelman and Mullet, 1997). JA accumulation is induced in response to wounding, pathogen or insect attack and abiotic stresses leading to activation of defensive or protective mechanisms (Turner *et al.*, 2002). Despite extensive work in recent years, assigning a specific role to JA has proven difficult owing to complex interactions with the ethylene and salicylic acid signalling pathways (Thomma *et al.*, 2001a; Kunkel and Brooks, 2002). JA is a 12-carbon fatty acid-derivative, synthesised from linolenic acid via the inducible octadecanoid pathway (Creelman and Mullet, 1997; Turner *et al.*, 2002). It may be expected to bind to a receptor; however, no such molecule has been discovered so far. Few other components of the signalling pathways downstream of JA are known, despite several screens in *A. thaliana* aimed at identifying mutants insensitive to JA (Staswick *et al.*, 1992; Feys *et al.*, 1994) or mutants with constitutive JA responses (Ellis and Turner, 2001). All signalling mutations isolated are alleles of the genes *coi1* (coronatine-insensitive) and *jar1* (jasmonate-resistant). COI1 is an F-box

protein (Xie *et al.*, 1998), involved in ubiquitin-mediated protein destruction (Bai *et al.*, 1996), and JAR1 has similarity to the auxin-induced GH3 gene product from soybean (Staswick, personal communication in Turner *et al.*, 2002).

1.3.3.3. Salicylic acid

SA, synthesised from phenylalanine, was originally identified as an essential component for induction of systemic acquired resistance (SAR), which renders the plant resistant to normally virulent pathogens by systemic induction of defence responses (e.g. *PR-1* expression) (Gaffney *et al.*, 1993). SAR is triggered following infection with a necrotrophic pathogen and correlates with increases in endogenous SA levels throughout the plant; it can also be initiated by application of SA or SA analogues. Subsequently, over a period of hours to days after the primary infection, a long-lasting and enhanced resistance to secondary challenge by the same or unrelated pathogens develops systemically (Durner *et al.*, 1997). SA was shown to be essential for the development of SAR through analysis of transgenic plants expressing the bacterial *NahG* gene (Gaffney *et al.*, 1993). The encoded enzyme, salicylate hydroxylase, inactivates SA by converting it to catechol. Thus, *NahG* plants are unable to accumulate SA and also incapable of developing SAR, indicating that SA accumulation is required for establishing systemic resistance. The role of SA is not limited to protection against a secondary infection but this molecule also functions in other disease resistance processes. Thus, *NahG* plants are compromised in PR protein induction and disease resistance in response to infection with avirulent pathogens (Delaney *et al.*, 1994). In addition, many mutants

with reduced SA levels (e.g. *pad4* (Zhou *et al.*, 1998)) are hyper-susceptible to pathogen infection.

UV-B irradiation was also shown to cause increases in SA levels and up-regulation of *PR* genes in response to UV-B irradiation was inhibited in *NahG* plants, indicating a role for SA in this signalling pathway (Surplus *et al.*, 1998).

1.3.3.3.1 Interaction of SA with H_2O_2

Initially, SA was placed upstream of H_2O_2 production after the isolation of a SA-binding protein in tobacco with catalase activity (Neuenschwander *et al.*, 1995). This activity was inhibited on binding of SA, thereby indirectly increasing H_2O_2 levels. However, no decrease in catalase activity could be detected in pathogen-inoculated leaves (Bi *et al.*, 1995) and increased H_2O_2 levels in tobacco plants with reduced catalase levels stimulated SA production (Chamnongpol *et al.*, 1998). In addition, application of SA to tobacco epidermal peels did not result in increased levels of AOS (Allan and Fluhr, 1997) and H_2O_2 was able to induce PR protein expression in wild-type but not *NahG* plants (Bi *et al.*, 1995), placing SA downstream of H_2O_2. Subsequently, a synergistic effect of these two molecules was revealed by the observation that simultaneous addition of SA and avirulent (or virulent) bacteria increases the amplitude of the oxidative burst (Shirasu *et al.*, 1997). Hence, SA and H_2O_2 generated during the oxidative burst have been placed into a positive feedback loop (Draper, 1997).

1.3.4. Transcription factors

It has been estimated that the *A. thaliana* genome encodes at least 1533 transcription factors, which represents approximately 5.9 % of the total estimated genes, in contrast to only 4.5 % in *Drosophila*, and 3.5 % in *C. elegans* and *S. cerevisiae* (Riechmann *et al.*, 2000). The largest families of transcription factors in *A. thaliana* are constituted by the MYB group (~ 180 members) and the APETALA2 / ethylene-responsive element binding protein (AP2 / EREBP) group (~ 150 members) (Riechmann and Ratcliffe, 2000). Several families are specific to plants (*e.g.* the AP2 / EREBP and the WRKY transcription factors); whereas, others that are present in small numbers in animals and yeast have been significantly amplified (*e.g* the MYB and basic-region leucine-zipper (bZIP) transcription factors)) (Riechmann and Ratcliffe, 2000).

1.3.4.1. Transcription factors in plant defence and stress responses

Many plant genes are transcriptionally regulated in response to pathogen attack or environmental stresses. Some of the transcription factors responsible for mediating these changes have been shown play a role in stress tolerance. For example, overexpression of the CRT/DRE-BINDING FACTOR1 (CBF1) conferred cold tolerance in *A. thaliana* (Jaglo-Ottosen *et al.*, 1998); whereas, overexpression of the *A. thaliana ERF1* gene caused enhanced resistance to two different necrotrophic fungi, but reduced resistance to *Pseudomonas syringae* (Berrocal-Lobo *et al.*, 2002). In addition, a recent study examined mRNA levels of 402 distinct transcription factors under various environmental stresses by microarray analysis and found that the majority of genes are expressed differentially after various stress

treatments (Chen *et al.*, 2002). Distinct but overlapping expression patterns indicate the existence of a complex regulatory network of signals that allow plants to respond optimally to their changing environment. Four families of transcription factors in particular have been linked to changes in gene expression in plant stress responses: the ethylene-responsive-element-binding-factors (ERFs) (see section 5.1), the WRKY proteins (see section 1.4.5), the bZIP proteins and the MYB proteins (Singh *et al.*, 2002).

1.4. Pathogen attack

Plant pathogens can be placed into two groups according to their mode of growth on the host plant. Necrotrophic pathogens secrete toxins or enzymes to kill and break down plant tissue and subsequently colonise the dead cells through absorption of nutrients (Thomma *et al.*, 2001b). The bacterium *Pseudomonas syringae* and the fungi *Alternaria brassicicola* and *Botrytis cinerea* fall into this group. Biotrophic pathogens, on the other hand, retrieve nutrients from living plant cells, and cannot survive on dead tissue. During infection, biotrophs avoid host defence responses by evading recognition, or by producing suppressors of defence responses. This group of pathogens includes the fungi *Peronospora parasitica* (downy mildew) and *Erysiphe orontii* (powdery mildew) (Thomma *et al.*, 2001b).

1.4.1. Plant resistance

Plants defend themselves from pathogen attack by activating a range of defence responses (see section 1.4.2). The speed with which these responses are activated is a key factor in determining the 'winner' of the plant-pathogen conflict (see section

1.4.4). Plant defence responses can be divided into three general pathways: non-host resistance pathways; gene-for-gene resistance pathways, which function during responses to avirulent pathogens; and, pathways that limit the spread of virulent pathogens. Further downstream, a fourth pathway, the SAR pathway, leads to strong resistance against normally virulent pathogens, pre-empting a second attack (see section 1.3.3.3).

1.4.1.1. Non-host resistance

Resistance of an entire plant species to a specific pathogen is termed non-host resistance and is the most common form of disease resistance; thus, most plant-pathogen contacts do not lead to disease (Heath, 2000; Nürnberger and Brunner, 2002). This form of resistance is generally controlled by a number of genes so that individual factors may segregate within a species without compromising overall resistance (Heath, 2000). As pathogens have rarely altered their host species range over recorded history, non-host resistance is very stable over time. The first line of defence to halt pathogen access and/or spread is constituted by preformed anti-microbial compounds such as peptides, proteins and secondary metabolites (Broekaert *et al.*, 1997). In addition to these constitutive defence mechanisms, inducible responses are triggered by elicitors. Elicitors are formed by pathogen-derived surface structures (exogenous elicitors), or plant cell wall fragments (endogenous elicitors) that are likely to be released by pathogen-derived hydrolytic enzymes (Nürnberger and Scheel, 2001). Fungal cell wall components (e.g. chitosan), bacterial proteins (e.g. harpin and flagellin) as well as plant cell wall oligogalacturonides are examples of general elicitors. Recently, a plant receptor for

bacterial flagellin was identified and shown to bind to a 22 amino acid fragment of the flagellin protein (which builds up the filament of eubacterial flagella) (Gomez-Gomez *et al.*, 1999).

1.4.1.2. Gene-for-gene resistance or host resistance

In contrast to non-host resistance, gene-for-gene resistance is expressed by plant genotypes within an otherwise susceptible host species and is often controlled by segregation of a single resistance (*R*) gene (Heath, 2000). In this scenario, colonization can be prevented following specific pathogen recognition mechanisms, which are triggered by interactions between *R* gene products from the plant with the matching avirulence (*avr*) gene products from the pathogen in a 'gene-for-gene' recognition event (Flohr, 1971). Disease resistance ensues only if corresponding *R* and *avr* genes are present in both host and pathogen (incompatible interaction); if either is inactive or absent, the plant is susceptible to infection (compatible interaction) (Flohr, 1971). The persistence of pathogen *avr* genes, despite the expected selective pressure exerted through *R* gene-induced defences, indicates that *avr* gene products play an important role in pathogen virulence on susceptible hosts (Nimchuck *et al.*, 2001). Accordingly, different classes of Avr proteins are implicated in interference with plant defence responses or in enhancing growth of the pathogen (Nimchuck *et al.*, 2001).

1.4.1.3. Basal resistance

The identification of mutants with enhanced susceptibility (*eds*) to virulent pathogens revealed the existence of inducible basal defence pathways which inhibit pathogen

spread after successful infection and onset of disease (Parker *et al.*, 1996). When infected with virulent strains of *P. parasitica*, the *eds1* mutant shows earlier sporulation and elevated production of sporangiophores as compared to the wild-type. [The mutation also impairs certain gene-for-gene resistance pathways and non-host resistance pathways, see section 1.4.3.2.] This phenotype is also exhibited by other mutants, *e.g.* the *non-expressor of PR-genes1* (*npr1)* mutant, identified on the basis of failure to induce *PR1* expression (Cao *et al.*, 1994), and the *phytoalexin-deficient4* (*pad4*) mutant, which displays reduced camalexin (the *A. thaliana* phytoalexin) accumulation in response to virulent pathogen attack (Reuber *et al.*, 1998).

1.4.2. The plant strikes back – plant defence responses

Potential strategies for plants to inhibit pathogens are erection of structural barriers that prevent pathogen access and enzymatic and chemical defences that interfere with pathogen metabolism (Glazebrook *et al.*, 1997). Induction of *PATHOGENESiS-RELATED* (*PR*) genes, callose deposition to strengthen the cell wall, as well as generation of antimicrobial phytoalexins, are well documented responses to pathogen attack. The most common effect of gene-for-gene resistance, also frequently observed in non-host resistance, is the hypersensitive response (HR), a rapid, genetically programmed death of cells at the infection site which helps to isolate the pathogen (Glazebrook *et al.*, 1997). Triggering of the HR response has been attributed to the generation of AOS in the oxidative burst (see section 1.7.4.3), in conjunction with production of nitric oxide (NO) (Delledonne *et al.*, 2001) (see section 1.7.4.3). However, little is known about the actual mechanisms of non-host

resistance. With the exception of the HR, the host response to virulent pathogens involves activation of many of the same defence-related responses that are activated by avirulent pathogens, although these responses are often activated more slowly or weakly (Reuber *et al.*, 1998).

1.4.3. Signalling downstream of pathogen recognition in *A. thaliana*

1.4.3.1. Early events

Early events following pathogen recognition involve ion fluxes across the plasma membrane followed by an oxidative burst. Treatment of parsley cell cultures with Pep-13, a peptide elicitor from *Phythophthora sojae*, stimulated rapid Ca^{2+} influx across the plasma membrane (within 2 – 4 min), with concomitant effluxes of Cl^- and K^+. In addition, uptake of protons lead to alkalinisation of the culture medium (Jabs *et al.*, 1997; Zimmermann *et al.*, 1997). This was followed by an increase in H_2O_2 within 4 – 6 min, reaching a first maximum at 15 – 20 min followed by a second, more sustained elevation at 3 – 6 hours. A similar timing for AOS generation was seen in elicitor-treated soybean suspension cultures (Levine *et al.*, 1994). Inhibition of the ion fluxes by channel blockers abolished H_2O_2 production as well as phytoalexin accumulation. Signalling events upstream of the oxidative burst are discussed in more detail in section 1.7.3.

1.4.3.2. Downstream signalling molecules

Several genes are required for resistance mediated by a number of different *R* genes. *EDS1* and *non-race specific disease resistance* (*NDR1)* are each required for the function of different *R* gene classes, indicating that two separate pathways

exist downstream of R protein activation. *R* genes that require *EDS1* also require *PAD4*, whereas those that require *NDR1* also require *avrPphB-susceptible2* (*PBS2)* for the majority of resistance responses, placing additional genes into each pathway. However, there are also several examples of *R* genes that function independently of both *EDS1* and *NDR1*, such as *RPP7*, *RPP8* and *RPP13* (resistance to *P. parasitica*), which require neither of these genes. Thus, at least three signalling pathways exist. *NDR1* encodes a protein with two predicted transmembrane domains and may therefore function to hold R proteins close to the membrane. *EDS1* and *PAD4* encode proteins with similarity to triacyl glycerol lipases. Their function is suggested to involve generation or degradation of a signal molecule. In addition, mutations in either gene leads to defects in SA accumulation and expression of both genes can be transcriptionally activated by SA, pointing to a role of *EDS1* and *PAD4* upstream of SA but possibly in a signal amplification loop. As mentioned in section 1.4.1.3, the *eds1* and *pad4* mutants not only show a loss of resistance to certain avirulent pathogens but also display increased susceptibility to virulent pathogens (Glazebrook *et al.*, 1997; Zhou *et al.*, 1998). Downstream of *EDS1* and *PAD4*, the *NPR1* gene is necessary both for SA-induced expression of *PR* genes such as *PR-1*, *BGL2* and *PR-5* and for the establishment of SAR (Cao *et al.*, 1994).

1.4.4. Common elements in the different resistance types

In recent years, analysis of disease resistance mutants has demonstrated that non-host, basal and *R* gene mediated resistance are mediated by the same underlying signalling pathways. Thus, the *eds1* mutant is not only impaired in resistance

conferred by certain *R*-genes but also allows enhanced growth of virulent *P. parasitica* isolates (Parker *et al.*, 1996). In addition, *P. parasitica* isolates derived from *Brassica oleracea* were also capable of sporulation on *eds1*, but not on any other *A. thaliana* ecotype tested, indicating a break-down in non-host resistance. Other mutants, *e.g. pad4* (Zhou *et al.*, 1998), *npr1* (Cao *et al.*, 1994), *sid1* and *sid2* (salicylic acid-induction deficient) (Navrath and Métraux, 1999), are also affected in susceptibility to avirulent and virulent isolates of *P. syringae* and *P. parasitica*. SA may thus play a central role in this signalling network. Accordingly, many defence responses that are characteristic of SAR are also observed in local *R* gene mediated resistance and in local growth limitation of virulent pathogens (Maleck *et al.*, 2001). This apparent paradox was explained by differences in timing of the defence response. In a compatible interaction, defence responses are initiated while the pathogen is already spreading through the host tissue and may thus be too slow to stop pathogen growth. By contrast, pathogens attacking SAR-induced tissue immediately encounter pre-formed defences hindering tissue colonization.

1.4.5. Promoter elements in pathogen-triggered gene induction: the W-box

W-boxes are responsible for pathogen- and elicitor-triggered expression such as defence proteins (*e.g. PR* genes in parsley (Rushton *et al.*, 1996)) and regulatory proteins (*e.g. RLK4* and *NPR1* in *Arabidopsis* (Du and Chen, 2000; Yu *et al.*, 2001)). The sequence of W-boxes [(T)(T)TGAC(C/T)] contains a short, invariant core (TGAC), which is essential for function and binding of the WRKY transcription factors. Several of these elements frequently cluster within short promoter stretches and can act synergistically (Eulgem, 1999). In *A. thaliana*, the W-box (TTGAC) is

shared by 26 defence genes with similar induction profiles to *PR-1*, as shown in microarray analysis of SAR gene expression (Maleck *et al.*, 2001). On average, these genes displayed 4.3 copies of the promoter element in 1 kb promoters, compared to 2.1 copies expected for random distribution. Consistent with this, another microarray experiment investigating gene expression changes in *A. thaliana* in response to *P. syringae* infiltration identified a promoter sequence similar to the W-box [(T/C/G)(T/C/G)(A/T)GAC(C/T)T]) at high frequency in the promoters of up-regulated defence genes (Chen *et al.*, 2002).

1.5. Wounding

Wounding is the result of a large number of stresses plants encounter, such as mechanical damage from wind, sand, hail and rain, cell wall degradation during bacterial and fungal pathogen attack, as well as, herbivore feeding and insect attack. Open wound sites caused by any of these mechanisms could facilitate infection by opportunistic pathogens (Reymond *et al.*, 2000). For protection, plants have evolved a variety of inducible chemical defences which are triggered systemically in response to wounding, which share many components with the defence mounted against bacterial or fungal attack (Durrant *et al.*, 2000). In addition, deterrents that decrease digestibility and nutritional value of the plant, and volatile signals that attract insect predators such as wasps and mites, are generated (Ryan, 2000). In a cDNA microarray experiment, mechanical wounding of *A. thaliana* leaves was shown to change the expression levels for 91 out of 150 defence-associated genes, demonstrating large-scale induction of protective mechanisms (Reymond *et al.*, 2000).

1.5.1. Signalling in response to wounding

Most research on wound signalling has been conducted upon tomato (*Lycopersicon esculentum*). In this system, wounding causes processing of the prosystemin protein at the wound site, resulting in release of the 18-amino-acid peptide hormone systemin (reviewed in Ryan, 2000). However, prosystemin has been isolated from solanaceous plants only (Constabel *et al.*, 1998), and does not appear to be present in other species such as *A. thaliana*. Accumulation of small cell wall components may also play a role in triggering appropriate responses. For example, oligogalacturonides (OGs) were shown to accumulate as a consequence of fungal attack in tomato (Benhamou *et al.*, 1990). In response to wounding, plants were shown to actively produce these cell wall fragments through systemic induction of polygalacturonase, a cell wall degrading enzyme yielding OG products (Bergey *et al.*, 1999). OGs generated during pathogen infection and herbivore attack were shown to elicit an oxidative burst (see section 1.7) leading to induction of *PROTEINASE INHIBITOR (PIN)* genes (which protect against insect attack) (Doares *et al.*, 1995). Increased production of OGs during wounding may therefore trigger defence mechanisms in anticipation of pathogen attack at the open wound site. In addition, wounding, as well as exposure to elicitors such as chitins, oligosaccharides, OGs (Doares *et al.*, 1995; Gundlach *et al.*, 1992), and yeast extracts (Parchmann *et al.*, 1997), leads to production of JA, which has been shown to be necessary for induction of numerous downstream genes (Reymond *et al.*, 2000).

1.6. Overlap between the described stress responses

Recently, gene expression profiling has provided evidence for extensive overlap in gene induction between *R* gene activation and wounding (Durrant *et al.*, 2000; Cheong *et al.*, 2002). Signalling molecules also appear to be shared between pathogen resistance, SA accumulation and wounding (see also sections 1.4.4 and 1.5.1). For example, the activities of two tobacco MAPKs, wound-inducible protein kinase (WIPK), and salicylic acid-inducible protein kinase (SIPK) (see section 4.1), are elevated in response to wounding (Zhang and Klessig, 1998a; Seo *et al.*, 1999) and in response to *R* gene recognition (Romeis *et al.*, 1999) (see section 4.1). Convergence of pathogen- and wounding- triggered responses was also revealed by analysis of promoter elements (Rushton *et al.*, 2002). In this study, tetramers of pathogen-inducible promoter elements, *e.g.* the W-box, were able to direct wound-induced gene expression. Hence, many common elements between pathogen resistance and the wounding response exist, suggesting that they may share perception and signalling mechanisms.

1.7. Oxidative burst

The active generation of AOS in plant cells, in a process termed the oxidative burst, was first demonstrated in potato tubers in response to fungal infection (Doke, 1983). Since then, oxidative bursts have been demonstrated in response to a wide variety of stresses, *e.g.* wounding (Doke, 1997; Orozco-Cadenas and Ryan, 1999), ozone fumigation (Wohlgemut *et al.*, 2002), irradiation with UV-B (Rao *et al.*, 1996; Allan and Fluhr, 1997), mechanical stress (Yahraus *et al.*, 1995), application of abscisic

acid (Pei *et al.*, 2000), hyperosmotic shock (Coelho *et al.*, 2002) and auxin (Joo *et al.*, 2001).

1.7.1. Mechanisms of AOS generation

R gene-mediated recognition of pathogens often results in the programmed execution of challenged host cells, producing a visible area of cell death that surrounds the site of attempted pathogen ingress (Dangl and Jones, 2001). An early characteristic feature of this hypersensitive response (HR) is the rapid generation of $^{\bullet}O_2^-$ and/or H_2O_2 (reviewed in Tenhaken *et al.*, 1995; Doke, 1997; Lamb and Dixon, 1997; Wojtaszek, 1997; Grant and Loake, 2000). This 'oxidative burst' was first demonstrated in potato tuber tissue following inoculation with an avirulent, but not with a virulent, race of *Phytophthora infestans* (Doke, 1983). Likewise, a variety of nonrace-specific fungal elicitors and endogenous oligogalacturonide elicitors derived from the plant cell wall rapidly induced the oxidative burst within 2 min of exposure to plant cells (Lamb and Dixon, 1997). A number of possible mechanisms responsible for AOS generation have been identified. Among these are plasma membrane-localised NADPH-dependent oxidases (Desikan *et al.*, 1996; Keller *et al.*, 1998), cell wall peroxidases (Bolwell *et al.*, 1998), and apoplastic amine, diamine, and polyamine oxidase-type enzymes (Allan and Fluhr, 1997). This abundance of mechanisms may reflect variation in the oxidative burst generation in different plant species, or in response to different stimuli (Wojtaszek, 1997).

Most attention has focussed on NADPH-dependent oxidases, which show similarity to the mammalian neutrophil oxidases, and catalyse the reaction $O_2 + NADPH \rightarrow {}^{\bullet}O_2^- + NADP^+ + H^+$. The mammalian protein complex is composed of at least five

components: two plasma membrane subunits ($gp91^{phox}$ and $p22^{phox}$) forming a heterodimeric flavocytochrome b_{-558}, and three cytosolic regulatory proteins ($p40^{phox}$, $p47^{phox}$, $p67^{phox}$), which are phosphorylated after stimulation and translocate to the plasma membrane to form the active enzyme (Segal and Abo, 1993). The $^{\bullet}O_2^-$ thus generated, and its dismutation product H_2O_2, are probably used to kill phagocytosed bacteria in the cell vacuole while the neutrophil cell stays alive.

Rice homologues of $gp91^{phox}$ were identified by sequence similarity to ESTs (Groom *et al.*, 1996) and used to isolate an *A. thaliana* homologue (Keller *et al.*, 1998). This respiratory burst oxidase homologue A (*RBOHA*) gene was found to encode a protein with a large hydrophilic N-terminal domain (not present in the mammalian ortholog), containing two Ca^{2+}-binding EF-hand motifs and extended similarity to a human GTPase activating protein. Eight *AtRBOH* genes have so far been identified (Torres *et al.*, 2002). Genes encoding other components of the NADPH oxidase complex have not been identified, which may indicate that regulation of the oxidative burst differs significantly in plants and animals. Accordingly, the ability of isolated plant gp^{phox} protein to generate $^{\bullet}O_2^-$ has been demonstrated, indicating that, unlike the mammalian enzyme, the plant RBOH protein does not require additional subunits for its function (Sagi and Fluhr, 2001). Instead, different members of the RBOH family may play distinct roles in response to different stresses. Consistent with this, the *A. thaliana* mutant *atrbohD,* but not *atrbohF,* showed reduced H_2O_2 accumulation after inoculation with avirulent *P. syringae* and *P. parasitica* whereas both genes play a role in the HR (see section 1.7.4.3) (Torres *et al.*, 2002).

Unlike NADPH oxidases, cell wall peroxidases generate H_2O_2 directly, by-passing the $^{\bullet}O_2^-$ dismutation step (Wojtaszek, 1997). Evidence for the involvement of

peroxidases in the generation of H_2O_2 during oxidative bursts was supplied by the observation that peroxidase isoforms produce H_2O_2 *in vitro* at an alkaline pH, which is characteristically found in the apoplast following pathogen recognition (Bolwell and Wojtaszek, 1997). Furthermore, peroxidases are secreted at infection sites (McLusky *et al.*, 1999).

Supporting the hypothesis that plant species may differ in their oxidative burst mechanisms (Wojtaszek, 1997), French bean cell cultures, but not rose cell cultures, failed to produce detectable $^{\bullet}O_2^-$ following elicitor challenge (Bolwell *et al.*, 1998). Moreover, simultaneous AOS production from distinct sources has been demonstrated (Allan and Fluhr, 1997; Grant *et al.*, 2000a). $^{\bullet}OH$ can also be detected by electron spin resonance analysis in elicitor-treated rice cells and is likely to be generated from H_2O_2 through the Fenton reaction (see section 1.1.1) (Kuchitsu *et al.*, 1995). Accordingly, $^{\bullet}OH$ generation was inhibited by exogenous CAT and iron chelator. In addition to active AOS generation, antioxidant enzymes such as APX and CAT are suppressed following pathogen recognition, a process which was suggested to enhance downstream effects by further increasing AOS levels (Mittler *et al.*, 1998). Similarly, gibberellin-induced programmed cell death in barley aleurone was shown to be dependent on H_2O_2 produced as a result of reduced antioxidant activity (Fath *et al.*, 2001).

1.7.2. The oxidative burst in compatible and incompatible interactions

The kinetics of H_2O_2 production in response to elicitor or pathogen treatment depend on recognition by the plant. Challenge of soybean suspension cultures with both an avirulent and a virulent strain of *P. syringae* pv. *glycinea* resulted in rapid

but transient generation of H_2O_2 (maximum 1 h after inoculation); however, only the avirulent pathogen triggered a sustained second oxidative burst (starting 3 h and peaking 5 h after inoculation) (Levine *et al.*, 1994). Similar timing was seen in elicitor-treated parsley cell suspension cultures (Jabs *et al.*, 1997). An earlier study in rice determined that the compatible interaction with a fungal pathogen triggered a delayed oxidative burst compared to the incompatible interaction (Sekizawa *et al*, 1985; reviewed in (Doke, 1997)). Treatment of *A. thaliana* leaf slices with flagellin elicitor triggered H_2O_2 generation within 4 min of application in ecotypes expressing the flagellin receptor FLS2 but not the flagellin-insensitive ecotype Ws-0 (Gomez-Gomez *et al.*, 1999), indicating that H_2O_2 generation can be receptor-specific.

1.7.3. Regulation of AOS production

Due to the cytotoxic nature of AOS, their generation by the plant itself must be tightly regulated (see section 1.1.1).

1.7.3.1. Regulation of NADPH oxidase activity

1.7.3.1.1 Calcium

The presence of EF-hands in the $gp91^{phox}$ subunit suggests that Ca^{2+} may play an important role in the regulation of NADPH oxidase activity. Accordingly, pathogen or elicitor challenge has been shown to trigger a rise in $[Ca^{2+}]_{cyt}$ which is necessary for the oxidative burst and HR response (Chandra and Low, 1997; Jabs *et al.*, 1997; Zimmermann *et al.*, 1997; Piedras *et al.*, 1998; Xu and Heath, 1998; Grant *et al.*, 2000b), (see also section 1.4.3.1). The NADPH oxidase subunit may bind Ca^{2+} released after pathogen recognition or abiotic stress treatment with subsequent

conformational changes initiating enzyme activity. Accordingly, the $^{\bullet}O_2^-$-generating activity of plant gp91^{phox} is stimulated by Ca^{2+} (Sagi and Fluhr, 2001). Ca^{2+} may also affect NADPH oxidase activity indirectly as NAD kinase, an enzyme which catalyses the final step in the production of NADPH, is dependent on calmodulin for activation (Harding *et al.*, 1997).

1.7.3.1.2 Protein kinases

Studies employing inhibitors of kinases and phosphatases have implicated protein phosphorylation in the control of the oxidative burst (Levine *et al.*, 1994; Chandra and Low, 1995; Miura *et al.*, 1995; Rajasekhar *et al.*, 1999). Genetic evidence for a role for kinases upstream of H_2O_2 generation was supplied by positional cloning of the *OST1* (*OPEN STOMATA1*) gene, an *A. thaliana* ser/thr kinase (Mustilli *et al.*, 2002). The *ost1* mutant fails to close its stomata or accumulate H_2O_2 in response to ABA application, but externally applied H_2O_2 triggered the same degree of stomatal closing as in the wild type, placing the OST1 kinase upstream of H_2O_2 generation.

In addition, a MAPK signal cascade was implicated in triggering the oxidative burst (Ren *et al.*, 2002). *A. thaliana* plants expressing constitutively active mutant forms of *AtMEK4* and *AtMEK5* under an inducible promoter were generated. Induction of these transgenes led to generation of H_2O_2, followed by HR-like cell death (see section 1.7.4.3). Similarly, a CDPK activated by elicitor treatment of tobacco cell suspension cultures was not affected by diphenyleneiodonium chloride (DPI) treatment, an inhibitor of NAPDPH oxidases (but see also section 4.3.1.1), placing this kinase upstream of the oxidative burst (Romeis *et al.*, 2000).

1.7.3.2. Regulation of cell wall-associated peroxidases

Cell wall peroxidase activity was stimulated *in vitro* through alkalinisation of the medium (Bolwell and Wojtaszek, 1997). As a rise in apoplastic pH is observed following pathogen recognition (Jabs *et al.*, 1997; Zimmermann *et al.*, 1997), this may be a regulatory mechanism for H_2O_2 production. In addition, co-localisation of peroxidase activity and H_2O_2 accumulation at *Botrytis allii* infection sites in onion epidermal cells suggested that secretion of peroxidases may be directed to the site of attempted pathogen penetration (McLusky *et al.*, 1999). This would increase AOS production at the necessary location.

1.7.4. Function of AOS-generated in response to pathogen attack

1.7.4.1. Direct anti-microbial activity

AOS may directly affect growth and survival of the attacking pathogen. Thus, H_2O_2 has been shown to inhibit the germination of spores of several fungal pathogens (Peng and Kuc, 1992) and potato expressing a fungal glucose oxidase (a H_2O_2-generating enzyme) showed enhanced resistance to *Erwinina caratovora* (Wu *et al.*, 1995). However, *in vivo* effects of altered AOS levels may also reflect resistance obtained by any of the mechanisms described below.

1.7.4.2. Cell wall cross-linking

Cross-linking of cell wall structural proteins is a rapid response in incompatible or non-host interactions (but not compatible interactions), and protects against further pathogen penetration through wall strengthening (Bradley *et al.*, 1992; Brisson *et al.*, 1994). H_2O_2 accumulation following the oxidative burst is believed to drive the

formation of protein cross-links, manifesting itself in rapid insolubilisation of cell wall proteins and increase in cell wall resistance to enzymatic digestion (Brisson *et al.*, 1994). However, the identity of the cross-linking molecules and the chemical processes involved are unknown.

1.7.4.3. HR formation

Attempted infection of plants by a non-host or an avirulent strain of pathogen results in rapid collapse of the challenged host cells in a process termed the HR (Levine *et al.*, 1994). AOS generated by the oxidative burst are thought to be key players in causing the HR. Accordingly, soybean cell cultures challenged with an avirulent (but not a virulent) strain of *P. syringae* triggered sustained accumulation of H_2O_2 and increased cell death (Levine *et al.*, 1994). Cell death was inhibited by treatment with DPI and kinase inhibitors, which also blocked the oxidative burst, and enhanced by incubation with the catalase inhibitor 3-amino-1,2,4-triazole. The *A. thaliana* plants mutants *atrbohD* and *atrbohF* exhibited reduced cell death in response to inoculation with avirulent *P. syringae*, providing genetic evidence for a role of NADPH oxidases in the HR (Torres *et al.*, 2002). In a different experimental approach, endogenous AOS levels were increased by exposing transgenic tobacco plants with reduced catalase levels to high light intensities (Chamnongpol *et al.*, 1998). The resulting AOS production was accompanied by development of HR-like lesions. In addition to H_2O_2, NO, a gaseous molecule, is produced in response to pathogen attack. NO levels relative to H_2O_2 and $^{\bullet}O_2^-$ levels were shown to be involved in the regulation of cell death (Delledonne *et al.*, 2001). Thus, at least in

some systems, other mechanisms in addition to the oxidative burst may operate to trigger a complete HR response.

1.7.4.4. Defence gene induction and signalling

In animal cells, $^{\bullet}O_2^-$ and H_2O_2 are produced not only in neutrophils, but also in other cell types in response to ligand stimulation (Finkel, 1998). This oxidative burst plays a role in intracellular signal transduction. For example, stimulation of vascular smooth muscle cells with platelet-derived growth factor resulted in a rapid increase in AOS and concomitant tyrosine phosphorylation. Exogenous H_2O_2 mimicked growth-factor-induced phosphorylation whereas overexpression of catalase blunted it (Sundarasan *et al.*, 1995). Similarly, H_2O_2 generated in soybean cell suspension cultures in response to challenge with avirulent (but not virulent) *P. syringae* was shown to induce expression of *GST* (Levine *et al.*, 1994). H_2O_2 was shown to function as a mobile signal by introducing a pair of dialysis membranes between two cell suspension cultures. Addition of avirulent *P. syringae* to one culture caused cell death only in these challenged cells, but triggered *GST* transcript accumulation in the uninfected suspension culture. If catalase was included in the compartment between the dialysis membranes, *GST* induction was blocked in the unchallenged cultures, confirming that H_2O_2 acts as a diffusible signal. Similarly, endogenous generation of H_2O_2, caused by exposure of tobacco plants containing an antisense catalase gene to high light intensities (see section 1.7.4.3), resulted in HR-like cell death at the site of illumination, and induced PR proteins in light-shielded adjacent tissue as well as systemic tissues (Chamnongpol *et al.*, 1998). This latter observation supports a paper by Alvarez *et al* (Alvarez *et al.*, 1998), demonstrating

the existence of 'microbursts' in systemic leaf tissue of tomato challenged with *P. syringae.* The small oxidative bursts, mainly found near vein tissue, caused cell death in a small number of cells and were not seen if leaves were detached immediately after infiltration. Co-infiltration of DPI with the pathogen reduced the local oxidative burst, the systemic microbursts, and the development of SAR; whereas, local infiltration of an H_2O_2-generating system induced systemic microbursts and subsequently SAR. Hence, H_2O_2 appears to function as a local and systemic signalling molecule in plant resistance. Similarly, local H_2O_2 generation and systemic microbursts were observed in response to wounding (Orozco-Cardenas *et al.*, 2001). Surprisingly, Torres *et al.*, 2002) report that *atrboh* mutants (devoid of the oxidative burst) still induced SAR by inoculation with avirulent *P. syringae*. The authors do not state if plants mutant in several of the *ATRBOH* genes were tested; thus, failure to suppress SAR establishment in a single *atrboh* mutant may reflect redundancy within the gene family.

1.7.5. The oxidative burst in response to wounding

Occurrence of an oxidative burst in response to wounding was demonstrated by detection of $^{\bullet}O_2^-$ in potato tuber after slicing (Doke, 1997). In tomato, H_2O_2 levels increased at wound sites within 1 h after wounding (Orozco-Cadenas and Ryan, 1999) and H_2O_2 accumulation was observed in the cell walls of wounded and unwounded (systemic) leaves after 4 h (Orozco-Cardenas *et al.*, 2001). The build-up of H_2O_2, as well as induction of defence genes, could be abolished by treatment with inhibitors of NADPH oxidases (DPI, imidazole and pyridine), indicating that these enzymes are the source of AOS (Orozco-Cardenas *et al.*, 2001). H_2O_2 accumulation

in response to wounding was also detected in 14 other plant species from six families, including in *A. thaliana* (Orozco-Cardenas *et al.*, 2001). Thus, signal propagation to other parts of the plant, subsequent to pathogen recognition and wounding, may involve small oxidative bursts triggered in systemic tissues (Alvarez *et al.*, 1998; Orozco-Cardenas *et al.*, 2001). The identity of the mobile molecule causing these microbursts is not known.

1.8. The cell wall – a common sensor in wounding and pathogen stress?

Wounding and attempted penetration by a pathogen, such as fungal hyphae, would be expected to generate not only chemical signals in the form of elicitors, but also mechanical signals derived from degradation, puncture, or deformation of the plant's cell wall or plasma membrane. Detection of this mechanical stress and the change in the state of the cell wall may be a more universal sensor of pathogen invasion than relying on the recognition of specific molecules which are subject to strong selection pressures (Heath, 2000). The role of the oxidative burst in response to other stresses causing distortion of the cell wall and plasma membrane such as freeze/thaw injury or hormone-induced cell elongation has not been investigated so far.

Evidence for a connection between the stress response signals and the cell wall was provided through characterisation of the *cev1* (*constitutive expression of VSP1)* mutant (Ellis *et al.*, 2002). This mutant accumulates anthocyanin, constitutively expresses a number of defence-related genes, and displays enhanced resistance to three powdery mildew pathogens. The mutation was shown to lie within the cellulose synthase gene *CesA3*. *cev1* roots have reduced amounts of cellulose,

indicating that a change in the cell wall architecture of the mutant, or signalling properties of non-incorporated cell wall components, lead to activation of the JA and ethylene stress response pathways. This is supported by the observation that treatment of *A. thaliana* with cellulose biosynthesis inhibitors reproduce the *cev1* phenotype.

The ability of plant cells to monitor and respond to signals at the cell wall has been demonstrated. Thus, AOS generation was detected following mechanical stimulation of parsley cells by touching the cell wall continuously for at least 5 – 10 minutes with a tungsten needle (Gus-Mayer *et al.*, 1998). In addition to the oxidative burst, needle contact with the cell wall enhanced cytoplasmic streaming and nuclear migration toward the site of stimulation as is observed during fungal penetration (Gross *et al.*, 1993). Similarly, AOS production (Mellersh *et al.*, 2002) and nuclear migration (Heath, 1997) were also observed at sites of localised enzymatic cell wall degradation.

1.8.1. Cell wall to plasma membrane signalling

The observation that external processes can trigger intracellular reactions suggests that signals emanating from the cell wall are able to reach and 'traverse' the plasma membrane. In mammalian cells, plasma membrane-bound receptors, known as integrins, connect the extracellular matrix (ECM) with the intracellular cytoskeleton and thus provide a link for signalling interactions between the cell and its environment. These molecules were shown to bind ligands in the ECM that contain Arg-Gly-Asp (RGD) motifs (Giancotti and Ruoslahti, 1999). Despite the lack of sequence homologues of integrins in plant genomes, there is some evidence for

functional homologues of these molecules in *A. thaliana* (Canut *et al.*, 1998; Laval *et al.*, 1999; Nagpal and Quatrano, 1999). For example, addition of RGD peptides has been shown to have physiological effects in plants including loss of plasma membrane-cell wall adhesion in plasmolysed *A. thaliana* cells (Canut *et al.*, 1998).

A role for cell wall – plasma membrane adhesion points for defence induction in response to fungal attack was demonstrated by Mellersh & Heath, 2001. Application of RGD peptides to cow pea or pea leaves disrupted attachment points between the cell wall and the plasma membrane This treatment entailed a decrease in recognition of incompatible rust fungi, manifesting itself in reduced H_2O_2 and callose production. In compatible interactions, the cell wall – plasma membrane adhesions appeared to be weakened underneath infection sites and addition of RGD peptides did not cause a change in infection efficiency for these species, indicating that interference with cell wall-to-cytosol signalling may be a means for pathogens to escape detection by the plant's defence system. Accordingly, pre-inoculation with incompatible fungi that increase cell wall – plasma membrane adhesion reduced penetration efficiency of compatible fungi (Mellersh and Heath, 2001).

In summary, these results indicate that signals emanating from pathogen attack or wounding at the cell wall can be perceived and transmitted to the intracellular cytoskeleton where they cause induction of the defence system including generation of H_2O_2 and callose deposition. A recent study by Coelho *et al.*, 2002, with *Fucus* embryonic cells, also implicated cell wall-plasma membrane signalling in response to hyperosmotic stress. Subsequent to stress application, AOS generation and elevations in $[Ca^{2+}]_{cyt}$ occurred particularly at sites of membrane-cell wall adhesions.

Thus, plant cells may be able to sense and respond to changes in environmental conditions by monitoring deformations in the cell wall and plasma membrane.

Thesis outline

The present study characterised the signalling network connecting AOS perception and activation of defence mechanisms further. The work can be divided into three parts. In the first part, a role for Ca^{2+} signalling in response to AOS treatment was demonstrated (Chapter 3). In the second part, evidence implicating OX1, a putative ser/thr kinase in H_2O_2 signalling is presented (Chapter 4). Finally, the third part details the relationship between AOS challenge and gene induction of members of the *ERF* transcription factor family (Chapter 5)

2 Materials and Methods

2.1 Chemicals

Chemicals were obtained from the following companies, unless stated otherwise, at AnalaR or equivalent quality.

BDH Laboratory Supplies, Poole, UK (BDH, UK)

GibcoBRL Life Technologies Ltd., Paisley, UK (GibcoBRL, UK)

Melford Laboratories, Ipswich, UK (Melford, UK)

Sigma-Aldrich Company Ltd., Ltd., Crawley, UK (Sigma, UK)

Duchefa Biochemie BV, Haarlem, The Netherlands (Duchefa, NL)

2.2 Antibiotics

Ampicillin and kanamycin were obtained from Melford, UK; streptomycin and spectinomycin from Sigma, UK and hygromycin, rifampicin and timentin from Duchefa, NL.

2.3 Enzymes

DNA and RNA modifying enzymes were obtained from New England Biolabs, Hitchin, UK (NEB, UK), GibcoBRL, UK, TaKaRa Shuzo Co. Ltd, Shiga, Japan and Bioline Ltd., London, UK.

Cellulase 'Onozuka' R-10 was obtained from Yakult Honsha Co. Ltd., Yakult Pharmaceutical Industry Co. Ltd., Tokyo, Japan

2.4 Nucleotides

Radionuclide ([α – ^{32}P]-dCTP, Redivue 10 mCi/ml) was obtained from AmershamPharmacia Biotech, Little Chalfont, UK (AmershamPharmacia, UK) Nucleotides were obtained from NEB, UK

2.5 Peptides

Flagellin 22 (Gomez-Gomez *et al.*, 1999) was a gift from Scott Peck, Sainsbury Laboratories, Norwich.

2.6 Seeds

Arabidopsis thaliana (*A. thaliana*) seeds were obtained from Lehle Seeds, Texas, USA (Lehle, USA).

2.7 Bacterial strains

Escherichia coli (*E.coli*) strain DH5α (GibcoBRL, UK) and *Agrobacterium tumefaciens* (*A. tumefaciens*) strain C58C1 (Deblaere *et al.*, 1985) were used.

2.8 *Peronospora parasitica* isolates

All *Peronospora parasitica* (*P. parasitica*) isolates were a gift from Anne Rehmany, HRI Wellesbourne, UK

2.9 Primers and probes

All primers listed in Table 2.1 are specific for regions within their respective cDNAs or genomic DNA; whereas, the kinase and 'phosphatase' primers are more degenerate with complementarity to regions conserved in all kinases (regions VI and VIII, Hanks and Quinn, 1991, primers designed by Dr Joy Boyce, University of Oxford). All hybridisation probes for Northern analysis were amplified from cDNA synthesised from seedlings treated for 1 h with 10 mM H_2O_2. Direct sequencing was used to verify the identity of the PCR product before use in Northern analysis.

Primers	direction	Primer sequence (5' → 3')	annealing temperature (°C)
M13 (sequencing from pUC18 or bluescript plasmids)	for rev	GGAAACAGCTATGACCATG (M13reverse) GTAAAACGACGGCCAGT (M13(-20)forward)	50
TUB (for control in RT-PCR)	for rev	GTGAACTCCATCTCGTCCAT CCTGATAACTTCGTCTTTGG	55
Probes for Northern analysis			
GST1 (At2g29450)	for re	TTGCTTCTTGCTCTTAACCC (GST1for) CTCAACCTTCTCCAAATTCC (GST1rev)	55
APX1 (At1g07890)	for rev	TGACGAAGAACTACCCAACC (apx-for) TAAGCATCAGCAAACCCAAG (apx-rev)	55
AOS (At5g42650)	for rev	TCCACAAGTCGTGGCTTTAC (AOSynth_for) AATCTCTCCGGCACAAACTC (AOSynth_rev)	56
ACX1 (At4g16760)	for rev	CTGATGGGTACCAAGAATAC (ACX1_for) AATTCCGCCATATGACGATC (ACX1_rev)	56
THI2.2 (also RT-PCR) (At1g66100)	for rev	TCGAGTTGTCTTGACATTAG (THI2.2_for) ACGCATTTTCAACTGCATTC (THI2.2_rev)	55
ECS1 (At1g31580)	for rev	ATGGCATCTTCTATAGTCTC (ECS1_for) TGACTTGGTGAGTTTTTTGG (ECS1_rev)	55
***OX1* primers**			
differential display for kinases	for rev	CCGTCGACGA(CT)T(AGCT)AA(AG)CC(ACGT)AA (VIBsense) GCGAATTC(CT)TC(AGCT)GG(AGCT)A(AG)(AG)TA (CT)TC (VIII anti)	55

OX1 (sequencing)	for	GTCGACATTATGCTAGAGGG (band6for) CCGGGACAGAATCTCAATTC (ki2) GCCAGACAATGTGATGATCC (ki3) GTCGATTGGTGGTCGTTAGG (ki4) TGGTGATAAGGGAACCGATG (ki5) AACGTTGAGGAAATCAAGGG (OX1constseq)	50
	rev	GTACACCATAGTCCATAGAC (kirev) GCCCTGTCTTAGAGTTAAGA (ki5'RACE300) AAATCTGATAATCTCGTCGG (ki5'RACE400) TGTCGACGTTAGTTAACTCC (kiseq1) ACAACTCCTTTAGCTCCACG (kiseq2) GTCAAGTGCTAATACAAGCT (5'revcheck) ACGTATTCCTCTGTTCCGAC (seqki3)	50
OX1 promoter (sequencing)	1 2 3 4 5	ATGGCAACTGTCCAAATGAG (OX1prom1) TGATACGAGATTCTCATCAG (OX1prom2) GCAATTTTTGGGCCATTGGG (OX1prom3) AACGCATGGCAACGAATCTC (OX1prom4) CGTTCAATGCCTTGGAAGAC (OX1prom5)	50
analysis of *OX1* 5' UTR	- 165 - 88 - 42 - 28	AGGCAAAGCAAACGAGTGGAC (5'A) AGTCGCCTACTACGTAGAAC (5'B) ATTGCTGTCTTAACTCTAACG (5'C) TCTAACGGAGTTAACTAACG (5'D)	55
OX1 Knock-out PCR	for rev JL202 JL270 Con-1A Con-1B	TAAAGTGTAGGCGAATAGCTGGAGACT (knockoutfor) GTATCATTCATTAGGAGAATGGGAGATTG (knockoutrev) CATTTTATAATAACGCTGCGGACATCTAC TTTCTCCATATTGACCATCATACTCATTG CGTCTAGGTGGTTCAGTACCTGTTGAATG TTTATCGAAGAAACATGTCGTTGAACCAG	65
OX2 probe	for rev	ATGAGCAACCACCTCTTACC (OX2for) TACCTTAAGCACCAAATCCC (OX2rev)	60
RT-PCR: *OX1* *OX2*	for rev for rev	GTCGACATTATGCTAGAGGG (band6for) ATCGGTTCCCTTATCACCAC (OX1RTPCRrev) ACGTCGATTTTCGAAATCTC (ox2RTPCRforB) ATCAACTTCGACCATCTAGA (ox2RTPCRrevB)	60
OX1 constructs			
OX1 constitutive mutant	for rev	GCGCGTCGACATAACAATGCTAGAGGGAGATGAGAAAC (ox1constfor) GCGCACTAGTACTCCTCTGAAGAAATCATG (ox1constrev)	58
OX1 antisense construct	for rev	GCGCACTAGTATGCTAGAGGGAGATGAGAAAC (ox1antifor) GCGCGTCGACACTCCTCTGAAGAAATCATG (ox1antirev)	58
pER8-specific probe	for rev	ACTAGTCGATCCAGGCCTCC (ER8for) CTCTTATCCATCCATTTGCA (ER8rev)	58
OX1-specific probe	for rev	TGGTGATAAGGGAACCGATG (ki5) GTACACCATAGTCCATAGAC (kirev)	56
OX1 promoter::GUS construct	for rev	GCGCGGATCCCGCTGGGATAATCTCAAAGG (YFPorGUSOX1for) CGCGCTGCAGATAATGTCGACGTTAGTTAAC (GUSOx1rev)	60
OX1promoter (-385 to -317) ::*minimal35S promoter::GUS* construct	for rev	GCGCTTCGAACCACGTAAAACGTCACCCCTGACGTCAC ATCCTCTAGAACACCACGTGTTTGTCTTAAACACGACGA GGATATCTCCACTGACGTAAG (PromOx1GUSfor) GTTGTAAAACGACGGCCAGT (Ox1promGUSrev)	58

***ERF* primers**			
differential display for phospha-tases	for rev	GGTGA(CT)TC(AGT)(ACT)G(AGT)GC(AGCT)CT(GCT) (CT)T(AGT) (PP2C Degen F (Red)) (AGT)(AT)(AC)(AG)TCCCA(AT)A(AGC)(ACT)CC(AG)TCA (GC)(AT)(ACT)CC (PP2C Degen R (Red))	50
ERF1 probe (At4g17500)	for rev	GTCCATACGACGACACTTAC (ERF1for) TTCTCCTTCTTGACCGGAAC (ERF1revS)	58
ERF1 RT-PCR	for rev	as above (ERF1for) AGCTCCGTTCTCGTTAGAAG (ERF1rev)	58
ERF4 (At3g15210)	for rev	CTGAGCTTTTAACGGTGTCG (ERF4forS) CAACATGGGGTGAAACAAAG (ERF4rev)	58
ERF4 RT-PCR	for rev	ATCCGAGAATGGCCAAGATG (ERF4for) as above (ERF4rev)	58
ERF5 (At5g47230)	for rev	AAACATCTACTCGACGAGGC (ERF5for) TTAAGCTCCGGTTCAAACTG (ERF5revS)	58
ERF5 RT-PCR	for rev	as above (ERF5for) TCGCATCTACTCGACGAGGC (ERF5rev)	58
ERF6 (At4g17490)	for rev	TCCTCCAAAATGGCTACACC (ERF6forB) TTGAACAGTGACACGAGGAG (ERF6revS)	58
ERF6 RT-PCR	for rev	as above (ERF6forB) CAACAAGCTGACCCAAACAG (ERF6rev)	58
ERF7 (At1g53170)	for rev	CACACACAGATCTCTTCTTC (ERF7for) AATCGCATGTAACGGTTTCG (ERF7rev)	58
ERF10 (At1g03800)	for rev	AAGAGAATGTCACTACGGCC (ERF10for) TTGCGTTGAGGTCAAGATCC (ERF10rev)	58

Table 2.1: Primers for PCR reactions
Primer names, sequences and annealing temperatures for primers used in PCR reactions are listed. The primer direction relative to the direction of the amplified sequence is indicated (forward or reverse). The exact name under which the primer was ordered from MWG-Biotech AG, Ebersberg, Germany, is given in brackets behind the corresponding sequence.

2.9.1 *OX1* probe

An EST corresponding to an *OX1* cDNA clone inserted into pBluescript II SK$^-$ (AV539923) was located using the Basic Local Alignment Search Tool (BLAST) program (Altschul *et al.*, 1997) and obtained from the Kazusa DNA Research Institute (Chiba, Japan, http: //www.kazusa.or.jp/). The EST was sequenced using M13 primers and found to include all but the 460 bp of the 5' end of the coding

region as well as 257 bp of the 3' UTR. The insert was purified after restriction with EcoRI and XhoI.

2.9.2 *β-TUBULIN* probe

The products obtained by amplification with degenerate primers for β-tubulins were cloned into *E. coli*, re-isolated and sequenced (all steps carried out by Sarah Scrase-Field, University of Oxford). Plasmids containing four different β-tubulins were mixed in a 1:1:1:1 ratio. Inserts were purified after restriction with SalI and NotI (size approximately 1 kb, two bands).

2.9.3 *PR-1* probe

Plasmid containing the *PR-1* probe was a gift from Dr Murray Grant, Wye College, UK. The insert was sequenced and found to comprise the complete cDNA (At2g14610, approximately 850 bp). To obtain probe DNA, restriction with SacI and KpnI was carried out and the insert was purified.

2.9.4 *PDF1.2* and *CHITB* probe

Plasmids (λ-PRL2) containing the *PDF1.2* cDNA (37F10T7) and *CHITB* cDNA (92G1T7) were ordered from the ABRC DNA Stock Center, Ohio State University. The identity of the sequences was confirmed by sequencing as At5g44420.1 (*PDF1.2a*) and At3g12500 (*BASIC ENDOCHITINASE B*), respectively. The plasmids were restricted with SalI and NotI and probes purified (approximate size: 420 bp (*PDF1.2*) and 1080 pb (*CHITB*)).

2.10 Plasmids

pUC18 (Amersham, UK), pBlueScript SK- (Stratagene, La Jolla, CA, USA (Stratagene, USA)), pBin19 (Bevan, 1984), pBI121 (Jefferson *et al.*, 1987) and pER8 (Zuo *et al.*, 2000) were used for cloning.

2.11 Sterilisation

2.11.1 Chemicals and solutions

2.11.1.1 Autoclaving

All thermostable chemicals in solution were sterilised by autoclaving at 121 °C, 30 psi, for 20 min.

2.11.1.2 Filter sterilising

All heat-labile solutions were filter sterilised using 0.2 µm syringe-filters obtained from Nalgene, Nalge Nunc International, Rochester, USA.

2.11.2 Surface sterilisation of *A. thaliana* seed

2.11.2.1 Ethanol sterilisation

Commercial seed and clean seed to be germinated and grown on agar plates were sterilised by addition of 70 % ethanol and shaking for 5 min. The seed was subsequently left to dry on filter paper in a sterile flow cabinet.

2.11.2.2 Bleach sterilisation

Seed obtained after dipping in *A. tumefaciens*, or to be grown on peat plugs in greenhouses, were sterilised in 70 % ethanol as described in section 2.11.2.1 but subsequently shaken for 10 min in 10 % sodium hypochlorite solution (final

concentration: 1.2 % (w/v)), 0.25 % (w/v) SDS. After four washes in sterile water in the flow cabinet, the seed was dispensed directly onto agar plates and left to dry.

2.12 Growth media and conditions

2.12.1 Bacterial growth media and conditions

Bacteria were grown on solid (1.5 % (w/v) agar, 2 % (w/v) Luria-Bertani (LB) medium (Sigma, UK), and in liquid culture, (2 % (w/v) LB) supplemented with antibiotics and/or inducing chemicals as appropriate (see section 2.12.3). Bacteria were incubated at 37 °C (*E. coli*) or 28 °C (*A. tumefaciens*), static for solid culture or shaking at 200 rpm for liquid culture.

2.12.2 Plant growth media and conditions

2.12.2.1 Germination and growth on MS agar plates

Sterilised *A. thaliana* seeds (section 2.11.2) were sown on 0.8 % (w/v) plant tissue culture grade agar (Sigma, UK) supplemented with 1 x MS nutrients (micro- and macroelements including vitamins, Duchefa, NL) and the appropriate antibiotic if required. The plates were sealed with micropore tape (Millipore, Watford, UK). After two to five days of stratification at 4 °C in the dark, plates were transferred to a growth chamber (21 °C, 16 h light, 8 h dark, 60 µM m^{-2} s^{-1} light intensity). If required, seedlings were transferred to peat plugs after they had reached an age of at least 6 days and grown to maturity in a greenhouse. Seed from individual plants was obtained by using the Aracon system (BetaTech bvba, Gent, Belgium), which isolates each plant in a transparent plastic tube.

2.12.2.2 Germination and growth on peat plugs

Sterilised *A. thaliana* seeds (2.11.2) were stratified in 0.15 % agar in the dark at 4 °C for two to three days. The seed suspension was pipetted onto re-hydrated peat plugs (Jiffy Products Ltd, Peterborough, UK) in boxes, the lids were replaced and boxes transferred to a growth cabinet (see section 2.13.2). After four to five days, the lids were slightly opened to allow gas exchange and decrease humidity.

2.12.3 Additions of antibiotics, chemical inducers and substrates

Antibiotics, chemical inducers and substrates added to MS and LB media are listed in table 2.2.

Selection plates for:	Antibiotic	Concentration (µg / ml)	Vector conferring resistance	Blue-white selection
E. coli	ampicillin	100	pUC18, pBlueScript	yes
	spectinomycin	50	pER8	no
	kanamycin	100	2.12.3.1.1 pBin19	yes
A. tumefaciens	streptomycin	300	2.12.3.1.2 pER8	no
	spectinomycin	100	pER8	no
	kanamycin	100	2.12.3.1.3 pBin19	no
	rifampicin (in DMSO)	100	2.12.3.1.4 *A. tumefaciens* helper plasmid	-
A. thaliana	kanamycin	50	pBin19	-
	hygromycin	50	pER8	-
	timentin (ticarcillin / clavulanic acid 15:1)	200	- (general anti-bacterial agent)	-

Table 2.2: Antibiotics, chemical inducers and substrates

Antibiotics were added to autoclaved LB or MS agar cooled to at least ~ 50 °C. For bacterial blue-white selection plates, 476 µg/ml (2 mM) of the chemical inducer IPTG (Melford, UK) and 40 µg/ml of the substrate X-gal (Melford, UK; in DMF) were added along with the selecting antibiotic. Transformants were able to grow on antibiotic plates as the introduced plasmid conferred resistance; white bacterial

colonies indicated the presence of insert in the plasmid which disrupts the galactosidase gene, preventing conversion of X-gal substrate into its blue product.

2.13 Plant treatments and phenotypic analysis

2.13.1 Stress and inhibitor treatment of seedlings in solution

Seedlings (6 - 7 days old) were transferred from MS agar plates into H_2O and left for 2 h to 3 h (as indicated) to recover from damage caused by the transfer before further treatment. If chemical stress agents were used, 1 ml of 5 x stress solution (as indicated) was added to seedlings floating in 4 ml H_2O in wells of 6-well plates, and the plates slightly swirled to allow mixing. For inhibitor studies, seedlings were placed into 3 ml of H_2O; 1 ml of 5 x inhibitor solution (as indicated) was added and the sample left for 20 to 40 min (as indicated) before addition of 1 ml of 5 x stress solution or H_2O. For cold treatments, seedlings were floated in 5 ml H_2O in 50 ml Falcon tubes for 3 h before transfer to a water bath of the indicated temperature. 14 day old plants were carefully extracted from the MS agar and directly placed into 25 ml of H_2O_2 or H_2O in Petri dishes (diameter 8.5 cm). Unless stated otherwise, chemicals were dissolved in H_2O to the indicated concentration. Jasmonic acid was prepared by dissolving 6 µl methyl jasmonate in 25 µl ethanol before addition of 25 ml H_2O to yield a 1 mM stock solution. Seedlings were treated in 1:10 and 1:20 dilutions (100 µM and 50 µM, respectively), taking care to use separate well plates for control and treated samples (methyl jasmonate is volatile and could affect the control samples). ABA (Sigma, UK) was made up as a 100 mM stock in ethanol.

2.13.2 Infection with *P. parasitica*

Distilled H_2O was added to infected *A. thaliana* tissue with sporulating *P. parasitica* and the spores released by vortexing. The spore suspension was removed and adjusted to 5 – 6 x 10^4 spores per ml using a haemocytometer (10 squares per suspension were counted with each square holding a volume of 10^{-4} ml) (Improved Neubauer Weber, England). The suspension was sprayed onto the seedlings grown on peat plugs in several small bursts with the help of an airbrush power back (Humbrol Ltd., Hull, UK). The seedlings were placed under a transparent dome to keep humidity near 100 % and moved into a growth cabinet at 16 °C with a 8 h light/16 h dark cycle. Onset of sporulation generally occurred after 4 – 5 days.

2.14 Aequorin techniques

2.14.1 Reconstitution of apoaequorin

At all stages of protocols described below, the luminophore coelenterazine (ProLume, Woburn, MA, USA) was handled in reduced light conditions.

2.14.1.1 In vitro *reconstitution of plant extract*

In vitro reconstitution was carried out as described by Knight *et al.*, 1991. 5 seedlings per sample were harvested into liquid nitrogen and homogenised in 100 µl MO medium (10 mM Tris-HCl (pH 7.4), 0.5 M NaCl, 5 mM EDTA, 5 mM β-mercaptoethanol, 0.1 % (w/v) gelatine) (Knight *et al.*, 1991). After addition of another 400 µl of MO medium, the suspension was microfuged at ≤ 13000 rpm for 10 minutes to pellet insoluble material. 100 µM coelenterazine stock in methanol

was added to 100 µl aliquots of the supernatant to a final concentration of 1 µM. The extract was incubated in the dark for 1 – 4 h at room temperature to allow reconstitution to occur.

2.14.1.2 In vivo *reconstitution of seedlings*

Aequorin expressing seedlings or plants (RLD1.1) grown on MS agar were transferred into H_2O and coelenterazine solution (final concentration: 10 µM, 1 % methanol) was added. Reconstitution was allowed to proceed for a minimum of 16 hours at 21 °C in the dark (Knight *et al.*, 1991). 5 – 7 day old seedlings (~ 100 / well in 6-well plates) were floated on 2 ml solution whereas 14 and 21 day old plants (~ 25 / petri dish, 8.5 cm diameter) were placed into 20 ml of solution.

2.14.2 Aequorin assays using the luminometer

A digital chemiluminometer with discriminator was used (Thorn EMI electron tubes), fitted with a cooling unit for the photomultiplier tube (to approximately – 25 ºC) in order to reduce background noise (Knight *et al.*, 1996; Knight *et al.*, 1991).

2.14.2.1 *Discharge of* in vitro-*reconstituted extract*

10 µl of the reconstituted extract was added to 500 µl Tris-EDTA buffer (200 mM Tris-HCl (pH 7.0), 0.5 mM EDTA) in a clear plastic cuvette (12 mm diameter, Sarstedt Ltd., Leicester, UK (Sarstedt, UK)). After insertion of the cuvette into the chamber of the luminometer (A. J. Neuroinstruments, Abingdon, Oxon, UK), 500 µl 50 mM $CaCl_2$ was added through an injection port using a syringe. Luminescence was counted over a 10 s interval.

2.14.2.2 $[Ca^{2+}]_{cyt}$ measurements of stimulated seedlings

After aequorin reconstitution, RLD1.1 seedlings were placed individually into plastic cuvettes (Sarstedt, UK) containing 0.5 ml water. Following a resting period of 5 min or 25 - 45 min (as indicated) to recover from the touch response, the cuvettes were individually inserted into the luminometer chamber and luminescence counts were recorded at 0.1 s or 1 s intervals. After 5 s of counting, 0.5 ml of solution containing the stimulating agent was added from a syringe through a luminometer port and measurements continued over the indicated time periods. Remaining aequorin was discharged by addition of 1 ml $CaCl_2$ solution (final concentration 1 M, 10 % ethanol), and counts recorded for a further 5 min until values were within 1 % of the highest discharge value.

2.14.2.3 Calibration of data obtained using the luminometer

The luminescence counts obtained were calibrated by applying equation 2.1 which takes into account the double logarithmic relationship between the concentration of free calcium present in cells and the remaining aequorin discharged at any point in time.

$$pCa = 0.332588 (-\log k) + 5.5593 ,$$

where k = luminescence counts s^{-1}/ total luminescence counts

Equation 2.1: Calibration of aequorin luminescence counts (Fricker *et al.*, 1999)

This calibration equation was determined empirically and works on the assumption that all aequorin is discharged from all cells and all emitted light is detected.

2.14.3 $[Ca^{2+}]_{cyt}$ imaging in the CCD camera

Changes in $[Ca^{2+}]_{cyt}$ were imaged with the help of a three microchannel plate intensified CCD camera (Photek 216, Photek Ltd., Hastings, UK). Photon emissions were stored by the camera as an array of pixels and the x-y co-ordinates of the images were established by the software (IFS216 Software, Photek Ltd.). This data was used to analyse changes in $[Ca^{2+}]_{cyt}$ over time as well as in different parts of the plant.

2.14.3.1 $[Ca^{2+}]_{cyt}$ imaging on plates

Following aequorin reconstitution, 6, 7, 14 or 21 day old plants were laid onto moist filter paper (Whatman, Grade 1) placed on top of 0.8 % agar. Special care was taken that the entire length of the root was in contact with the paper. For experiments investigating signalling between different parts of the plant, the leaves or (part of) the roots were placed on top of an extra layer of parafilm with a moist square of filter paper on top to prevent drying of the plant tissue. The second filter paper was not in contact with the underlying large filter paper.

After a rest period of 30 - 45 min, the filter paper with the plants was transferred onto a 0.8 % agar plate containing 10 mM H_2O_2 or 10 µM menadione (prepared on the same day). This "stress" plate was immediately placed into a specially constructed dark box underneath the CCD camera.

2.14.3.2 $[Ca^{2+}]_{cyt}$ imaging in solution

A single reconstituted seedling (7 days old) was placed into 1 ml of H_2O (in a 6 well plate well) and left to rest for 30 min – 1 h. 0.5 ml of 30 mM H_2O_2 was added,

swirled very gently and briefly and the well plate placed underneath the CCD camera.

2.14.4 $[Ca^{2+}]_{cyt}$ signalling mutant screen

RLD1.1 seedlings (6 days old) of an EMS mutagenised population were screened on 10 mM H_2O_2 plates under the CCD camera and their Ca^{2+} signatures compared with those of non-mutagenised RLD1.1 seedlings. Mutants with altered calcium signatures were transferred onto peat plugs and grown up. Seed was collected for individual plants and seedlings of each line, reconstituted in 1 ml coelenterazine solution (10 seedlings per well in 24 well plates), were re-screened under the camera. Total aequorin levels of the remaining lines were determined by *in vitro* aequorin assays. Lines with high aequorin levels were re-screened again under the camera and by luminometry.

2.15 DNA techniques

2.15.1 Plant genomic DNA extraction

2.15.1.1 SHORTY DNA prep

All steps were carried out on ice where possible.

Approximately 100 seedlings (5 days old) grown on MS agar plates were harvested into 1.5 ml Eppendorf tubes and frozen in liquid nitrogen. After grinding the tissue using a plastic micropestle, 550 µl extraction buffer (200 mM Tris-HCl, pH 9.0, 400 mM LiCl, 25 mM EDTA, 1 % (w/v) SDS (releases protein from DNA)) and 550 µl phenol mix (Tris-HCl, pH 8/choloroform/isoamyl alcohol (25/24/1) (separates protein

and nucleic acid, with latter in the aqueous upper phase) were added to the still frozen powder and mixed by vortexing the tube for 20 s. The tubes were centrifuged for 5 min at maximum speed at 4 °C and the upper phase (~ 500 µl) removed to a tube with 550 µl phenol mix, followed by vortexing and another 5 min centrifugation. The upper phase (~ 500 µl ml) was added to 500 µl isopropyl alcohol, mixed by inversion and the DNA left to precipitate at room temperature. After a further 10 min centrifugation, the supernatant was removed and the pellet left to air-dry. The DNA was re-suspended in 500 µl TNE (0.01 M Tris-HCl, pH 8, 0.1 M NaCl, 1 mM EDTA) and treated with 20 µg RNase (Sigma, UK; stock: 10 mg/ml in 0.2 M sodium phosphate buffer, pH 6.4)) for 10 min at 37 °C. Another 550 µl phenol mix was added, the contents of the tubes mixed by inversion and centrifuged for 5 min, 4 °C at maximum speed. The supernatant (~ 475 µl) was added to 750 µl isopropyl alcohol and left to precipitate at room temperature for 20 min. After 10 min centrifugation, the supernatant was decanted and the pellet rinsed with 80 % ethanol. The wash was removed after 30 s centrifugation and the pellet left to air-dry. The DNA was re-suspended in 500 µl of 10 mM Tris-HCl, pH 8.0 by shaking for 1 h at 37 °C.

(Adapted from the protocol on the Wisconsin Knockout facility website: www.biotech.wisc.edu/NewServicesAndResearch/Arabidopsis/FindingYourPlant.asp)

2.15.1.2 Simple DNA prep

a) 8 – 10 cotyledons or 3 – 4 flower heads were collected into 1.5 ml Eppendorf tubes and frozen in liquid nitrogen. After grinding the tissue with a plastic micropestle, 500 µl extraction buffer (see section 2.15.1.1) were added, mixed and

the tubes centrifuged for 5 min at maximum speed. 0.35 ml of the supernatant was transferred to a tube containing 350 µl isopropanol, mixed by inversion and centrifuged for 10 min. Subsequently, the supernatant was removed and the pellet left to air-dry. The DNA was re-suspended in 400 µl of 10 mM Tris-HCl, pH 8.0 by shaking for 1 h at room temperature.

(Adapted from the protocol on the Wisconsin Knockout facility website: www.biotech.wisc.edu/NewServicesAndResearch/Arabidopsis/FindingYourPlant.asp)

b) All steps of the protocol were carried out at room temperature unless stated otherwise. Approximately 20 seedlings (7 days old) were collected into a 1.5 ml Eppendorf tube, frozen in liquid nitrogen and ground to powder with a plastic micropestle. 200 µl of Edwards extraction buffer (200 mM Tris-HCl, pH 7.5, 250 ml NaCl, 25 mM EDTA, pH 8.0, 0.5 % SDS) were added to the frozen powder and the tube vortexed. After a 1 min centrifugation at maximum speed, 150 µl of the supernatant were added to 150 µl of isopropanol, mixed by inversion and left at room temperature for 2 min to allow the DNA to precipitate. The tubes were centrifuged for another 5 min, the supernatant was removed and the pellet left to air-dry. The DNA was re-suspended in 50 µl of 10 mM Tris-HCl, pH 8.0.

(Adapted from Goodman's modification of the Edwards method)

2.15.1.3 Dellaporta method

Approximately 200 seedlings were collected into 1.5 ml Eppendorf tubes and frozen in liquid nitrogen. After grinding the frozen tissue to powder, 750 µl of extraction buffer (100 mM Tris-HCl, pH 8.0, 50 mM EDTA, 500 mM NaCl, 10 mM β-

mercaptoethanol) and 100 µl of 10 % SDS were added. The tubes were incubated for 20 min at 65 °C followed by a 5 min centrifugation. 250 µl KAc (5 M) were added and the extract incubated for 10 min on ice. After 10 min centrifugation, 600 µl of isopropanol were added and the tubes left at – 70 °C for 10 min. Following another 10 min spin, the supernatant was removed and the pellet was dissolved in 700 µl 1 x TE buffer (10 mM Tris-HCl, pH 8.0, 1 mM EDTA). 75 µl of 3 M NaAc and 500 µl isopropanol were added and the tubes left for 10 min at room temperature. After a 10 min centrifugation, the supernatant was removed, the pellet washed in 80 % ethanol and left to air-dry. The DNA was re-suspended in 50 µl TE buffer by incubation at 65 °C (10 min).

2.15.2 DNA separation by electrophoresis and DNA gel extraction

2.15.2.1 DNA size separation by agarose gel electrophoresis

1 % (w/v) electrophoresis grade agarose was melted by heating in 0.5 x TBE (45 mM Tris-boreate, pH 8.0, 1 mM EDTA). After cooling to approximately 50 °C, ethidium bromide was added to a final concentration of 5 µg/ml and the molten gel poured into the gel tank. 0.5 x TBE was used as the running buffer.

DNA solutions were loaded in 1 x loading buffer (0.25 % (w/v) bromophenol blue, 0.25 % (w/v) xylene cyanole FF, 40 % (w/v) sucrose). The gel was electrophoresed to satisfactory resolution at 30 – 40 mAmp with voltage non-limiting. Nucleic acid bands were visualised on a UV-transillumintor (wavelength 254 nm) (UVP Laboratory Products, Upland, CA, USA). Fragment size was approximated by comparing positions with molecular size standards run on the same gel (1 kb ladder or 100 bp ladder, NEB, UK) whereas the quantity of DNA was estimated by

comparing fluorescence intensities with bands of the DNA low mass ladder (GibcoBRL, UK).

2.15.2.2 DNA separation by polyacrylamide gel electrophoresis

Electrophoresis of DNA fragments through polyacrylamide gels allows a higher resolution of bands than agarose gel electrophoresis due to the smaller pore size. 40 ml of gel mix (8 ml of 30 % acrylamide:bisacrylamide mixture (BioRad, Hercules, CA, USA(BioRad, USA)) in 1 x TBE) was prepared, 200 µl of 10 % (w/v) ammonium persulphate and 70 µl TEMED added to start polymerisation and the mix poured between 20 x 15 cm glass plates separated by 0.75 mm spacers. The resulting 6.67 % polyacrylamide gel was loaded with PCR product containing 1 x DNA sample buffer and run at 150 V, Amps not limiting, until the bromophenol blue dye had just run off the end. Subsequently, the gel was incubated in SYBR Green I solution (1:10,000 dilution in 1 x TBE ; 10,000 x stock in DMSO, Molecular Probes, Eugene, OR, USA) on a shaker for 1 h. Bands were visualised on the UV-transilluminator (UVP, USA)

2.15.2.3 Extraction of DNA from agarose gels

Gel slices containing the DNA of interest were cut from the agarose gel on a UV-transilluminator (UVP, USA) with a sharp razor blade. Elution was performed with the help of gel extraction kits (QIAquick or Qiagen MinElute gel extraction kit, Qiagen, Crawley, UK) according to the manufacturer's instructions. In short, the gel slice was melted in buffer containing guanidium salt and isopropanol added (this provides chaotropic salts, adjusts the pH and depletes the nucleic acid hydration

shell to allow binding of the DNA to the column). The solution was applied to a spin column containing a silica-gel membrane (anion-exchange column). After spinning, the DNA bound to the membrane was washed with buffer PE (containing ethanol) and eluted with water or 10 mM Tris-HCl, pH 8.5 (elution occurs at basic pH and low salt buffer). The quantity of DNA recovered was estimated as described in section 2.15.6.

2.15.2.4 Elution of DNA from the polyacrylamide gel

The band of interest was cut out with a sharp razor blade on the transilluminator, chopped up inside an Eppendorf tube and eluted by shaking overnight in elution buffer (0.5 M ammonium acetate, 10 mM magnesium acetate, 1 mM EDTA, pH 8, 0.1 % SDS). Subsequently, the tube was spun at 4 °C for 1 min (at 13000 rpm), the supernatant removed into a fresh tube and 2 volumes of ethanol added. After leaving the sample at –20 °C for 10 minutes, the tube was spun for 10 min at 13000 rpm, 4 °C. The pellet was washed in 70 % ethanol, spun again for 5 minutes and then air-dried before re-suspension in 20 µl TE buffer (10 mM Tris-HCl, 1 mM EDTA, pH 8).

2.15.3 Ethanol precipitation

DNA samples in solution were precipitated by addition of sodium acetate (final concentration 0.3 M, pH 5.2) and 2.5 volumes of 100 % ethanol and incubation at room temperature for 15 min (ethanol depletes the hydration shell and exposes negatively charged phosphate groups which are bound by the added counter-ion (here Na^+). This reduces the repulsive forces between the polynucleotide chains so

that a precipitate can form (Sambrook and Russell, 2001). The DNA was pelleted by centrifugation (20 min, 14000 rpm, ≥ 16 °C to prevent salt co-precipitation). The pellet was washed with 70 % ethanol, air-dried and re-suspended in 10 mM Tris-HCl, pH 8.5.

2.15.4 Digestion of DNA with restriction enzymes

All restriction enzymes were from NEB, UK. DNA digestion with restriction enzymes was carried out according to the manufacturer's instructions, using the recommended 1 x salt buffer (NEB buffers, supplied with the enzyme) with bovine serum albumin (100 µg/ml). A volume containing 5 – 10 units of enzyme was used in each digest and constituted ≤ 10 % of the total volume. Digests were incubated at 37 °C for 1 – 2 h. For digests with enzymes that require different buffers, digestions were performed sequentially: the enzyme with the lower salt buffer was added first and incubated. Subsequently, buffer conditions were adjusted and the second enzyme was added followed by a second incubation.

2.15.5 Amplification of DNA fragments by PCR

2.15.5.1 DNA polymerases

Table 2.3 gives details of reaction mixes used for different DNA polymerases.

DNA polymerase	Final volume (µl)	PCR buffer	$MgCl_2$ (mM)	dNTP mix (mM each)	Enzyme (units)	Special treatment
Taq (GibcoBRL, UK)	50	20 mM Tris-HCl, pH 8.4 50 mM KCl	1.5	0.2	2.5	
BioTaq (Bioline)	50	16 mM $(NH_4)_2SO_4$ 67 mM Tris-HCl, pH 8.8, 0.01 % Tween-20	1.5	0.2	2.5	
Immolase (Bioline)	50	16 mM $(NH_4)_2SO_4$ 67 mM Tris-HCl, pH 8.8, 0.01 % Tween-20	1.5	0.2	2.5	pre-incubation at 95 °C for 7 min (heat-activated enzyme)
TaKaRa ExTaq (TaKaRa)	100	not specified	2	0.4 (supplied with TaKaRa dNTP mix)	2.5	PCR conditions: 96 °C for 5 min, then addition of enzyme, then 94 °C for 15 s 65 °C for 30 s 72 °C for 2 min for 36 cycles, then 72 °C for 4 min, primers were used at 0.12 µM
TaKaRa Pyrobest (TaKaRa)	100	not specified	in buffer	0.4 (supplied with TaKaRa dNTP mix)	2.5	PCR conditions: 98 °C for 10 s 55 °C - 60 °C for 30 s 72 °C for 1 min for 30 cycles

Table 2.3: PCR conditions used for different DNA polymerases.
Mg^{2+} ions form soluble complexes with dNTPs and template DNA to produce the actual substrate that the polymerase recognises.

2.15.5.2 Oligonucleotide primers

Primers were designed to consist of at least 40 % G and C bases. If a restriction site sequence was present, a 4 bp G and C 'clamp' was added at the 5' end which aids recognition of the target sequence by the restriction enzyme. All primers were used at a final concentration of 2 µM unless stated otherwise. For standard PCR reactions, 20 bp oligonucleotides were used. Primers were checked through a

BLAST search (www.arabidopsis.org/blast/) to ensure that they were unique to the sequence to be amplified.

2.15.5.3 DNA Template

Approximately 0.1 - 1 ng of plasmid or PCR product served as template in all reactions unless stated otherwise; if product was amplified from cDNA, 10 µl of a 1:10 dilution for rare cDNA (*e.g.* kinases) and 1:50 or 1:100 for abundant cDNA templates was added.

2.15.5.4 PCR programs

The reaction mixes were either overlaid with 50 µl wax (Chill-out 14 liquid wax, MJ Research Inc., Waltham, MA, USA) to prevent evaporation during the PCR cycles or a thermal cycler with heated lid was used. The PCR block was pre-heated to 95 °C before insertion of the PCR tubes.

Unless otherwise specified in table 2.3, the PCR machine was programmed to hold each temperature for 5 min in the first cycle (to allow complete denaturation of the template) followed by 25 – 35 cycles of 1 min at 95 °C for denaturation, 1 min/kb at 55 - 62 °C for annealing and 1 min at 72 °C for extension. After the specified number of cycles had been completed, the samples were left for 10 minutes at 72 °C to complete the final extension cycle. The annealing temperature was optimised empirically but originally chosen on the basis of the melting temperature of the primers, which was calculated using equation 2.2:

T_m = [2 °C x (number of A and T bases)] + [4 °C x (number of C and G bases)]

Equation 2.2: Calculation of T_m values for oligonucleotide primers

Primers were designed with similar T_m values and the annealing temperature was chosen to lie 5 to 10 °C lower than their melting temperature.

In RT-PCR experiments, each cDNA sample was amplified in duplicate or triplicate.

2.15.6 Quantification of DNA

DNA was quantified either by electrophoresis of a known volume of DNA and comparison of ethidium bromide fluorescence intensity with that of a known amount of mass ladder (GibcoBRL, UK) or by spectrophotometry (UNICAM 5625, Rochester, NY, USA) of a known dilution of DNA in water at a wavelength of 280 nm (50 µg/ml double-stranded DNA yield an absorption reading of 1).

2.15.7 Sequencing

Sequencing templates were either plasmids or PCR products. The sequencing reaction mix (20 µl final volume) was composed of template (250 ng or closest), 4 µl 2.5 x sequencing buffer (200 mM Tris-HCl, pH 9, 5 mM $MgCl_2$), 4 µl BigDye mix (enzyme, nucleotides) and 200 nM primer. The reaction mix was placed into the PCR machine and heated for 1 minute at 96 °C before undergoing 25 cycles of 30 seconds at 96 °C, 15 seconds at 50 °C and 4 minutes at 60 °C. The reaction product was ethanol precipitated and air-dried before sequencing was carried out in an automated sequencer (Applied Biosystems automatic capillary action) housed in the Department of Plant Sciences, University of Oxford.

2.15.8 Southern analysis (from PCR product)

PCR product was electrophoresed on a TBE agarose gel (1 %) (see section 2.15.2.2).

2.15.8.1 Denaturation of DNA

DNA was denatured by incubating the agarose gel for 45 min at room temperature in denaturation solution (1.5 M NaCl, 0.5 M NaOH, gently shaking). After several rinses in deionised H_2O, the gel was neutralised for 45 min in neutralisation solution (1 M Tris-HCl, pH 7.4, 1.5 M NaCl), and transferred to fresh neutralisation solution after 30 min.

2.15.8.2 Transfer of DNA from gel onto nylon membrane

The DNA was transferred onto a positively charged nylon membrane (Roche Diagnostics GmbH, Mannheim, Germany (Roche, Germany)) by capillary action. The DNA gel was placed on top of a glass plate covered by 3M paper in contact with a reservoir of 10 x SSC (1.5 M NaCl, 0.15 M Na citrate, pH 7). Positively charged nylon membrane (pre-wet in water and 1 x SSC) was laid onto the gel and any air bubbles expelled by rolling a glass rod over the surface. 2 sheets of 3M paper (pre-wet in 1 x SSC), a layer of paper tissues, a glass plate and a weight were placed (in this order) on top of the membrane. The following morning, the membrane was rinsed for 5 min in 6 x SSC (to remove any agarose), air-dried for 30 min and the blotted DNA fixed to the membrane by UV-crosslinking (on auto-crosslink setting, 254 nm, Stratalinker, Stratagene, USA).

DNA probe synthesis and hybridisation of labelled probe to the membrane was carried out as described in sections 2.19.3.2 and 2.19.3.3.

2.16 Cloning of DNA fragments

2.16.1 Gap-fill synthesis

PCR reactions with regular Taq polymerase enzyme often result in incomplete filling at the termini and thus sticky ends. In order to fill in these gaps, 2.5 units (1 µl) of *Pfu* DNA polymerase (Stratagene, USA) and 1 µl dNTP mix (10 mM) were added directly to the PCR solution. The mixture was incubated in a PCR block for 30 min at 72 ° and the fragment purified by agarose gel electrophoresis and gel extraction before further treatment.

2.16.2 Cloning by blunt-ended ligation (pUC18 plasmid)

2.16.2.1 Phosphorylation of the insert

pUC18 vector was obtained (AmershamPharmacia, UK) in an unphosphorylated, linearised form to prevent re-circularisation. In order to allow ligation of the insert into the plasmid, approximately 200 ng of fragment was phosphorylated by treatment with 10 units (1 µl) of T4 polynucleotide kinase (NEB, UK) in 1 x ligase buffer (50 mM Tris-HCl, pH 7.5, 10 mM $MgCl_2$, 10 mM DTT, 1 mM ATP, 25 µg/µl BSA). The mixture was incubated in a PCR block for 45 min at 37 °C followed by 20 min at 65 °C to inactivate the enzyme.

2.16.2.2 Ligation

The amounts of insert and vector to be used in the ligation reaction were calculated according to equation 2.3. (The concentration of pUC 18 was 0.1 µg/µl.)

$$3 \times \text{amount of vector (ng)} \times \frac{\text{size of insert (bp)}}{\text{size of vector (bp)}} = \text{amount of insert (ng)}$$

Equation 2.3

Insert and plasmid DNA were incubated overnight at 14 °C with 200 units (1 µl) of T4 DNA ligase (NEB, UK) in 1 x ligase buffer (see section 2.16.2.1, adjusted for new volume) and in 1 mM freshly added ATP (NEB, UK). Generally, the total reaction volume was 10 µl. The enzyme was inactivated the following day by a 10 min incubation at 65 °C. A control ligation without insert was carried out alongside.

2.16.3 Cloning by sticky-end ligation (into BlueScript, pBin19 and pER8)

2.16.3.1 Dephosphorylation of vector DNA

Vectors restricted with a single enzyme (and thus able to re-circularise) were treated with bacterial alkaline phosphatase (BAP, GibcoBRL, UK) after digestion. This enzyme hydrolyses 3' and 5' phosphates from DNA, thus preventing ligation of complementary termini of the vector without insert. 75 units (0.5 µl) of BAP were added to 100 µl of DNA solution in 1 x dephosphorylation buffer (10 mM Tris-HCl, pH 8.0). The mixture was incubated at 65 °C for 60 min. To stop enzyme activity, 1 µl of 0.5 M EDTA, pH 8.0 were added followed by a 10 min incubation at 50 °C. The DNA was purified by electrophoresis and gel extraction prior to further treatment.

If vectors were cut with more than one enzyme yielding incompatible termini, dephosphorylation was unnecessary and DNA was used directly after purification from the restriction digest.

2.16.3.2 Ligation

The amounts of insert and vector to be used were calculated and the reaction mix set up as described in section 2.16.3.1, except that fresh ligase buffer was used making separate addition of ATP unnecessary.

2.16.4 Bacterial plasmid DNA purification

Plasmid DNA isolation was carried out according to the instructions of the HYBAID RECOVERY Quick Mini Spin Kit Protocol (ThermoHybaid, Ashford, UK) or Qiaprep Miniprep Handbook (for small amounts, *i.e.* mini-preps) or the Qiagen maxi-prep kit (for larger amounts, *i.e.* maxi-preps) (Qiagen, UK).

2.16.4.1 Plasmid mini-preps

Cells from 1.5 – 5 ml of liquid culture were harvested by centrifugation at 13000 rpm for 1 min. The pellet was resuspended in the recommended volume of resuspension medium (50 mM Tris-HCl pH 7.5 – 8.0, 10 mM EDTA, 100 µg/ml RNase A). The recommended volume of alkaline lysis buffer (200 mM NaOH, (denatures chromosomal DNA, plasmid DNA and proteins) and 1 % (w/v) SDS (solubilises the cell membrane)), was added and the solution left to stand for < 5 min to release plasmid DNA from the cell without release of cell-wall-bound chromosomal DNA. The lysate was subsequently neutralised with neutralisation buffer (potassium

acetate and guanidium hydrochloride (which also removes nucleic acid binding proteins and disrupts non-specific interactions)) leading to trapping of denatured proteins, chromosomal DNA and cellular debris in salt-detergent complexes (the plasmid DNA, smaller and covalently closed, renatures under these condition and remains in solution) and cleared by centrifugation. The supernatant was subsequently applied to a spin column containing a silica membrane and the column was washed with wash solution (containing ethanol). Plasmid DNA was eluted from the column with elution buffer (10 mM Tris-HCl, pH 8) pre-heated to 70 °C.

2.16.4.2 Plasmid maxi-preps

If not detailed, see section 2.16.4.1 for buffer compositions.

Cells from 100 ml of culture solution were harvested by centrifugation at 6000 g for 15 min at 4 °C). Cells were re-suspended in 10 ml re-suspension buffer. After addition of 10 ml lysis buffer, the mixture was left to incubate for up to 5 min at room temperature. The lysate was neutralised by addition of 10 ml cold neutralisation buffer (3.0 M KAc, pH 5.5) and the mixture incubated on ice for 20 min. The lysate was incubated for 10 min in a QIAfilter cartridge which causes the precipitate to float to the top of the solution and subsequently cleared by filtration. The filtrate was run into a silica-resin containing column (anion-exchange). After washing the column twice with 30 ml wash buffer (buffer QC: 1.0 M NaCl, 50 mM MOPS, pH 7.0, 15 % (v/v) isopropanol), plasmid DNA was eluted in 15 ml elution buffer (buffer QF: 1.25 M NaCl, 50 mM Tris-HCl, pH 8.5, 15 % (v/v) isopropanol). To remove salt from the plasmid solution, the DNA was precipitated by addition of 0.7 volumes of

isopropanol and pelleted by centrifugation at ≥ 15,000 rpm at 4 °C. The pellet was washed twice in 70 % ethanol, air-dried and re-dissolved in 10 mM Tris-HCl, pH 8.5.

2.17 Cloning into bacterial cells

2.17.1 Preparation of competent cells

2.17.1.1 Preparation of competent E. coli *DH5α*

100 ml of LB broth were inoculated with 1 ml *E. coli* DH5α liquid overnight culture and incubated shaking at 37 °C until an OD_{600} of 0.2 to 0.3 was reached (approximately 1.5 h). At this point, cells were harvested by 5 min centrifugation at 3500 *g*, 4 °C and re-suspended in 50 ml ice cold $CaCl_2$ (100 mM). The suspension was left on ice for 20 min and harvested by 5 min centrifugation at 3500 *g*, 4 °C. Cells were re-suspended in 10 ml $CaCl_2$ (0.1 M) and 2 ml glycerol (4 °C) was added (final concentration: 17 % (v/v)). 200 µl of cells were aliquoted into chilled tubes and frozen in liquid nitrogen before storage in the - 80 °C freezer.

2.17.1.2 Preparation of competent A. tumefaciens *C58C1*

50 ml of LB broth was inoculated with 4 ml *A. tumefaciens* C58C1 overnight culture and incubated shaking at 28 °C until the culture reached an OD_{600} of 0.5 to 1.0 (approximately 4 to 6 h). Cells were harvested by 5 min centrifugation at 3000 *g*, 4 °C and re-suspended in 2 ml of ice-cold $CaCl_2$ (20 mM). 100 µl of cells were aliquoted into chilled tubes and frozen in liquied nitrogen before storage in the - 80 °C freezer.

2.17.2 Transformation of competent bacterial cells

2.17.2.1 Transformation of E. coli *strains*

A 200 µl aliquot of competent cells was thawed on ice for 45 min before addition of 1 - 10 ng of DNA in a volume not exceeding 10 % of the total reaction volume. After a further 15 – 30 min on ice, the cells were heat shocked at 42 °C for 2 min and 1 ml of LB was added. The tube was gently shaken at 37 °C for 1 h before 100 µl or 200 µl of cells were plated out on LB plates containing the appropriate antibiotics. Cells were incubated at 37 °C until visible colonies appeared.

2.17.2.2 Transformation of A. tumefaciens *strains*

A 100 µl aliquot of frozen competent cells was thawed on ice. Approximately 1 µg of DNA was added (in a volume ≤ 12 µl) and the cells heat shocked for 5 min at 37 °C. After addition of 1 ml LB, the tubes were shaken gently at 27 °C for 2 to 4 h. Subsequently, the cells were pelleted by centrifugation, all but ~ 200 µl were removed, the pellet re-suspended in the remaining supernatant and the suspension plated out onto a LB plate containing rifampicin (100 µg/ml), to inhibit growth of bacteria other than *A. tumefaciens*, and other appropriate antibiotics for transformant selection. Cells were incubated at 28 °C until visible colonies appeared (generally 2 days).

2.18 Isolation of the *ox1* knock-out mutant line

Largely, the protocol given by the Arabidopsis Knock-out Facility on http://www.biotech.wisc.edu/NewServicesAndResearch/Arabidopsis/Guidelines.asp was followed and proceedings are also detailed in Appendix A, section A.1.

Suitable primers 2150 bp upstream (5') and 1160 bp downstream (3') of the predicted *OX1* start and stop codon, respectively, were designed and tested for suitability by comparison with a standard control reaction using primers Con-1A and Con1-B (specified by the protocol, all PCR reactions with TaKaRa ExTaq polymerase). After the first round PCR reactions were received from the Knock-out facility, the product was electrophoresed on 1 % agarose gels and a Southern blot was performed (see section 2.15.8). DNA in pools with a signal was amplified by PCR using the nested T-DNA border primer JL270 and the *OX1* knock-out forward or reverse primer. The product was purified and sequenced using JL270 as primer. In round 2 of the screen, PCR products were again electrophoresed and positives subjected to PCR amplification followed by sequencing. For round 3, approximately 100 seeds per seed pool were sown onto MS agar plates, seedlings were grown for 7 days before harvesting, and genomic DNA was extracted (Shorty method, see section 2.15.1.1). Seed pools containing the insertion were identified by PCR as above. The seed pool containing the insertion was sown out again and seedlings transferred to peat plugs. After emergence of the fourth leaf, 8 – 9 cotyledons from plants in one row (one cotyledon/plant) were harvested and DNA extracted (simple DNA extraction method, see section 2.15.1.2). Again, plant rows containing plants with the insertion were identified by PCR. The identity of the PCR product was verified by restriction enzyme digestion (*NdeI*, single cut). Flower buds of single plants in the two positive rows were collected, DNA extracted (simple DNA extraction method) and PCR performed. The three plants with the insertion were grown up to seed and harvested separately. Seed was bulked for further experiments.

2.19 Ribonucleic acid techniques

2.19.1 RNA extraction

2.19.1.1 RNA mini-preps

50 to 100 seven day old seedlings or 16 to 20 small leaves were collected into a 1.5 ml Eppendorf tube and frozen in liquid nitrogen. If the seedlings had been treated in solution, the sample was blotted dry on tissue paper before freezing.

RNA was extracted using the RNeasy Plant Total RNA kit (Qiagen, UK) according to the manufacturer's protocol. Frozen tubes containing the samples were placed into a metal block at –80 °C and tissue ground up with sterile micropestles. 450 µl of buffer RLT supplemented with β-mercaptoethanol (10 µl/ml) was added and the solution vortexed. After a 2 min incubation at 56 °C to break up the tissue, the solution was homogenised in a QiaShredder spin column. The flow-through was mixed with 0.5 volumes (225 µl) ethanol (100 %) and applied to the RNeasy mini spin column containing an RNA binding membrane. The membrane was washed once with buffer RW1 and twice with buffer RPE (containing ethanol) before elution of the RNA in 50 µl RNase-free H_2O.

2.19.1.2 cDNA synthesis

2.5 µg RNA were suspended with 0.5 µg oligo-$(dT)_{12-18}$ (GibcoBRL, UK, 500 µg /ml) in a final volume of 12 µl, denatured for 10 min at 70 °C and immediately transferred to ice to allow annealing of the oligo-$(dT)_{12-18}$ to the poly-A tail of the RNA. The following were added to the reaction mix: 4 µl of 5 x first strand buffer (250 mM Tris-HCl, pH 8.3, 375 mM KCl, 15 mM $MgCl_2$), 2 µl of 100 mM DTT, 1 µl of 10 mM RNase-free dNTPs and 1 µl superscript II enzyme (200 U/µl, GibcoBRL, UK). This

reaction mixture was incubated at 42 °C for 50 minutes to allow cDNA synthesis followed by 15 minutes at 72 °C to inactivate the enzyme. For differential display analysis, each sample was produced in triplicate.

2.19.1.3 DNAse treatment of RNA samples

RNA was incubated for 15 min at 25 °C with RNase-free DNase (GibcoBRL, UK) at a concentration of 1 unit/µg RNA in 1 x DNase reaction buffer (20 mM Tris-HCl; pH 8.4, 2 mM $MgCl_2$, 50 mM KCl). The enzyme was inactivated by addition of EDTA (final concentration: 2.5 mM) and heating to 65 °C for 10 min. The treated RNA was directly used for cDNA synthesis and RT-PCR analysis.

2.19.1.4 RNA quantification

The optical density at 260 nm of a 1:50 or 1:100 dilution of the RNA samples was recorded in a UNICAM 5625 UV/VIS spectrophotometer in order to determine the RNA concentration (OD_{260} 1 = 40 µg RNA/ml).

2.19.2 RNA separation by agarose gel electrophoresis

2.19.2.1 RNA sample preparation for gel loading

A volume of RNA solution containing 10 µg was dessicated under vacuum (in a speed vac) and re-suspended in 5 µl RNase-free water and 15 µl of RNA sample loading buffer (62.5 % (v/v) deionised formamide, 1.14 M formaldehyde, 1.25 x MOPS (0.025 M), 200 µg/ml xylene cyanole, 200 µg/ml bromophenol blue, 50 µg/ml ethidium bromide). Immediately prior to loading, the RNA samples were denatured for 10 min at 65 °C and placed on ice.

2.19.2.2 Agarose gel electrophoresis

RNA samples were fractionated on a gel containing 1 % (w/v) electrophoresis grade agarose, 0.6 % (v/v) formaldehyde (2.2 M) and 1x MOPS buffer (20 mM MOPS, 5 mM NaAc, 1 mM EDTA, pH 7.0) in a total volume of 150 ml. The loaded gel was run at approximately 65 mAmp, volts not limiting, until satisfactory resolution had occurred. The running buffer was composed of 0.6 % (v/v) formaldehyde (2.2 M) and 1 x MOPS buffer. After satisfactory separation, the gel was imaged and recorded on the UV-transilluminator (UVP, USA).

2.19.3 Northern analysis

2.19.3.1 Transfer of RNA from gel onto nylon membrane

The RNA was transferred onto a positively charged nylon membrane (Roche, Germany) by capillary action. The RNA gel was placed on top of a glass plate covered by 3M paper in contact with a reservoir of 20 x SSC (3 M NaCl, 0.3 M Na citrate, pH 7). Positively charged nylon membrane (pre-wet in water and 1 x SSC) was laid onto the gel and any air bubbles expelled by rolling a glass rod over the surface. 2 sheets of 3M paper (pre-wet in 1 x SSC), a layer of paper tissues, a glass plate and a weight were placed (in this order) on top of the membrane. The following morning, the blotted RNA was fixed to the membrane by UV-crosslinking (auto-crosslink setting, 254 nm, Stratalinker, Stratagene, USA).

2.19.3.2 DNA probe synthesis

DNA-probes for Northern analysis were obtained by two different approaches: through PCR amplification from cDNA by specific primers (Table 2.1) or through

digestion of an insert-containing plasmid isolated from *E. coli.* 50 ng or 25 ng (for two probes) of purified probe in a volume of 47.5 µl were denatured for 5 min at 95 °C and placed on ice. The chilled solution was added to a *Ready To Go* DNA labelling bead (AmershamPharmacia, UK) which, when re-suspended, contains a buffered aqueous solution of dATP, dGTP, dTTP, random nonamer and Klenow large fragment polymerase. 2.5 µl (25 µCi) of [α-^{32}P]dCTP (AmershamPharmacia, UK) was added and the tube incubated for 30 min to 1 h in a 37 °C waterbath to let probe synthesis proceed. Unincorporated nucleotides were subsequently removed by spinning the solution for 2 min at 3000 *g* through a in a ProbeQuant G-50 Microspin column (AmershamPharmacia, UK) (size exclusion chromatography). The eluted labelled probe was denatured by a 5 min incubation at 95 °C, chilled on ice, and added to the hybridisation buffer (see section 2.19.3.3).

2.19.3.3 Hybridisation of ^{32}P-labelled DNA probe to RNA blots

Pre-hybridisation solution containing 50 % (v/v) formamide, 5 x SSC, 0.5 % SDS, 5 x Denhardt's reagent (final concentrations: 0.1 % Ficoll; 0.1 % polyvinylpyrrolidone (PVP); 0.1 % bovine serum albumin, filter sterilised), and 100 µg/ml denatured salmon sperm DNA (Sigma, UK) was heated to 42 °C and added to the membrane in a hybridisation bottle (ThermoHybaid, UK). After a minimum of 2 hours incubation in a mini rotary hybridisation oven (ThermoHybaid, UK) at 42 °C, the radioactively labelled probe (section 2.19.3.2) was added to the solution. The bottle was placed back into the oven for overnight incubation. The following day, the membrane was washed twice for 15 minutes at 42 °C in each 2 x SSC, 1 x SSC and 0.1 x SSC (all

wash solutions contained 0.1 % SDS and were pre-heated to 42 °C). Subsequently, the blot was wrapped in cling film.

2.19.3.4 Detection of hybridisation and normalisation of gene induction data

The wrapped blots were placed for approximately 24 hours onto a GS-505 sample exposure platform (BioRad, USA) together with a Molecular Imager Imaging Screen-BI (BioRad, USA) which had previously been erased using a GS-505 Screen Eraser (BioRad, USA). The imaging screen contains a microscopic storage phosphor layer which is sensitive to radiation emissions from isotopic decay (by transfer of electrons between the embedded elements cerium and samarium). After exposure, the latent image was recovered by scanning the screen with an infrared laser scanning system (GS-525 Molecular Imager System (BioRad, USA)). As the laser illuminates the screen surface, the transferred electrons move back to cerium. This is coupled to the emission of photons which are counted by a photomultiplier tube. The signal is recorded as a digitised image in the host computer and can be quantified by processing the image with the Molecular Analyst software (BioRad, USA). In order to normalise induction data for differences in RNA loading, counts obtained for each band were normalised by calculating the gene-of-interest/β-tubulin ratio (on the assumption that β-tubulin mRNA levels remained constant during the course of the experiment).

To obtain images of higher resolution in addition to the phosphorimager scan, the blot was transferred onto a sheet of Biomax ML film (Kodak) inside an autoradiography cassette with intensifying screens. After 2 h to 14 days (one ½ life

of ^{32}P) at –80 °C, depending on the strength of the signal, the film was developed using an X-OMAT.

2.19.3.5 Removing radioactive probe from the RNA membrane

Before re-probing with other DNA probes, blots were stripped of the labelled probe by briefly washing them in water before incubation for 1 hour at 68 °C in 50 % (v/v) formamide, 50 mM Tris-HCl (pH 8), and 1 % (w/v) SDS (total volume: 50 ml). Finally, the membranes were rinsed in 2 x SSC and tested for residual radioactive signal in the phosphorimager.

2.20 Transformation of plants

2.20.1 *A. tumefaciens*-mediated transformation of *A. thaliana* by floral dip

The protocol described in Clough and Bent, 1998 (Clough and Bent, 1998) was followed. *A. thaliana* plants were grown on soil and their primary flowering bolt was clipped, causing numerous secondary flowering stems to emerge. An overnight culture of *A. tumefaciens* C58C1 cells transformed with a binary vector carrying the transgene of interest was used to inoculate a flask of LB (1/100 dilution) with the appropriate antibiotics. The culture was grown to a density of OD_{600} of 0.8 – 1.2 and harvested by centrifugation at 4800 rpm at room temperature. Cells were re-suspended in the same volume of dipping medium (5 % (w/v) sucrose, 0.05 % (v/v) Silwet L-77). The aerial parts of *A. thaliana* plants 7 – 10 days after clipping of the primary bolts were completely submerged in the cell suspension for ~ 5 s. Subsequently, the plants were laid sideways onto a tray with moistened paper towel, covered in plastic wrap to maintain high humidity and returned to the growth cabinet

for ~ 24 h. They were then uncovered, placed in an upright position and left to set seed.

2.20.2 Selection of *A. thaliana* primary transformants

Seed harvested from dipped *A. thaliana* plants was bleach sterilised (see section 2.11.2.2) and plated out on MS agar supplemented with 200 µg/ml timentin and antibiotics selecting for the presence of the vector (see section 2.12.3, Table 2.2). Plants displaying a resistant phenotype (non-bleaching on kanamycin; vigorous growth on hygromycin) were rescued, transferred to peat plugs and grown to maturity.

2.21 GUS assays

2.21.1 in vitro

The GUS-Light kit for chemiluminescent detection of GUS reporter gene activity in cell extracts (Tropix, Inc.; Bedford, MA, USA) was used for all *in vitro* assays. All solutions were supplied with the kit.

Twenty 7 day old seedlings per sample were frozen following treatment and ground up in 150 µl lysis buffer (50 mM $NaPO_4$, pH 7; 10 mM EDTA, 0.1 % sodium lauyrl sarcosine, 0.1 % Triton X-100, 10 mM β-mercaptoethanol). Homogenates were centrifuged for 2 min at maximum speed and the supernatant transferred into a fresh tube. 5 µl of this GUS extract was mixed with 15 µl lysis buffer, placed into a luminometer cuvette and 180 µl GUS reaction buffer (1 % glucuron chemiluminescent substrate, 0.1 M $NaPO_4$, pH 7.0; 10 mM EDTA) was added. The

solution was allowed to incubate for exactly 60 min at room temperature to allow processing of the substrate by GUS enzyme present in the extract. The cuvette was subsequently placed into the luminometer and 300 µl light emission accelerator was injected through the injection port. Luminescence was counted immediately in 5 s intervals and the second interval measured was recorded.

2.21.2 in vivo

Seedlings were stained for GUS activity by submersion in staining solution (50 mM $NaPO_4$, pH 7.2; 0.5 mM $K_3Fe(CN)_6$; 0.5 mM $K_4Fe(CN)_6$; 10 mM EDTA; 0.01 % (v/v) Triton; 2 mM X-gluc substrate (Melford, UK) in DMF (stock solution: 100 mM) and vacuum infiltration to 400 mmHg for 3 min. Samples were incubated at 37 °C until the desired staining intensity was reached (generally overnight) and de-stained in 80 % ethanol. Seedlings were mounted on microscope slides in 50 % glycerol and images taken with a Nikon Coolpix 990 digital camera mounted on a Leica DM R microscope.

3. Calcium signalling in response to AOS treatment

3.1. Introduction

Ca^{2+} elevations in response to AOS treatment have been reported in a number of different systems. For example, H_2O_2 treatment of mammalian smooth muscle cells results in a rise in $[Ca^{2+}]_{cyt}$ (Suzuki *et al.*, 1997). In *Commelina communis* guard cells, low concentrations of superoxide, generated by application of methyl viologen, and H_2O_2 triggered rapid increases in $[Ca^{2+}]_{cyt}$, as measured by changes in Fura-2 fluorescence (McAinsh *et al.*, 1996). The rise in $[Ca^{2+}]_{cyt}$ as well as ensuing stomatal closure were inhibited by the Ca^{2+} ion chelator EGTA, indicating that external Ca^{2+} is required for the Ca^{2+} signature and downstream response. H_2O_2 challenge of whole tobacco seedlings expressing recombinant aequorin resulted in a rapid, transient elevation of $[Ca^{2+}]_{cyt}$ which was inhibited by lanthanum, a Ca^{2+} channel blocker, and ruthenium red, an inhibitor of Ca^{2+} release from internal stores (Price *et al.*, 1994). Transient increases in $[Ca^{2+}]_{cyt}$ were also measured in aequorin-expressing *A. thaliana* seedlings challenged by O_3 fumigation (Clayton *et al.*, 1999). In the latter study, $[Ca^{2+}]_{cyt}$ levels were monitored over a period of 60 min which revealed a dose-dependent biphasic Ca^{2+} signature, with a rapid first peak followed by a second, prolonged rise in $[Ca^{2+}]_{cyt}$. The second $[Ca^{2+}]_{cyt}$ peak was shown to be required for downstream induction of *GST*. In summary, external application of AOS engendered increases in $[Ca^{2+}]_{cyt}$. Activation of Ca^{2+}-permeable channels in response to AOS treatment was demonstrated in *A. thaliana* guard cells by patch-clamping. Pei *et al* (Pei *et al.*, 2000). showed that application of H_2O_2 stimulated Ca^{2+} influx through a hyperpolarisation-activated Ca^{2+}-permeable channel, followed by partial stomatal closing. The Ca^{2+} influx was also detected in response to ABA

treatment, which was shown to generate H_2O_2 in a DPI-sensitive oxidative burst. Thus, endogenously generated AOS are able to increase $[Ca^{2+}]_{cyt}$.

3.1.1. The calcium signature

In tobacco and *A. thaliana*, changes in $[Ca^{2+}]_{cyt}$ have been correlated with induction of protective mechanisms in a number of stresses, including oxidative stress (H_2O_2 (Price *et al.*, 1994; McAinsh *et al.*, 1996); O_3 (Clayton *et al.*, 1999)), cold (Knight *et al.*, 1996), drought and salinity (Knight *et al.*, 1998) and hypo-osmotic shock (Cessna *et al.*, 1998). It is difficult to envisage how a single second messenger is able to mediate end-responses specific to each stimulus and to produce graded, dose-dependent responses. Two factors have been suggested for regulation of the observed specificity. The first factor is the growth history of the cell which leads to differing gene expression patterns (Allan *et al.*, 1994) and/or plasma membrane voltages (Blatt, 1999). These parameters determine whether the cell employs a Ca^{2+}-dependent signalling pathway to transduce a signal. The second factor is the 'calcium signature' of each stimulus, characterised by a specific amplitude, location and temporal pattern of the Ca^{2+} signal which encodes information on the particular stress (McAinsh and Hetherington, 1998). In animal cells, all three of these variables have been shown to regulate different downstream effects (Gu and Spitzer, 1995; Dolmetsch *et al.*, 1997; Hardingham *et al.*, 1997; Li *et al.*, 1998; Ducibella *et al.*, 2002). Less is known about the effects of different calcium signatures in plant cells, but evidence for a similar 'information code' is accumulating. For example, the *A. thaliana de-etiolated 3* (*det3*) mutant exhibits a prolonged $[Ca^{2+}]_{cyt}$ elevation in response to external Ca^{2+} and H_2O_2, unlike wild-type plants which show oscillations

(Allen *et al.*, 2000). In contrast to the wild-type, *det3* fails to close its stomata in response to these treatments but imposing specific Ca^{2+} spikes by repetitive membrane hyperpolarisation and depolarisation induced stomatal closure in both, *det3* and the wild-type. Furthermore, a study on *Fucus* rhizoid cells (Goddard *et al.*, 2000) demonstrated differential location of the $[Ca^{2+}]$ rise depending on stimulus strength (hypo-osmotic shock). This was related to the level of the changes in cell volume and inhibition of cell division and could be mimicked by photo-release of caged IP_3 in the appropriate area.

3.1.2. The oxidative burst and calcium

The relationship between H_2O_2 generated in oxidative bursts and calcium has been difficult to characterise. On the one hand, challenge with elicitors or avirulent pathogens triggers $[Ca^{2+}]_{cyt}$ elevations that are necessary for induction of the oxidative burst (Chandra and Low, 1997; Grant *et al.*, 2000b). On the other hand, H_2O_2 accumulation or treatment has been shown to trigger dose-dependent increases in $[Ca^{2+}]_{cyt}$ (Price *et al.*, 1994; McAinsh *et al.*, 1996) that are necessary for the development of AOS-mediated cell death (Levine *et al.*, 1996). To complicate matters, ozone application has been shown to cause a rise in $[Ca^{2+}]_{cyt}$ (Clayton *et al.*, 1999) and trigger an oxidative burst (Pellinen *et al.*, 1999). As O_3 is believed to dissolve in the apoplast, yielding AOS species such as H_2O_2 (Wohlgemut *et al.*, 2002), this would indicate the presence of a signalling chain going from H_2O_2 to $[Ca^{2+}]_{cyt}$ to H_2O_2 and again to $[Ca^{2+}]_{cyt}$. Consistent with this finding, AOS produced in an oxidative burst were shown to contribute to the biphasic Ca^{2+} signature triggered by elicitor treatment of tobacco cell cultures as addition of DPI or catalase reduced

the height of the Ca^{2+} peaks (Lecourieux *et al.*, 2002). The first Ca^{2+} peak was not only reduced in amplitude but was also of shorter duration, indicating that AOS generation triggered rapidly after the initial rise in Ca^{2+} may sustain Ca^{2+} influx into the cytosol. Similarly, Coelho *et al* (Coelho *et al.*, 2002) demonstrated the presence of H_2O_2-activated Ca^{2+}-permeable channels in *Fucus* rhizoid cells by patch-clamping. In this system, AOS produced in a hyperosmotically triggered oxidative burst was shown to be required for the generation of a cytosolic calcium wave which in turn was required for subsequent AOS production in the mitochondria, placing AOS upstream as well as downstream of increases in $[Ca^{2+}]_{cyt}$. In agreement with these results, *A. thaliana* cell cultures exposed to H_2O_2 led to increased H_2O_2 production in the mitochondria (in this case, resulting in programmed cell death), indicating a link between early H_2O_2 signalling and subsequent mitochondrial H_2O_2 production (Tiwari *et al.*, 2002).

3.1.3. Distinction between different AOS

Despite rapid reactions converting one species into another (see section 1.1.1), different AOS treatments have been shown to trigger distinct downstream responses, indicating that the plant must be able to distinguish between them. For example, phytoalexin biosynthesis can be induced only by apoplastic $^{\bullet}O_2^-$ production in parsley cells (Jabs *et al.*, 1997); whereas H_2O_2, but not $^{\bullet}O_2^-$, induces transcription of heat shock proteins in tomato suspension cultures (Banzet *et al.*, 1998) and cytosolic *APX* in germinating rice embryos (Morita *et al.*, 1999). $^{\bullet}O_2^-$ and H_2O_2 generated as a consequence of UV-B irradiation also have different effects on gene induction (Mackerness *et al.*, 2001). Thus, *PR-1* transcript levels were

regulated by H_2O_2 derived from $^{\bullet}O_2^-$; whereas, *PDF1.2* levels were regulated by $^{\bullet}O_2^-$ but not H_2O_2. Localisation of the AOS may be an important factor in this process, as molecules such as $^{\bullet}O_2^-$ and $^{\bullet}OH$ cannot cross membranes, while H_2O_2 can (Allan and Fluhr, 1997, see also section 1.2).

3.1.4. Glutathione and the cellular redox state

Irrespective of differences in reactivity and localisation, all AOS treatments affect the cellular redox balance. Considerable amounts of non-protein thiols are present in plants which function as antioxidants by keeping other redox-active molecules in a reduced state (Noctor and Foyer, 1998). Glutathione, a Glu – Cys – Gly tripeptide, is the major thiol compound, present at concentrations of up to 10 mM in the chloroplast (Foyer *et al.*, 1997). Two molecules of the reduced form, GSH, are oxidised to a dimer, connected by a disulphide bond, GSSG. Under most conditions, glutathione is found largely in the reduced form (90 – 99 %) (Foyer *et al.*, 1997). By providing a 'store' for reducing power within the cell, glutathione acts as a redox buffer. Concomitantly, oxidative conditions increase GSH synthesis in *A. thaliana* cell suspension cultures whereas depletion of glutathione by treatment with buthionine sulfoximine, an inhibitor of glutathione synthesis (Griffith and Meister, 1979), renders them susceptible to oxidative damage (May and Leaver, 1993). GSSG is re-converted to two molecules of GSH through the action of GSH reductase with NADPH as a reductant (see Figure 1.2).

It has been suggested that the GSH/GSSG ratio, indicative of the cellular redox balance, may be involved in AOS perception (Dröge, 2002). For example, the bacterial OxyR protein (see section 1.1.3) can be activated either directly by

hydrogen peroxide or alternatively by changes in the intracellular GSH/GSSG balance, suggesting that the increase in H_2O_2 is sensed in this manner (Dröge, 2002). In plants, treatments that affected the GSH/GSSG ratios in opposite ways had the opposite effects on the H_2O_2-triggered rise in $[Ca^{2+}]_{cyt}$, even though accumulation of H_2O_2 was enhanced in both cases (Price *et al.*, 1994). Pre-treatment with BSO heightened the rise in $[Ca^{2+}]_{cyt}$ whereas inhibition of APX1 activity by treatment with hydroxyurea or hydroxylamine, which should increase the GSH/GSSG ration by blocking the ascorbate – glutathione cycle (see Figure 1.2), lowered the $[Ca^{2+}]_{cyt}$ elevation. These observations indicate that it is not H_2O_2 accumulation *per se* which is sensed by the plant but its effect on the GSH/GSSG ratio, possibly via redox-sensing mechanisms (see section 1.1.3). Accordingly, H_2O_2 generated in an elicitor-triggered oxidative burst in tobacco epidermal peels was shown to alter the GSH/GSSG ratio (Allan and Fluhr, 1997).

The aim of this study was to

- test the hypothesis that plant cells can distinguish between different AOS and trigger distinct calcium signatures,
- investigate the importance of the calcium signature in mediating downstream responses by modulating the calcium signature, and
- examine the involvement of the cellular redox state in determining the size of $[Ca^{2+}]_{cyt}$ elevations and downstream effects.

3.2. Results

3.2.1. $[Ca^{2+}]_{cyt}$ elevations in response to AOS treatment

Changes in cytosolic calcium concentrations were investigated using *A. thaliana* RLD1 seedlings stably transformed with the apoaequorin gene (Knight *et al.*, 1996). Once reconstituted with its luminophore coelenterazine to produce aequorin, this protein emits blue light upon binding of calcium ions. The light can be measured by luminometry, yielding information on timing and magnitude of the response, or with a photon-counting camera, supplying additional spatial information.

3.2.1.1. H_2O_2 and $^{\bullet}O_2^-$ (menadione)

3.2.1.1.1 Timing and magnitude of the Ca^{2+} signature

In order to determine whether H_2O_2 and $O_2^{\bullet-}$ trigger increases in $[Ca^{2+}]_{cyt}$, reconstituted seedlings were treated with different concentrations of H_2O_2 and menadione (a generator of $O_2^{\bullet-}$ through redox cycling (Thor *et al.*, 1982)) and emitted light was measured using a luminometer (Figure 3.1). A rise in $[Ca^{2+}]_{cyt}$ was detected starting 15 s after stress application and reaching a maximum after 35 – 45 s. The magnitude of increase in $[Ca^{2+}]_{cyt}$ was dependent on the concentration of H_2O_2 or menadione administered, with 10 mM H_2O_2 and 10 µM menadione resulting in $[Ca^{2+}]_{cyt}$ peak values of approximately 0.6 µM and 0.4 µM, respectively. An early small peak at 5 s is triggered by the injected solution moving the seedling in the cuvette (touch response Knight *et al.*, 1991). Seedlings treated in these experiments did not manifest any signs of damage and were viable when placed back into water or onto agar plates (data not shown), indicating that the increase in $[Ca^{2+}]_{cyt}$ was not part of a cytotoxic response. For further investigation, 10 mM for H_2O_2 and 10 µM

for menadione were chosen due to the consistent responses elicited at these concentrations. The calcium signal triggered by H_2O_2 and mendione was also investigated over longer time periods following stress application (Figure 3.2).

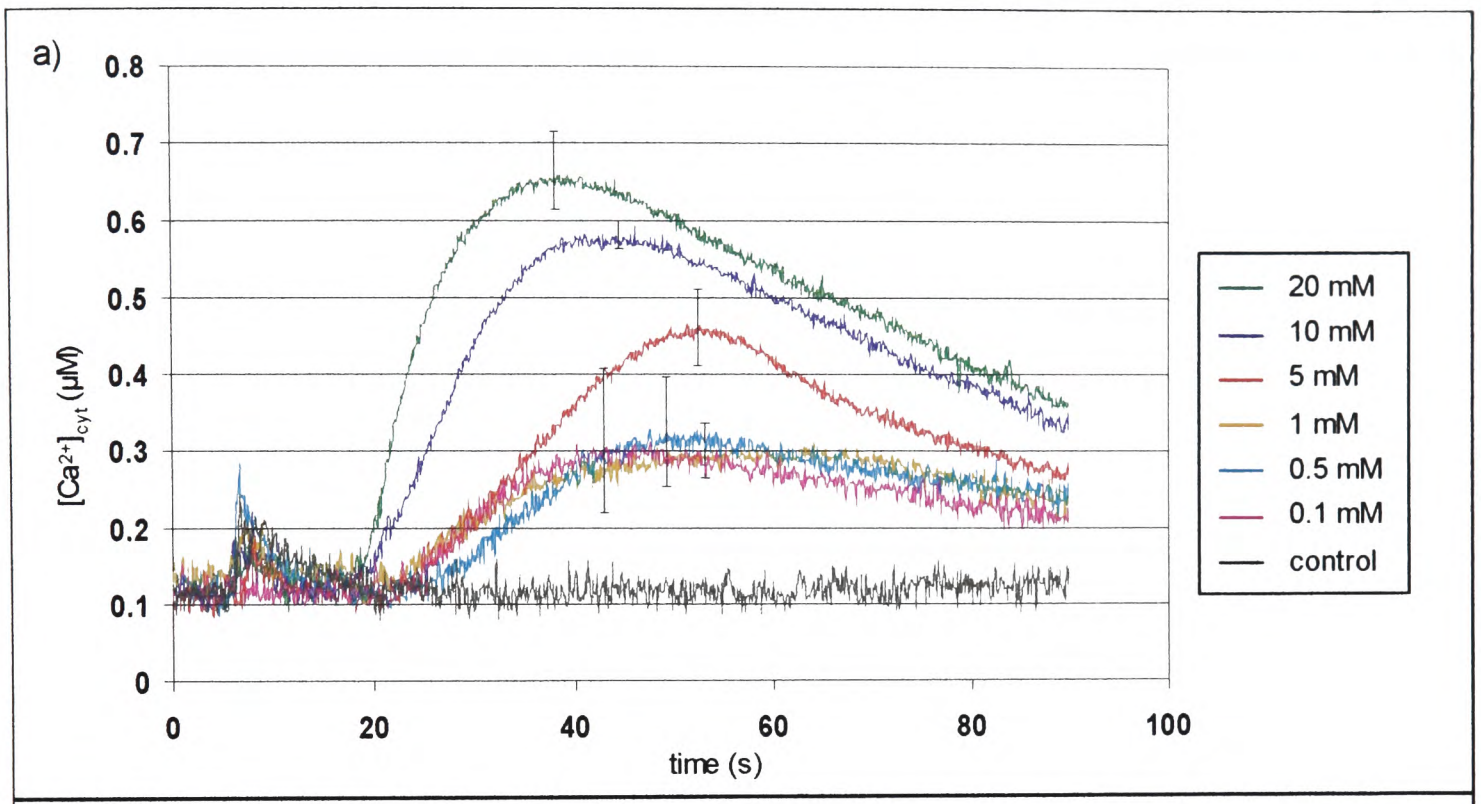

Figure 3.1: Increase in $[Ca^{2+}]_{cyt}$ in response to different concentrations of H_2O_2 and menadione $[Ca^{2+}]_{cyt}$ was measured by luminometry as described in Methods. 6 day old reconstituted RLD1.1 seedlings were placed individually into plastic cuvettes containing 0.5 ml H_2O and left to rest for 5 min. At 5 s, a) H_2O_2 or b) menadione was added to the final concentrations indicated in the legend. At 90 s, remaining aequorin was discharged. Traces represent the mean of five individual seedlings with error bars indicating standard error at that time point.

The results showed that a second increase in $[Ca^{2+}]_{cyt}$ was elicited by H_2O_2 treatment. This elevation displayed more variability in height and timing (peak at 7 – 20 min) than the first $[Ca^{2+}]_{cyt}$ peak and was yet more variable or even absent if seedlings were not allowed to rest after transfer and before challenge with H_2O_2 (Figure 3.3). Menadione treatment did not evoke a second peak irrespective of the preceding rest period (Figure 3.2 b) or the menadione concentration used, as a second peak was also not observed at the lethal concentration of 100 µM (data not shown).

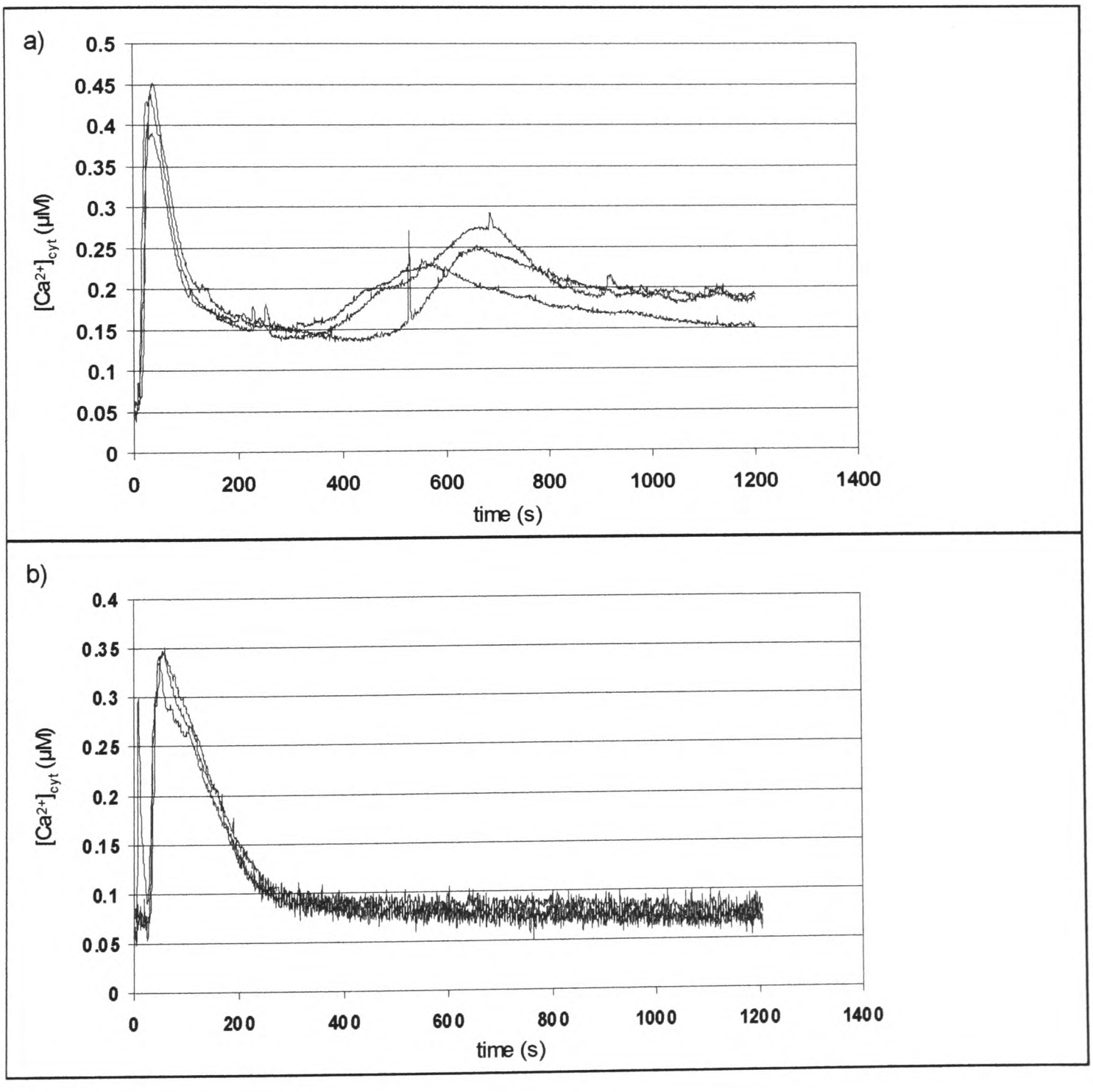

Previous page:
Figure 3.2: Increase in $[Ca^{2+}]_{cyt}$ in response to H_2O_2 and menadione
$[Ca^{2+}]_{cyt}$ was measured by luminometry as described in Methods. 7 day old reconstituted RLD1.1 seedlings were placed individually into plastic cuvettes containing 0.5 ml H_2O and left to rest for 25 to 45 min. a) H_2O_2 (final concentration 10 mM) or b) menadione (final concentration 10 µM) was added at 5 s. At 1200 s, remaining aequorin was discharged. Traces represent the responses of three individual seedlings.

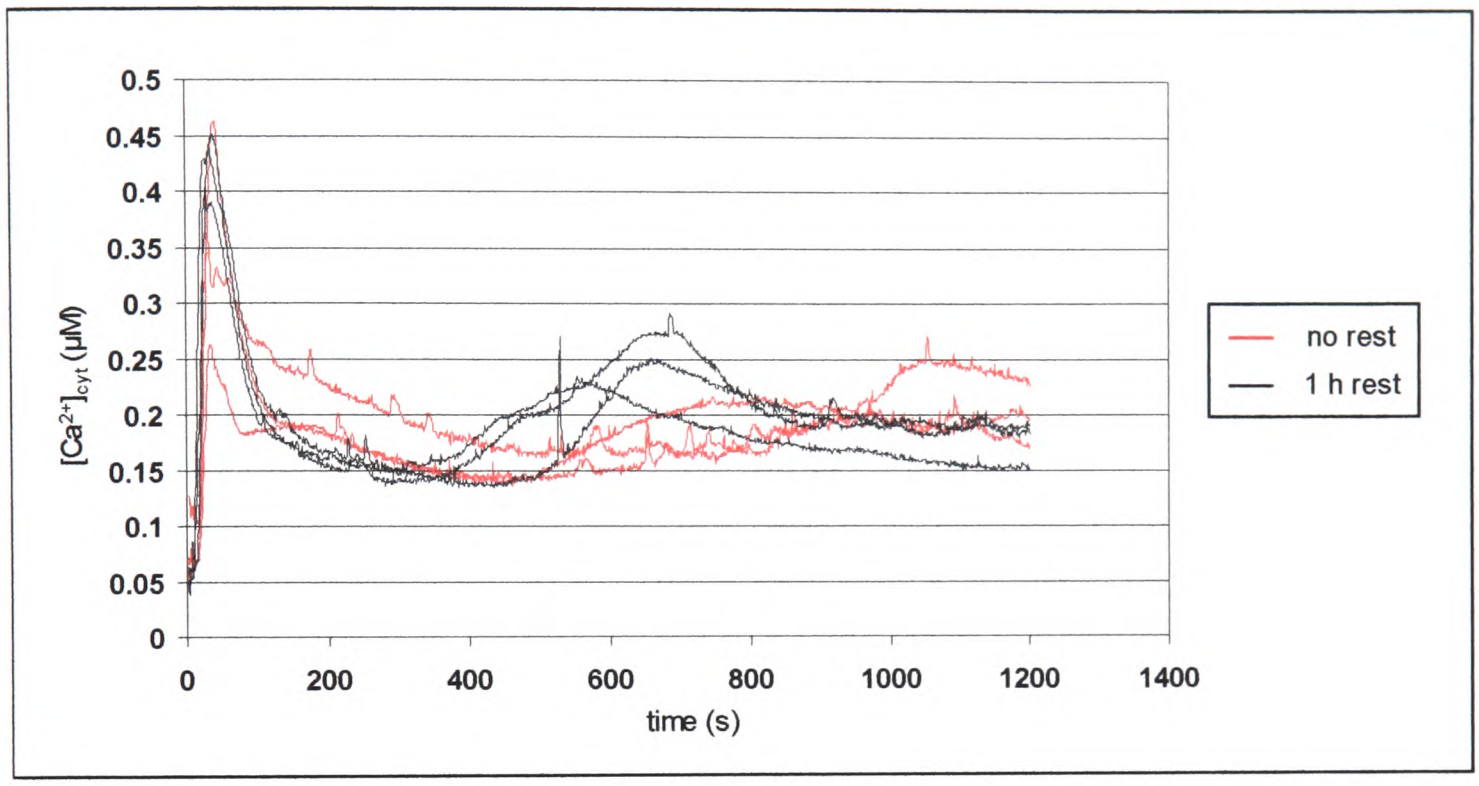

Figure 3.3:
Resting after seedling transfer affects the second $[Ca^{2+}]_{cyt}$ peak in response to H_2O_2
$[Ca^{2+}]_{cyt}$ was measured by luminometry as described in Methods. 7 day old reconstituted RLD1.1 seedlings were placed individually into plastic cuvettes containing 0.5 ml H_2O. H_2O_2 (final concentration: 10 mM) was either added immediately and luminescence counted or the seedlings were left to rest for 1 h before challenge. At 1200 s, remaining aequorin was discharged. Traces represent the responses of three individual seedlings per treatment.

3.2.1.1.2 Localisation of the $[Ca^{2+}]_{cyt}$ elevations

The spatial characteristics of the calcium signal were investigated by imaging reconstituted seedlings under the photon-counting camera following transfer onto agar plates containing 10 mM H_2O_2 or 10 µM menadione. Consistent with the luminometry data, seedlings responded to H_2O_2 with two $[Ca^{2+}]_{cyt}$ elevations (Figure 3.4). The exact timing of the first peak is difficult to state as the time taken from transfer of seedlings to start of image integration may vary slightly (between 10 – 20 seconds); however, generally $[Ca^{2+}]_{cyt}$ began to rise after 25 – 30 seconds and

reached a peak at 45 – 60 s. The small delay compared to the timing detected by luminometry may stem from the different stress application: under the camera, seedlings are not directly immersed in solution but the oxidative stress agent has to diffuse from the agar into the filterpaper to reach the plant. The first increase in $[Ca^{2+}]_{cyt}$ was always located in the cotyledons/leaves but was variable in the root. It is possible that data extracted from images of the upper root included aerial parts of the plant (hypocotyl), accounting for some of this variability. The second peak was located exclusively in the root, particularly the lower root. This response was variable in the type of root tissue involved as well as in timing, with peak times measured between 5 –20 minutes after stress application. To obtain a measure of the consistency of the root signal, 25 seedlings were imaged on the same H_2O_2 plate and the mean of the responses was calculated (Figure 3.5). The height of the second luminescence peak of the lower roots was thus shown to reach only one third of the early peak measured from the cotyledons. However, as the lower root signal was of much longer duration, 40.5 % of the total luminescence was detected in this tissue as opposed to 22.5 % in the cotyledons (Figure 3.5 b). In order to eliminate the possibility that luminescence differences between tissues were due to differences in aequorin content, 10 seedlings were cooled repeatedly to 2 °C under the camera and subsequently discharged of remaining aequorin by $CaCl_2$ addition in the luminometer. Cooling triggers $[Ca^{2+}]_{cyt}$ release in all plant tissues (Knight *et al.*, 1996). Cotyledons, upper root half and lower root half contained 37 % (± 3.8), 38 % (± 2.8) and 25 % (± 2.6) of total luminescence, respectively. Thus, the higher luminescence detected in the lower root as compared to the cotyledons was not due to a higher content in aequorin.

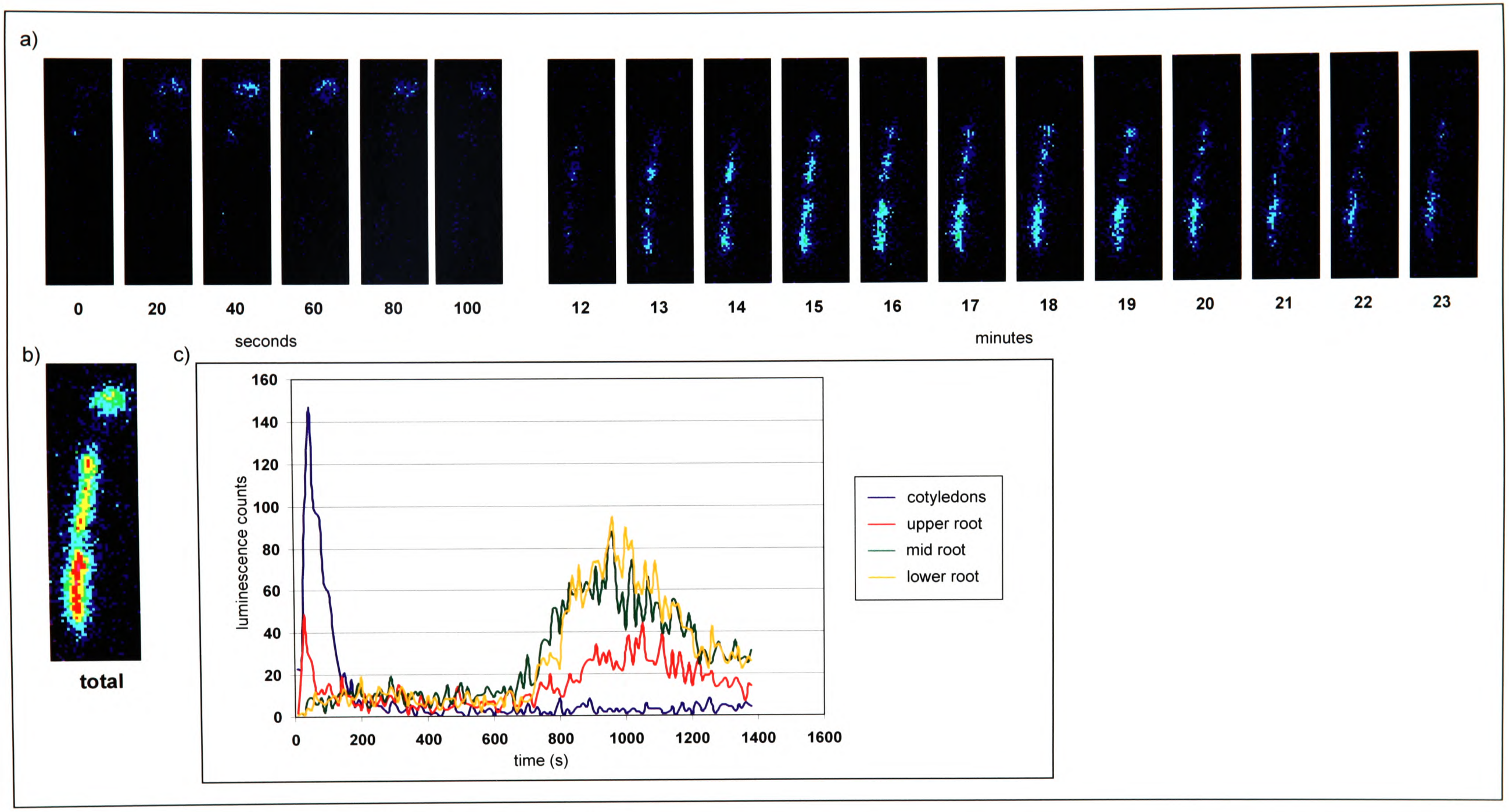

Figure 3.4: Localisation of increases in $[Ca^{2+}]_{cyt}$ in response to H_2O_2
$[Ca^{2+}]_{cyt}$ was measured under the camera as described in Methods. 7 day old reconstituted RLD1.1 seedlings were transferred to moist filter paper and left to rest for 45 min. After transfer of the filter paper onto agar plates containing 10 mM H_2O_2, luminescence was counted for 23 min. Images represent the total photon counts for an individual seedling over a) consecutive 20 s or 1 min intervals and b) the total 23 min period. Luminescence measured in different parts of this seedling over the 23 min interval is depicted in d).

a)

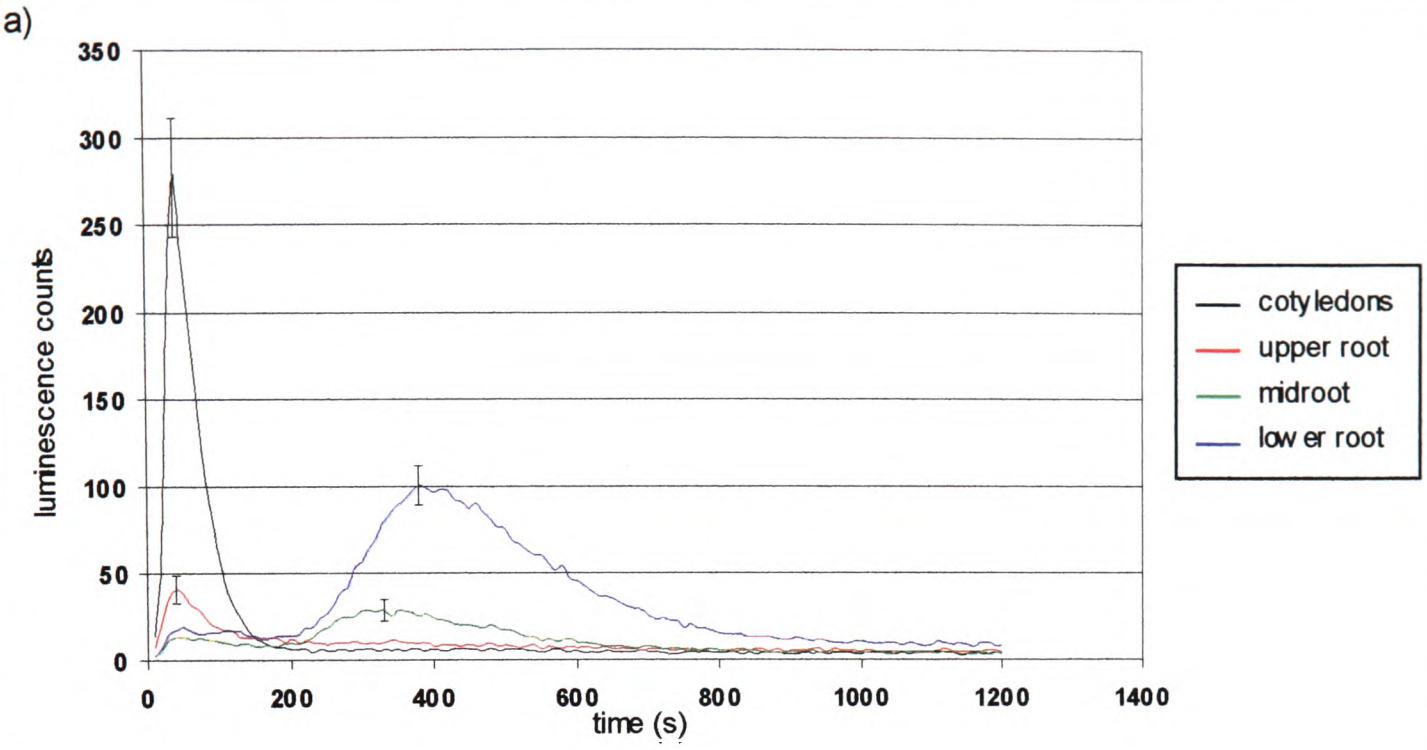

b)

	% of cotyledon peak height	% of total luminescence
cotyledons	(100)	22.5
upper root	11	14
mid root	22	23
lower root	33	40.5

Figure 3.5: Localisation of increases in $[Ca^{2+}]_{cyt}$ in response to H_2O_2
$[Ca^{2+}]_{cyt}$ was measured under the camera as described in Methods and Figure 3.4. Luminescence was counted for 20 min. a) Traces represent mean luminescence counts of 25 seedlings imaged on the same stress plate. Error bars indicate standard error at that time point. b) The maximum count value of luminescence (peak height) given off by the cotyledons was taken as 100 % and compared to the peak heights of different root sections. The percentage of total luminescence for each part of the seedling was calculated ([sum of counts for section / sum of all parts] *100)

To confirm that the observed localisations of the two $[Ca^{2+}]_{cyt}$ peaks also occur under luminometry conditions, seedlings were imaged floating in liquid (Figure 3.6). Again, the early peak was observed in the cotyledons and upper root followed by a later but more prolonged $[Ca^{2+}]_{cyt}$ elevation in the lower root sections. Thus, localisation of the Ca^{2+} elevations is unaffected by the method of H_2O_2 challenge, allowing direct comparison of data obtained by luminometry and imaging.

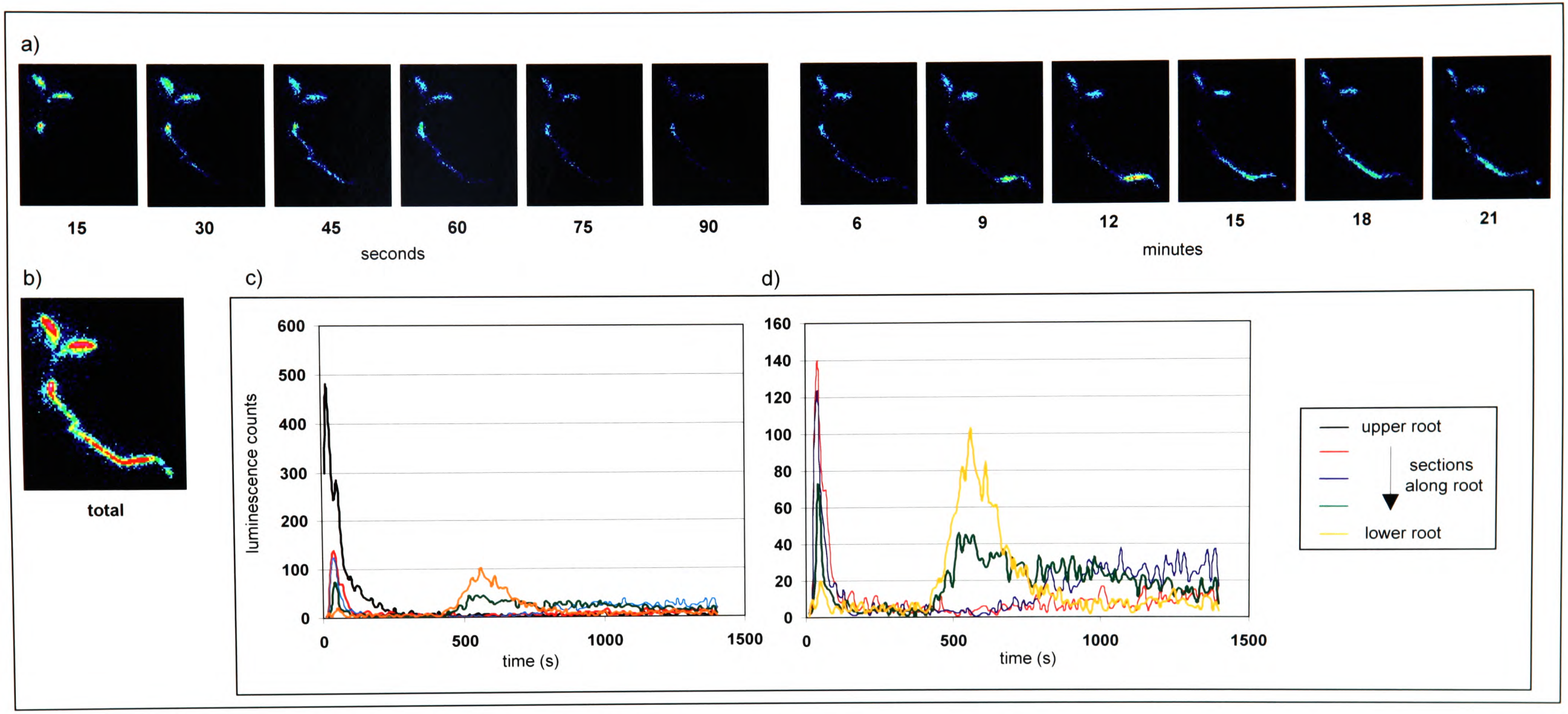

Figure 3.6: Localisation of increases in $[Ca^{2+}]_{cyt}$ in response to H_2O_2
$[Ca^{2+}]_{cyt}$ was measured under the camera as described in Methods. 7 day old reconstituted RLD1.1 seedlings were transferred into 1 ml H_2O in a well plate and left to rest for 1 h before addition of H_2O_2 (final concentration 10 mM). Luminescence was counted for 23 min. Images represent the total photon count for an individual seedling over a) consecutive 15 s or 3 min intervals and b) the total 23 min period. Luminescence measured in different parts of this seedling's root over the 23 min period is depicted in c) and d) (upper root was removed from d) in order to improve distinction between other root sections).

The calcium signal in 14 day old plants (Figure 3.7) and 21 day old plants (data not shown) was comparable to that in 7 day old seedlings. At this stage, lateral roots have formed. Increases in $[Ca^{2+}]_{cyt}$ in these tissues were found to be relatively strong and appeared to start in the part of the side root proximal to the main root and move into the more distal parts (Figure 3.7 a and c).

Consistent with the results obtained by luminometry, imaging menadione application detected only an early peak, with a timing similar to that of the first rise in $[Ca^{2+}]_{cyt}$ triggered by H_2O_2 treatment (Figure 3.8). With both stress agents, $[Ca^{2+}]_{cyt}$ increased in the cotyledons; however, in menadione treated seedlings, the signal was subsequently found to move down from the root crown into the root.

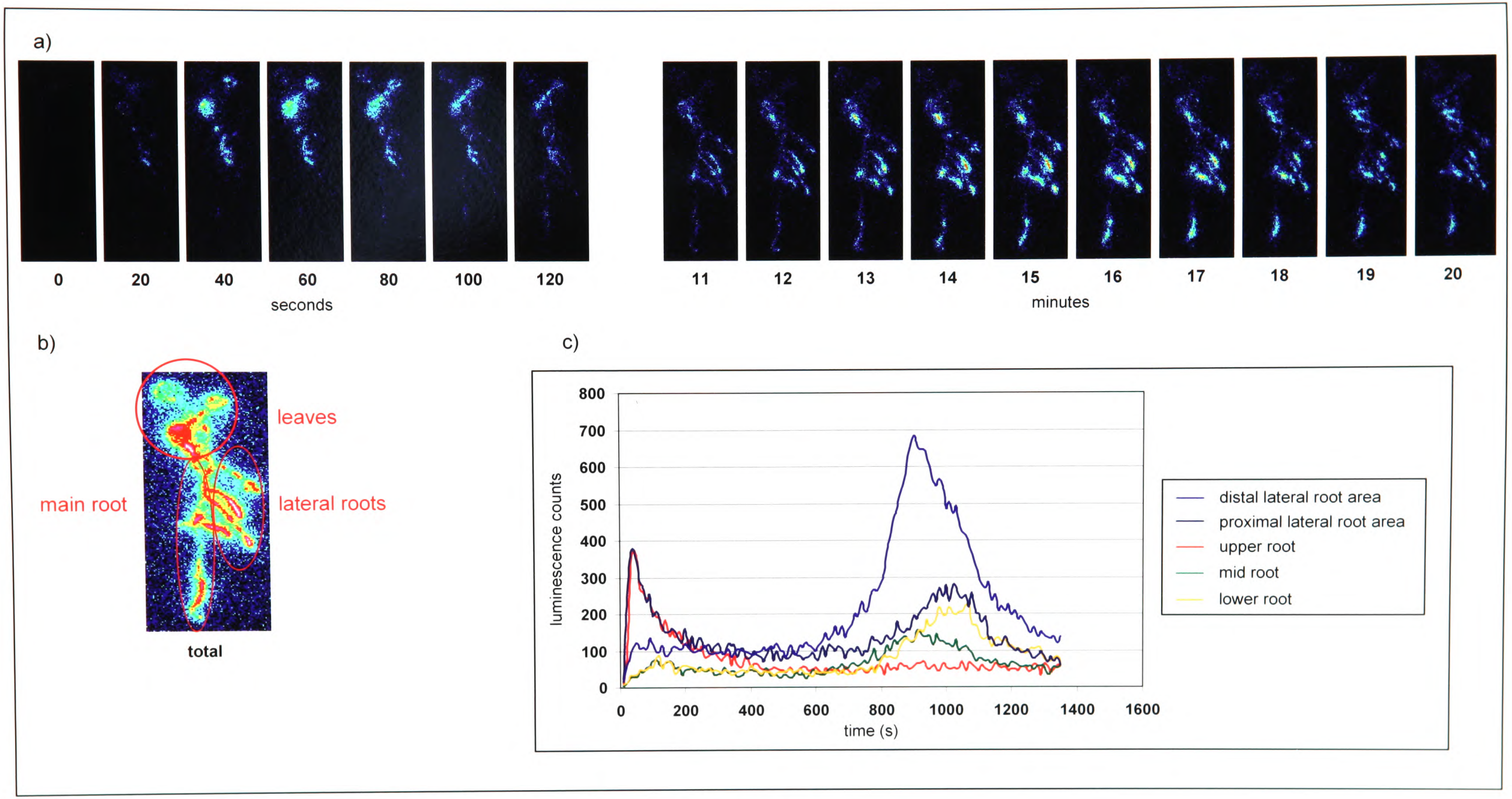

Figure 3.7: Localisation of increases in $[Ca^{2+}]_{cyt}$ in response to H_2O_2 in 14 day old plants
$[Ca^{2+}]_{cyt}$ was measured under the camera as described in Methods. 14 day old reconstituted RLD1.1 plants were transferred to moist filter paper and left to rest for 45 min. After transfer of the filter paper onto agar plates containing 10 mM H_2O_2, luminescence was counted for 23 min. Images represent the total photon counts for an individual plant over a) consecutive 20 s or 1 min intervals and b) the total 23 min period. Luminescence measured in different root sections of the same plant over the 23 min interval is depicted in c) (leaves are omitted in order to improve distinction between the root areas).

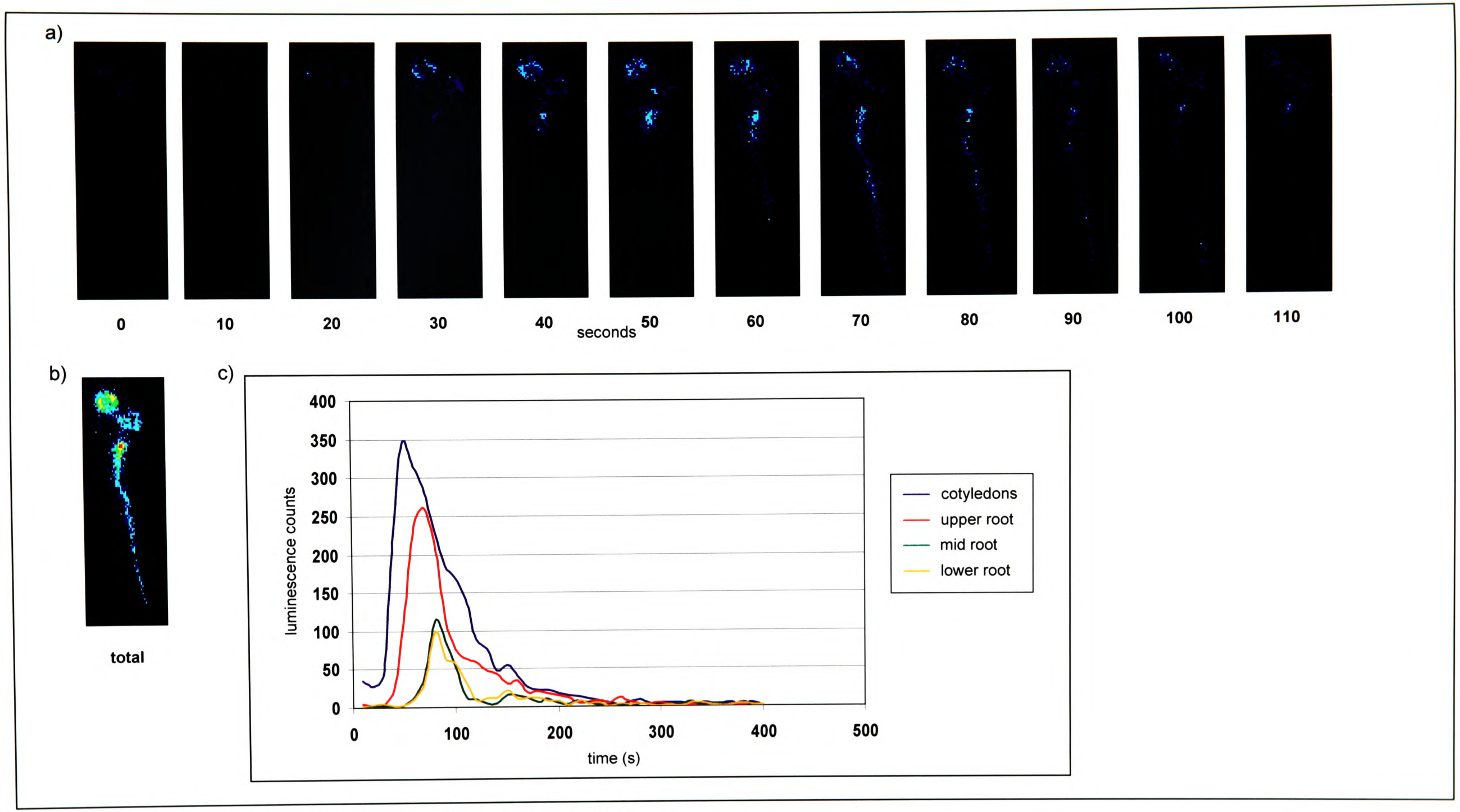

Figure 3.8: Localisation of increases in $[Ca^{2+}]_{cyt}$ in response to menadione
$[Ca^{2+}]_{cyt}$ was measured under the camera as described in Methods. 7 day old reconstituted RLD1.1 seedlings were transferred to moist filter paper and left to rest for 45 min. After transfer of the filter paper onto agar plates containing 10μM menadione, luminescence was counted for 400 s. Images represent the total photon counts for an individual seedling over a) consecutive 10 s intervals or b) the total 400 s period. Luminescence measured in different parts of this seedling over the 400 s period is depicted in c).

3.2.1.2. Ozone

Seedlings were fumigated with 500 ppb O_3 in a luminometer cuvette. $[Ca^{2+}]_{cyt}$ levels started rising 20 – 25 s after onset of fumigation, reaching a maximum of 0.43 µM ± 0.026 (n = 6) at 35 – 40 s (Figure 3.9). A second, biphasic elevation was observed with a first peak at 7 min and a second peak at 15 min.

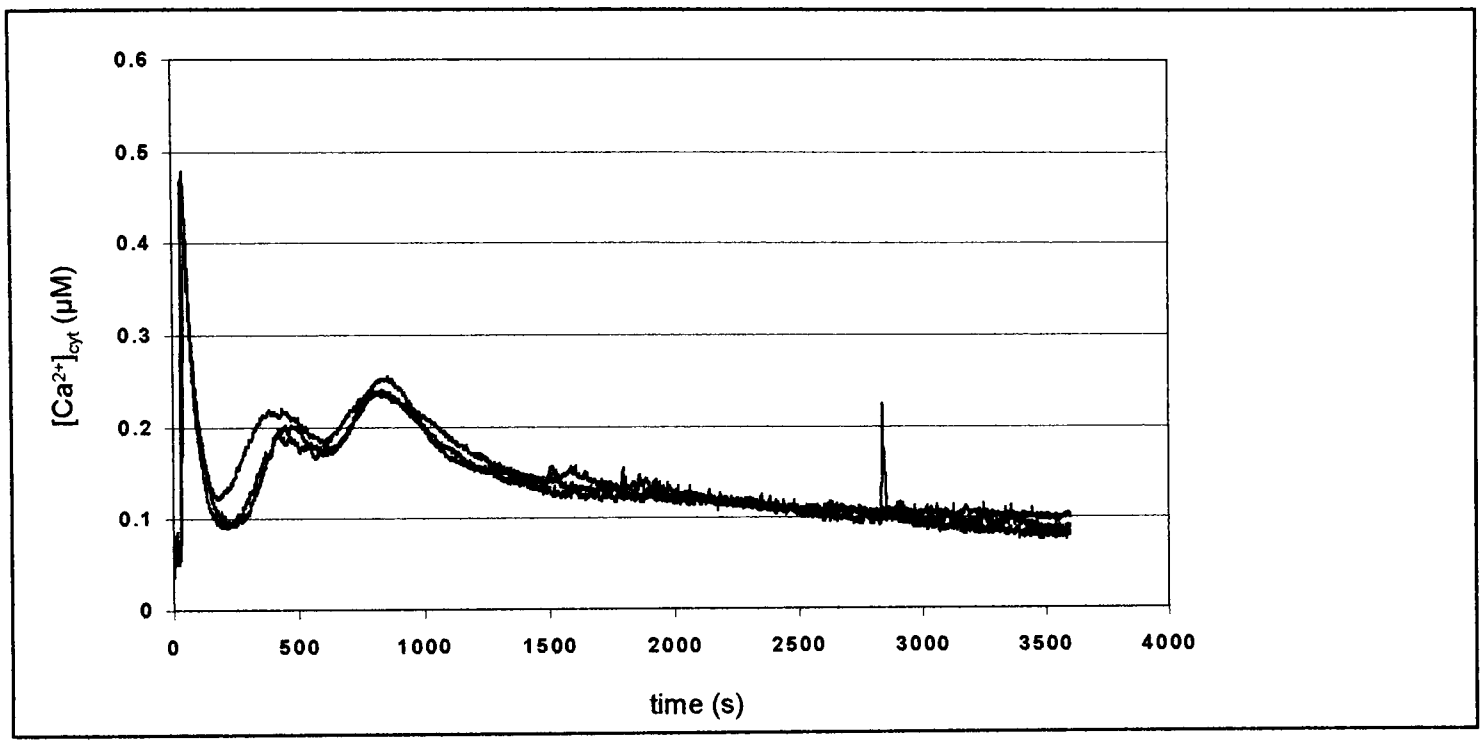

Figure 3.9: Increase in $[Ca^{2+}]_{cyt}$ in response to O_3
$[Ca^{2+}]_{cyt}$ was measured by luminometry as described in Methods. 7 day old RLD1.1 seedlings, reconstituted for 28 h, were placed individually into plastic cuvettes on a strip of moist filter paper and left to rest for 30 min. At 5 s, 500 ppb O_3 or air was allowed to enter the cuvette at a flow rate of 100 ml / min. At 3600 s, the seedling was transferred into a cuvette containing 0.5 ml H_2O and the remaining aequorin was discharged. Traces represent the responses of three individual seedlings.

3.2.1.3. Communication between different parts of seedlings during the H_2O_2 response

3.2.1.3.1 Dependence of the second $[Ca^{2+}]_{cyt}$ elevation on the continued presence of H_2O_2

To determine whether the second $[Ca^{2+}]_{cyt}$ peak of the H_2O_2 response is dependent on the continued presence of H_2O_2 or whether it is triggered by the first $[Ca^{2+}]_{cyt}$ peak independently of H_2O_2, seedlings were incubated in 10 mM H_2O_2 for the duration of the first peak only (Figure 3.10 a), until the start of the second peak (Figure 3.10 b) or until after the onset of the second peak (Figure 3.10 c) before transfer into H_2O in a luminometer cuvette. By removing H_2O_2 at different points during second Ca^{2+} rise, it was determined that the presence of H_2O_2 is required at all stages for the second $[Ca^{2+}]_{cyt}$ elevation to occur/continue.

3.2.1.3.2 Communication between different parts of the seedling

Sections of 14 day old plants were protected from contact with the H_2O_2-containing agar plate and imaged under the photon-counting camera to determine whether different tissues within the plant communicate the $[Ca^{2+}]_{cyt}$ signal to unchallenged tissues (Figure 3.11). The images obtained indicate that the signal spreads into the protected areas to a small extent (e.g. Figure 3.11 c), but a full $[Ca^{2+}]_{cyt}$ signal is only triggered if tissues are in direct contact with H_2O_2.

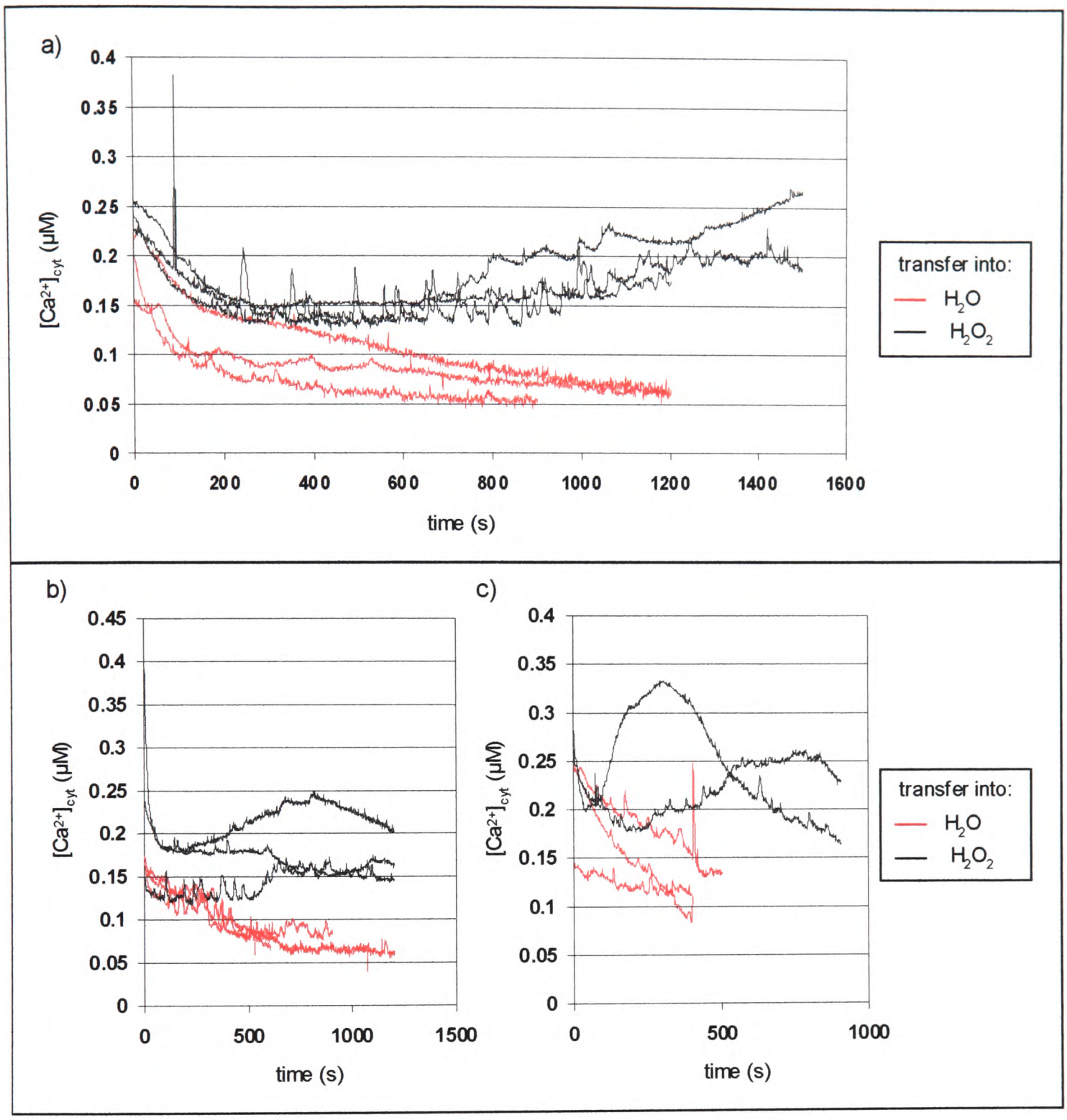

Figure 3.10: Dependence of the second $[Ca^{2+}]_{cyt}$ peak on the continued presence of H_2O_2
$[Ca^{2+}]_{cyt}$ was measured by luminometry as described in Methods. 7 day old reconstituted RLD1.1 seedlings were placed into 10 mM H_2O_2 for a) 1 min, b) 7 min or c) 9 min before transfer into plastic cuvettes containing 1 ml of 10 mM H_2O_2 or H_2O. Luminescence was counted immediately. Remaining aequorin was discharged at 460 s to 1500 s integration. Traces represent the responses of 2 – 3 individual seedlings per treatment.

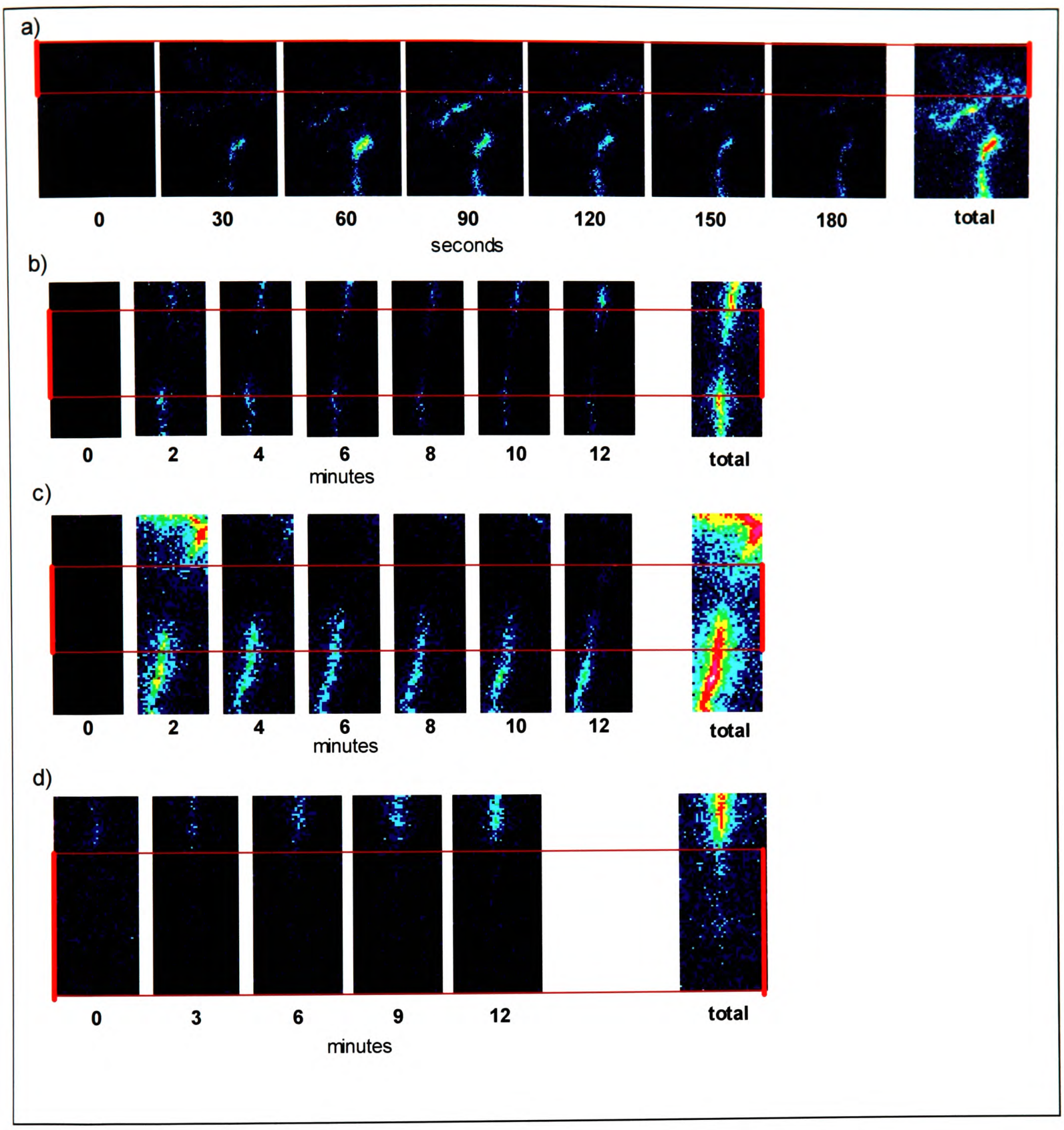

Figure 3.11: Communication between different parts of the plant
$[Ca^{2+}]_{cyt}$ was measured under the camera as described in Methods. a) Leaves, b) the upper root, c) the midroot and d) the lower root of a reconstituted 14 day old RLD1.1 plant were placed on a layer of parafilm and damp filter paper, indicated here by a red line. After a rest period of 45 min, the plants were transferred to a 10 mM H_2O_2 agar plate and imaged for 30 min. Images represent the total photon counts for an individual plant over consecutive a) 30 s, b), c) and d) 1 min periods.

3.2.1.4. Response of different root cell types to H_2O_2

Reconstituted seedlings expressing aequorin in different cell types of the root (epidermis, cortex and endodermis) were challenged with 10 mM H_2O_2 in a luminometer cuvette. All cell types tested were able to respond (Figure 3.12). In epidermal cells, a response with two $[Ca^{2+}]_{cyt}$ peaks comparable to the total plant response was triggered (Figure 3.12 a, peaks at 35 – 55 s and 400 – 600 s), whereas cortical cells exhibited a first peak at 50 s followed by a slow $[Ca^{2+}]_{cyt}$ elevation which was still increasing at 1200 s (Figure 3.12 b). Endodermal cells responded with a small first $[Ca^{2+}]_{cyt}$ elevation at 50 – 60 s and a second $[Ca^{2+}]_{cyt}$ peak at a slightly later time than the epidermis (peak at 600 – 800 s) (Figure 3.12 c).

Next page

Figure 3.12: Increase in $[Ca^{2+}]_{cyt}$ in response to 10 mM H_2O_2 in different root cell types
$[Ca^{2+}]_{cyt}$ was measured by luminometry as described in Methods. 7 day old reconstituted seedlings expressing aequorin in a) root epidermal cells, b) root cortical cells and c) root endodermal cells (Kiegle *et al.*, 2000a) were placed individually into plastic cuvettes containing 0.5 ml H_2O and left to rest for 30 min. H_2O_2 (final concentration 10 mM) was added at 5 s. At 1200 s, remaining aequorin was discharged. Background counts were subtracted from seedling luminescence counts. Traces represent the responses of three individual seedlings.

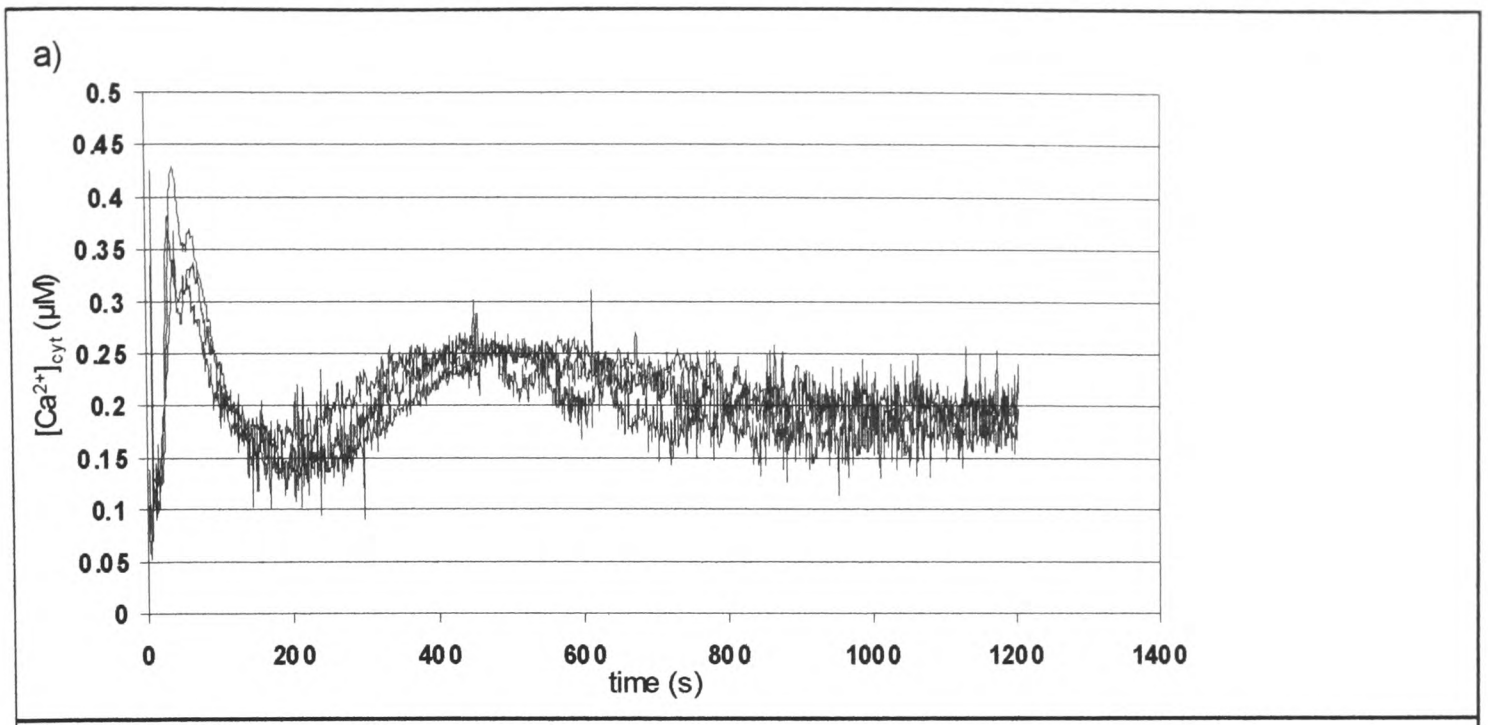
a)
0.5
0.45
0.4
0.35
0.3
0.25
0.2
0.15
0.1
0.05
0
[Ca2+]cyt (µM)
0
200
400
600
800
1000
1200
1400
time (s)

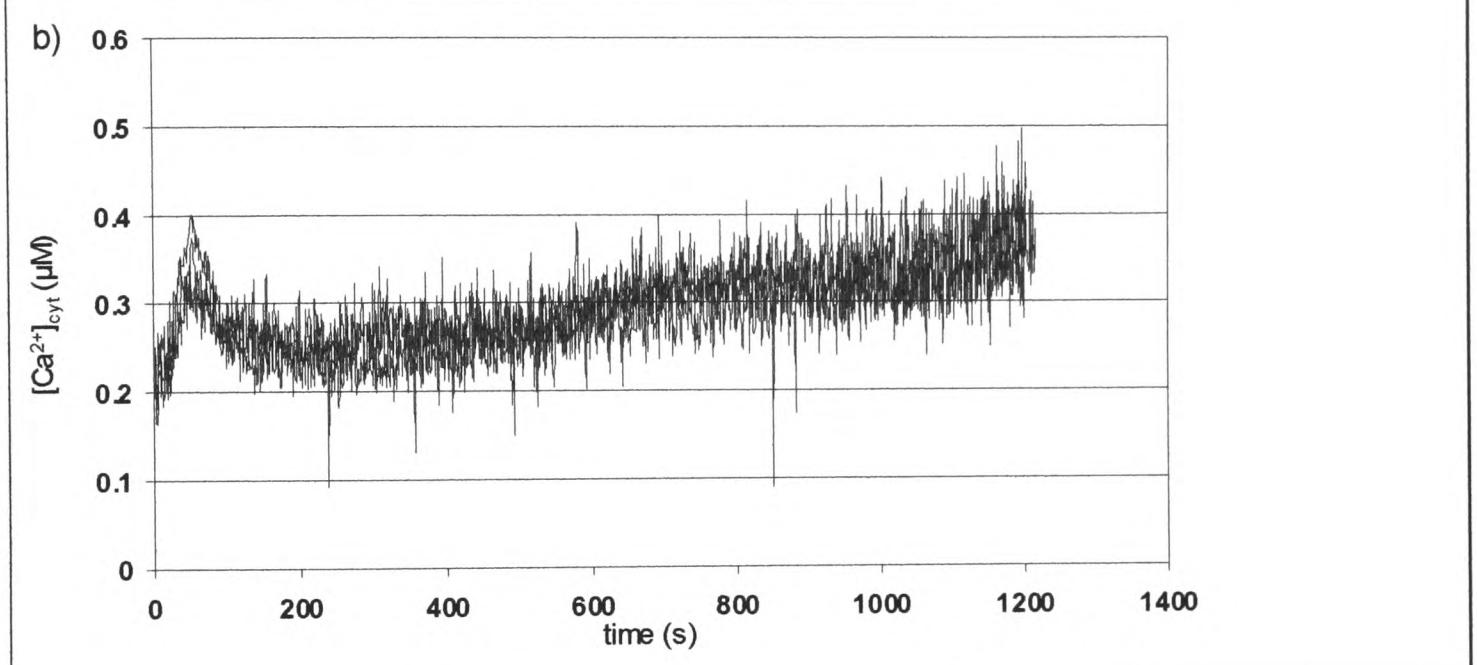
b)
0.6
0.5
0.4
0.3
0.2
0.1
0
[Ca2+]cyt (µM)
0
200
400
600
800
1000
1200
1400
time (s)

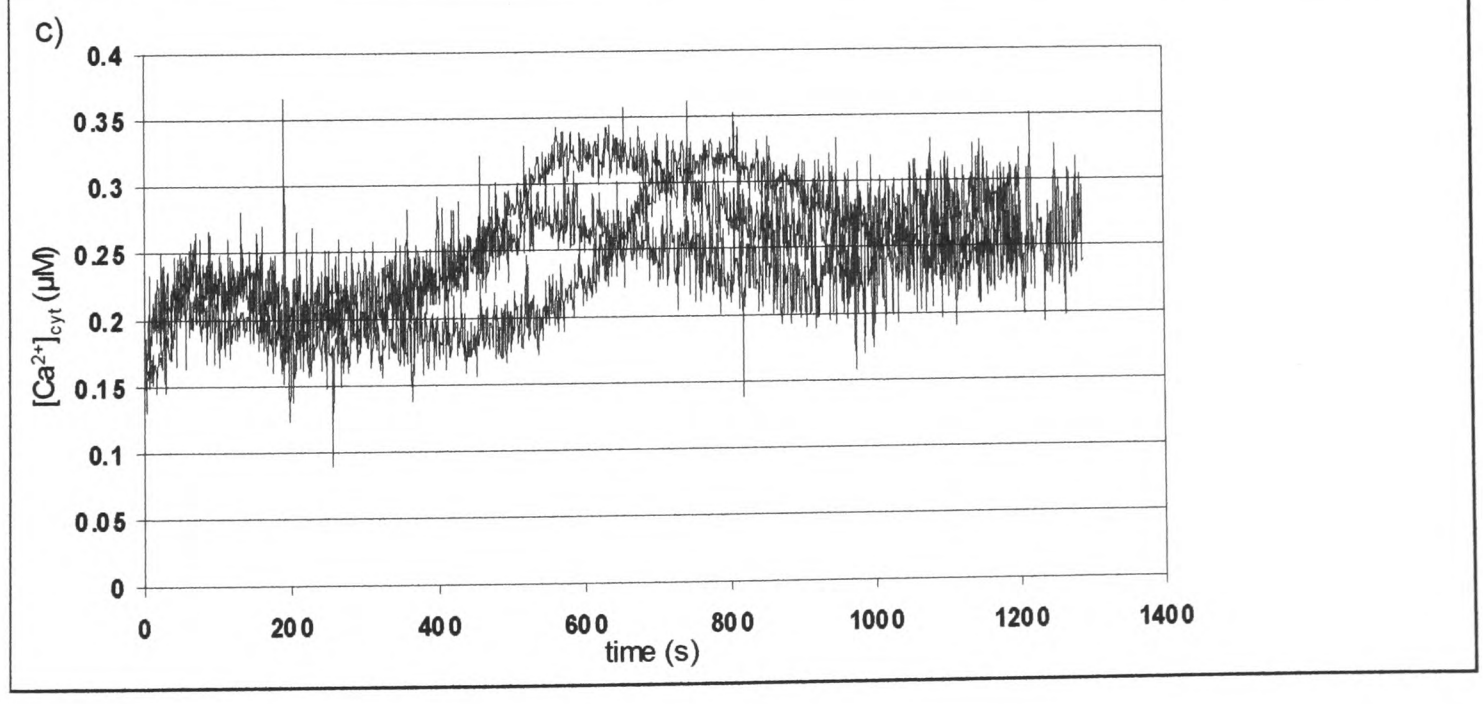
c)
0.4
0.35
0.3
0.25
0.2
0.15
0.1
0.05
0
[Ca2+]cyt (µM)
0
200
400
600
800
1000
1200
1400
time (s)

3.2.1.5. Modulation of the Ca^{2+} signature

3.2.1.5.1 Ca^{2+} channel blockers

To modulate the Ca^{2+} signature, reconstituted seedlings were incubated for 30 min - 1 h in various inhibitors prior to stress treatment (Figure 3.13). It was found that $LaCl_3$, a blocker of plasma membrane Ca^{2+}-channels (Tester and MacRobbie, 1990) and ruthenium red, a putative antagonist of intracellular calcium channels (Cibulsky and Sather, 1999), strongly inhibited the early increase in $[Ca^{2+}]_{cyt}$, particularly in response to menadione (Figure 3.13 b). Verapamil was also effective; however, this compound was shown to cause discharge of aequorin in the absence of H_2O_2 (data not shown), whereas nifedipine did not decrease the $[Ca^{2+}]_{cyt}$ elevation. Ruthenium red caused induction of *GST1* transcription in the absence of H_2O_2 (data not shown) and was therefore not further investigated. $LaCl_3$ was able to inhibit the first $[Ca^{2+}]_{cyt}$ peak of the H_2O_2 response at concentrations as low as 0.1 mM (from 0.44 µM ± 0.016 to 0.20 µM ± 0.01 for 0.1 mM $LaCl_3$; n = 4) (Figure 3.14). The effect upon the second $[Ca^{2+}]_{cyt}$ elevation was variable but generally caused this peak to be delayed and decreased (Figure 3.15; first peak is reduced from 0.435 µM ± 0.025 to 0.271 µM ± 0.020; n=4). 0.1 mM $LaCl_3$ affected the O_3-induced $[Ca^{2+}]_{cyt}$ signature in a similar manner: the first peak was decreased (from 0.43 µM ± 0.026 to 0.33 µM ± 0.014; n = 6) whereas the second peak was delayed and decreased but more prolonged (Figure 3.16).

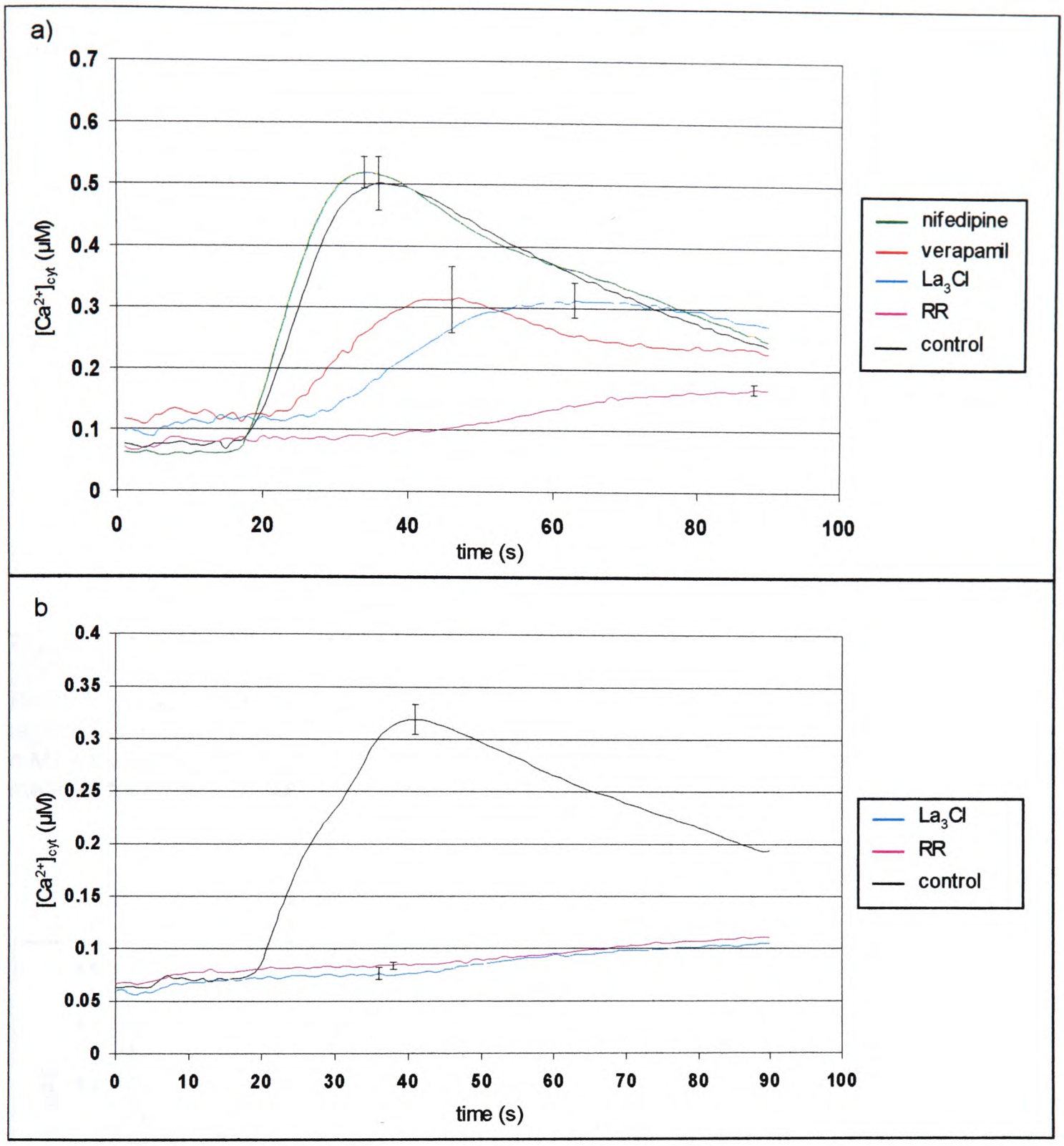

Figure 3.13: Effect of Ca^{2+} channel blockers on the H_2O_2 -induced $[Ca^{2+}]_{cyt}$ signature
$[Ca^{2+}]_{cyt}$ was measured by luminometry as described in Methods. 6 day old reconstituted RLD1.1 seedlings were incubated for 1 h in inhibitor solution or H_2O (control) in the dark (10 mM $LaCl_3$, 1 mM verapamil, 200 µM nifedipine, 100 µM ruthenium red) prior to transfer into luminometer cuvettes. a) H_2O_2 (final concentration 10 mM) and b) menadione (10 µM) was added at 5 s integration. At 90 s, remaining aequorin was discharged. Traces represent the mean of five samples with error bars indicating standard error at that time point.

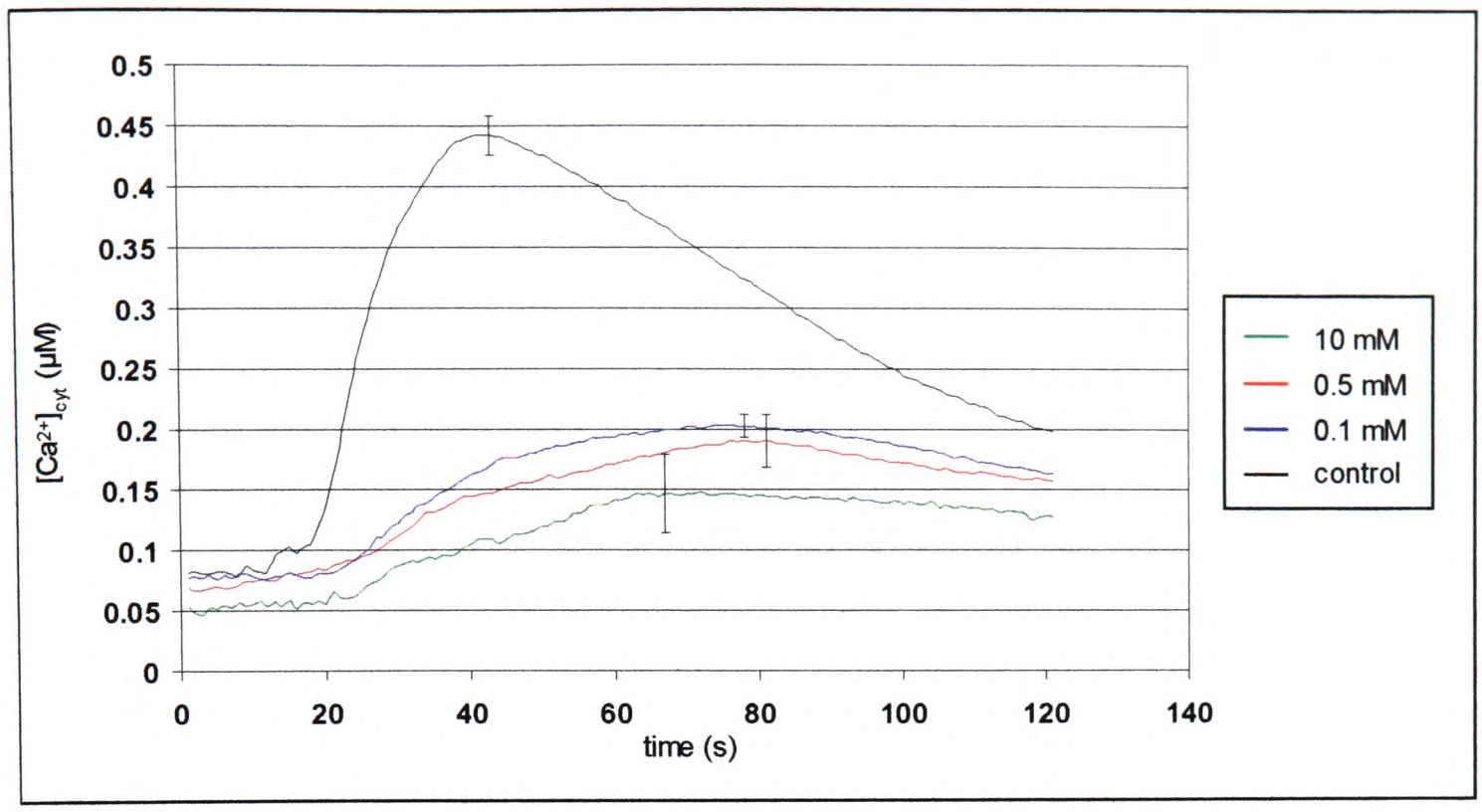

Figure 3.14: Inhibition of the first H_2O_2-induced $[Ca^{2+}]_{cyt}$ peak after incubation in $LaCl_3$
$[Ca^{2+}]_{cyt}$ was measured by luminometry as described in Methods. 7 day old reconstituted RLD1.1 seedlings were incubated for 1 h in $LaCl_3$ solution (concentrations indicated in the legend) or H_2O (control) prior to transfer into plastic cuvettes. H_2O_2 (final concentration 10 mM) was added at 5 s. At 90 s, remaining aequorin was discharged. Traces represent the mean of four samples with error bars indicating standard error at that time point.

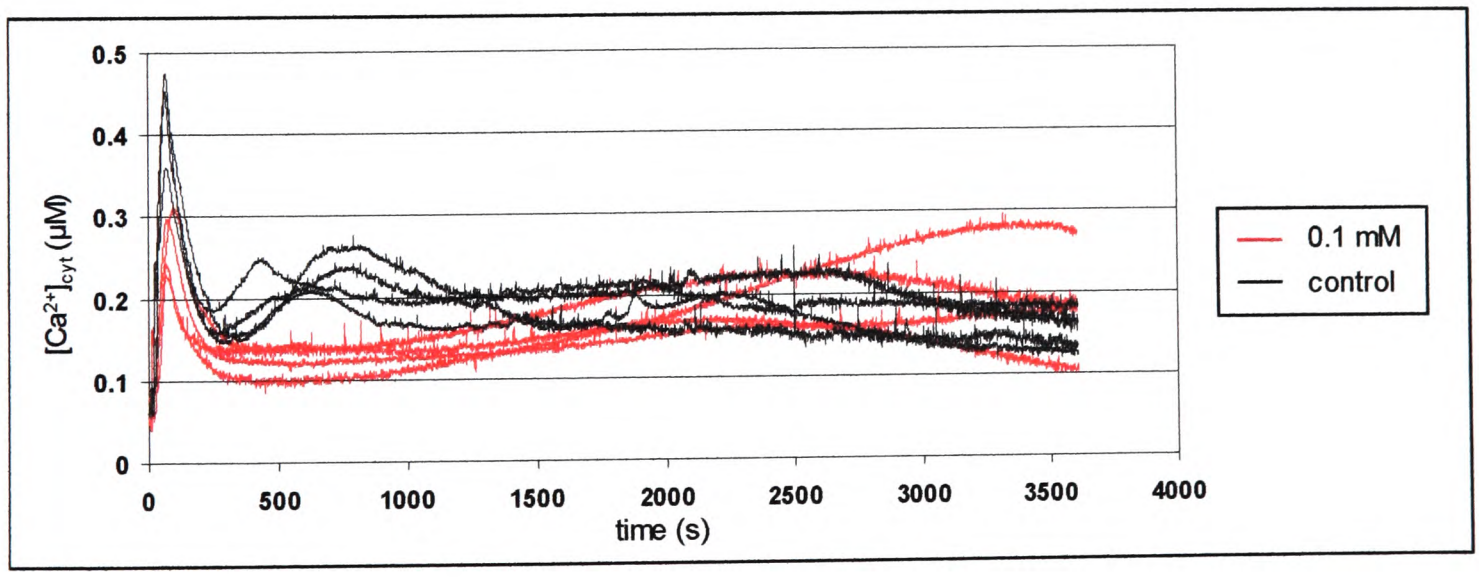

Figure 3.15: Effect of 0.2 mM $LaCl_3$ on the H_2O_2-induced Ca^{2+} signature
$[Ca^{2+}]_{cyt}$ was measured by luminometry as described in Methods. 7 day old reconstituted seedlings were incubated individually in 0.5 ml of 0.2 mM $LaCl_3$ solution or H_2O (control) for 30 min inside a plastic cuvette. H_2O_2 (final concentration 10 mM) was added at 5 s. At 3600 s, remaining aequorin was discharged. Traces represent the responses of three individual seedlings per treatment.

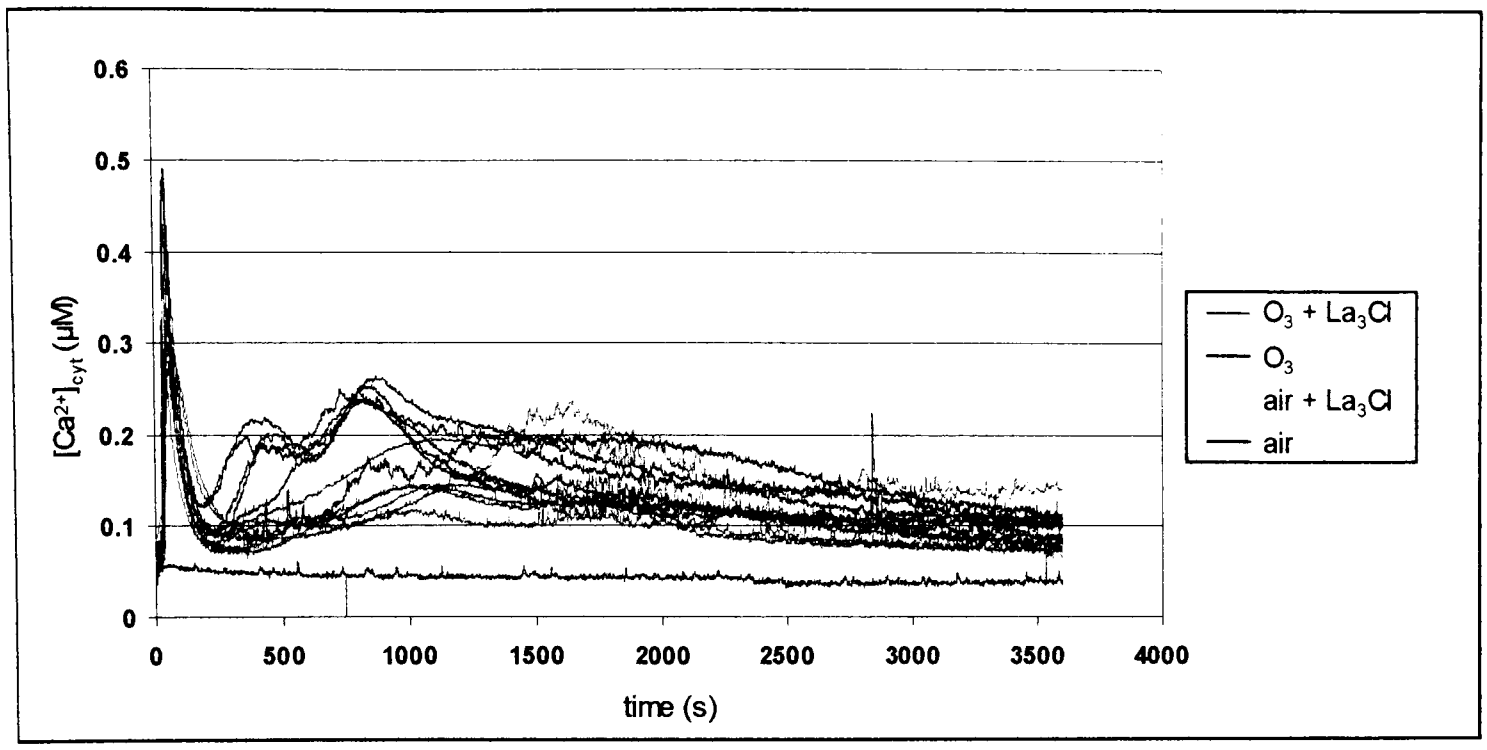

Figure 3.16: Effect of 0.1 mM $LaCl_3$ on the O_3-induced Ca^{2+} signature
$[Ca^{2+}]_{cyt}$ was measured by luminometry as described in Methods. 7 day old RLD1.1 seedlings, reconstituted for 28 h, were incubated in 0.1 mM $LaCl_3$ solution or H_2O for 30 min. Subsequently, individual seedlings were placed on filter paper strips soaked in 0.1 mM $LaCl_3$ solution or H_2O, placed inside plastic cuvettes and left to rest for 30 min. At 5 s, 500 ppb O_3 or air was allowed to enter the cuvette at a flow rate of 100 ml / min. At 3600 s, the seedling was transferred into a cuvette containing 0.5 ml H_2O and remaining aequorin was discharged. Traces represent responses of six individual seedlings for O_3 treatments and one seedling for air controls.

3.2.1.5.2 Ca^{2+} chelators

Ca^{2+} chelators bind and thus remove Ca^{2+} ions from solution (Tsien, 1980).

• EGTA

The effect of EGTA on the Ca^{2+} signature of treated seedlings was dependent on the presence of chelator both before and during stress: if seedlings were transferred into H_2O after pre-incubation, subsequent challenge with H_2O_2 or menadione increased the first $[Ca^{2+}]_{cyt}$ peak strongly (Figures 3.17 a and 3.18), whereas transfer into fresh EGTA solution inhibited the $[Ca^{2+}]_{cyt}$ elevation upon H_2O_2 addition but still increased it in menadione challenged seedlings. In addition, the usual delay of 15 s between stress application and $[Ca^{2+}]_{cyt}$ rise (Figure 3.1) was absent after

incubation in EGTA, irrespective if seedlings were transferred into fresh EGTA solution or water before challenge. Thus, $[Ca^{2+}]_{cyt}$ levels rose immediately after addition of H_2O_2 or menadione (Figure 3.17 a and 3.18).

• BAPTA

BAPTA decreased the Ca^{2+} response in H_2O_2- and menadione-treated seedlings (Figures 3.17 b and 3.18). However, as for EGTA (but to a lesser degree), $[Ca^{2+}]_{cyt}$ rose immediately on addition of H_2O_2 or menadione if seedlings were transferred into H_2O before stress challenge. This immediate rise was less frequently observed when seedlings were transferred into fresh BAPTA solution.

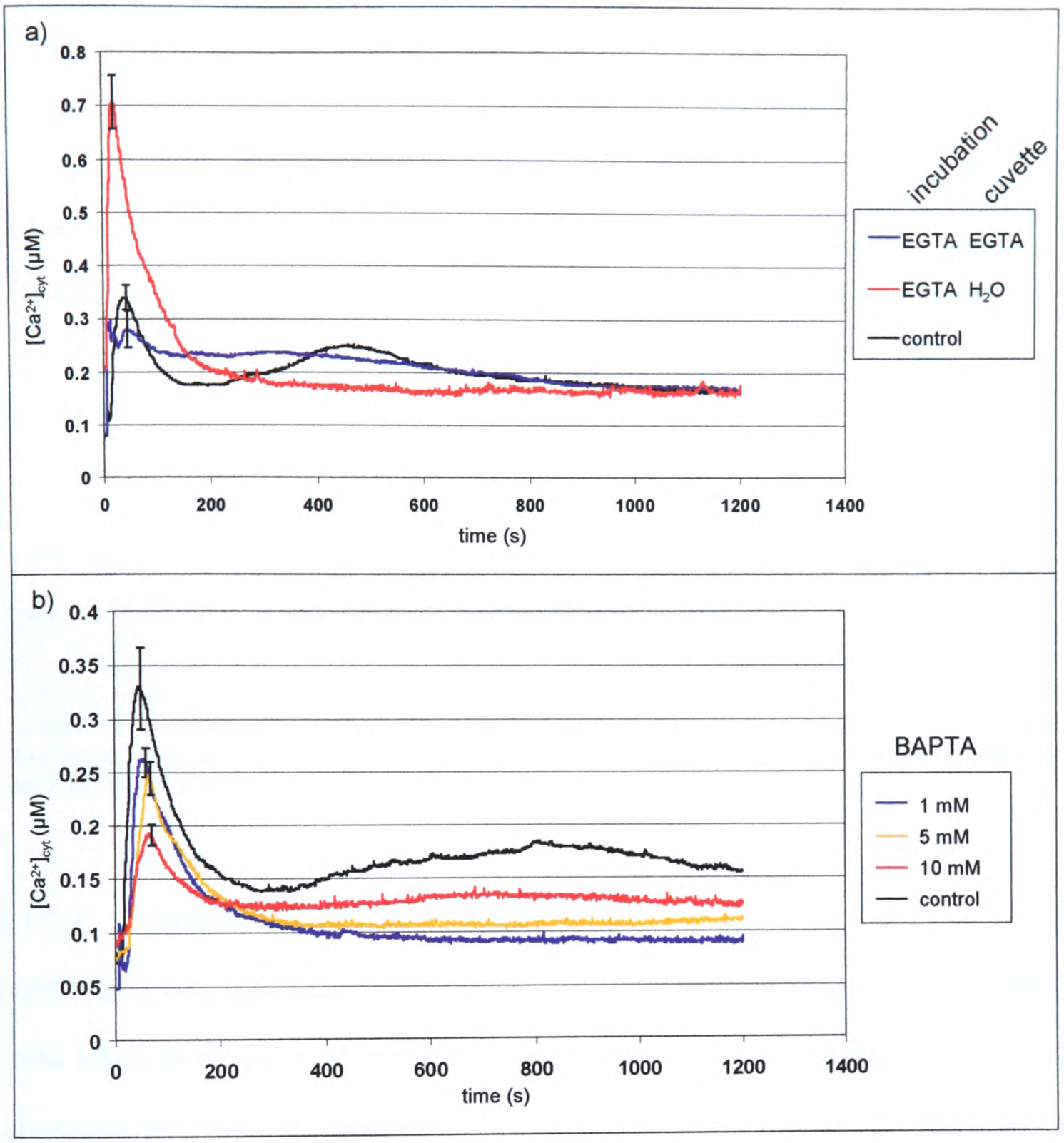

Figure 3.17: Effect of Ca^{2+} chelators on the H_2O_2-induced Ca^{2+} signature
$[Ca^{2+}]_{cyt}$ was measured by luminometry as described in Methods. 7 day old reconstituted seedlings were incubated for a) 30 min in 10 mM EGTA (pH 8.7) and b) 35 – 50 min in BAPTA (pH 7.3) at the indicated concentrations. Control seedlings were incubated in H_2O. In a), individual seedlings were transferred into cuvettes containing either fresh EGTA or H_2O before challenge with H_2O_2 (final concentration: 10 mM) at 5 s. In b), seedlings were incubated in the same cuvette to which H_2O_2 (final concentration 10 mM) was added at 5 s. At 1200 s, remaining aequorin was discharged. Traces represent the the mean of a) 3 and b) 4 seedlings with error bars indicating standard error at that time point.

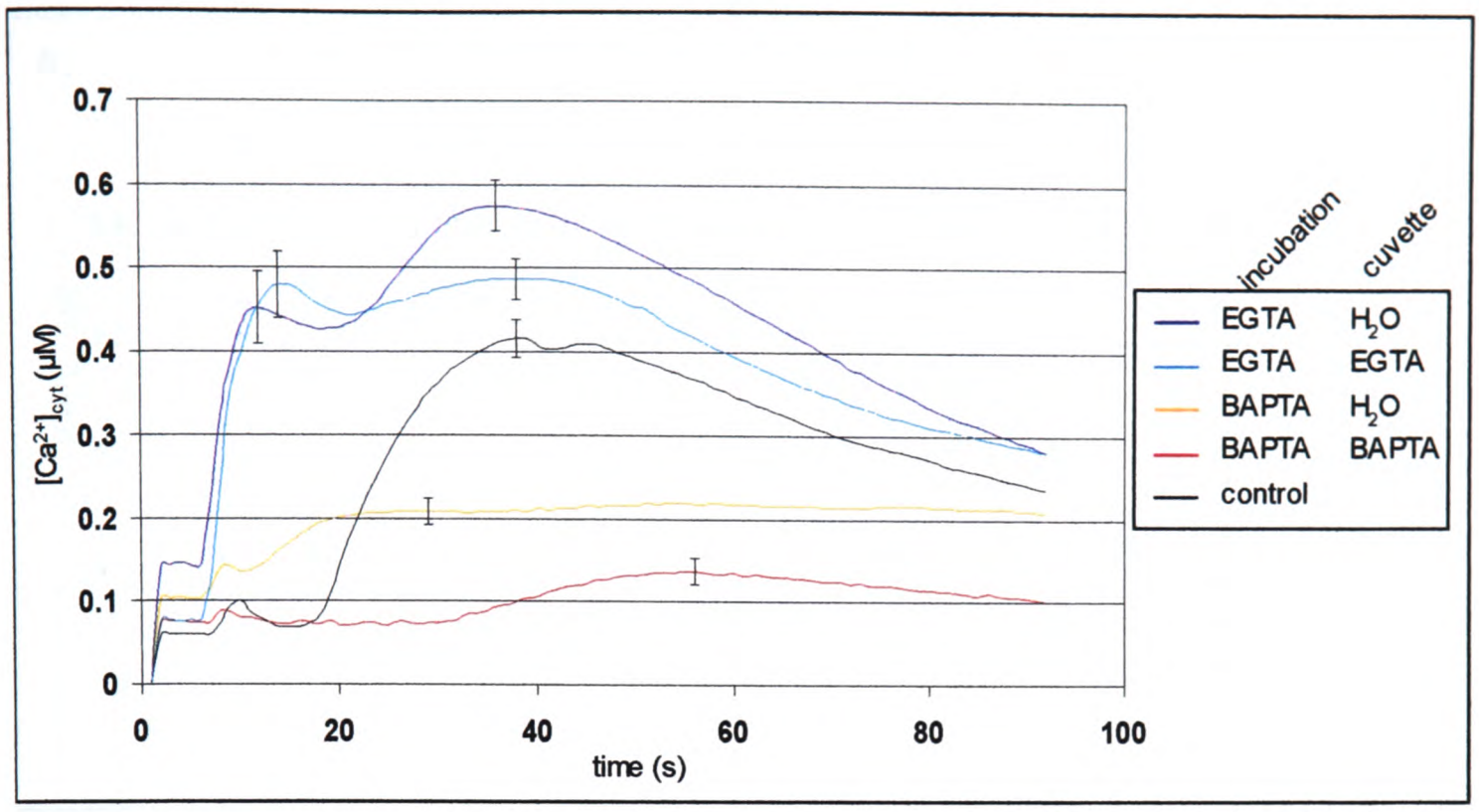

Figure 3.18: Effect of Ca^{2+} chelators on the menadione-induced $[Ca^{2+}]_{cyt}$ signature
$[Ca^{2+}]_{cyt}$ was measured by luminometry as described in Methods. 7 day old reconstituted RLD1.1 seedlings were incubated for 1 h in 10 mM EGTA, pH 8, 10 mM BAPTA, pH 8 or H_2O (control) prior to transfer into plastic cuvettes containing 0.5 ml of either H_2O, EGTA or BAPTA. H_2O_2 (final concentration 10 mM) was added at 5 s. At 90 s, remaining aequorin was discharged. Traces represent the mean of five seedlings with error bars indicating standard error at that time point.

3.2.1.5.3 Glutathione synthesis inhibitor BSO

Glutathione levels, and thus redox buffer capacity, were decreased by incubation in 10 mM BSO, an inhibitor of glutathione synthesis (Griffith and Meister, 1979), prior to challenge with H_2O_2 or menadione. In both cases, the first $[Ca^{2+}]_{cyt}$ elevation was significantly increased, *e.g.* from 0.31 µM ± 0.024 to 0.45 µM ± 0.013 (n = 5) for H_2O_2 challenge (Figure 3.19, a and b). The treatment also appears to have a stabilising effect on the second $[Ca^{2+}]_{cyt}$ peak in the H_2O_2 response: in batches of seedlings that did not exhibit a second peak under control conditions, BSO incubation increased the occurrence and height of the second peak (Figure 3.20; here first peak enhanced from 0.40 µM ± 0.011 to 0.48 µM ± 0.034; n=5).

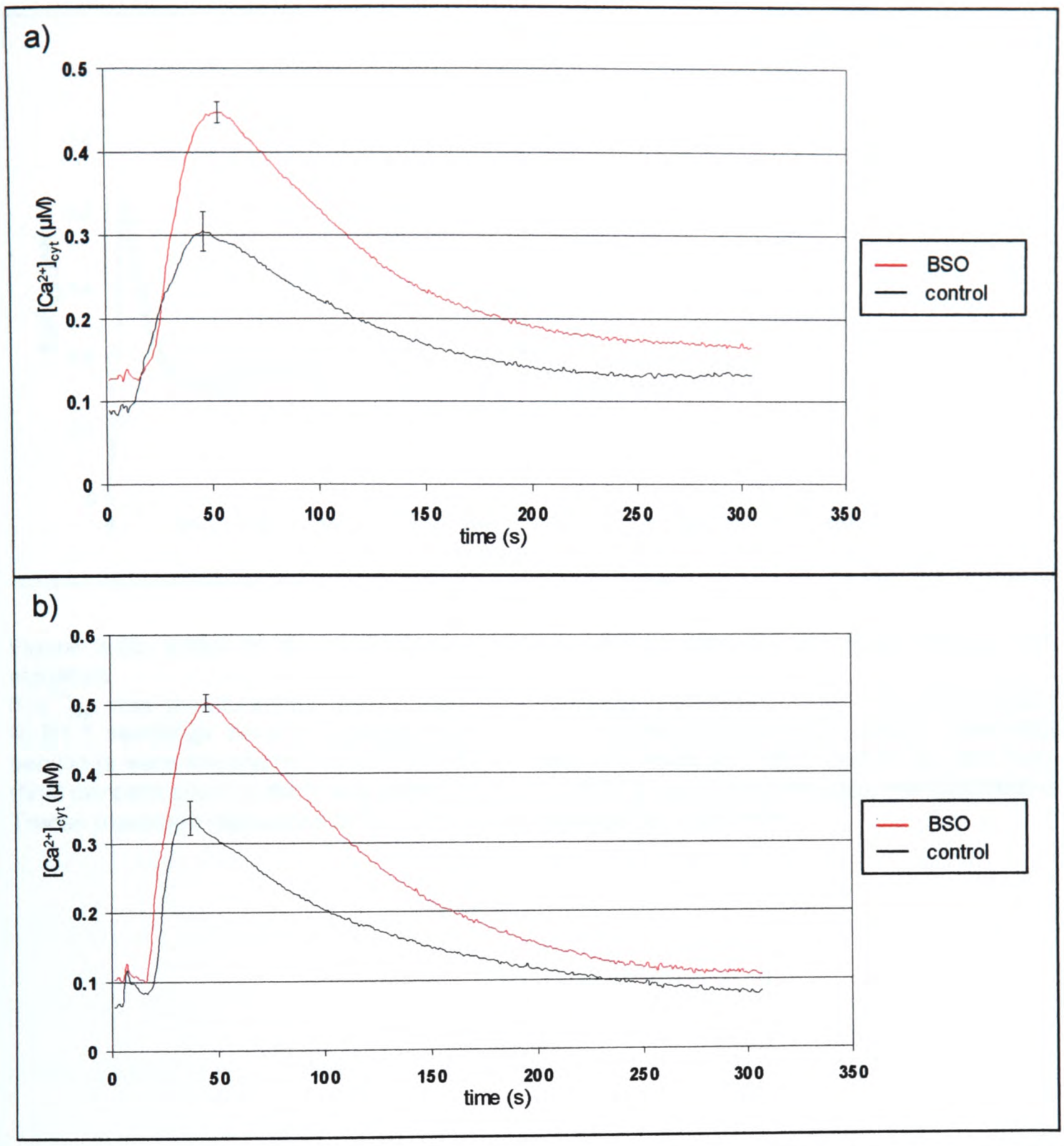

Figure 3.19: Effect of reduced glutathione levels on the H_2O_2- and menadione-induced early $[Ca^{2+}]_{cyt}$ peaks

$[Ca^{2+}]_{cyt}$ was measured by luminometry as described in Methods. 7 day old reconstituted seedlings were incubated for 3 – 5 h in 10 mM BSO or H_2O (control), transferred individually into plastic cuvettes and left to rest for 5 min. a) H_2O_2 (final concentration 10 mM) and b) menadione (final concentration 10 µM) was added at 5 s. At 300 s, remaining aequorin was discharged. Traces represent the mean of five seedlings with error bars indicating standard error at that time point.

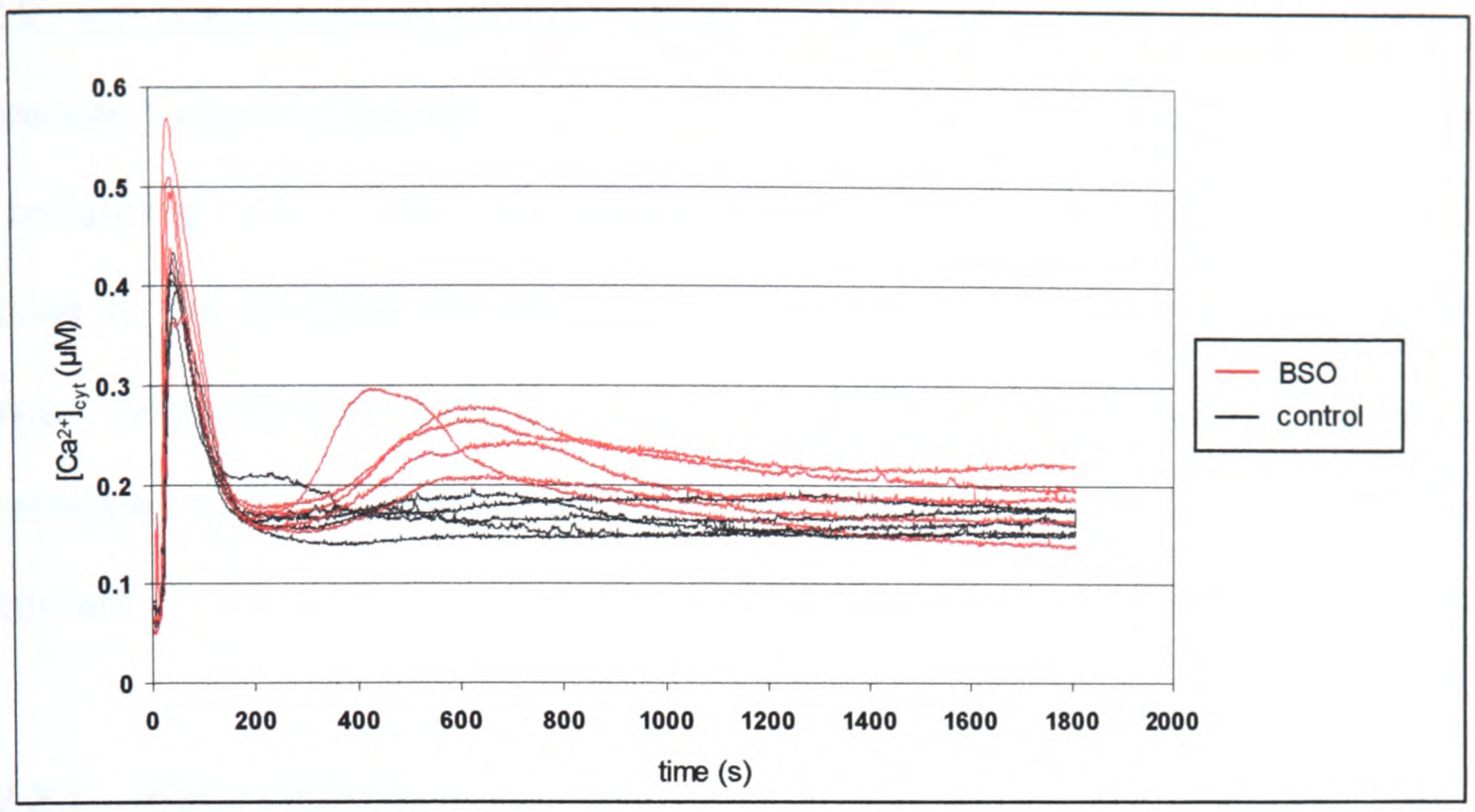

Figure 3.20: Effect of the glutathione synthesis inhibitor BSO on the H_2O_2-induced Ca^{2+} signature

$[Ca^{2+}]_{cyt}$ was measured by luminometry as described in Methods. 7 day old reconstituted RLD1.1 seedlings were incubated for 4 – 6 h in 10 mM BSO or H_2O (control). Individual seedlings were transferred into 0.5 ml H_2O in plastic cuvettes and left to rest for 30 min. H_2O_2 (final concentration 10 mM) was added at 5 s. At 1800 s, remaining aequorin was discharged. Traces represent responses of five individual seedlings per treatment.

3.2.2. The role of calcium in the induction of antioxidant defenses

It has been shown that plants are able to perceive oxidative stress and compensate by enhancing defence responses which either neutralise the AOS before damage is caused or are involved in repair mechanisms (Bowler *et al.*, 1992; Sharma and Davis, 1994; Conklin and Last, 1995). Induction of antioxidant genes was investigated for their dependence upon calcium signalling following oxidative stress treatment.

3.2.2.1. Gene induction in response to H_2O_2 and menadione treatment

The genes for several antioxidant enzymes were tested for induction of expression in response to H_2O_2 and menadione treatment by Northern analysis (Figure 3.21). *GST1*, encoding an enzyme involved in detoxification by conjugating radicals with glutathione (see section 1.1.2), was induced in a concentration dependent manner in response to H_2O_2, with strong induction at 10 mM for all time points (1, 3, and 6 h; Figure 3.21 a). *APX1*, encoding an enzyme of the Halliwell-Asada pathway, was induced strongly at 5 mM and 10 mM H_2O_2 at all time points but exhibited a higher basal level of induction in control samples than *GST1*. 10 mM H_2O_2 was chosen for future experiments – in line with the $[Ca^{2+}]_{cyt}$ measurements — as this was the concentration at which both genes were consistently up-regulated and which allowed survival of the seedlings (data not shown). The *CAT3* gene, involved in the break-down of H_2O_2 to H_2O and molecular oxygen, was also tested for induction in response to H_2O_2 treatment but showed strong circadian regulation of expression (data not shown), consistent with previous findings (Zhong and McClung, 1996). This gene was therefore not investigated further.

Menadione treatment (Figure 3.21 b) induced *GST1* consistently to significant levels only at concentrations that proved lethal to the seedlings (100 µM). *APX1* mRNA levels were increased at the viable concentration of 10 µM; however, high basal levels of this gene complicated interpretation of induction data; therefore, further gene induction experiments concentrated on the response to H_2O_2.

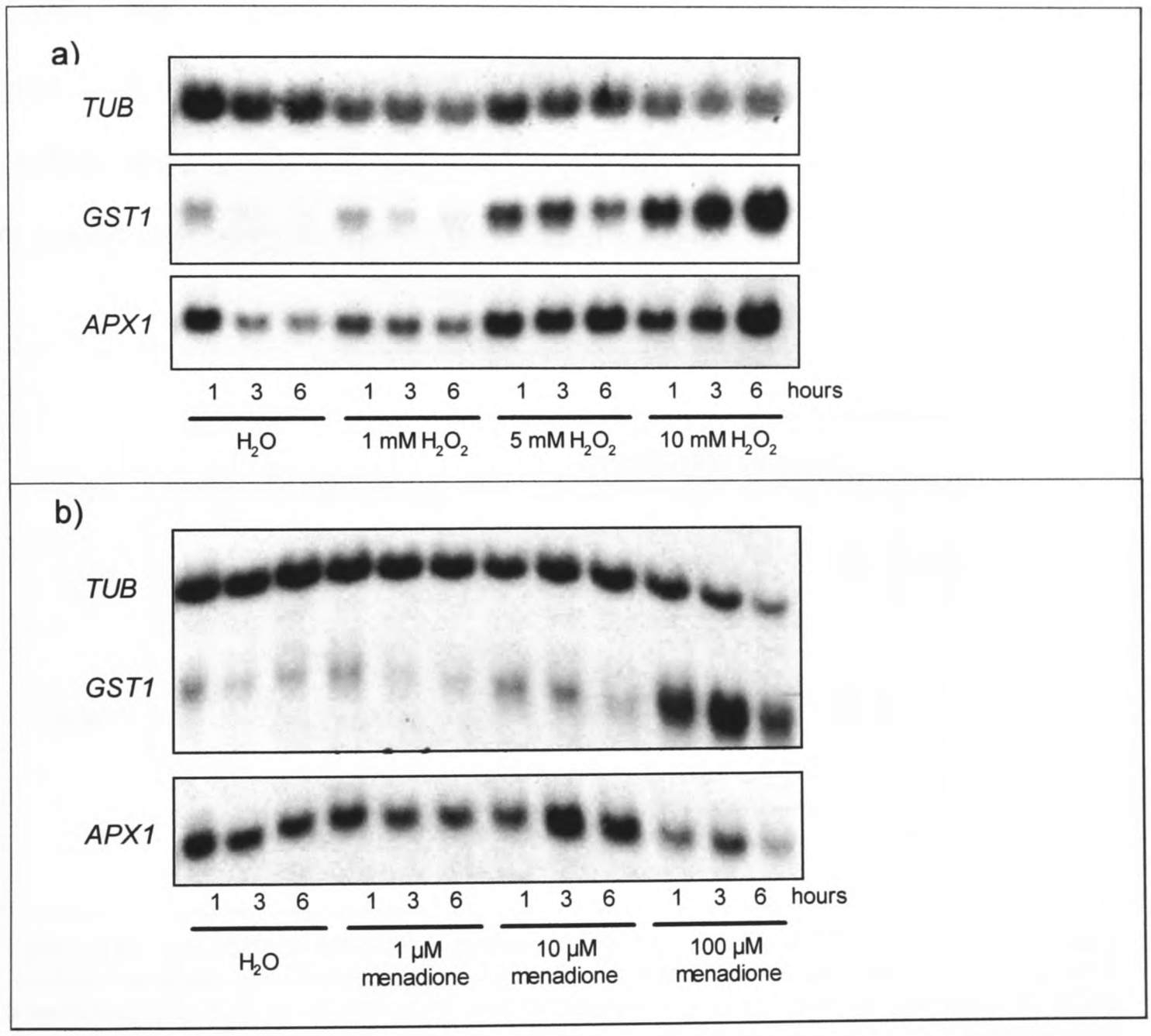

Figure 3.21: Induction of antioxidant enzyme genes in response to H_2O_2 and menadione
Northern analysis was carried out as described in Methods. 6 day old RLD1 seedlings were incubated in H_2O or different concentrations of a) H_2O_2 and b) menadione for 1, 3, or 6 hours as indicated. Total RNA was extracted from the samples, electrophoresed and transferred to nylon membrane. *GST1*, *APX1* and *β-TUBULIN* probes were labelled and hybridised to the RNA on the membrane.

3.2.2.2. Relating the H_2O_2-triggered calcium signature to antioxidant gene induction

3.2.2.2.1 Localisation

As the two peaks of the Ca^{2+} signature triggered by H_2O_2 are located in different parts of the plant, antioxidant gene induction was investigated separately in the root and shoot to determine if both elevations caused an increase in mRNA levels. *GST1* and *APX1* were induced in the shoot in response to treatment with 10 mM H_2O_2 (Figure 3.22). Increased levels of *GST1* were also observed in the root; however, the mRNA showed signs of degradation (smearing). *APX1* levels were higher in the H_2O control root samples than in the treated samples.

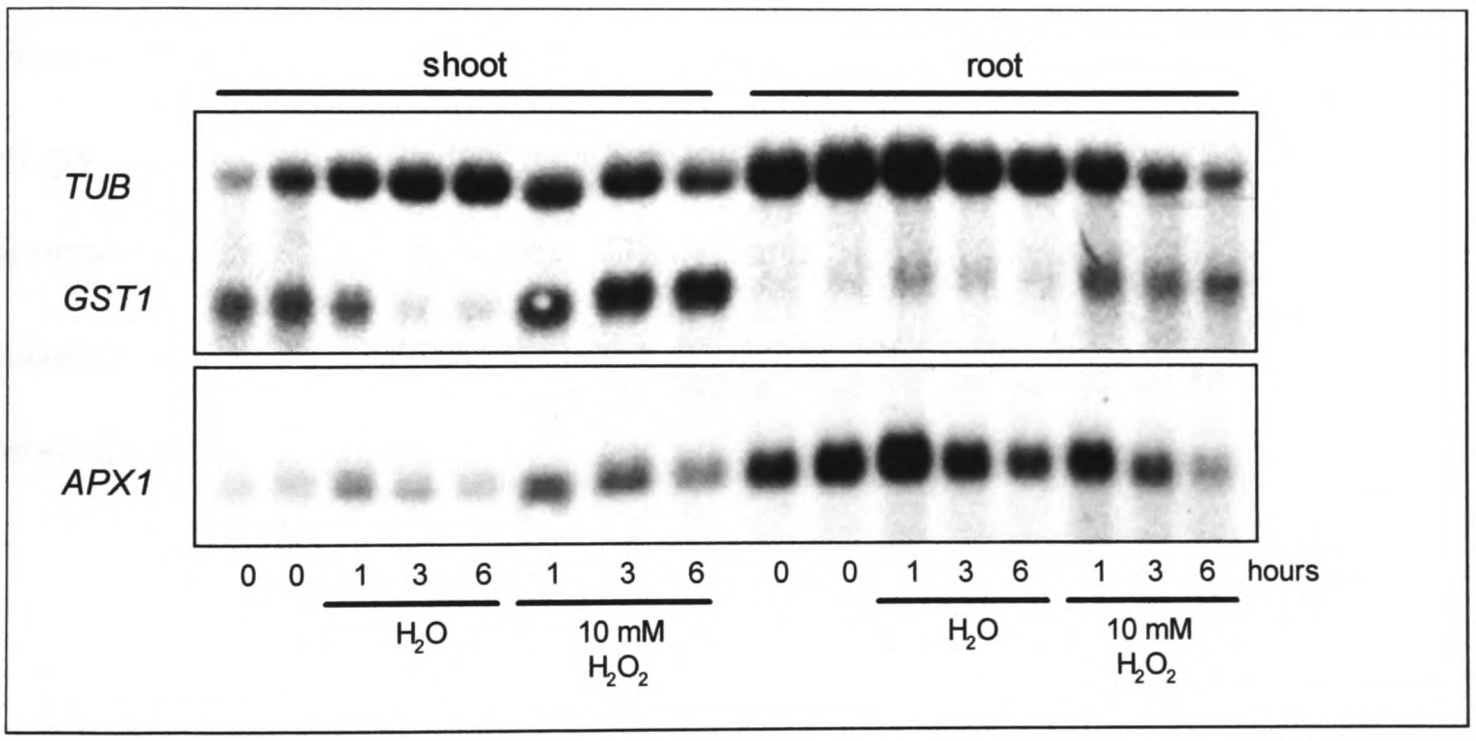

Figure 3.22: Induction of antioxidant genes in response to H_2O_2 in different parts of the plant Northern analysis was carried out as described in Methods. 14 day old RLD1 plants were transferred into H_2O or 10 mM H_2O_2 and incubated 1, 3, or 6 hours as indicated. 25 plants per sample were lined up on a smooth surface and severed at the root / shoot junction. Root and shoot tissue was collected into tubes and frozen separately. Total RNA was extracted from the samples, electrophoresed and transferred to nylon membrane. *GST1*, *APX1* and *β-TUBULIN* probes were labelled and hybridised to the RNA on the membrane.

3.2.2.2.2 Timing

Experiments in section 3.2.1.3.1 demonstrated that H_2O_2 must be present for the second $[Ca^{2+}]_{cyt}$ peak to occur. It was thus investigated whether the complete duration of the Ca^{2+} signature is required for full antioxidant gene induction. Seedlings were placed into 10 mM H_2O_2 solution for 3 min, 5 min or 20 min before transfer back into H_2O. Removal occurred thus at time points after the first but before the second $[Ca^{2+}]_{cyt}$ peak, at the beginning of the second $[Ca^{2+}]_{cyt}$ elevation and at the end of the second $[Ca^{2+}]_{cyt}$ elevation, respectively. The seedlings were left in water for 1 h, 3 h or 6 h (from the time of transfer into H_2O_2) for gene induction to proceed. The results suggest that full *GST1* and *APX1* induction at the 3 h and 6 h time points requires the presence of H_2O_2 beyond the duration of the Ca^{2+} signature (Figure 3.23). At the early time point of 1 h, *GST1* appears to be more strongly induced after shorter incubations; however, this may be the result of touch response during the transfers. *GST1* and *APX1* levels increase with longer incubation in H_2O_2. Comparable results were obtained when this experiment was repeated (data not shown).

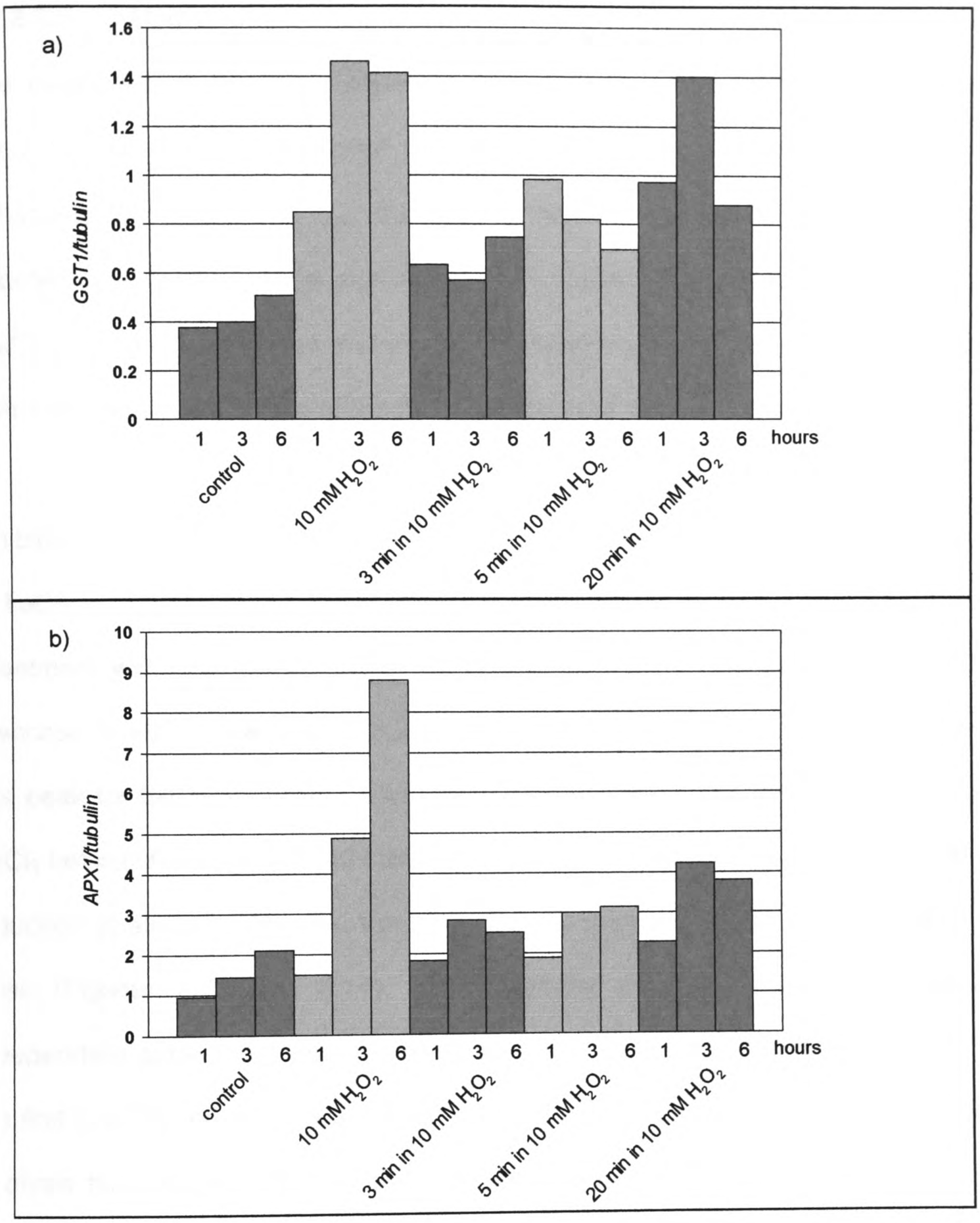

Figure 3.23: Dependence of antioxidant gene induction on the presence of the second H_2O_2-induced Ca^{2+} elevation

Northern analysis and normalisation of gene induction data was carried out as described in Methods. 7 day old RLD1 seedlings were transferred into H_2O and left to recover for 3 h before addition of H_2O_2 (final concentration 10 mM). After 3 min, 5 min or 20 min incubation, the seedlings were briefly rinsed in H_2O and placed into fresh H_2O. Samples were frozen 1, 3 or 6 h from addition of H_2O_2. The '10 mM H_2O_2' samples remained in H_2O_2-solution at all times times whereas the 'control' samples remained in H_2O. Total RNA was extracted, electrophoresed and transferred to nylon membrane. *GST1*, *APX1* and *β-TUBULIN* probes were labelled and hybridised to the RNA on the membrane. Bars represent *GST1* (a) and *APX1* (b) gene induction relative to *β-TUBULIN* mRNA levels.

3.2.2.2.3 Magnitude

The magnitude of the Ca^{2+} response has been proposed to encode information about the level of stress applied (Dolmetsch *et al.*, 1997). Thus, by inhibiting or enhancing the rise in $[Ca^{2+}]_{cyt}$, the level of antioxidant gene induction should be affected accordingly if gene expression were dependent on the magnitude of the $[Ca^{2+}]_{cyt}$ elevation. This was investigated by Northern analysis of seedlings treated with inhibitors or enhancers of the $[Ca^{2+}]_{cyt}$ signature as shown in section 3.2.1.5.

Inhibition

- $LaCl_3$

Treatment with channel blockers was shown to inhibit the first $[Ca^{2+}]_{cyt}$ peak in response to H_2O_2 (see section 3.2.1.5.1, Figures 3.14 and 3.15). The necessity of this peak for full gene induction was thus investigated by incubating seedlings with $LaCl_3$ before challenge with 10 mM H_2O_2. $LaCl_3$ treatment reduced *GST1* and *APX1* induction at all concentrations that had also been shown to inhibit the first $[Ca^{2+}]_{cyt}$ peak (Figures 3.24 and 3.14). This reduction was reproduced in a second independent experiment treating seedlings in 0.1 mM $LaCl_3$ (data not shown). As the first $[Ca^{2+}]_{cyt}$ elevation was shown to occur predominantly in the shoot, Northern analysis for gene induction in the cotyledons was carried out (Figure 3.25). The result indicates a reduction in *GST1* levels comparable to the data obtained from whole seedlings; however, a much smaller effect on *APX1* induction was observed.

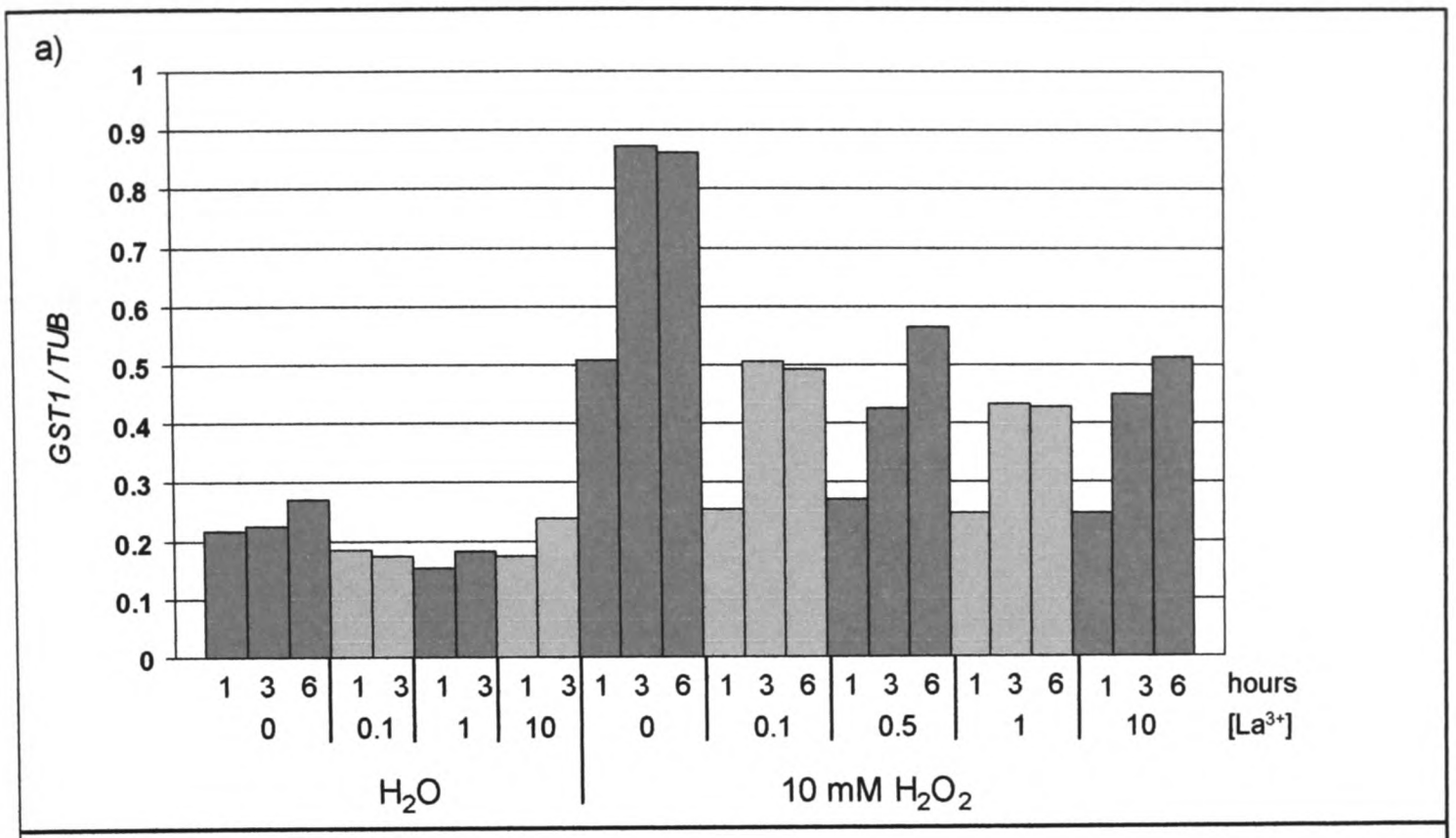

Figure 3.24: Inhibition of antioxidant gene induction by $LaCl_3$ treatment
Northern analysis and normalisation of gene induction data was carried out as described in Methods. 7 day old RLD1 seedlings were transferred into H_2O and allowed to recover for 2 h before addition of $LaCl_3$ solution (final concentration as indicated). Control samples remained in H_2O. After 1 h incubation, samples were placed into fresh $LaCl_3$ and H_2O_2 was added where indicated (final concentrations $LaCl_3$:as before; H_2O_2: 10 mM). Samples were removed and frozen after 1 h, 3 h or 6 h. Total RNA was extracted, electrophoresed and transferred to nylon membrane. *GST1*, *APX1* and *β-TUBULIN* probes were labelled and hybridised to the RNA on the membrane. Bars represent *GST1* (a) and *APX1* (b) gene induction relative to *β-TUBULIN* mRNA levels.

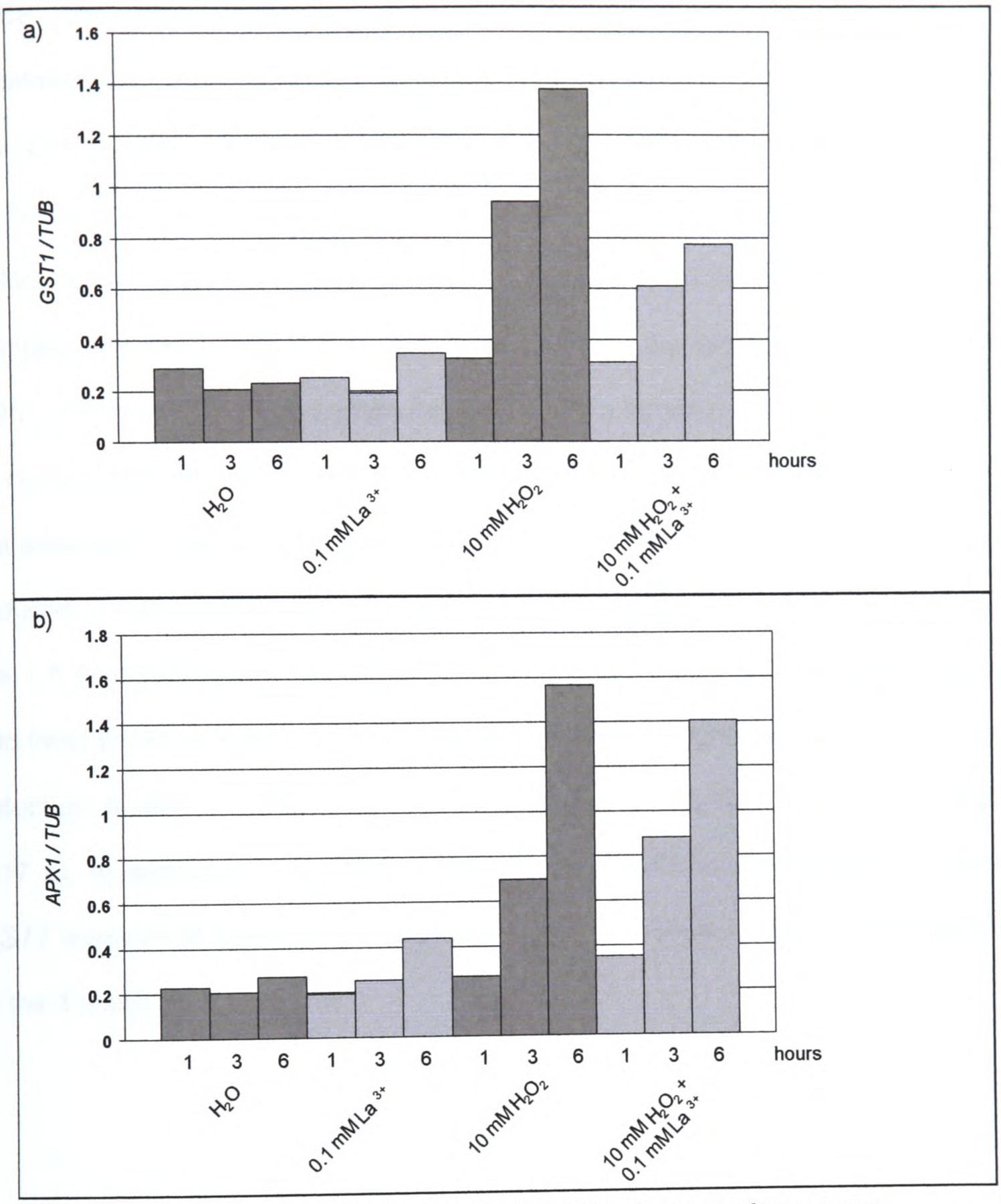

Figure 3.25: Inhibition of antioxidant gene induction in the shoot by $LaCl_3$ treatment
Northern analysis and normalisation of gene induction data was carried out as described in Methods. 8 day old RLD1 seedlings were transferred into H_2O and allowed to recover for 3 h before addition of $LaCl_3$ solution (final concentration: 0.2 mM). Control samples remained in H_2O. After 40 min incubation, samples were placed into fresh $LaCl_3$) and H_2O_2 was added where indicated (final concentrations $LaCl_3$: 0.1 mM; H_2O_2: 10 mM). Samples were removed after 1 h, 3 h or 6 h, lined up on a smooth surface and severed at the hypocotyl/root junction. After freezing the shoot tissue, total RNA was extracted, electrophoresed and transferred to nylon membrane. *GST1*, *APX1* and *β-TUBULIN* probes were labelled and hybridised to the RNA on the membrane. Bars represent *GST1* (a) and *APX1* (b) gene induction relative to *β-TUBULIN* mRNA levels.

- Ca^{2+} chelators

Treatment with the Ca^{2+} chelators EGTA and BAPTA was shown to decrease the first $[Ca^{2+}]_{cyt}$ peak if the chelator was present during H_2O_2 challenge and, in the case of EGTA, increase the Ca^{2+} response if the seedlings were transferred into H_2O before H_2O_2 addition (section 3.2.1.5.2, Figure 3.17). *GST1* was increased in all samples involving chelator treatment, particularly at the late 6 h time point (Figure 3.26), indicating that these compounds constitute a stress on the cell in the absence of H_2O_2. *APX1* showed induction at 6 h in the BAPTA and EGTA control samples, but were low at the earlier 1 h and 3 h time points. The 3 h and 6 h time points were reduced in H_2O_2-treated samples that had been incubated in BAPTA or EGTA, but the 1 h sample showed increased *APX1* levels. Transfer of EGTA treated samples into fresh EGTA or into H_2O_2 did not appear to cause a significant difference in gene induction despite the large effect this exerted on the first $[Ca^{2+}]_{cyt}$ peak (see Figure 3.17 a). In summary, the effect of BAPTA and EGTA is complicated, increasing *GST1* levels in all treatments and decreasing *APX1* levels in H_2O_2-treated samples at the 3 h and 6 h time points.

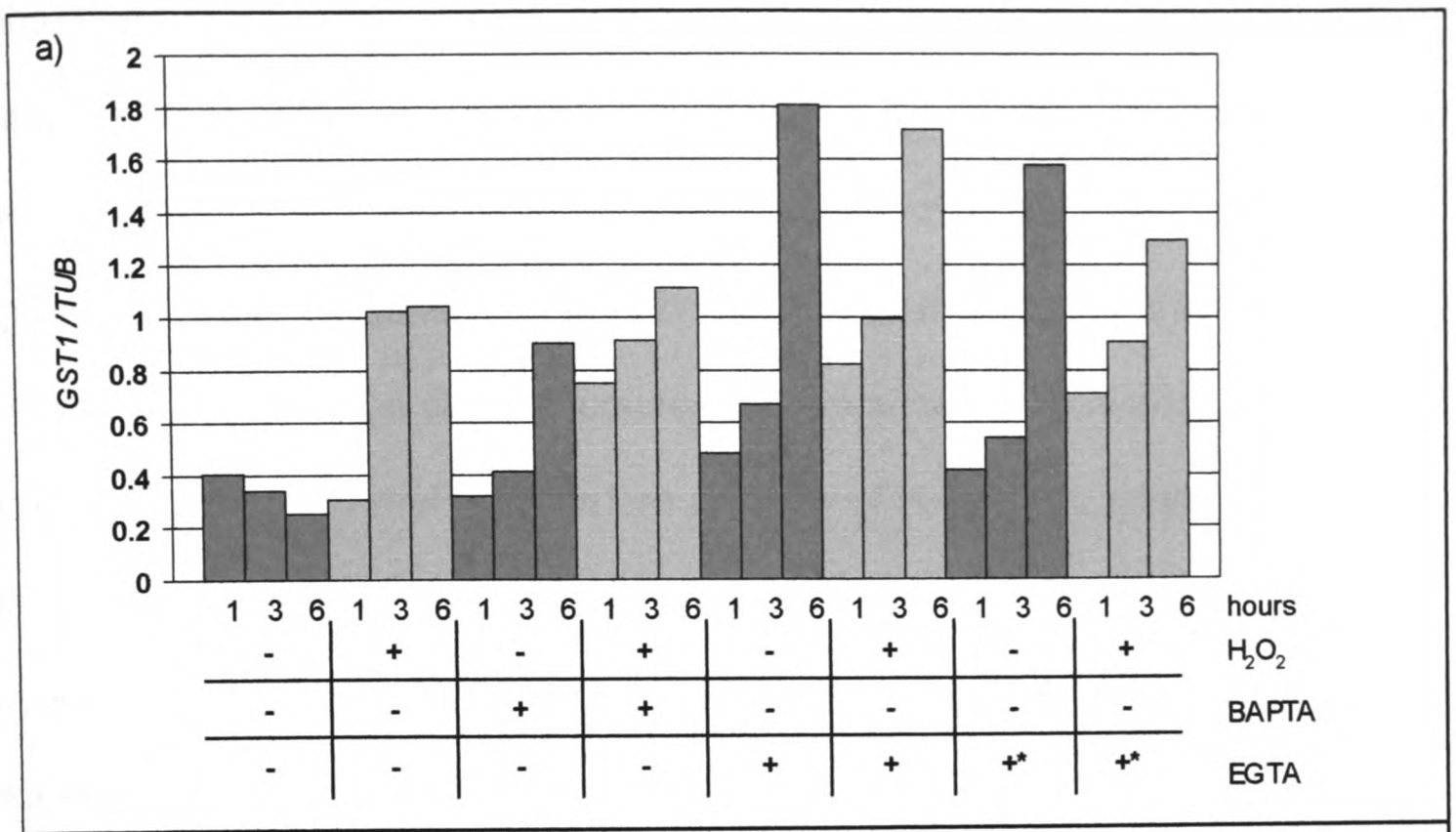

Figure 3.26: Effect of chelator treatment on antioxidant gene induction
Northern analysis and normalisation of gene induction data was carried out as described in Methods. 7 day old RLD1 seedlings were transferred into H_2O and allowed to recover for 2.5 h before addition of EGTA or BAPTA solution (final concentrations: 10 mM and 1 mM, respectively). Control samples remained in H_2O. After 30 min incubation, samples were placed into H_2O (control samples and EGTA samples with *) or fresh chelator solution. H_2O_2 was added where indicated (final concentrations: EGTA and BAPTA: as before; H_2O_2: 10 mM). Samples were frozen after 1 h, 3 h or 6 h. Total RNA was extracted, electrophoresed and transferred to nylon membrane. *GST1*, *APX1* and *β-TUBULIN* probes were labelled and hybridised to the RNA on the membrane. Bars represent *GST1* (a) and *APX1* (b) gene induction relative to *β-TUBULIN* mRNA levels.

Enhancement

Treatment with BSO, an inhibitor of glutathione synthesis, was shown to increase the first $[Ca^{2+}]_{cyt}$ elevation in response to H_2O_2 treatment (see section 3.2.1.5.3, Figure 3.19 a) and stabilise the second peak (Figure 3.20). In order to determine if this enhancement in the Ca^{2+} response affects antioxidant gene induction, seedlings were incubated in 10 mM BSO before addition of H_2O_2 (final concentration: 10 mM, Figure 3.27). A small enhancement in the increase in *GST1* and *APX1* levels was observed for BSO-treated samples as compared to control samples. This increase was reproduced in a second independent experiment (data not shown).

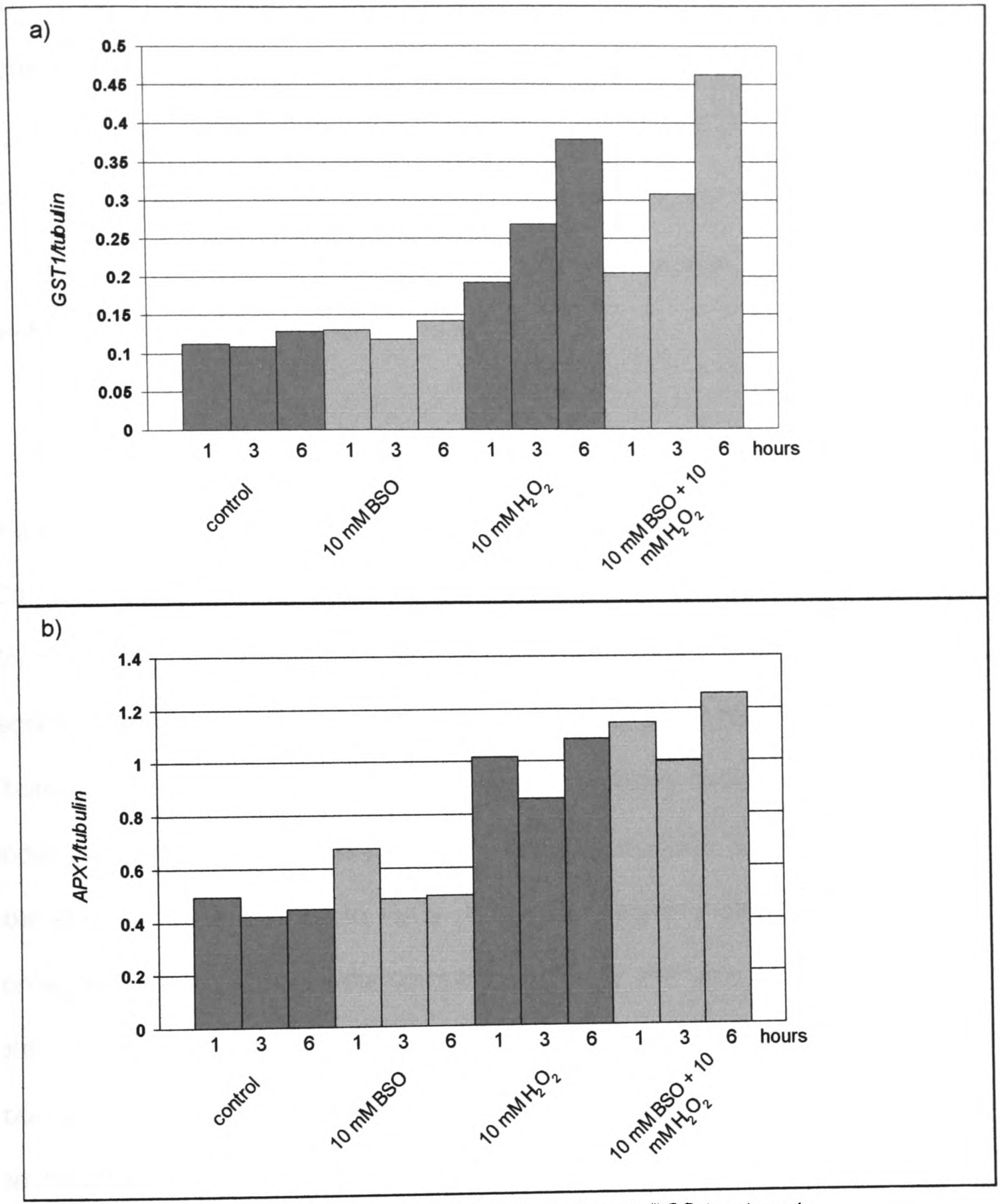

Figure 3.27: Enhancement of antioxidant gene induction by BSO treatment
Northern analysis and normalisation of gene induction data was carried out as described in Methods. 7 day old RLD1 seedlings were incubated in 5 ml BSO (10 mM) or H_2O ('control') for 16 h (overnight, in the dark). H_2O_2 (final concentration 10 mM) or H_2O was added the following day and samples removed and frozen after 1 h, 3 h or 6 h as indicated. Total RNA was extracted, electrophoresed and transferred to nylon membrane. *GST1*, *APX1* and *β-TUBULIN* probes were labelled and hybridised to the RNA on the membrane. Bars represent *GST1* (a) and *APX1* (b) gene induction relative to *β-TUBULIN* mRNA levels.

3.2.3. Calcium signalling mutants

Increases in $[Ca^{2+}]_{cyt}$ have been measured within seconds of stress application (see Figure 3.1, also Knight *et al.*, 1996) which suggests that Ca^{2+} elevations function as early components of signal transduction chains. Thus, by identifying mutants that are impaired in their Ca^{2+} response to a specific stimulus, it may be possible to identify the stress sensor mechanism itself.

3.2.3.1. Screen for mutants in the H_2O_2 calcium response

In order to identify genes involved in H_2O_2 perception and signalling upstream of the $[Ca^{2+}]_{cyt}$ response, RLD1.1 seed was mutagenised with EMS (by Lehle Seeds, Round Rock, TX, USA). 5 – 6 day old seedlings of this population were reconstituted and screened for a reduced $[Ca^{2+}]_{cyt}$ signal under the camera. Thereby, 225 of approximately 2200 seedlings were isolated. After a re-screen under the camera with 10 seedling per line (Figure 3.28), 97 lines still showed an aberrant $[Ca^{2+}]_{cyt}$ response to H_2O_2. In *in vitro* aequorin assays, only 26 of these contained total aequorin levels comparable to the wild-type seedlings: the average total luminescence count of five RLD1.1 (non-mutagenised) samples was 5,100,000 counts whereas the majority of isolated putative mutant lines exhibited counts below the cut off set at 4,000,000 (mean of 1 – 3 samples). In a further re-screen under the camera, three of the 26 lines showed an altered $[Ca^{2+}]_{cyt}$ response to menadione and H_2O_2 but normal responses in subsequent cold treatments (Figure 3.29).

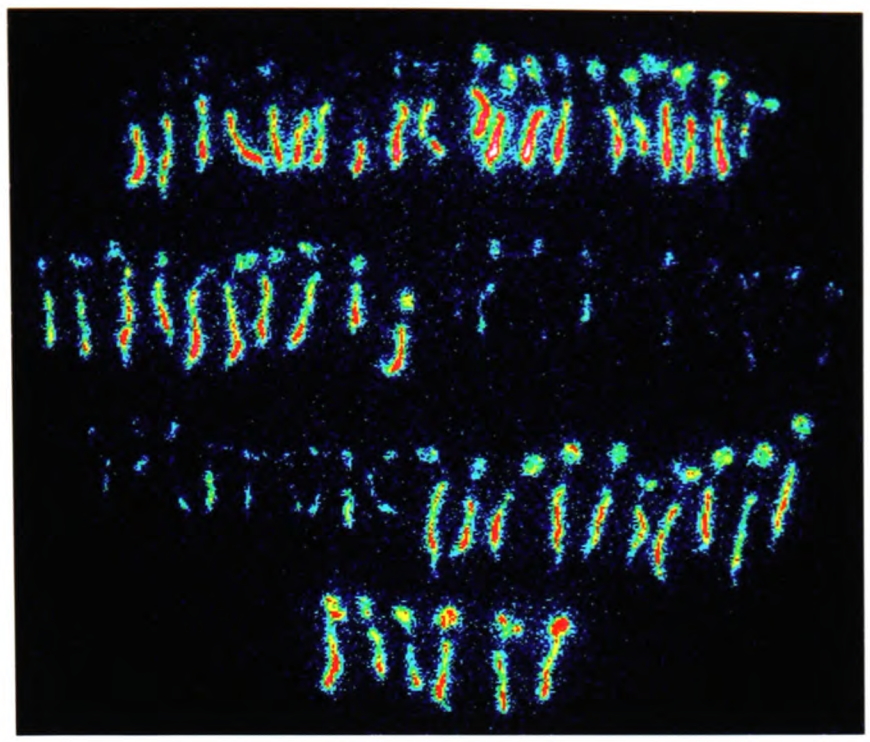

Figure 3.28: Re-screen of putative calcium signalling mutant lines
$[Ca^{2+}]_{cyt}$ was measured under the camera as described in Methods. Single EMS mutagenised RLD1.1 seedlings, isolated for their reduced Ca^{2+} signal in response to H_2O_2 challenge, were grown up and seed was harvested. Ten 6 day old seedlings of each line were re-screened on 10 mM H_2O_2 agar under the camera. The image above represents total photon counts over 25 min for six mutant lines (two lines in each row) and six wild-type seedlings in the bottom row.

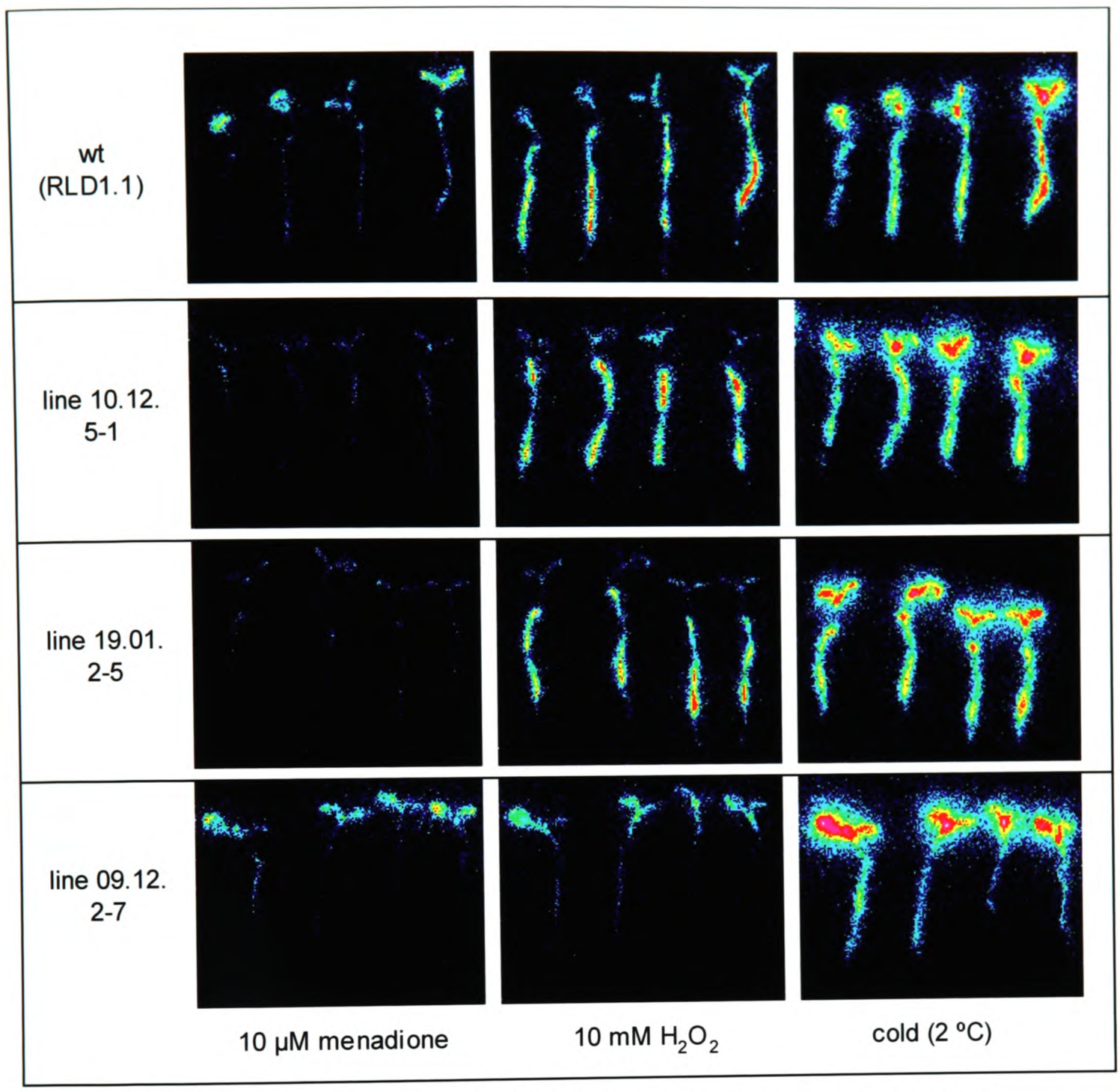

Figure 3.29: Mutants with a decreased Ca^{2+} signal in response to H_2O_2 but not cold
$[Ca^{2+}]_{cyt}$ was measured under the camera as described in Methods. 7 day old seedlings were lined up on moist filter paper and left to rest for 30 min. They were subsequently transferred (on the filter paper) to an agar plate containing 10 µM menadione and imaged for 30 min. The same seedlings were again transferred to a plate containing 10 mM H_2O_2 and imaged for another 30 min followed by cold treatment on the Peltier element in the camera (10 min at 4 °C). Images represent total luminescence counts.

3.2.3.2. Characterisation of the Ca^{2+} response in three mutant lines

Line 10.12. 5-1 and line 19.01. 2-5 showed a reduced signal in the cotyledons in response to H_2O_2 and menadone but exhibited a normal root response. Line 09.12. 2-7 showed a normal response in the cotyledons but a reduced second peak in the root. Further characterisation of the mutant lines by luminometry confirmed the

observations made under the camera for the former two mutant lines (10.12. 5-1 and 19.01. 2-5) (Figure 3.30) (but has not yet been carried out for line 09.12. 2-7).

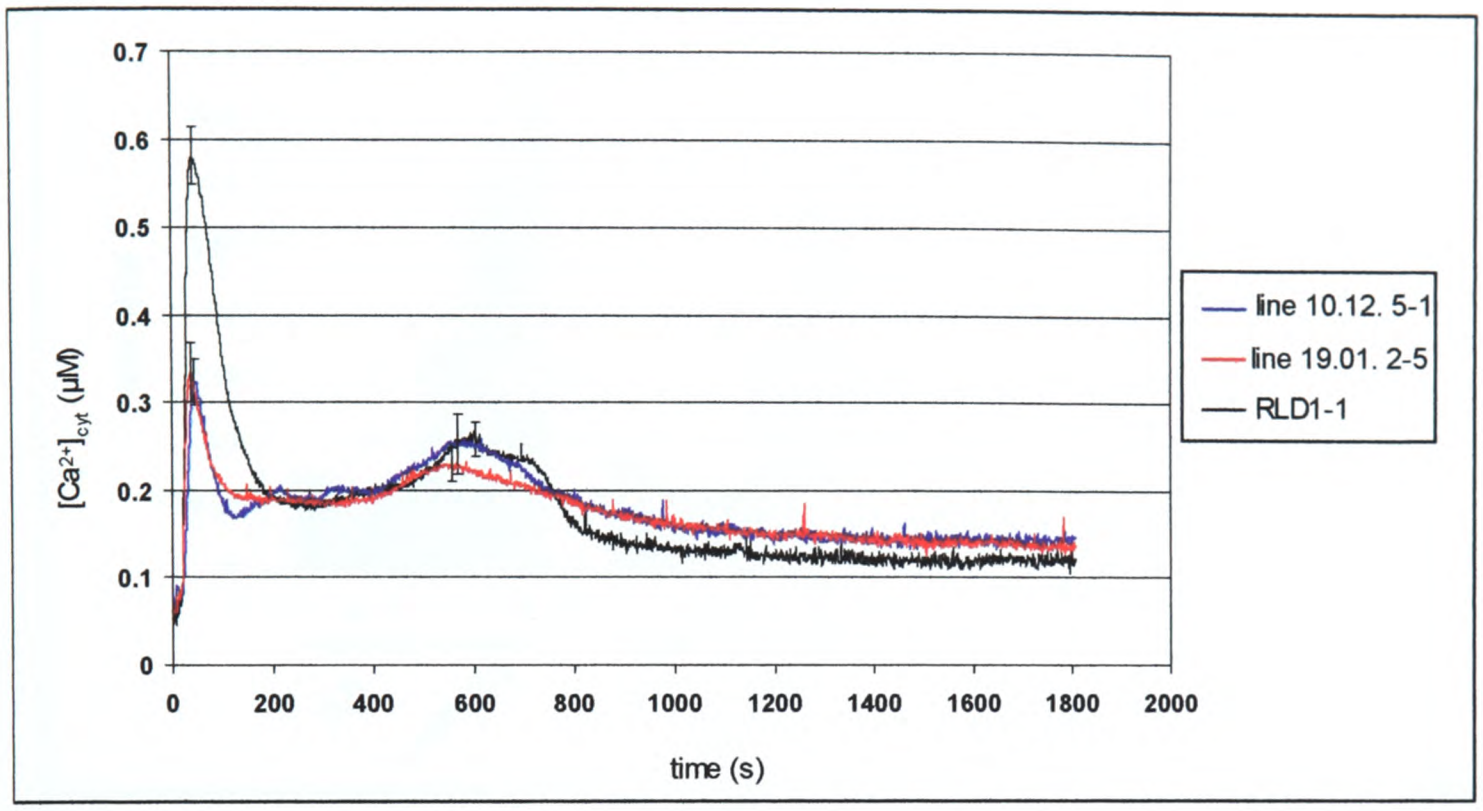

Figure 3.30: Reduced first $[Ca^{2+}]_{cyt}$ elevation in response to H_2O_2 in two mutant lines
$[Ca^{2+}]_{cyt}$ was measured by luminometry as described in Methods. 7 day old reconstituted seedlings were placed individually into plastic cuvettes containing 0.5 ml H_2O and left to rest for 30 min. At 5 s, H_2O_2 (final concentration: 10 mM) was added. At 1800 s, remaining aequorin was discharged. Traces represent the mean of three individual seedlings with error bars indicating standard error at that time point.

3.2.3.3. Comparison of GST1 *and* APX1 *induction in wild-type and signalling mutants*

Gene induction in response to 10 mM H_2O_2 in wild-type and mutant lines was compared to determine whether the reduced $[Ca^{2+}]_{cyt}$ response renders the mutant seedlings unable to fully induce antioxidant genes. Lines 10.12. 5-1 and 19.01. 2-5 (low signal in the cotyledons) induced *GST1* and *APX1* to the same extent as the RLD1.1 wild-type (Figure 3.31). Line 09.12. 2-7 (low root signal) showed increased mRNA levels of both genes in response to H_2O_2 challenge (Figure 3.32).

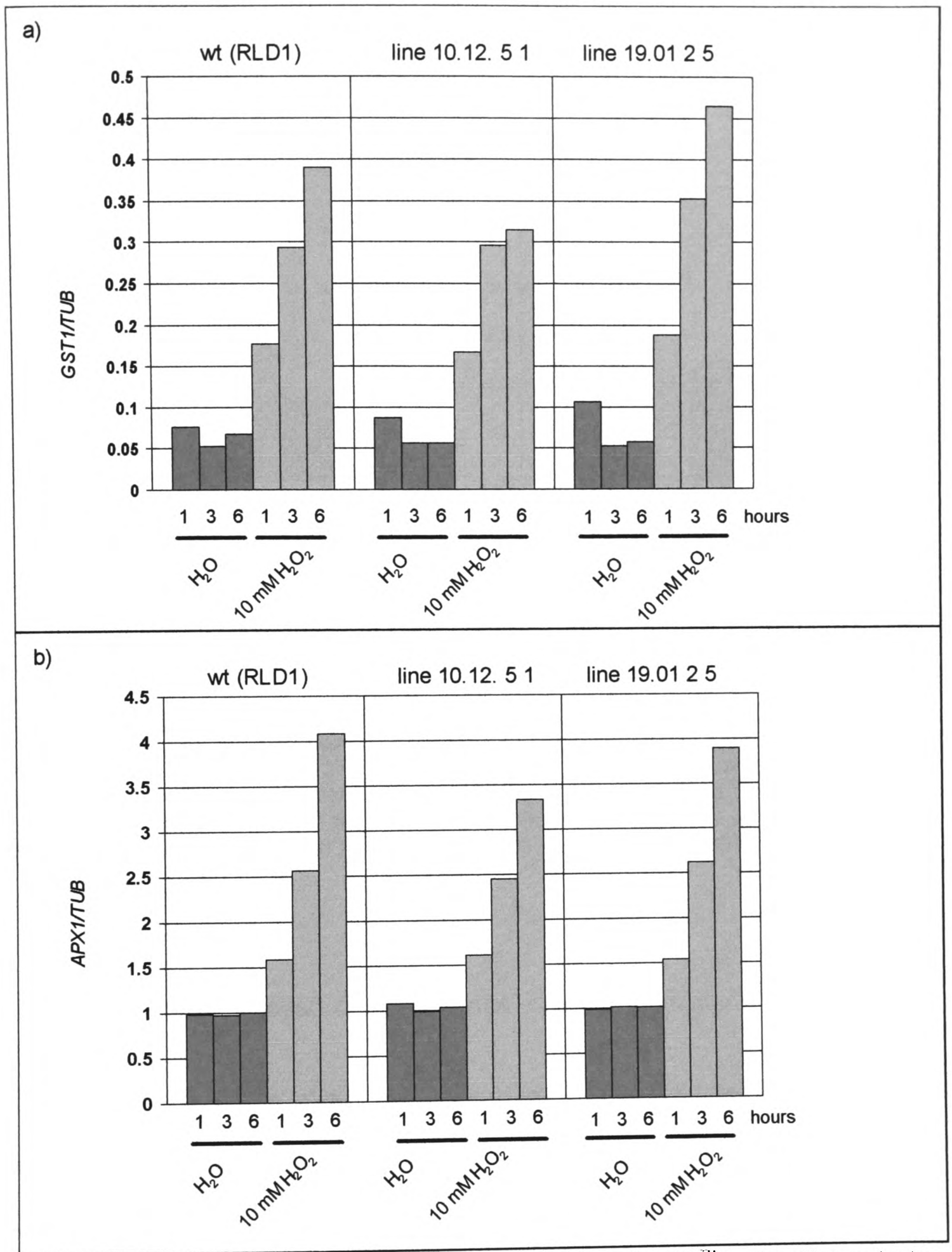

Figure 3.31: Antioxidant gene induction in response to H_2O_2 in the $[Ca^{2+}]_{cyt}$ signalling mutants (For legend, see Figure 3.32)

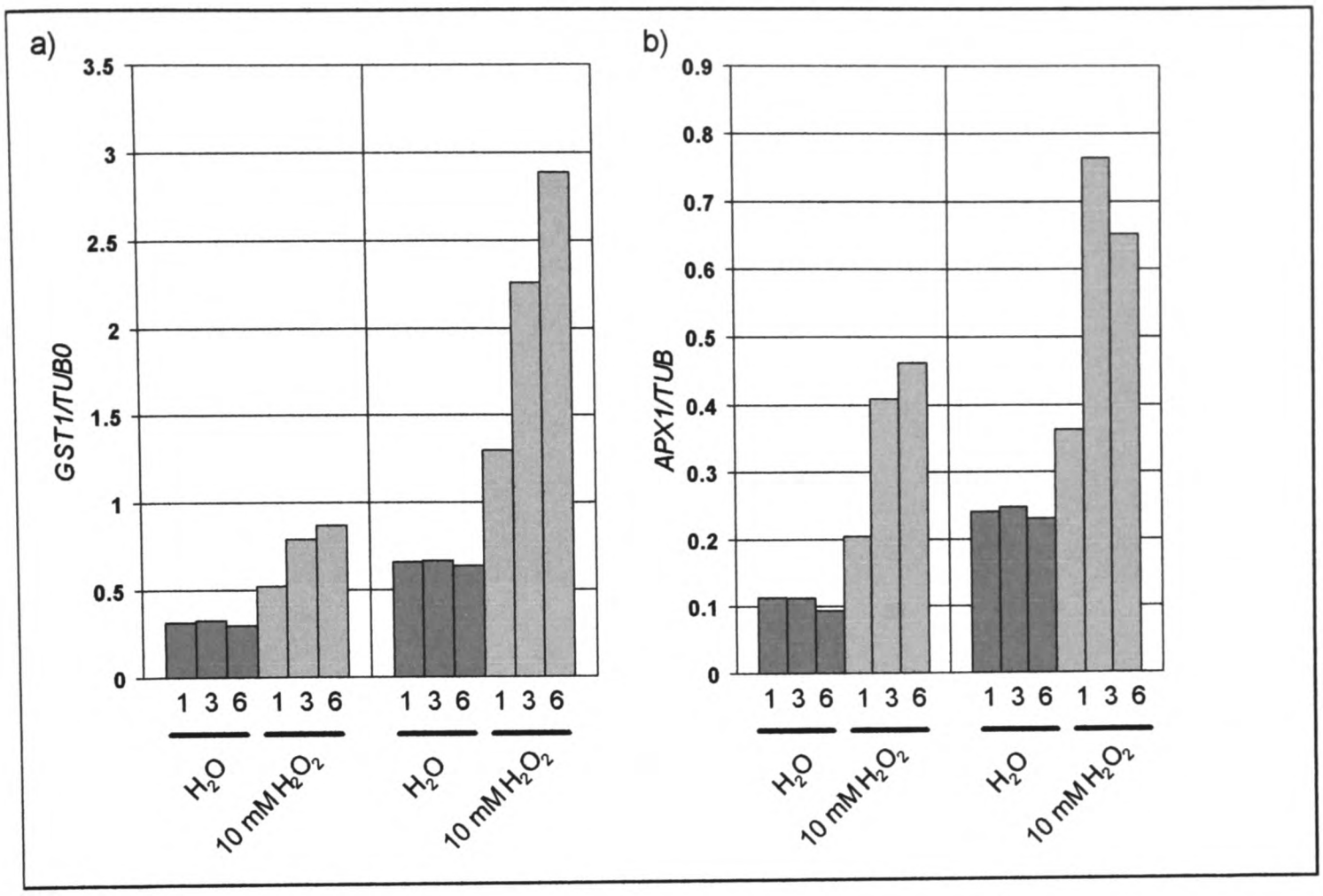

Figure 3.32: Antioxidant gene induction in response to H_2O_2 in the Ca^{2+} signalling mutant line 09.12. 2-7
Northern analysis and normalisation of gene induction data was carried out as described in Methods. 7 day old seedlings were transferred into H_2O and left to recover for 3 h before addition of H_2O_2 (final concentration 10 mM). After 1 h, 3 h and 6 h, samples were removed and frozen. Total RNA was extracted, electrophoresed and transferred to nylon membrane. *GST1*, *APX1* and *β-TUBULIN* probes were labelled and hybridised to the RNA on the membrane. Bars represent *GST1* (a) and *APX1* (b) gene induction relative to *β-TUBULIN* mRNA levels.

3.2.3.4. Phenotypic analysis of mutant lines – bleaching assay

Susceptibility to oxidative stress of mutant lines compared to the wild-type was assessed by transferring 7 day old seedlings to 10 mM H_2O_2 solution and monitoring bleaching of the cotyledons. Lines 10.12. 5-1 and 19.01. 2-5 did not show increased bleaching whereas line 09.12. 2-7 turned white within 3 days (Figure 3.33). Seedlings of this line are of a lighter green shade even before H_2O_2 treatment and have larger cotyledons than the wild-type or the other two mutant lines (data not shown).

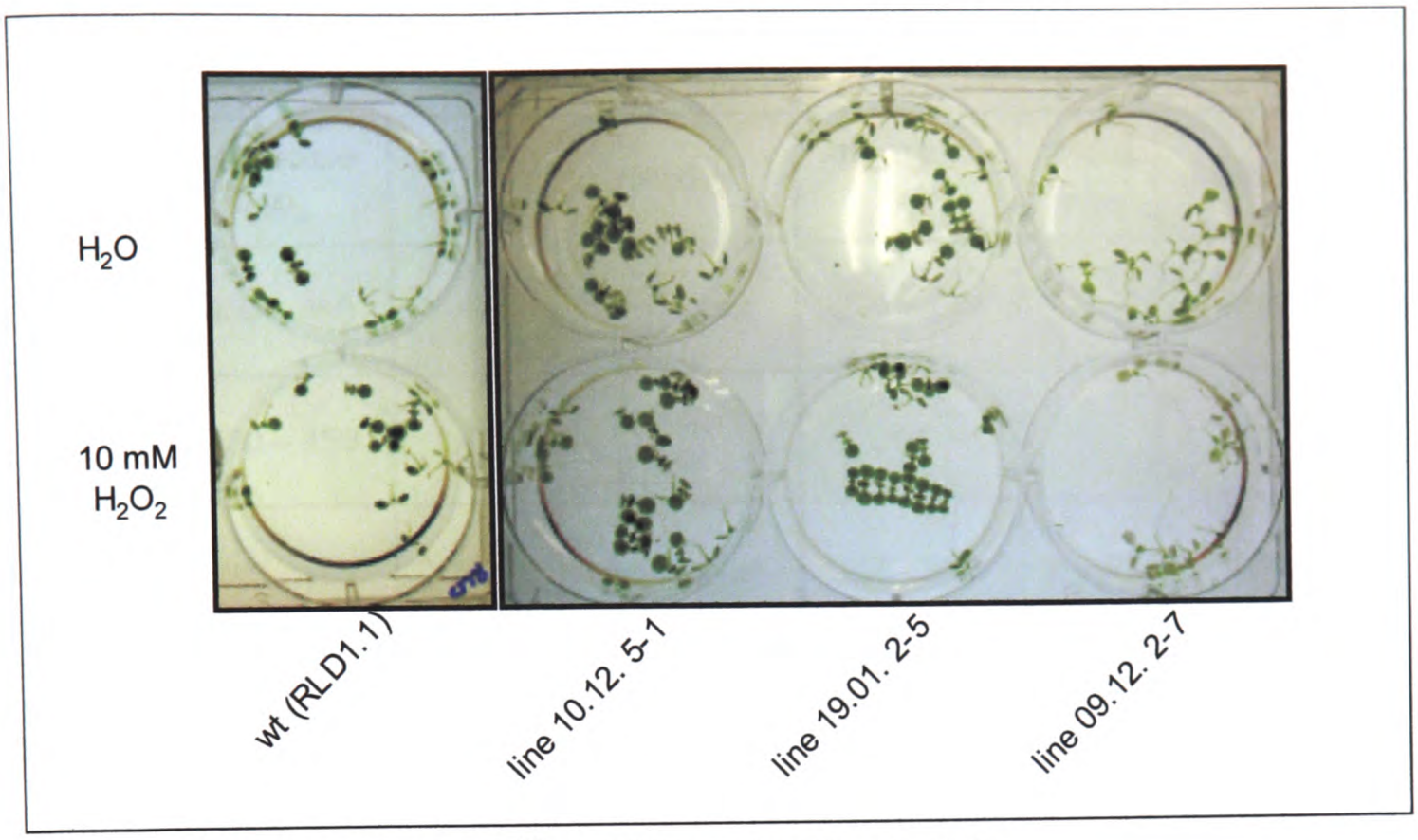

Figure 3.33: Survival assay of Ca^{2+} signalling mutant lines in H_2O_2
7 day old seedlings were transferred from MS agar plates into 10 mM H_2O_2 solution, placed into a growth cabinet (21 °C, 16 h light) and monitored for bleaching as an indicator of survival. The above image was taken 4 days after transfer.

3.3. Discussion

3.3.1. Specificity in calcium signalling in response to different AOS treatments

The specific calcium signature of a signalling pathway can be characterised by its amplitude, temporal pattern and location (McAinsh and Hetherington, 1998).

These three parameters were determined for $[Ca^{2+}]_{cyt}$ increases elicited by the oxidative stress agents H_2O_2, $^{\bullet}O_2^-$ (menadione) and ozone (summarised in Table 3.1), all of which have been shown to cause lipid peroxidation in plant cells (Pell *et al.*, 1997; Sweetlove *et al.*, 2002).

AOS	1st peak			2nd peak		
	magnitude (nM)	timing (s)	location	magnitude (nM)	timing (min)	location
H_2O_2	400 – 450	40	cotyledons	200 – 250	7 – 20	root
$O_2^{\bullet-}$	400 – 450	40	cotyledons + root	—	—	—
O_3	400 - 450	45	cotyledons*	200 - 250	7 – 20	root*

Table 3.1: Characteristics of the Ca^{2+} signatures triggered by different AOS treatments
Values indicate characteristics of $[Ca^{2+}]_{cyt}$ elevations in response to 10 mM H_2O_2, 10 µM menadione ($^{\bullet}O_2^-$) and 500 ppb ozone.
*: personal communication, Dr Nicola Evans, University of Lancaster

3.3.2. The rapid Ca^{2+} peak

A similar rapid $[Ca^{2+}]_{cyt}$ elevation was triggered by all AOS applied, starting 15 s after AOS addition with a maximum between 35 – 50 s and returning to near basal levels within 2 – 3 min (Figures 3.1 and 3.6). In addition, for both H_2O_2 and $^{\bullet}O_2^-$, the height of this Ca^{2+} rise was dose-dependent (Figure 3.1). This is consistent with previous reports of $[Ca^{2+}]_{cyt}$ elevations in response to H_2O_2 treatment in tobacco seedlings (Price *et al.*, 1994) and to O_3 fumigation in *A. thaliana* seedlings (Clayton *et al.*, 1999). Ca^{2+} elevations in response to menadione treatment have been observed in rat platelets (Mirabelli *et al.*, 1989) and human lung epithelial cells (McCormick *et al.*, 2000). In the latter study, it was proposed that menadione photochemistry rather than AOS production accounted for the observed rise in Ca^{2+}, supported by the observation that BSO treatment did not have an effect on the Ca^{2+} rise (McCormick *et al.*, 2000). However, in the present study, all experiments were carried out in the dark, making formation of photochemical products of menadione

unlikely, and AOS production was linked to the Ca^{2+} signature by demonstrating an effect of BSO on the height of the first Ca^{2+} peak (see section 3.2.1.5.3). Imaging under the photon-counting camera revealed that the early Ca^{2+} peak in response to H_2O_2 (Figures 3.4 and 3.7), $^{\bullet}O_2^-$ (Figure 3.8) and ozone (personal communication, Dr Nicola Evans, University of Lancaster) was located in the cotyledons.

3.3.3. The late Ca^{2+} peak

Interestingly, only H_2O_2 and ozone treatment triggered a second, late $[Ca^{2+}]_{cyt}$ rise, localised in the root, starting 4 – 10 min after stress application and lasting between 8 – 20 min (Figures 3.2 a and 3.5; Figure 3.9 and Dr Nicola Evans, personal communication, respectively). Further characterisation of this second Ca^{2+} elevation in response to H_2O_2 revealed that the root tissue needs to be in constant and direct contact with H_2O_2 for the full Ca^{2+} signature to occur (Figures 3.10 and 3.11). Challenge with menadione ($^{\bullet}O_2^-$) did not cause this second Ca^{2+} elevation (Figures 3.2 b and 3.8), indicating that the plant may be able to distinguish between different AOS treatments (see also section 6.2.3). It could be speculated that menadione generates $O_2^{\bullet-}$ in the shoot but not in the root, *e.g.* by redox cycling in the chloroplast. However, the early $[Ca^{2+}]_{cyt}$ elevation triggered in response to menadione treatment is also seen in parts of the root (Figure 3.8) and the response of this tissue is dependent on the presence of menadione (and hence not the result of shoot to root signalling, data not shown), indicating that $^{\bullet}O_2^-$ is indeed generated in root tissues.

3.3.3.1. *Variability*

In contrast to the first Ca^{2+} peak, the second Ca^{2+} peak triggered by H_2O_2 is much more variable in height and timing. The variability may be the result of differing conditions experienced by the plant prior to stress application. This explanation is supported by the finding that a 45 min rest period is required for the second elevation to occur at all (Figure 3.3), indicating that mechanical transfer of seedlings influences the Ca^{2+} signature.

3.3.3.2. *Accessibility of H_2O_2*

Challenging seedlings expressing aequorin in specific root cell types with H_2O_2 demonstrated that externally applied H_2O_2 has access to internal tissues and that the late second peak in the root is therefore not the result of delayed stimulation (Figure 3.12). Epidermal root cells displayed a pronounced early $[Ca^{2+}]_{cyt}$ elevation, possibly involving cells in the root crown that frequently exhibited a $[Ca^{2+}]_{cyt}$ rise concomitant with the shoot $[Ca^{2+}]_{cyt}$ increase (Figure 3.4).

The two phases of the Ca^{2+} signal thus indicate differences in the early signal transduction mechanism between shoot and root tissue. Interestingly, a recent study demonstrated that aequorin-expressing tobacco cell cultures also display a biphasic $[Ca^{2+}]_{cyt}$ signature in response to H_2O_2 challenge (Lecourieux *et al.*, 2002), with similar timing to the two $[Ca^{2+}]_{cyt}$ peaks observed in whole *A. thaliana* seedlings. It is surprising that both $[Ca^{2+}]_{cyt}$ peaks can be triggered in cell suspension culture cells despite the differential location in shoot and root in *A. thaliana* (Figure 3.4). Hence, either tobacco and *A. thaliana* differ in their Ca^{2+} signatures with respect to location

of the Ca^{2+} rise or some of the cells have differentiated within the cell suspension culture.

3.3.3.3. Possible role in cell death

It is possible that the root Ca^{2+} elevation is associated with cell death as the main root frequently ceases to grow subsequent to H_2O_2 treatment (data not shown), and as some RNA degradation is seen in H_2O_2-treated root samples (Figure 3.22). However, even if this signal were part of a death response, it is specific to H_2O_2 and ozone: treatment of seedlings with a lethal concentration of menadione (100 µM) did not trigger a second Ca^{2+} peak (data not shown). Application of 50 mM H_2O_2 to *A. thaliana* guard cells did not affect membrane integrity (Pei *et al.*, 2000) and infiltration of excised *A. thaliana* leaves with 10 mM H_2O_2 solution showed no substantial increase in cell death (Overmyer *et al.*, 2000), suggesting that at least the early (shoot-localised) Ca^{2+} signal observed in this study is not due to cytotoxic damage.

3.3.4. Which channels are activated by H_2O_2 and menadione?

Several channel blockers were tested for their ability to inhibit the H_2O_2- and menadione-triggered rapid rise in $[Ca^{2+}]_{cyt}$. Lanthanum chloride as well as ruthenium red were shown to be effective (Figure 3.13). Lanthanum also delayed and decreased the second $[Ca^{2+}]_{cyt}$ rise triggered by H_2O_2 and O_3 (Figures 3.15 and 3.16). In a number of plant species (the alga *Chara corallina*, *A. thaliana*, tomato and wheat), lanthanum has been shown to block plasma membrane Ca^{2+} channels (Tester and MacRobbie, 1990; Lewis and Spalding, 1998). Therefore, the ability of

lanthanum to decrease H_2O_2- and menadione-triggered $[Ca^{2+}]_{cyt}$ elevations indicates an extracellular origin of the Ca^{2+} ions. However, lanthanum also has been shown to block other cation channels, such as K^+ channels (Lewis and Spalding, 1998), and there is evidence that La^{3+} ions can enter the cytoplasm (Tester and MacRobbie, 1990) where they may block internal Ca^{2+} channels. Thus, the presented results can only be interpreted tentatively with respect to the origin of Ca^{2+} ions.

In animal cells, ruthenium red is a well known antagonist of (intracellular) ryanodine receptors, which are ion channels responsible for signal-dependent release of stored Ca^{2+} into the cytosol (Cibulsky and Sather, 1999). However, this compound also inhibits a wide range of Ca^{2+}-binding proteins and affects other cation channels, including plasma membrane-localised voltage-gated Ca^{2+} channels (Cibulsky and Sather, 1999). Therefore, inhibition of $[Ca^{2+}]_{cyt}$ elevations by ruthenium red does not indicate the source of Ca^{2+} ions.

If Ca^{2+} influx across the plasma membrane is essential for the H_2O_2- and menadione-triggered Ca^{2+} signatures, removal of the extracellular Ca^{2+} ions by chelation with EGTA and BAPTA would be expected to abolish the observed increases in $[Ca^{2+}]_{cyt}$. However, AOS challenge of seedlings incubated with EGTA or BAPTA frequently resulted in immediate $[Ca^{2+}]_{cyt}$ increases not seen with H_2O_2 or menadione treatment alone (compare Figures 3.17 a and 3.18 with Figure 3.1). This was particularly evident if seedlings were transferred back into water after incubation in chelator solution. A possible explanation for this observation is that chelator treatment leads to inhibition of Ca^{2+}-regulated Ca^{2+} ATPases. In control seedlings, these Ca^{2+} pumps are continuously active to remove Ca^{2+} ions 'leaking' into the cytosol. Chelator treatment could abolish this 'leak' and thus inhibit the Ca^{2+}-

dependent Ca^{2+} ATPase activity. By replacing external Ca^{2+} through transfer into fresh H_2O and immediately activating Ca^{2+} channels through H_2O_2 challenge, the influx of Ca^{2+} would not be buffered by Ca^{2+} pump activity, but instead cause an immediate and increased rise in $[Ca^{2+}]_{cyt}$. Alternatively, the effect on the calcium signature may result from the increased pH of the EGTA and BAPTA solutions (pH 7.3 – 8.7).

Transfer of seedlings into fresh BAPTA solution resulted in a decrease of the height of $[Ca^{2+}]_{cyt}$ elevations triggered by H_2O_2 and menadione challenge (Figures 3.17 b and 3.18), confirming that Ca^{2+} influx through plasma membrane Ca^{2+}-channels may be involved.

In conclusion, studies employing channel inhibitors and Ca^{2+} chelators indicate that H_2O_2 may trigger activation of plasma membrane Ca^{2+} channels. Further discussion on which type of Ca^{2+} channel may be activated upon H_2O_2 treatment is provided in Section 6.2.1.

3.3.5. The cellular redox balance – a possible sensing mechanism for oxidative stress

The rapid $[Ca^{2+}]_{cyt}$ elevation was similar in response to all AOS applied with respect to timing (*e.g.* Figures 3.1 and 3.9) and inhibition by lanthanum treatment (Figures 3.13 and 3.16). This consistent early peak may thus be triggered by changes in the cellular redox balance, an effect all AOS can be expected to have in common. In agreement with this hypothesis, reducing the cellular redox buffer by inhibition of glutathione synthesis, and thus reducing the ability of the cell to maintain a high GSH/GSSG ratio, led to an increase in the magnitude of the early Ca^{2+} peak in

response to H_2O_2 and menadione challenge (Figures 3.19). This result is consistent with a previous study in tobacco, demonstrating that treatments which increase or reduce the cellular GSH/GSSG ratio have opposite effects on the rise in $[Ca^{2+}]_{cyt}$ (Price *et al.*, 1994). BSO treatment was also shown to have a stabilising effect on the root-localised second Ca^{2+} peak in response to H_2O_2 challenge (Figure 3.20). This observation indicates that the redox balance also plays a role in this late $[Ca^{2+}]_{cyt}$ elevation. Hence, the signal transduction pathway in response to AOS may be mediated by redox signalling through changes in the GSH/GSSG ratio (see section 1.1.3) upstream of changes in $[Ca^{2+}]_{cyt}$. However, other additional mechanisms must be involved in H_2O_2 signalling in the lower root, as menadione treatment triggers a much smaller $[Ca^{2+}]_{cyt}$ elevation in this tissue than observed in response to H_2O_2 challenge (Figures 3.4 and 3.8).

3.3.6. A role for $[Ca^{2+}]_{cyt}$ elevations in AOS-mediated induction of antioxidant defenses

In order to establish a link between early AOS signalling events and antioxidant gene induction, the necessity of the Ca^{2+} signature for full induction of *GST1* and *APX1* was investigated. *GST1* (Levine *et al.*, 1994) and *APX1* (Storozhenko *et al.*, 1998) had previously been shown to be induced by AOS and oxidative stress treatment. In the present study, *GST1* and *APX1* transcript levels increased in response to H_2O_2 treatment (Figure 3.21 a) and this increase was located mainly in the shoot for *GST1* (Figure 3.22), coinciding with the location of the first Ca^{2+} elevation (Figure 3.4). On the other hand, *APX1* levels were high in the roots in control as well as H_2O_2-treated samples, possibly as a result of stress experienced

during removal of the plants from agar. In this experiment, changes in total *APX1* levels in response to H_2O_2 treatment would have been masked by the high background levels in the roots. However, plants used in this Northern analysis were 14 days old and thus had extensive roots which were difficult to remove from agar without damaging. All other Northern analysis data presented (except Figure 3.25) stem from 7 day old seedlings whose roots did not undergo the same amount of stress during transfer and thus may have had lower induction levels of *APX1*. Accordingly, *APX1* expression was markedly increased in response to H_2O_2 treatment in other experiments (Figures 3.21, 3.23, 3.24, 3.25, 3.26 b, 3.27 b).

3.3.6.1. Timing of the Ca^{2+} signature

The importance of the timing of the $[Ca^{2+}]_{cyt}$ elevations was investigated by interrupting the Ca^{2+} signature at different stages by removing seedlings from H_2O_2 solution (Figure 3.23). The continued presence of H_2O_2 was previously shown to be required for occurrence of the second Ca^{2+} peak (Figure 3.10). Northern analysis suggests that H_2O_2 needs to be present for the duration of the Ca^{2+} signature and beyond for full induction of *GST1* and *APX1* (Figure 3.23). This indicates that other signals, in addition to the relatively early calcium signal, operate at later time points in transducing H_2O_2 perception. Nevertheless, increases in expression of the two antioxidant genes reflect the length of incubation in H_2O_2, with longer incubations resulting in higher transcript levels (Figure 3.23).

3.3.6.2. *Magnitude of the $[Ca^{2+}]_{cyt}$ elevations*

The importance of the magnitude of the $[Ca^{2+}]_{cyt}$ elevations was investigated by modulating the height of the first Ca^{2+} peak. As previously demonstrated, incubation with the Ca^{2+} channel blocker lanthanum partially inhibited the first rise in Ca^{2+} in response to H_2O_2 treatment (Figures 3.14 and 3.15); whereas, reduction of the cellular glutathione content by incubation with BSO enhanced this peak (Figures 3.19 a and 3.20). Accordingly, lanthanum treatment decreased *GST1* and *APX1* induction in response to H_2O_2 treatment (Figure 3.24); whereas, incubation with BSO enhanced their expression slightly (Figure 3.27). The effect of lanthanum upon gene induction in the shoot, the site of the first Ca^{2+} elevation, was investigated. In this location, lanthanum treatment inhibited induction of *GST1*, whereas only a very small effect on *APX1* transcript levels was observed (Figure 3.25). Hence, the magnitude of the early $[Ca^{2+}]_{cyt}$ elevation in response to H_2O_2 treatment corresponded to the magnitude of *GST1* induction whereas induction of *APX1* was not affected in this tissue. However, lanthanum decreased H_2O_2-triggered induction of *APX1* transcript levels in whole seedlings (Figure 3.24), indicating that transcription of this gene may have been affected in the root tissue; hence the second $[Ca^{2+}]_{cyt}$ elevation may control *APX1* induction.

In a previous study, the role of the ozone-triggered biphasic Ca^{2+} signature in *GST1* induction was investigated (Clayton *et al.*, 1999). The authors speculated that only the second, but not the first, Ca^{2+} peak was inhibited by lanthanum treatment and consequently that this peak was involved in *GST1* induction. However, upon closer inspection of the data, the height of the first Ca^{2+} peak had also decreased.

Therefore, data presented here are consistent with these previous results (if not with the interpretation).

Changes in the Ca^{2+} signature in response to treatment with the calcium chelators EGTA and BAPTA (Figure 3.17) could not be related to changes in induction of *GST1* and *APX1* (Figure 3.26). Chelator treatment in the absence of AOS challenge caused strong induction of *GST1* and slight induction of *APX1*. In both cases, H_2O_2 treatment increased transcript levels even further. This could be linked to the immediate Ca^{2+} rise observed following addition of H_2O_2 and menadione (see above and section 3.2.1.5.2).

3.3.7. Calcium signalling mutants

The importance of the magnitude of the Ca^{2+} signature in response to H_2O_2 treatment was also investigated by a genetic approach which invovled screening EMS-mutagenised seedlings for altered Ca^{2+} responses. Thus, three lines were identified which displayed a reduced Ca^{2+} signature in response to H_2O_2 challenge but were able to respond normally to cold shock (Figures 3.29 and 3.30). In two of these lines (lines 10.12. 5-1 and 19.01. 2-5), the first Ca^{2+} elevation is decreased without change in the second rise. A third line (line 09.12. 2-7) displays a lower second Ca^{2+} peak but responds normally in the cotyledons. This indicates that the shoot and root signal are triggered by different mechanisms. However, it needs to be confirmed that root aequorin levels of the 'root mutant' are comparable to wild-type levels. Also, a low shoot signal could be caused by reduced access of H_2O_2, *e.g.* through a thicker cuticle, offering an explanation that does not involve altered Ca^{2+} responses. *GST1* and *APX1* induction upon H_2O_2 treatment was not altered in

the lines with a decreased first $[Ca^{2+}]_{cyt}$ elevation (Figure 3.31). This may indicate that downstream responses in general are not affected, and consequently that Ca^{2+} signalling is not involved in initiating protective mechanisms, or that the plant may be able to compensate for the mutation. Also, genes/processes other than *GST1* and *APX1* may be influenced but were not tested. In the root mutant (line 09.12. 2-7), *GST1* and *APX1* transcript levels were increased, even before stress challenge (Figure 3.32). In addition, this mutant bleached much faster in H_2O_2, despite increased transcript levels of antioxidant enzymes. Hence, other detoxification mechanisms could be disrupted in this line which cannot be compensated for by an increase in *GST1* and *APX1* levels. The phenotype may indicate an inability to transduce the oxidative stress signal due to the reduced Ca^{2+} signal, which the plant attempts to compensate for by increasing *GST1* and *APX1* transcription by Ca^{2+}-independent mechanisms (even during basal oxidative stress). However, other mutations, independent of the mutation affecting the Ca^{2+} signature, could also account for the altered phenotype of this line.

In summary, three main conclusions can be drawn from the presented data:

a) The plant may is able to distinguish between different AOS treatments as different Ca^{2+} signatures are generated in response to H_2O_2, $^{\bullet}O_2^-$ and O_3.

b) The first Ca^{2+} elevation is necessary for full induction of *GST1* transcription and its magnitude determines the strength of induction whereas the second Ca^{2+} elevation may be necessary for *APX1* induction.

c) AOS may be sensed through changes in the cellular redox status

4. OX1 – a protein kinase involved in H_2O_2 signalling

4.1. Introduction

4.1.1. Protein kinases involved in H_2O_2 signalling

Until recently, H_2O_2 was viewed mainly as a toxic molecule. However, the past decade has supplied numerous examples where H_2O_2 generation was initiated by the plant itself and where H_2O_2 functioned as a signalling molecule, necessary for triggering downstream responses (see section 1.2). Despite extensive data demonstrating the role of H_2O_2 in signalling, little is known about the identity of signalling components linking H_2O_2 generation to changes in gene expression. Protein phosphorylation catalysed by protein kinases is a common element in signal transduction cascades. Among the kinases, MAPK cascades are critical for the response of cells to changes in their environment (Buck *et al.*, 2001), *e.g.* in yeast in response to hyperosmolarity (O'Rourke *et al.*, 2002). In animal cells, MAPK activation in response to AOS accumulation has been reported. For example, the MAPKs, extracellular signal-regulated protein kinase2 (ERK2), the c-Jun N-terminal kinase and the p38 kinase were all rapidly activated by H_2O_2 treatment of human cell cultures (Guyton *et al.*, 1996).

Plant MAPK cascades have also been implicated in stress signalling. Thus, rapid activation of plant MAPKs can be induced by wounding (Seo *et al.*, 1995; Usami *et al.*, 1995; Ichimura *et al.*, 2000), cold (Jonak *et al.*, 1996; Ichimura *et al.*, 2000), osmotic stress (Ichimura *et al.*, 2000; Droillard *et al.*, 2002), virus infection (Zhang and Klessig, 1998b), elicitor treatment (Desikan *et al.*, 2001a) and pathogen attack (Romeis *et al.*, 1999). All these processes are associated with induction of H_2O_2

accumulation (see sections 1.2 and 1.7), pointing to a global role for H_2O_2 in MAPK cascade activation. In particular, two MAPKs have emerged that are activated by a wide range of these stresses as well as directly by challenge with H_2O_2: AtMPK3 and AtMPK6 in *A. thaliana* and their orthologues in tobacco (wound-inducible protein kinase (WIPK) and salicylic acid-inducible protein kinase (SIPK), respectively) and alfalfa (stress-activated MAPK (SAMK) and and salt stress-inducible MAPK (SIMK)).The activation pattern of AtMPK3 and AtMPK6 and their orthologues implicates these kinases in signal transduction events downstream of H_2O_2 and evidence in favour of this hypothesis is summarised below.

Little is known about the role of other classes of kinases in mediating responses to AOS. In animal cells, several protein kinase C (PKC) isoforms can be activated by H_2O_2, independently of the well-studied lipid second messenger diacylglycerol (Dröge, 2002). In plants, a receptor-like kinase gene, *RLK3*, induced by H_2O_2 (as well as menadione, salicylic acid and pathogen attack) was isolated from *A. thaliana* (Czernic *et al.*, 1999). Additionally, a range of kinase genes was induced by H_2O_2 in *A. thaliana* cell suspension cultures in a microarray experiment (Desikan *et al.*, 2001b). Recently, NDP kinase2 (NDPK2) was shown to be activated in response to H_2O_2 treatment, and overexpression of the corresponding gene conferred enhanced tolerance to several AOS-generating environmental stresses (Moon *et al.*, 2003). NDPK2 is known to play a role in maintaining intracellular levels of nucleotides, but has also been implicated in the signal transduction chain downstream of phytochrome A as well as in the UV-B and heat stress signalling. Upon H_2O_2 application, this kinase appears to regulate activation of the MAPKs AtMPK3 and AtMPK6, placing it upstream of the MAPK cascade (Moon *et al.*, 2003).

4.1.2. MAPK activation in response to direct H_2O_2 application

MAPK activation by H_2O_2 has been demonstrated in kinase activity assays. Thus, H_2O_2 treatment of *A. thaliana* suspension cultures, as well as infiltration of the H_2O_2-generating system glucose/glucose oxidase into *A. thaliana* leaves, resulted in activation of kinases with MAPK characteristics (Desikan *et al.*, 1999; Grant *et al.*, 2000a). Ozone fumigation, as well as H_2O_2 and $^{\bullet}O_2^-$ incubation of tobacco cell cultures, also activated a MAPK, probably SIPK, in a calcium-dependent process (Samuel *et al.*, 2000). AtMPK6, but not AtMPK4, was shown to be activated by H_2O_2 (and $^{\bullet}O_2^-$ treatment) in *A. thaliana* cell cultures (Yuasa *et al.*, 2001). In a transient transfection approach, a MAPKKK, ANP1, and two MAPKs, AtMPK3 and AtMPK6, were shown to be involved in the MAPK cascade triggered by H_2O_2 treatment of *A. thaliana* leaf protoplasts (Kovtun *et al.*, 2000). In the latter study, AtMPK3 and AtMPK6 were activated by H_2O_2 challenge and constitutively active forms of these kinases were able to induce the H_2O_2-responsive *GST6* promoter (fused to a luciferase reporter gene) in the absence of H_2O_2. In summary, H_2O_2 can activate MAPK cascades involving AtMPK3 and AtMPK6 and their homologues in other plant species, leading to activation of defence mechanisms.

4.1.3. MAPK activation as a result of oxidative burst-inducing stimuli

AtMPK3 and AtMPK6 are also activated in response to a range of stimuli shown to trigger oxidative bursts (see sections 1.2 and 1.7). Three of these MAPK-activating stresses are discussed below.

4.1.3.1. Wounding

Wounding induced activation of *A. thaliana* AtMPK4 and AtMPK6 (Ichimura *et al.*, 2000), tobacco SIPK (Zhang and Klessig, 1998a) and WIPK (Seo *et al.*, 1999) as well as alfalfa SAMK (Bögre *et al.*, 1997). Overexpression of WIPK was reported to increase JA levels and downstream expression of a protease inhibitor gene (Seo *et al.*, 1999), demonstrating a role for kinase activity in triggering defensive mechansims to wounding. However, a connection between wounding, H_2O_2 generation and MAPK activation has not been investigated.

4.1.3.2. Pathogenesis

Elicitor treatment has also been shown to initiate MAPK signalling. For example, MAPK cascade activation by the bacterial elicitor flagellin was demonstrated in leaf protoplasts transiently expressing a variety of MAPKs, MAPKKs and MAPKKKs (Asai *et al.*, 2002). The results map out a complete MAPK module (as well as activation of downstream transcription factors), including the MAPKKK AtMEKK1, the MAPKKs AtMKK4 and AtMKK5 and the MAPKs AtMPK3 and AtMPK6. Flagellin has been shown to cause H_2O_2 generation in *A. thaliana* leaves (Gomez-Gomez *et al.*, 1999); however, flagellin-mediated activation of these MAPKs differed from H_2O_2-triggered activation as constitutively active ANP1, which can mimic the H_2O_2

signal and induce the H_2O_2-responsive *GST6* promoter (Kovtun *et al.*, 2000), was unable to activate AtMKK4 and AtMKK5. In addition, constitutively active AtMKK4 and AtMKK5 were able to activate AtMPK3 and AtMPK6, which were also activated in response to H_2O_2, but did not induce expression of *GST6*. Therefore, the MAPK cascade triggered by flagellin and H_2O_2 both involved activation of AtMPK3 and AtMPK6 but differ in other respects (*e.g.* response gene induction). AtMPK6 (but not AtMPK3) was also shown to be rapidly activated in cell cultures and leaf strips by treatment with bacterial, fungal and plant-derived elicitors (Nuehse *et al.*, 2000). Accordingly, SIPK was activated in tobacco cell cultures by treatment with fungal and plant-derived elicitors (Zhang *et al.*, 1998) and both SIPK and WIPK were activated in tobacco leaves by viral infection, with activation of WIPK shown to depend on *R* gene interaction (Zhang and Klessig, 1998b). SIPK and WIPK were also activated in tobacco cells expressing a tomato resistance gene on elicitation with the complementary bacterial avirulence product (Romeis *et al.*, 1999). However, this activation was not dependent on the oxidative burst as demonstrated by pre-treatment with DPI. Similarly, infiltration of *A. thaliana* leaves with the bacterial elicitor harpin caused activation of AtMPK6 and AtMPK4, which was not affected by catalase or DPI; whereas, H_2O_2 treatment only activated AtMPK6 but not AtMPK4 (Desikan *et al.*, 2001a). Interestingly, the *Atmpk4* mutant displays increased resistance to virulent pathogens and constitutive *PR* gene expression due to elevated SA levels but is impaired in induction of the JA-responsive genes *PDF1.2* and *THI2.1* (Petersen *et al.*, 2000), indicating a role in pathogen- and wound-inducible signal transduction.

4.1.3.3. Ozone

The role of SIPK in mediating responses to ozone were investigated in transgenic tobacco lines overexpressing or suppressing (by RNAi) SIPK (Samuel and Ellis, 2002). Both, up-regulation and down-regulation of this kinase caused increased sensitivity to ozone manifest in lesion formation and increased accumulation of H_2O_2. Downstream induction of the antioxidant genes *APX* and *GST* was differently affected, indicating that lesion formation may be triggered by different mechanisms in the two transgenic lines: The SIPK suppressor may accumulate H_2O_2 due to delayed induction of both antioxidant enzymes whereas the overexpressor may induce increased H_2O_2 generation in an oxidative burst, similar to H_2O_2 accumulation seen in MAPK-mediated cell death (Ren *et al.*, 2002). This hypothesis is substantiated by the observation that expression of constitutively active NtMEK2, the upstream MAPKK of SIPK and WIPK, leads to cell death which is preceded by activation of endogenous SIPK and WIPK (Yang *et al.*, 2001). In addition, expression of constitutively active SIPK (but not WIPK) also leads to cell death (Zhang and Liu, 2001). Thus, the duration of SIPK activation may determine the outcome, with short activation triggering induction of cellular defenses and prolonged induction resulting in execution of a cell death program (Yang *et al.*, 2001).

In summary, both direct application of exogenous H_2O_2 and H_2O_2 originating from oxidative bursts involve activation of AtMPK3 and AtMPK6 in *A. thaliana* or their homologues in other plant species. This MAPK activation leads to induction of downstream processes. Despite the convergence on AtMPK3 and AtMPK6, different pathways employ distinct MAPK cascade modules, as demonstrated by the H_2O_2 and flagellin MAPK cascades (Kovtun *et al.*, 2000; Asai *et al.*, 2002). Differential induction of downstream genes indicates that additional factors determine the specificity of the downstream response.

The aim of this study was to

- identify other protein kinases involved in transducing a H_2O_2 signal
- placethe identified OX1 kinase into a signal transduction cascade linking stress perception and induction of protective mechanisms
- characterise the role of OX1 in response to various stresses and in developmental processes

4.2. Results

Kinases are common components of signal transduction cascades and have been shown to be involved in stress signalling pathways in many organisms including *A. thaliana*. Phosphorylation by kinases is a fast response following signal perception and does not require transcription of the kinase gene itself; however, a correlation between kinase activation and up-regulation of transcription of the kinase gene encoding it is often detected (Hirt, 1999).This observation was exploited to identify kinases involved in H_2O_2 signalling by differential display of kinase- encoding cDNA sequences, amplified by PCR. A kinase gene was identified in this way and given the name *OX1*, for *'OXIDATIVE STRESS-INDUCIBLE1'* kinase.

4.2.1. Isolation of *OX1*

4.2.1.1. Differential display of kinase cDNA fragments

7 day old RLD1 seedlings were incubated for various time periods in 10 mM H_2O_2. The cDNA obtained from these samples was used for PCR amplification using degenerate primers complementary to sequences conserved in kinases. After size fractionation of the amplified fragments, kinase gene induction was detected by comparing band intensities for H_2O_2 treatment with the water control. One fragment was present at a higher level in H_2O_2-treated samples (Figure 4.1). This fragment was cloned into pUC18 and sequenced.

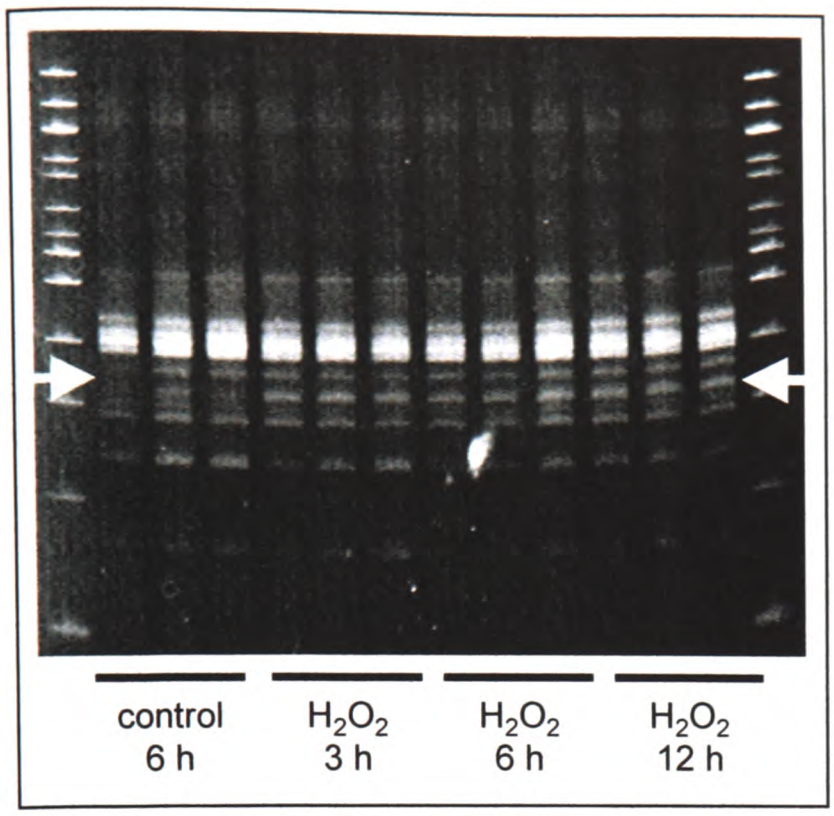

Figure 4.1: Differential display of kinase cDNAs induced by 10 mM H_2O_2
7 day old RLD1 seedlings were incubated for 3, 6 or 12 h in 10 mM H_2O_2 (each in triplicate) and the samples frozen in liquid nitrogen. RNA extraction, cDNA synthesis and PCR amplification of DNA with kinase-specific primers was performed as described in Methods. 15 µL samples of PCR product were fractionated on a 6.67 % TBE polyacrylamide gel, stained with SYBR Green and visualised on the UV-transilluminator. The white arrows indicate the position of the excised and cloned band (size ~ 300 bp). Markers: 100 bp ladder.

4.2.1.2. Identification of OX1

Two different sequences were recovered from the six clones sequenced. By performing a BLAST search for sequence homologies (Altschul *et al*, 1997), part of a genomic clone of chromosome 3 (AB026647) was found to be identical to one of the isolated sequences. The sequence falls into a predicted ORF (At3g25250) coding for a protein with similarity to protein kinases. The other fragment is part of a predicted ORF coding for a transmembrane protein (At5g41860) of unknown function.

In order to isolate the complete kinase gene, the adjacent sequence was entered into exon/intron prediction programs (*e.g.* Genscan, Chris Burge, MIT, http://genes.mit.edu/GENSCAN.html). A 1381 bp sequence was predicted with a 118 bp intron, corresponding to 421 amino acids and a protein of 47.6 kDa molecular weight. Two ESTs for At3g25250 were identified, AI998555 and AV539923 from Columbia rosettes and roots, respectively, but these do not extend to the 5' terminus of the predicted gene. The predicted start codon was verified by

PCR from cDNA using forward primers just upstream of the predicted start ATG (Figure 4.2). This analysis confirmed that the predicted ATG is present in the cDNA and that the 5' UTR is probably 40 to 80 bp long.

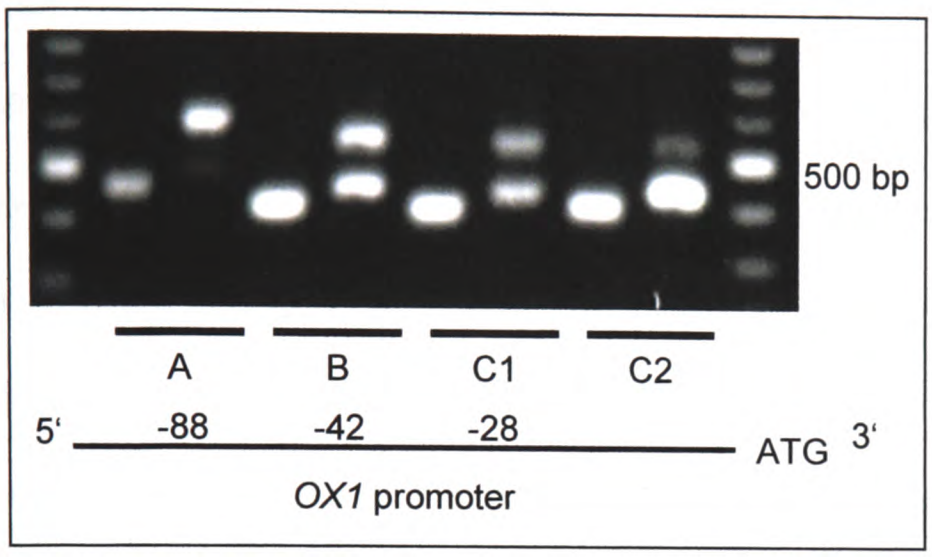

Figure 4.2: 5' UTR analysis of the *OX1* gene
Fragments of *OX1* were amplified by PCR using primers on either side of the predicted ATG. cDNA from 1 h, 10 mM H_2O_2 (A, B and C1) or 10 µM menadione (C2) was used as template. A, B and C are primers complementary to sequences upstream of the start codon at positions indicated in the diagram below the gel picture. For each of these primers, a PCR reaction with a reverse primer upstream (left lane, primer 'RACE400') or downstream (right lane, primer 'revcheck') of the intron was run. Presence of a large fragment (> 500 bp) indicates genomic contamination (as the intron is still present); thus, the presence of two bands in the right 'revcheck' lane points to PCR product from cDNA, not genomic DNA. The right lane for primer A does not include a small band, indicating that the complementary sequence is beyond the end of the cDNA. Therefore, the 5' UTR can be expected to include primer B but not primer A.

4.2.2. Characterisation of *OX1*

4.2.2.1. Classification

OX1 belongs to the family of IRE/NPH/PI dependent/S6 kinases (family 4.2.6) of the PlantsP kinase classification system (http://plantsp.sdsc.edu/plantsp/family/class.020318.html) which itself falls into the group of calcium response kinases (group 4.2). This classification system is based on 'all-against-all' comparison of 1114 sequences containing protein kinase domains using BLAST (Altschul *et al*, 1997). The predicted protein contains a conserved eukaryotic protein kinase domain (hmmpfam (HMMER2.1.1)) of 12 subdomains,

including a ser/thr kinase active site signature (prosite_scan) (Figure 4.3). The 12 kinase subdomains are located in the N-terminal 1000 bp of the gene, followed by a 280 bp C-terminus without homology to known sequences. The absence of conserved signal sequences in the amino acid sequence points to a cytosolic localisation. However, a number of putative N-myristoylation sites are present which may anchor the kinase to a membrane.

For further investigation of the *OX1* gene, several collections of 'knock-out' populations were screened for an *ox1* null-mutant. A homozygous *ox1* mutant was identified by screening the Wisconsin T-DNA insertion lines (Krysan *et al.*, 1999). The procedure carried out is detailed in Appendix A. The isolated line contains a T-DNA insertion in the coding sequence between the first and second conserved kinase domains (Figure 4.3). This yields a truncated protein lacking the catalytic site and is therefore expected to be non-functional. In addition, an *OX1promoter::GUS* reporter gene fusion was generated (see Appendix B.1) and transformed into *A. thaliana* in order to investigate tissue localisation of *OX1* gene induction. Plants with other transgenic constructs (inducible *OX1* constitutive mutant and antisense constructs, *OX1 promoter* (-385 to -317*)::GUS* reporter gene fusion construct) were also produced; however, further experiments with these lines were not successful (see Appendix B2 and B.3). In order to reveal differences in H_2O_2-triggered gene induction between the *ox1* null-mutant and the WS-2 wild-type, a microarray experiment was carried out at the NASC Affymetrix Facility (Nottingham, UK) comparing transcript levels after 3 h incubation in H_2O_2 or H_2O in *ox1* and WS-2. The raw data supplied by NASC was analysed by calculating signal value ratios and genes with more than 2.0 - 2.5 fold induction or repression (as indicated) are

displayed in Appendix C. Similar values for the majority of genes in the *ox1* mutant and wild-type confirmed that the different sample data sets were comparable.

4.2.2.2. Homologues of OX1

A BLAST search (Altschul *et al*, 1997) of the *OX1* nucleotide sequence revealed similarity to a number of protein kinases, with the highest ranking entry showing ~80 % identity in the kinase domain region but lacking 108 bp at the C-terminus (Figure 4.3). This homologue of *OX1* was named *OX2* and is located on chromosome 4. On the protein level, the two genes are 72 % identical (266 out of 369 amino acids). The protein most similar to OX1 and OX2 is a putative kinase with 43 % identity (155 out of 355 amino acids) to OX1 on the amino acid level. A putative kinase from potato (T07670) and a protein kinase from rice (B30322) show 36 % amino acid identity (137 out of 380 and 136 out of 372 amino acids, respectively).

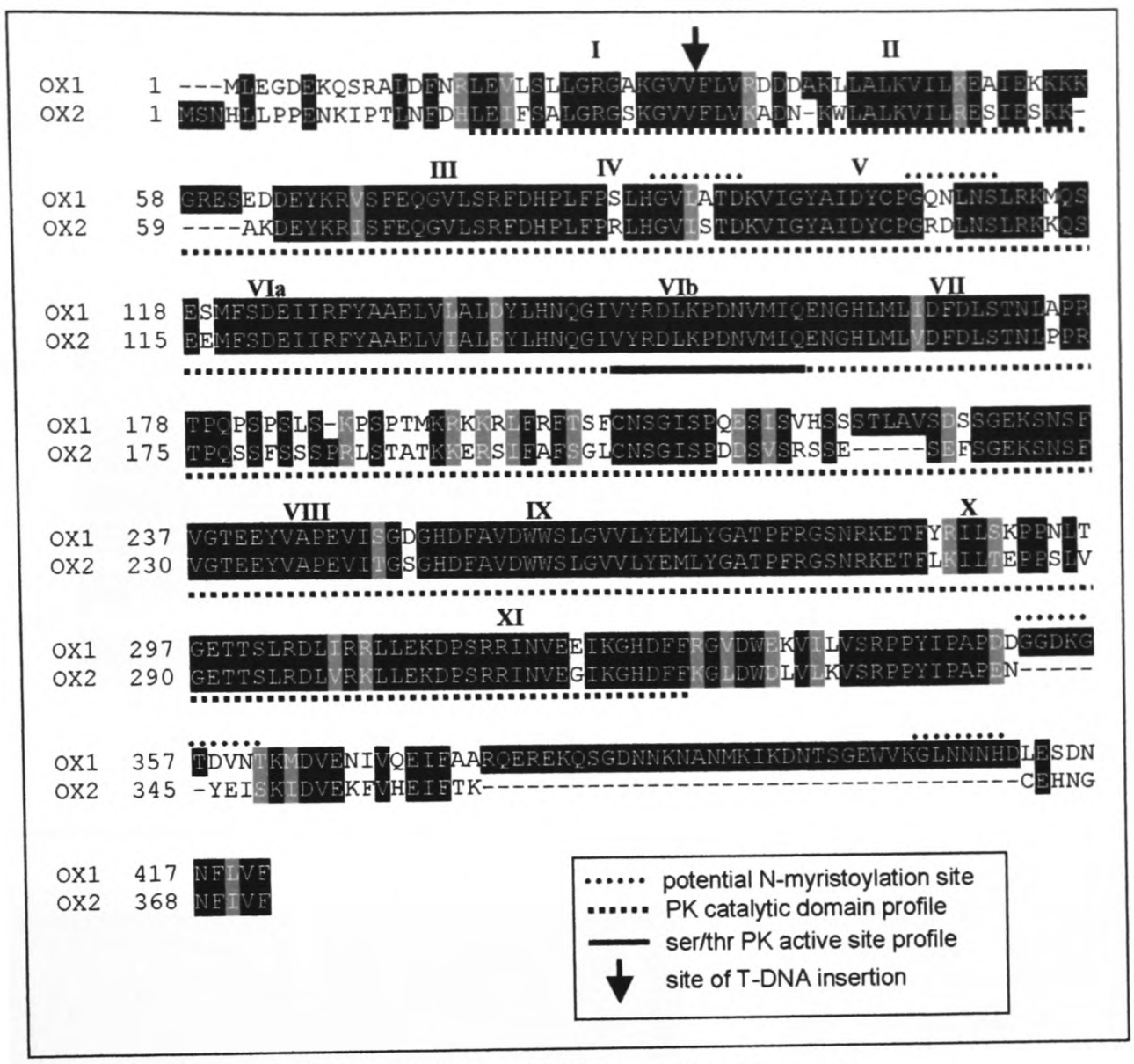

Figure 4.3: Alignment of the OX1 and OX2 protein sequences
OX1 and OX2 protein sequences were aligned in ClustalW (http://www.ebi.ac.uk/clustalw/) and shaded in Boxshade (http://www.ch.embnet.org/software/BOX_form.html). Black boxes represent identical amino acids whereas grey shading indicates amino acids with similar properties. Predicted protein domains were identified in Prosite (http://ca.expasy.org/prosite/). The Roman numerals above the sequence refer to the 12 domains conserved across the protein kinase family (Hanks and Quinn, 1991). The site of the T-DNA insertion is indicated by an arrow.

4.2.2.2.3 Expression of OX2

Expression of the closely related *OX2* gene in response to H_2O_2 was investigated by Northern analysis and RT-PCR. The expression levels of *OX2* were too low to be detected by Northern blot analysis (Figure 4.4). RT-PCR showed that *OX2* was expressed to much lower levels than *OX1* after induction with H_2O_2 and no consistent induction pattern for H_2O_2 treatment could be discerned (Figures 4.4 and

4.5). Thus, *OX2* is either not induced in response to H_2O_2 or the RNA levels are too low for detection by the attempted methods.

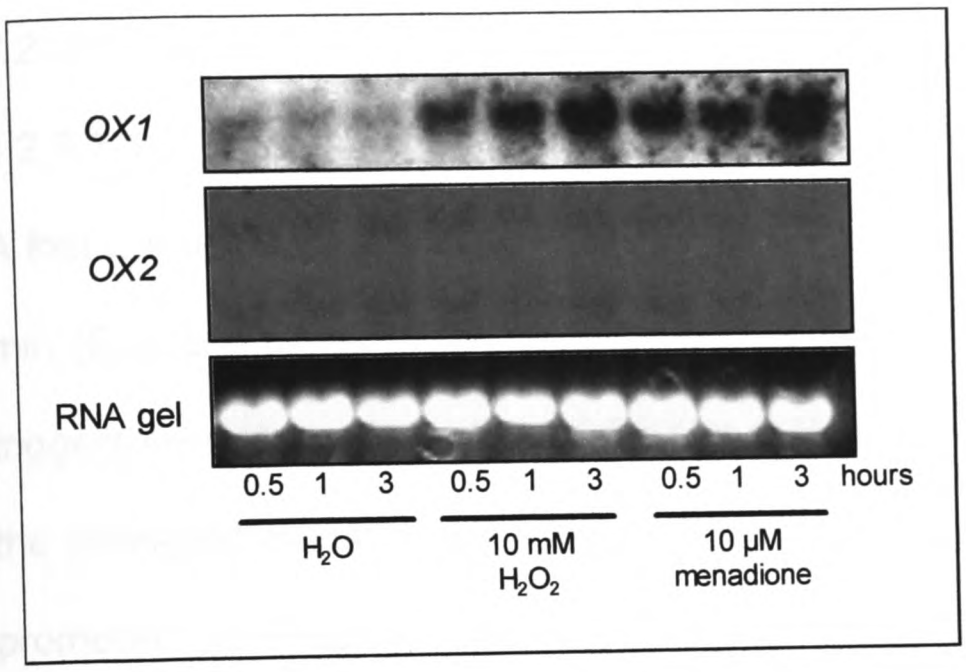

Figure 4.4: *OX2* expression in response to H_2O_2
7 day old RLD1 seedlings were transferred into H_2O and allowed to rest for 3 h before treatment with H_2O_2 or menadione for 0.5, 1 or 3 hours. The total RNA was extracted and Northern analysis was carried out as described under Methods. DNA probes used to hybridise to the membranes consisted of the kinase domains of *OX1* and *OX2* . The RNA stained with ethidium bromide is depicted as a loading control.

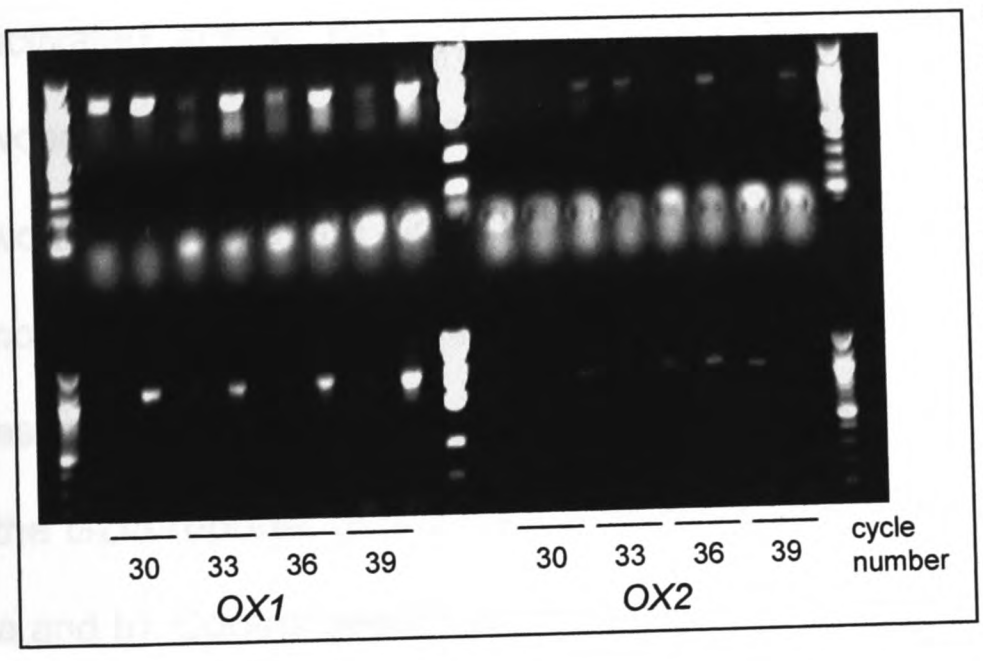

Figure 4.5: *OX2* expression in response to H_2O_2 treatment.
RT-PCR was carried out on cDNA obtained from RLD1 seedlings (7 days old) treated for 1 h in H_2O (left lane of each cycle number column) or 10 mM H_2O_2 (right lane). As a control for primer compatibility, two different sets of primers were used for *OX2* RT-PCR (upper row OX2RTPCRforA and revA; lower row OX2 RTPCRforB and revB). The bright band between the two PCR product rows is constituted of primers from the upper row PCR reactions.

4.2.3. Analysis of *OX1* induction

As shown in Figure 4.4, *OX1* transcript levels are elevated in response to H_2O_2 and menadione treatment. Under natural conditions, AOS concentrations rise as a secondary effect of a range of abiotic stresses (see section 1.1) or as a consequence of an oxidative burst (see section 1.2) in which the plant cell itself produces H_2O_2 and $O_2^{\bullet-}$, possibly to function as signalling molecules. Thus, changes in *OX1* induction were monitored in response to a range of abiotic and biotic

stresses by Northern analysis and with the help of a *OX1*promoter::*GUS* reporter gene fusion construct (see Appendix B.1).

4.2.3.1. Abiotic stresses

4.2.3.1.1 Wounding and cellulase

A fast but transient increase in *OX1* levels was caused by wounding, peaking at 30 min (Figure 4.6). Addition of cellulase, which hydrolyses cellulose in the cell wall, triggers very strong induction of *OX1* (*e.g.* Figures 4.6 and 4.13). This treatment had the strongest effect on *OX1* levels of all stresses tested. GUS staining of the *OX1* promoter::*GUS* fusion lines after cellulase treatment showed that the promoter was activated across the entire surface of the cotyledons (Figure 4.7 a); whereas, wounding with a sharp razor blade increased GUS levels only along the edge of the wounded tissue and along the severed vascular tissues (Figure 4.7 b). Staining was not simply the result of increased accessibility of histochemical substrates as GUS assays immediately after wounding, *e.g.* without incubation to allow for induction of the *GUS* reporter gene, did not reveal any GUS expression (see cuts in Figure 4.13 a and b). Control seedlings (in H_2O) did not show any staining (Figure 4.7 a)

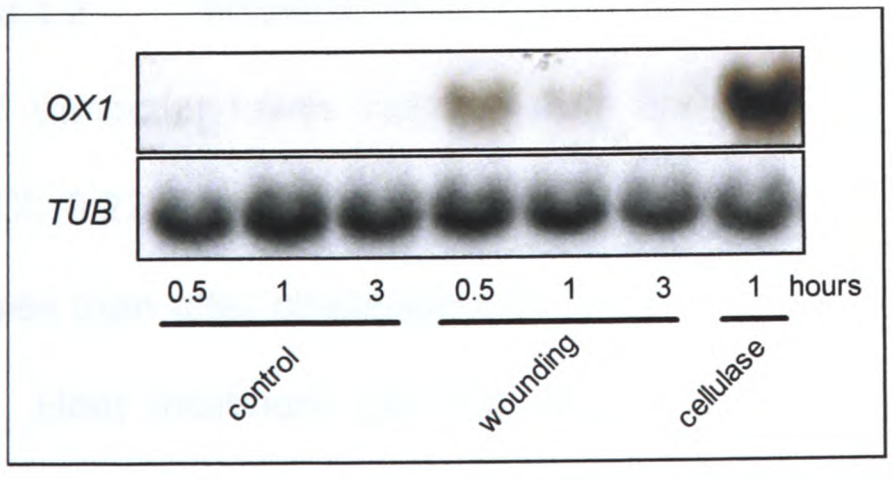

Figure 4.6: Induction of *OX1* in response to wounding and cellulase
Northern analysis was carried out as described in Methods. 7 day old Col-0 seedlings were transferred into H_2O and left to recover for 2.5 h. Seedlings were either wounded with tweezers until approximately 25 % of the cotyledon surface was damaged or challenged by addition of cellulase (final concentration: 0.01 % w/v). Control samples remained in H_2O.
After 0.5, 1 or 3 hours, samples were frozen and total RNA was extracted, electrophoresed and transferred to nylon membrane. *OX1* and *β-TUBULIN* probes were labelled and hybridised to the RNA on the membrane.

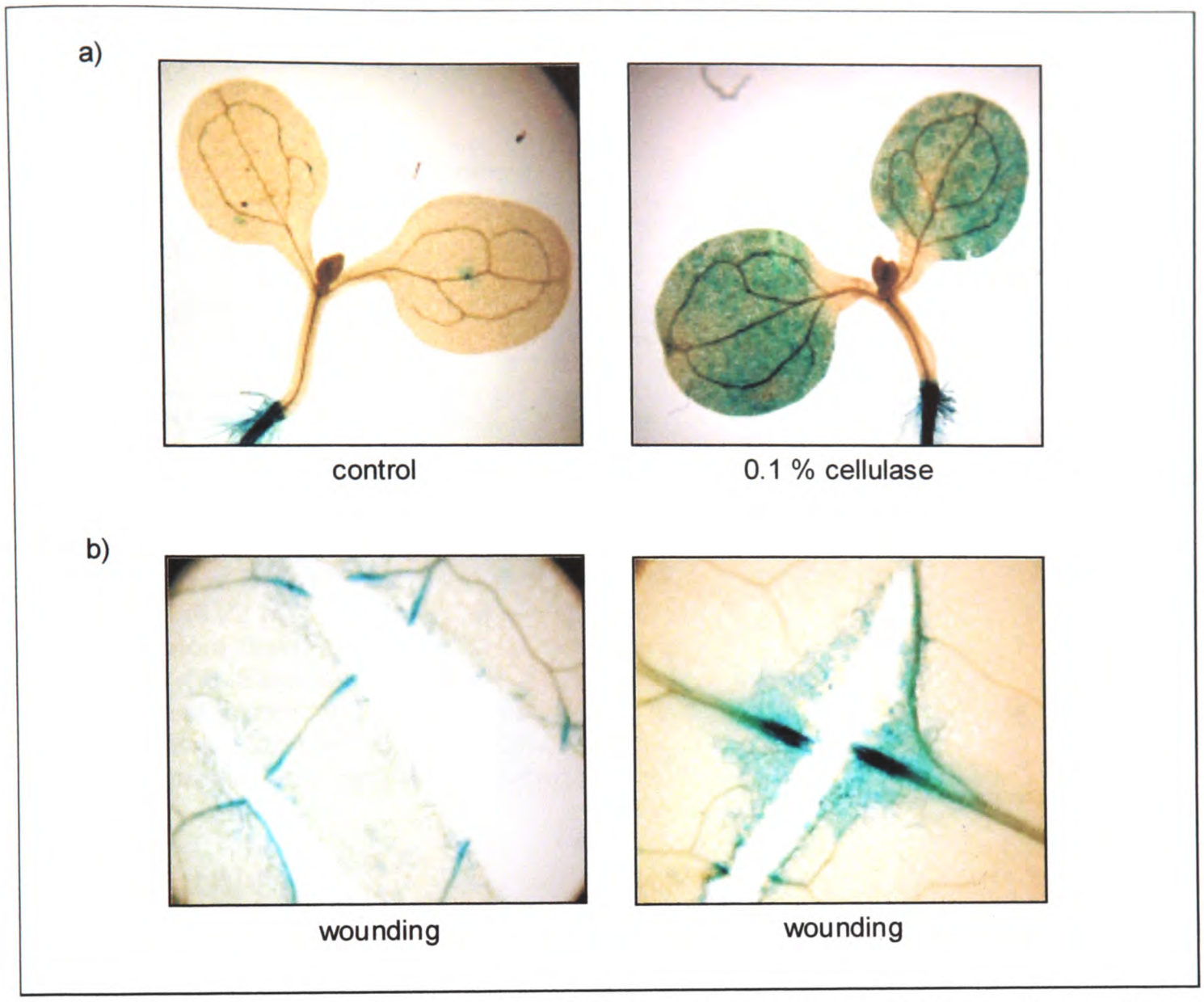

Figure 4.7: Localisation of *OX1*promoter activation in response to cellulase and wounding
In vivo GUS staining was performed as described in Methods. 7 day old Col-0 seedlings transformed with the *OX1*promoter::GUS construct were a) treated with 0.1 % (w/v) cellulase solution or b) cut with a sharp razor blade across the cotyledon surface. The control sample remained in H_2O without treatment. After 3 hours, tissues were stained for GUS expression. Images were taken with a Nikon Coolpix 990 digital camera mounted on a Leica DM R microscope. a) 250 x and b) 1000 x magnification; with up to an extra 2.8 x magnification (from no zoom to full zoom of the digital camera).

4.2.3.1.2 Temperature, drought and salt stress

OX1 transcript levels were slightly increased in response to treatment with salt (NaCl, 0.22 M), drought (mannitol, 0.44 M) and cold (4 °C) but to a much lower degree than after challenge with H_2O_2 (10 mM) and cellulase (0.1 % (w/v)) (Figure 4.8). Heat treatment (35 °C) did not have any effect on *OX1* induction when compared to control levels (H_2O only). In a second experiment, seedlings were

incubated at 37 °C; *OX1* was also not induced at this higher temperature (data not shown).

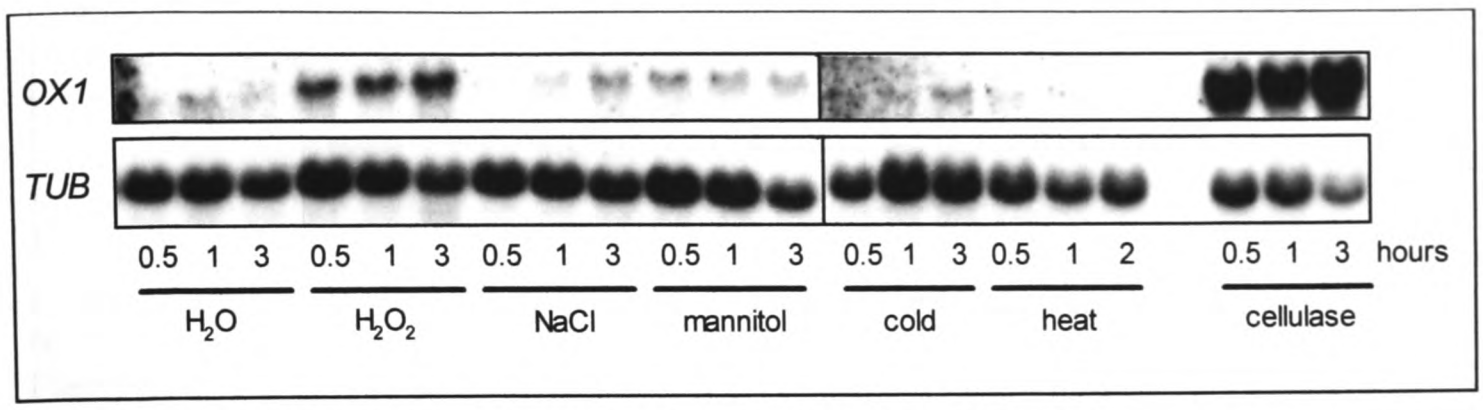

Figure 4.8: Induction of *OX1* by temperature, drought and salt stress
Northern analysis was carried out as described in Methods. 7 day old Col-0 seedlings were transferred into H_2O and left to recover for 3 h. Seedlings were incubated in H_2O, H_2O_2 (10 mM), NaCl (0.22 M), mannitol (0.44 M), cold (4 °C) or cellulase (0.1 % (w/v)) for 0.5 h, 1 h and 3 h before freezing. For heat treatment, seedlings were placed into a 35 °C waterbath and left for 1 h. Samples were frozen after 0.5 h and 1 h heating as well as 1 h after removal from the heat treatment (2 h time point). After 0.5, 1, 2 or 3 hours, samples were frozen and total RNA was extracted, electrophoresed and transferred to nylon membrane. *OX1* and *β-TUBULIN* probes were labelled and hybridised to the RNA on the membrane.

4.2.3.1.3 UV-B

UV-B treatment increased *OX1* transcript levels slightly (Figure 4.10).

4.2.3.2. Biotic stresses

4.2.3.2.1 Flagellin

Flagellin functions as a general elicitor of defence responses in all *A. thaliana* ecotypes tested, except WS-0, triggering generation of AOS in an oxidative burst (Gomez-Gomez *et al.*, 1999). Treatment with flagellin 22, the 22 amino acid peptide necessary and sufficient for recognition by the *A. thaliana* flagellin receptor (Gomez-Gomez *et al.*, 1999), increases *OX1* levels slightly in Col-0 but not WS-2 (Figure 4.9). This may reflect the inability of WS-2, similar to WS-0, to recognise the peptide. *OX1* levels are not increased in the DMSO control.

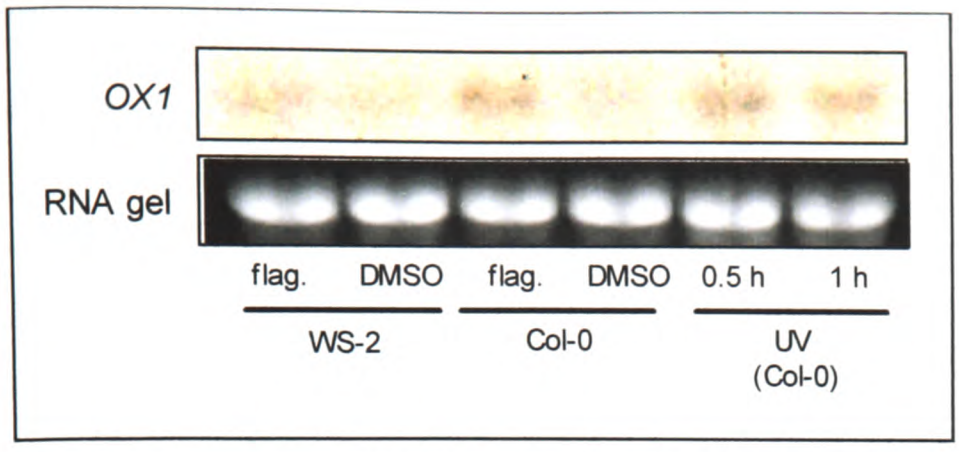

Figure 4.9: Induction of *OX1* by flagellin and UV-B
Northern analysis was carried out as described in Methods.
Flagellin treatment: 7 day old Col-0 and WS-2 seedlings were transferred into H_2O, left to recover for 2 h before addition of the flagellin fragment (22 amino acid peptide, 1 µM, in DMSO (1:1000)) or DMSO (1:1000). The samples were incubated for 1 h before freezing and extraction of total RNA.
UV-B treatment: a MS agar plate with 7 day old Col-0 seedlings was placed facing downwards on top of a UV-transilluminator (3UV transilluminator, UVP Laboratory Products, Upland, CA, USA) for 2 min. After a 5 min break, the seedlings were illuminated for another 2 min. Samples were frozen 30 min and 1 h after illumination and total RNA was extracted, electrophoresed and transferred to nylon membrane. *OX1* probe was labelled and hybridised to the RNA on the membrane. The image represents a scan from the phosphorimager. The RNA stained with ethidium bromide is depicted as a loading control.

4.2.3.2.2 Necrotrophic fungus (*Penicillium*)

Necrotrophic fungi secrete toxins or enzymes to kill and break down plant tissue and subsequently colonise the dead cells through absorbtion of nutrients (Thomma *et al.*, 2001a). Activation of the *OX1* promoter was detected in *in vitro* and *in vivo* GUS assays of seedlings transformed with the *OX1*promoter::*GUS* construct that had been infected by a necrotrophic fungus naturally present on the seed coat (Figure 4.10, data for *in vitro* assay not shown). The fungus was identified as a *Penicillium* isolate on the basis of its conidiophore structure (Figure 4.10 c). Strong GUS staining was observed in areas of fungal proliferation as gauged by conidiophores protruding from the leaf surface (Figure 4.10 c). Areas where the fungus penetrated the epidermal cell layer also stained strongly (Figure 4.10 a). In addition to staining

at fungal proliferation sites, infected seedlings showed strong staining in several structures at the bases of developing leaves that may represent stipules.

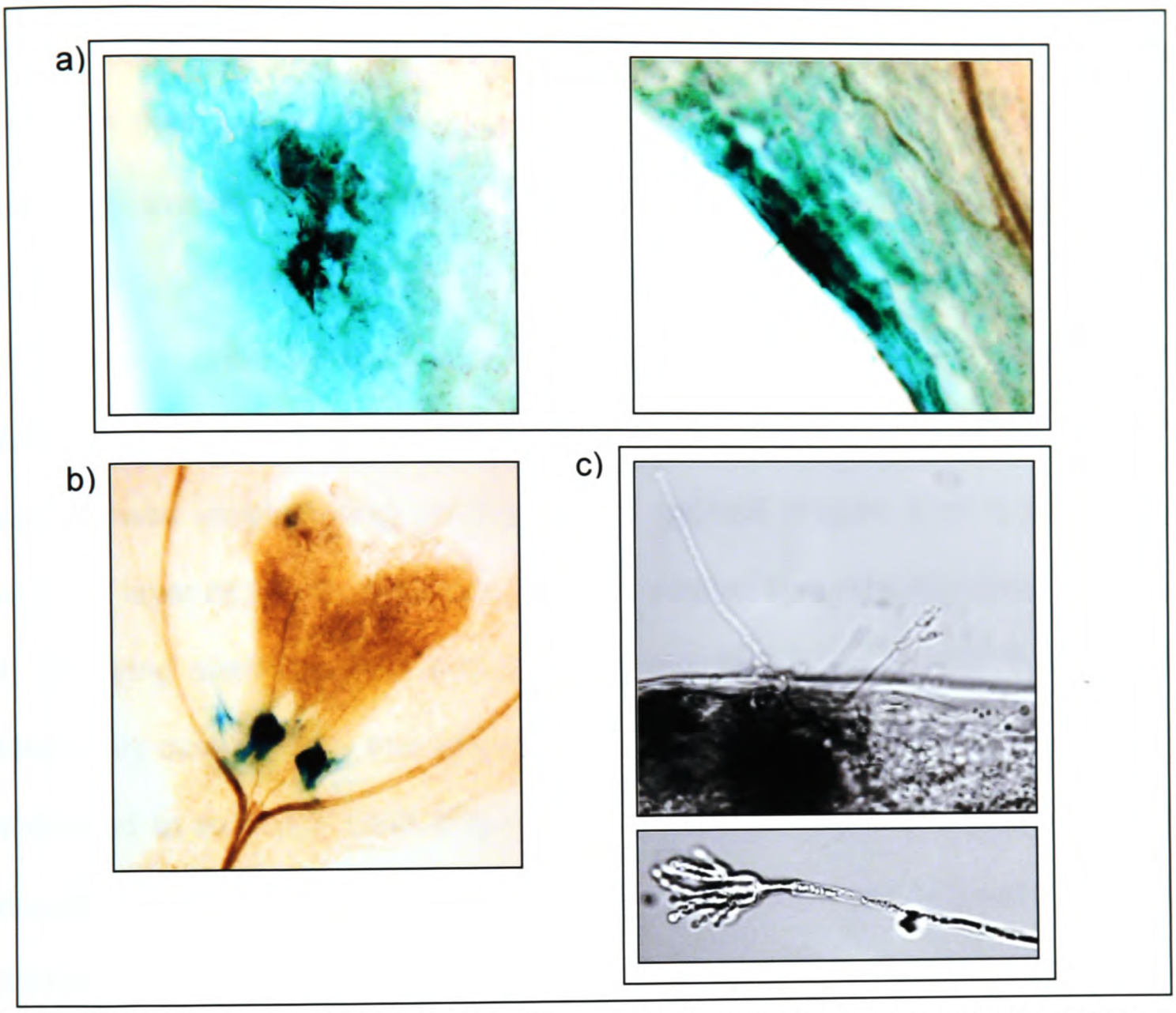

Figure 4.10: Localisation of *OX1* promoter activation in response to infection with a necrotophic *Penicillium* isolate

in vivo GUS staining was performed as described in Methods. Col-0 seed transformed with a *OX1*promoter::GUS construct (four independent lines) was left un-sterilised before sowing onto MS agar plates and vernalisation. Seedlings were grown for 7 days before staining for GUS expression. During this time, fungal spores present on the seed had germinated and colonised the seedlings and surrounding MS agar. a) Cotyledon surfaces in areas of fungal attack, manifest through presence of conidiophores. b) Emerging leaves of a seedling with infected cotyledons. c) Conidiophores of the fungus emanating from the cotyledon surface. a) and b): Images were taken with a Nikon Coolpix 990 digital camera mounted on a Leica DM R microscope, magnification a) 4000 x, b) 250 x magnification; with up to an extra 2.8 x magnification (from no zoom to full zoom of the digital camera). c): Images were taken with an Optronics camera (MIH038226), 4000 x and 10,000 magnification (upper and lower image, respectively).

4.2.3.2.3 Biotrophic fungus (*Peronospora parasitica*)

Biotrophic pathogens retrieve nutrients from living plant cells. Virulent strains are able to colonise plant tissues by evading recognition or by producing suppressors of defence responses whereas avirulent strains are recognised and subsequently limited in their growth through the plant response (Thomma *et al.*, 2001a). Col-0 seedlings transformed with a *OX1*promoter::*GUS* construct were infected with virulent and avirulent isolates of *Peronospora parasitica* (Koch and Slusarenko, 1990) and stained for GUS expression. When infected with the virulent isolates Maks 9 (Figure 4.11) and Emco 5 (data not shown) (Bittner-Eddy *et al.*, 1999), GUS staining was visible along growing fungal hyphae (Figure 4.11 b and c) in the adjacent layer of 2 to 4 cells and in cells penetrated by fungal haustoria (Figure 4.11 d). Spraying seedlings with spores of the avirulent isolate Emoy 2 (Holub *et al.*, 1994) only caused GUS expression in small patches of cells where the fungus had attempted to establish itself (Figure 4.12 a and b). These cell patches tended to include dead cells (brown colouration) at the penetration site (Figure 4.12 c and d), possibly the result of a HR. *P. parasitica* grown on wild-type seedlings stained only very faintly (data not shown), indicating low endogenous GUS activity.

Following page:
Figure 4.11: Localisation of *OX1* promoter activation in response to infection with a virulent *P. parasitica* isolate
Infection and *in vivo* GUS staining were performed as described in Methods. 4 week old Col-0 plants transformed with the *OX1*promoter::GUS construct (5 independent lines) were infected with the virulent *P. parasitica* isolate Maks 9. Leaves were detached from the plant 7 days after infection and stained for GUS expression. a) *A. thaliana* leaf infected with *P. parasitica* with sporangiophores covering part of the leaf surface. b) ,c) and d) GUS-stained leaves showing GUS expression in several cell layers along the fungal hyphae. Images were taken with a Nikon Coolpix 990 digital camera mounted on a Leica DM R microscope. b) 250 x, c) 1000 x and d) 4000 x magnification; with variation of an extra 2.8 x magnification (from no zoom to full zoom of the digital camera).

a)

b)

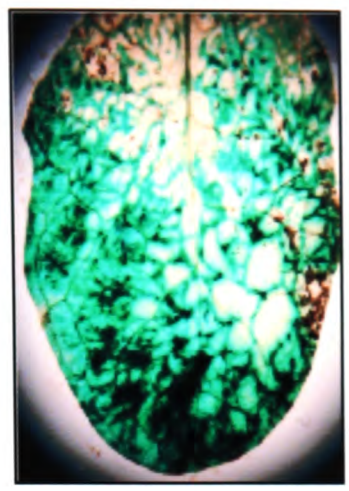

c)

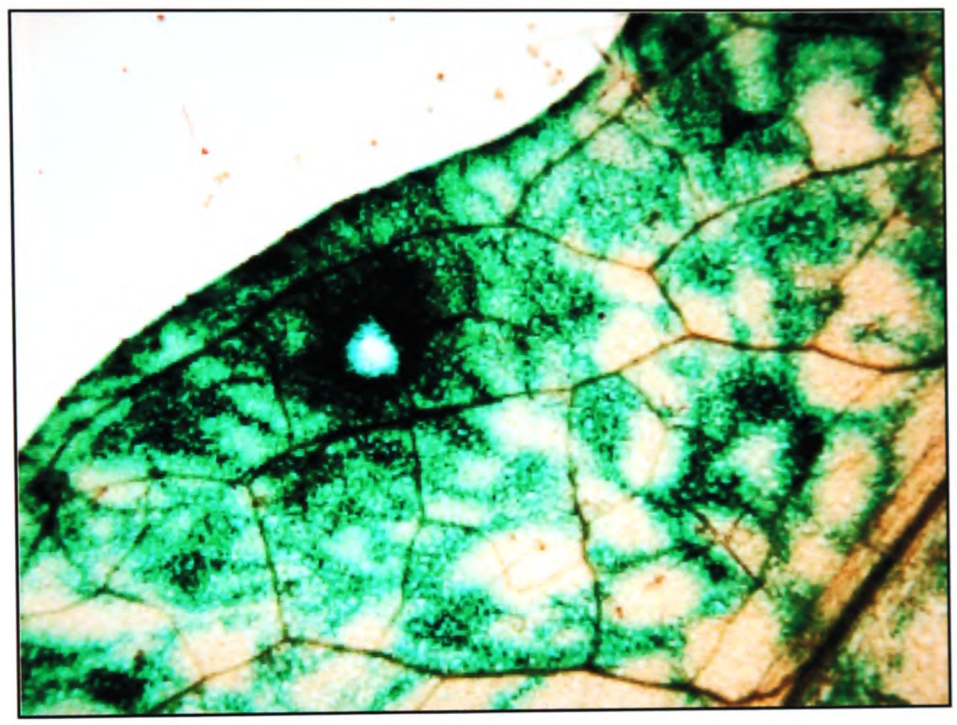

d)

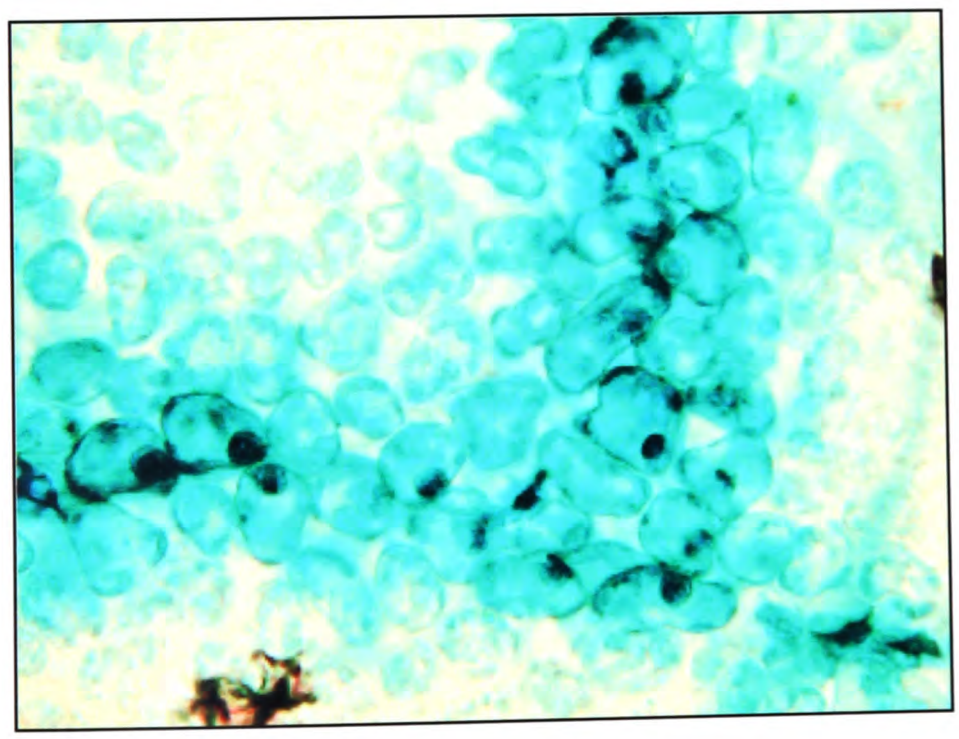

a)

b)

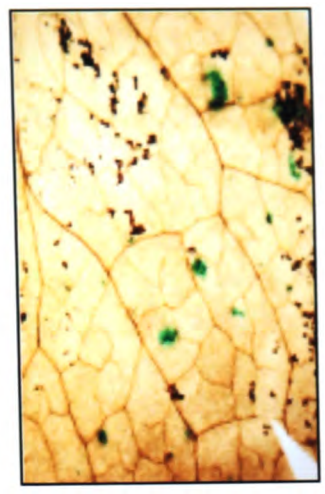

c)

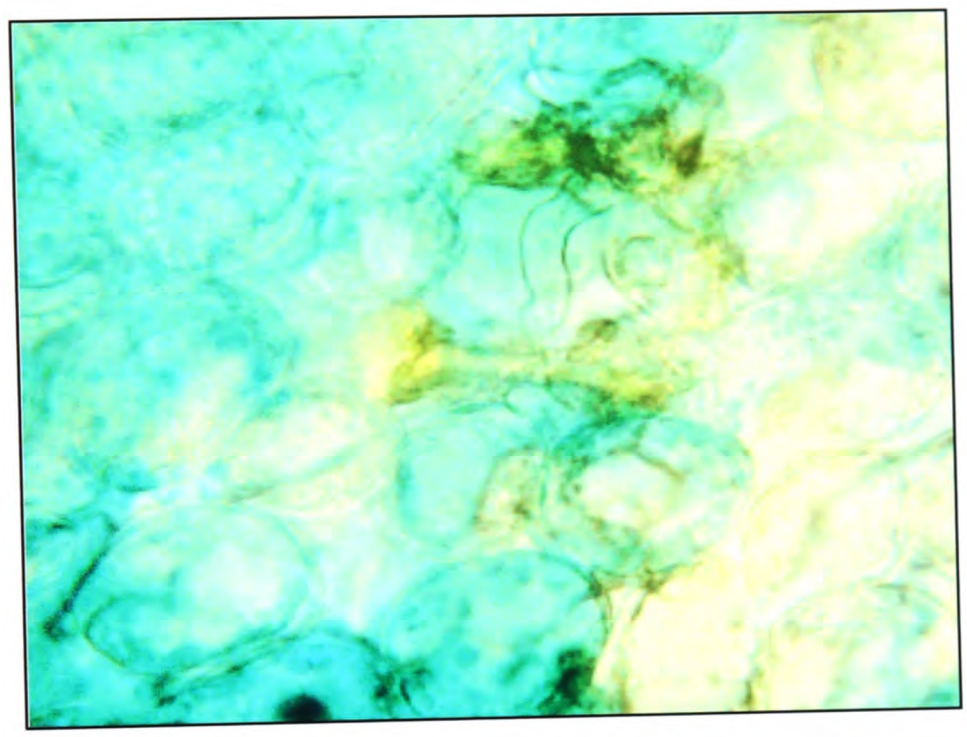

d)

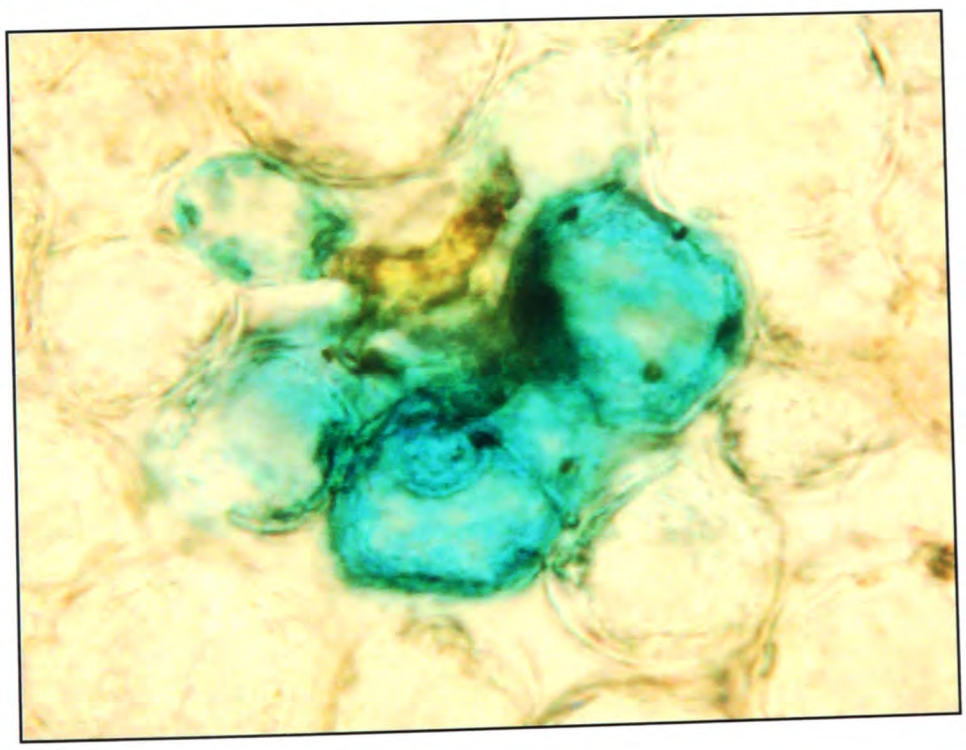

Previous page:
Figure 4.12: Localisation of *OX1* promoter activation in response to infection with an avirulent *P. parasitica* isolate
Infection and *in vivo* GUS staining were performed as described in Methods. 4 week old Col-0 plants transformed with a *OX1*promoter::GUS construct (5 independent lines) were infected with the avirulent *P. parasitica* isolate Emoy 2. Leaves were detached from the plant 7 days after infection and stained for GUS expression. a) and b): Leaves of *A. thaliana* plants with GUS staining visible at sites of attempted penetration by the pathogen. c) and d): Sites of attempted penetration, displaying GUS staining and plant cell death (brown colouration) around a short fungal hypha (c) and a single haustorium (d). Images were taken with a Nikon Coolpix 990 digital camera mounted on a Leica DM R. a) and b) 250 x, c) and d) d) 4000 x magnification; with up to an extra 2.8 x magnification (from no zoom to full zoom of the digital camera).

4.2.3.3. Plant hormones

4.2.3.3.1 Salicylic acid (SA)

SA is involved in disease resistance to certain pathogens as well as SAR induction (Gaffney *et al.*, 1993) (see section 1.3.3.3). *OX1* was not induced by incubation in SA under conditions that triggered induction of the SA-inducible *PR-1* gene (Figure 4.13).

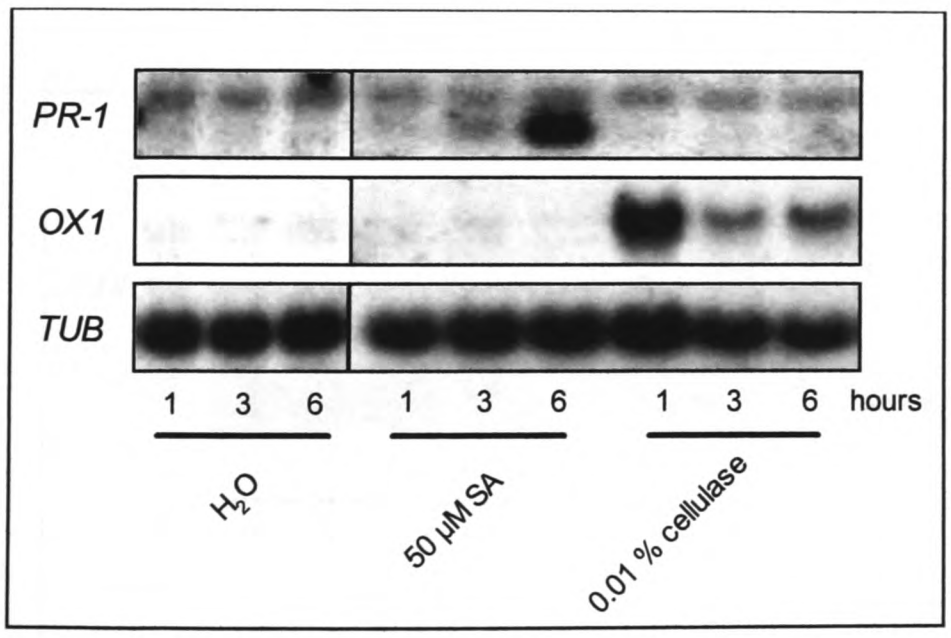

Figure 4.13: Induction of *OX1* by SA
Northern analysis was carried out as described in Methods. 7 day old RLD1 seedlings were transferred to H_2O and left to recover for 3 h. SA (final concentration: 50 µM) or cellulase (final concentration: 0.01 % (w/v)) were added. as indicated. Samples were frozen after 1 h, 3 h and 6 h incubation. Total RNA was extracted, electrophoresed and transferred to nylon membrane. *PR-1*, *OX1* and *β-TUBULIN* probes were labelled and hybridised to the RNA on the membrane.

4.2.3.3.2 Ethylene

Ethylene, together with JA, has been implicated in disease resistance to necrotrophic pathogens (Thomma *et al.*, 2001a) and induction of ISR (Pieterse and van Loon, 1999) (see section 1.3.3.1). Treatment with the ethylene precursor ACC did not increase *OX1* levels under conditions that induced the ethylene-responsive genes *CHITB* and *PDF1.2* (Thomma *et al.*, 1998) (Figure 4.14). The ethylene signalling mutants *etr1* and *ctr1* (deficient and constitutive in ethylene signalling, respectively) were also tested for *OX1* induction in response to H_2O_2 and cellulase (Fig. 4.15). No clear pattern of differences in *OX1* transcript levels was discernible.

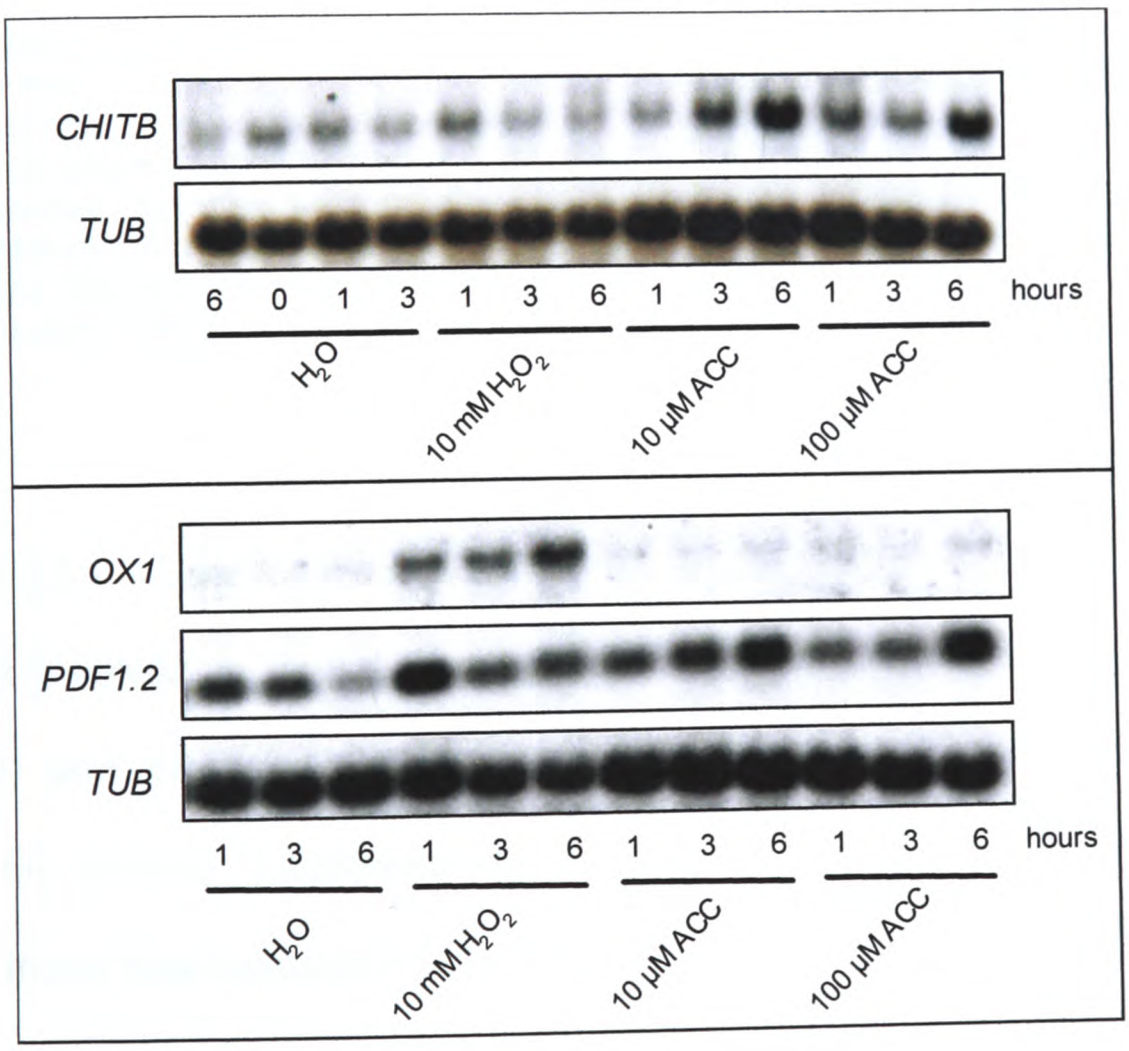

Figure 4.14: Induction of *OX1* by ACC
Northern analysis was carried out as described in Methods. 7 day old RLD1 seedlings were transferred to H_2O and left to recover for 3 h. H_2O_2 (final concentration: 10 mM) or ACC (final concentrations: 10 µM and 100 µM) were added as indicated. Samples were frozen after 1 h, 3 h and 6 h incubation and total RNA was extracted. Samples of 10 µg RNA each were electrophoresed and blotted separately. *CHITB*, *PDF1.2*, *OX1* and *β-TUBULIN* probes were labelled and hybridised to the RNA on the membrane.

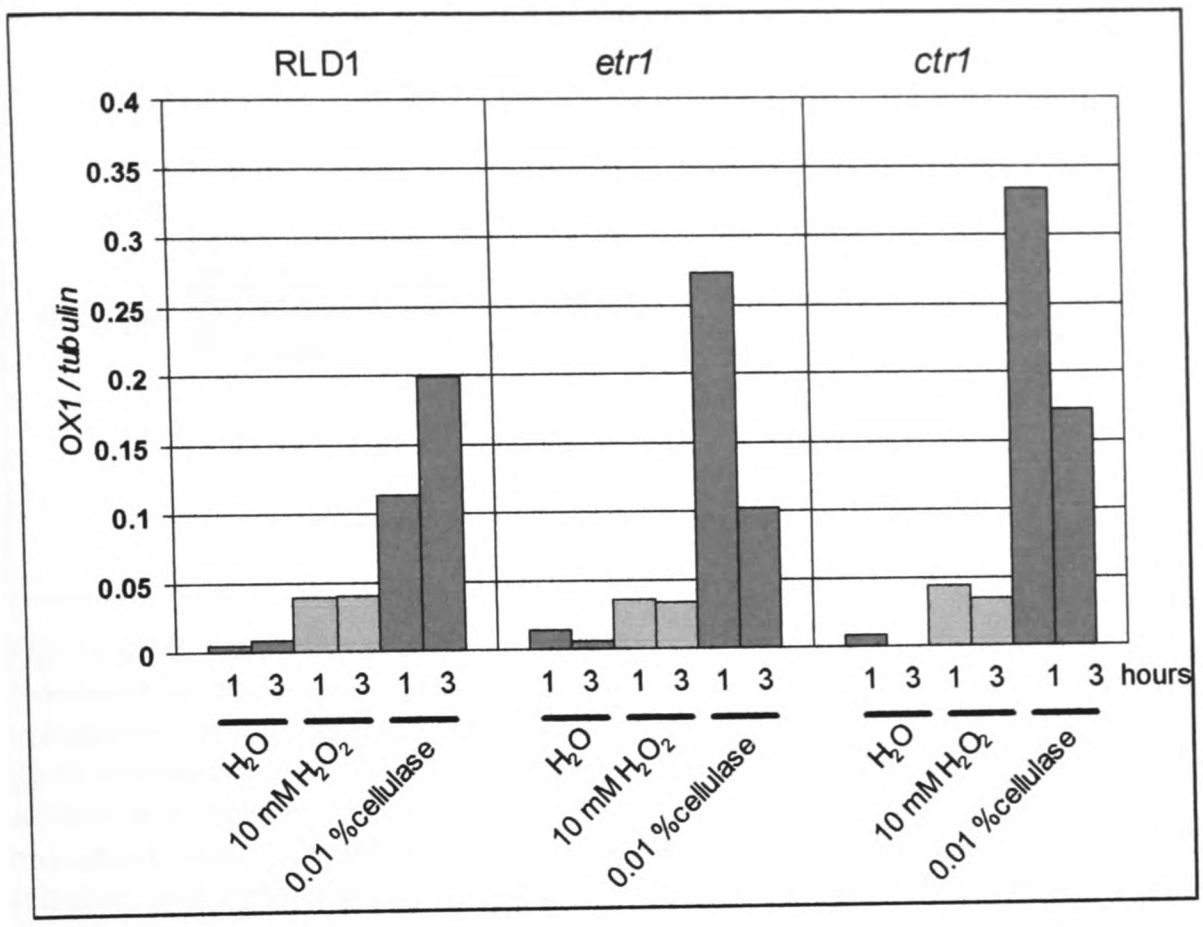

Figure 4.15: Induction of *OX1* in the ethylene signalling mutants *etr1* and *ctr1*
Northern analysis and normalisation of gene induction data was carried out as described in Methods. 7 day old seedlings were transferred to H_2O and left to recover for 30 min. H_2O_2 (final concentration: 10 mM) or cellulase (final concentration: 0.01 % (w/v)) were added as indicated. Samples were frozen after 1 h and 3 h incubation. Total RNA was extracted, electrophoresed and transferred to nylon membrane. *GST1*, *APX1* and *β-TUBULIN* probes were labelled and hybridised to the RNA on the membrane. Bars represent *OX1* gene induction relative to *β-TUBULIN* mRNA levels.

4.2.3.3.3 Jasmonic acid (JA)

JA is involved in signal transduction in response to wounding (Reymond *et al.*, 2000) and infection with necrotrophic pathogens (Thomma *et al.*, 2001a) (see section 1.3.3.2). Treatment with JA did not increase *OX1* transcript levels under conditions that induced the *ALLENE OXIDE SYNTHASE* (*AOS*) gene. *AOS* is a JA biosynthesis gene induced in response to JA treatment (Reymond *et al.*, 2000) (Figure 4.16).

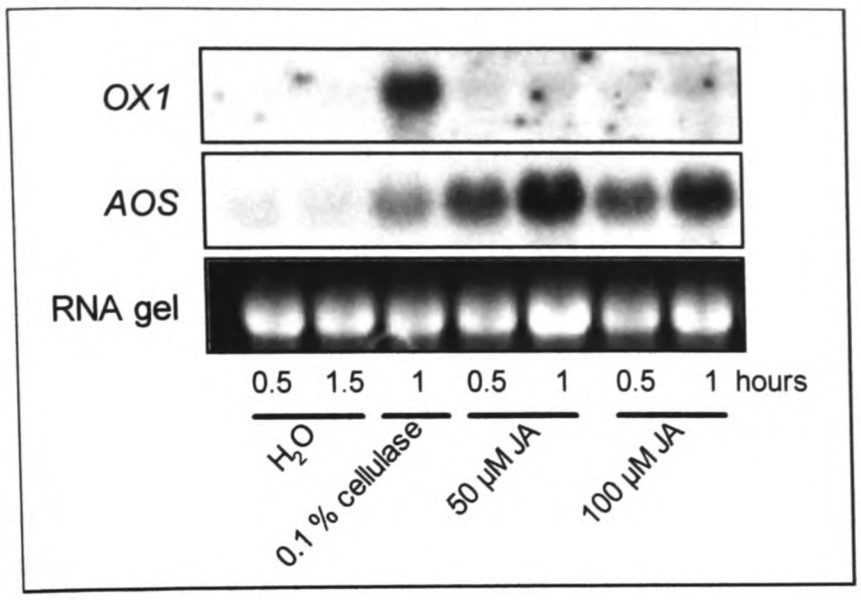

Figure 4.16: Induction of *OX1* by JA
Northern analysis was carried out as described in Methods. 7 day old Col-0 seedlings were transferred to H_2O and left to recover for 3 h. Cellulase (final concentration: 0.1 % (w/v)) or JA (final concentrations: 50 µM and 100 µM, 1:10,000 and 1:20,000 ethanol, respectively) were added as indicated. Samples were frozen after 0.5 h, 1 h and 1.5 h incubation. Total RNA was extracted, electrophoresed and transferred to nylon membrane. *OX1* and *AOS* probes were labelled and hybridised to the RNA on the membrane. RNA stained with ethidium bromide is depicted as a loading control.

4.2.3.3.4 Abscisic acid (ABA) and auxin

ABA is involved in the drought response and has been shown to be necessary for stomatal closure in a signalling cascade which also involves H_2O_2 (Pei *et al.*, 2000). Auxin mediates a range of processes, including apical dominance, root growth and root gravitropism (Joo *et al.*, 2001). *OX1* levels increased in response to treatment with ABA but not NAA, a synthetic analogue of auxin (Figure 4.17). *OX1* gene induction in the *ox1* mutant followed the same pattern but absolute transcript levels were higher when compared to the WS-2 wild-type, indicating either negative feedback regulation of the OX1 protein on *OX1* gene expression or enhanced stability of the truncated *OX1::T-DNA* mRNA compared to the native *OX1* mRNA. The larger transcript size in the *ox1* mutant suggests that native *OX1* transcript is absent.

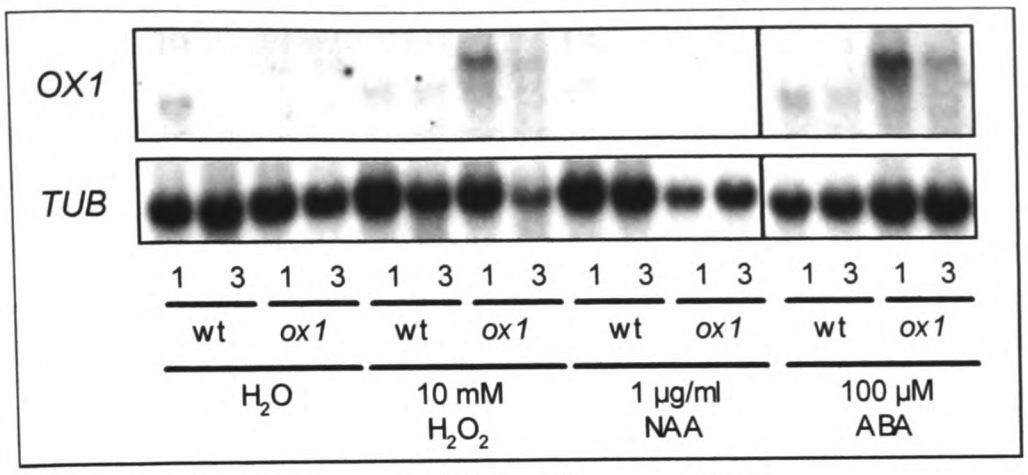

Figure 4.17: Induction of *OX1* by NAA and ABA
Northern analysis was carried out as described in Methods. 7 day old WS-2 or *ox1* seedlings were transferred to H_2O and left to recover for 3.5 h. H_2O_2 (final concentration: 10 mM), NAA (final concentration: 1 µg/ ml) or ABA (final concentration: 100 µM, 0.1 % ethanol) were added as indicated. Samples were frozen after 1 h and 3 h incubation. *OX1* and *AOS* probes were labelled and hybridised to the RNA on the membrane. Total RNA was extracted, electrophoresed and transferred to nylon membrane. *OX1* and *β-TUBULIN* probes were labelled and hybridised to the RNA on the membrane.

4.2.3.4. Different ecotypes

Different ecotypes were tested for induction of *OX1* in response to H_2O_2 and cellulase. All ecotypes tested displayed increased levels of *OX1* (Figure 4.18) but differed in the absolute level of induction. Again, the *ox1* mutant (see also Figure 4.17) shows enhanced *OX1* induction (in terms of absolute levels of transcripts) as compared to the WS-2 wild type and other ecotypes.

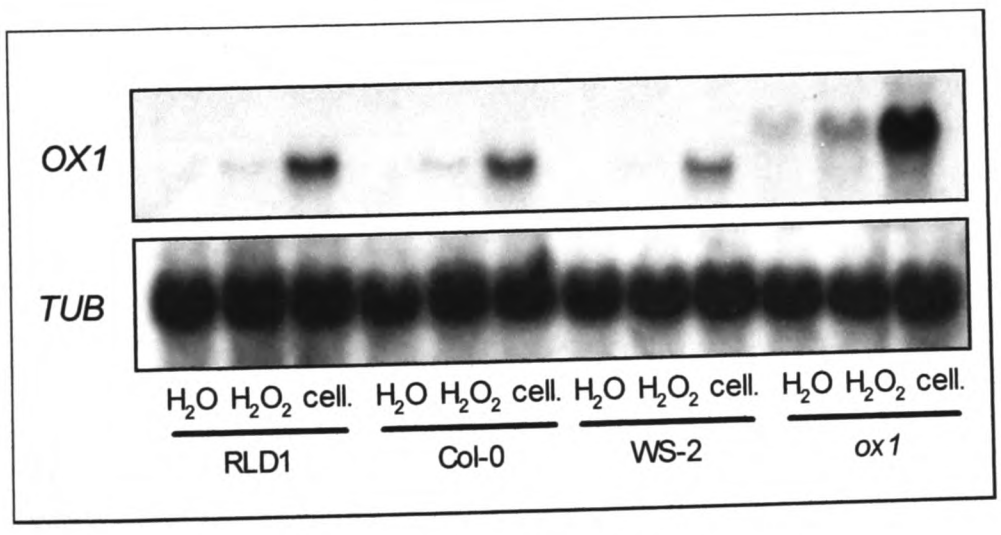

Figure 4.18: Induction of *OX1* in different ecotypes
Northern analysis was carried out as described in Methods. 7 day old seedlings (wt) of different ecotypes and *ox1* seedlings were transferred into H_2O and left to recover for 2 h. H_2O_2 (final concentration: 10 mM) or cellulase (final concentration: 0.02 % (w/v)) were added as indicated. Samples were frozen after 1 h incubation. Total RNA was extracted, electrophoresed and transferred to nylon membrane. *OX1* and *β-TUBULIN* probes were labelled and hybridised to the RNA on the membrane.

4.2.3.5. Involvement of NADPH oxidases

It had been proposed that oxidative bursts —the generation of H_2O_2 initiated by the plant in response to wide range of stresses (see section 1.2) – are the result of NADPH oxidase activation (Desikan *et al.*, 1996). In order to test whether *OX1* induction in response to cellulase treatment was the result of NADPH oxidase activation, seedlings were treated with DPI, an irreversible inhibitor of the oxidase activity (Figure 4.19). Unexpectedly, the increase in *OX1* levels was enhanced in samples treated with DPI. To further investigate the role of NADPH oxidases, eight lines, null-mutant each in one of the eight NADPH oxidase genes (A – H), were tested for changes in *OX1* induction in response to cellulase (data not shown). *OX1* levels were reduced in some of these lines, but not consistently so in two separate experiments; thus, no clear picture of the involvement of NADPH oxidases emerged from the experiments performed.

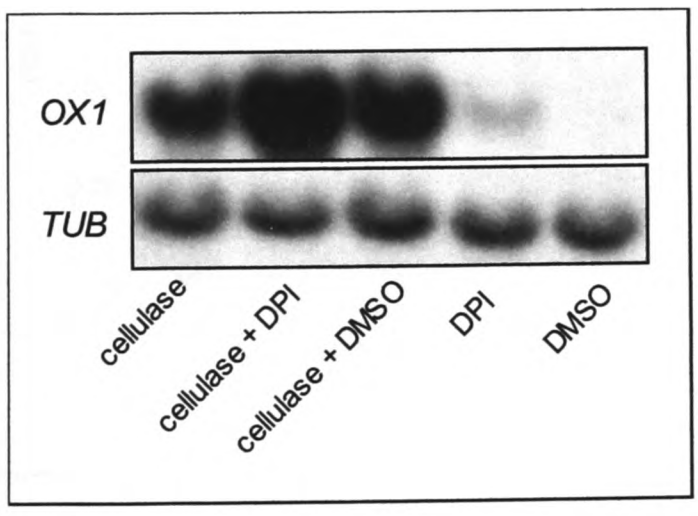

Figure 4.19: Effect of DPI on *OX1* induction in response to cellulase
Northern analysis was carried out as described in Methods. 7 day old Col-0 seedlings were transferred into H_2O and left to recover for 3 h. DPI in DMSO or DMSO (final concentration: 10 µM, 1:2000) were added and samples left to incubate for 15 min before addition of cellulase (final percentage: 0.01 % (w/v)). Samples were frozen after 1 h incubation and total RNA was extracted, electrophoresed and transferred to nylon membrane. *OX1* and *β-TUBULIN* probes were labelled and hybridised to the RNA on the membrane.

4.2.3.6. *Dependence of* OX1 *induction on calcium signalling*

Challenging seedlings with H_2O_2 was shown to cause increases in $[Ca^{2+}]_{cyt}$ (see section section 3.2.1.1.1, Figures 3.1 and 3.2) which could be inhibited by treatment with the channel blocker $LaCl_3$ (section 3.2.1.5.1, Figures 3.14 and 3.15). The effect of inhibition of the H_2O_2-triggered $[Ca^{2+}]_{cyt}$ signature upon *OX1* induction was investigated. $LaCl_3$ treatment reduced *OX1* induction at 1 h and 3 h time points at all concentrations that had also been shown to inhibit the first $[Ca^{2+}]_{cyt}$ peak (Figure 4.20). At the 6 h time point, *OX1* levels were slightly increased in the $LaCl_3$-treated samples.

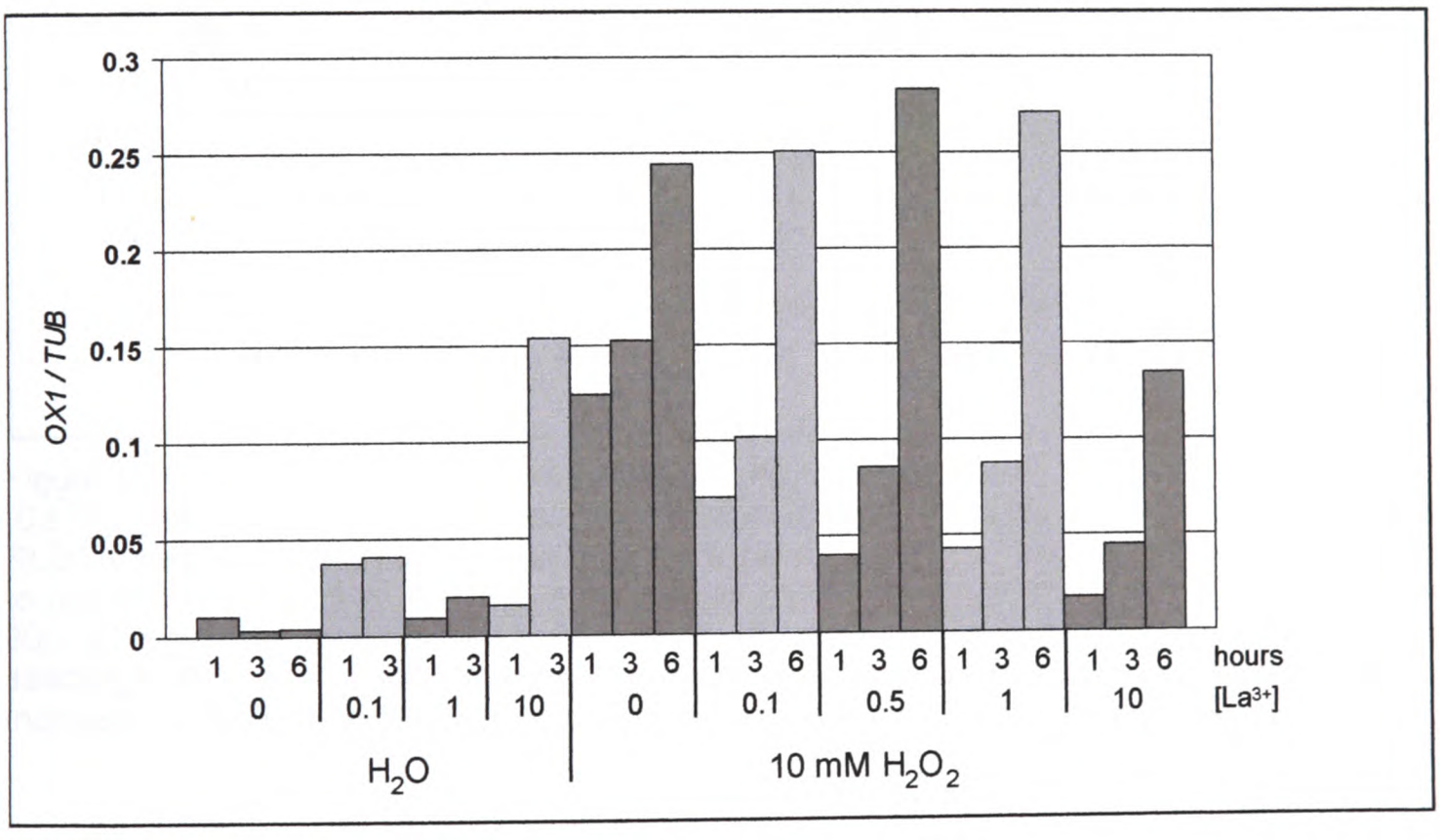

Figure 4.20: Inhibition of H_2O_2-triggered *OX1* induction by $LaCl_3$-treament
Northern analysis and normalisation of gene induction data was carried out as described in Methods. 7 day old RLD1 seedlings were transferred into H_2O and allowed to recover for 2 h before addition of $LaCl_3$ solution (final concentration as indicated). Control samples remained in H_2O. After 1 h incubation, samples were placed into fresh $LaCl_3$ and H_2O_2 was added where indicated (final concentrations $LaCl_3$: as before; H_2O_2: 10 mM). Samples were removed and frozen after 1 h, 3 h or 6 h. Total RNA was extracted, electrophoresed and transferred to nylon membrane. *OX1* and *β-TUBULIN* probes were labelled and hybridised to the RNA on the membrane. Bars represent *OX1* gene induction relative to *β-TUBULIN* mRNA levels.

In order to determine whether cellulase also increases $[Ca^{2+}]_{cyt}$, reconstituted aequorin-expressing RLD1.1 seedlings were treated with cellulase in the luminometer and emitted light was measured (Figure 4.21). A rise in $[Ca^{2+}]_{cyt}$ was detected starting 30 seconds after stress application and reaching a plateau after approximately 150 seconds. This rise in $[Ca^{2+}]_{cyt}$ could be inhibited by treatment with $LaCl_3$.

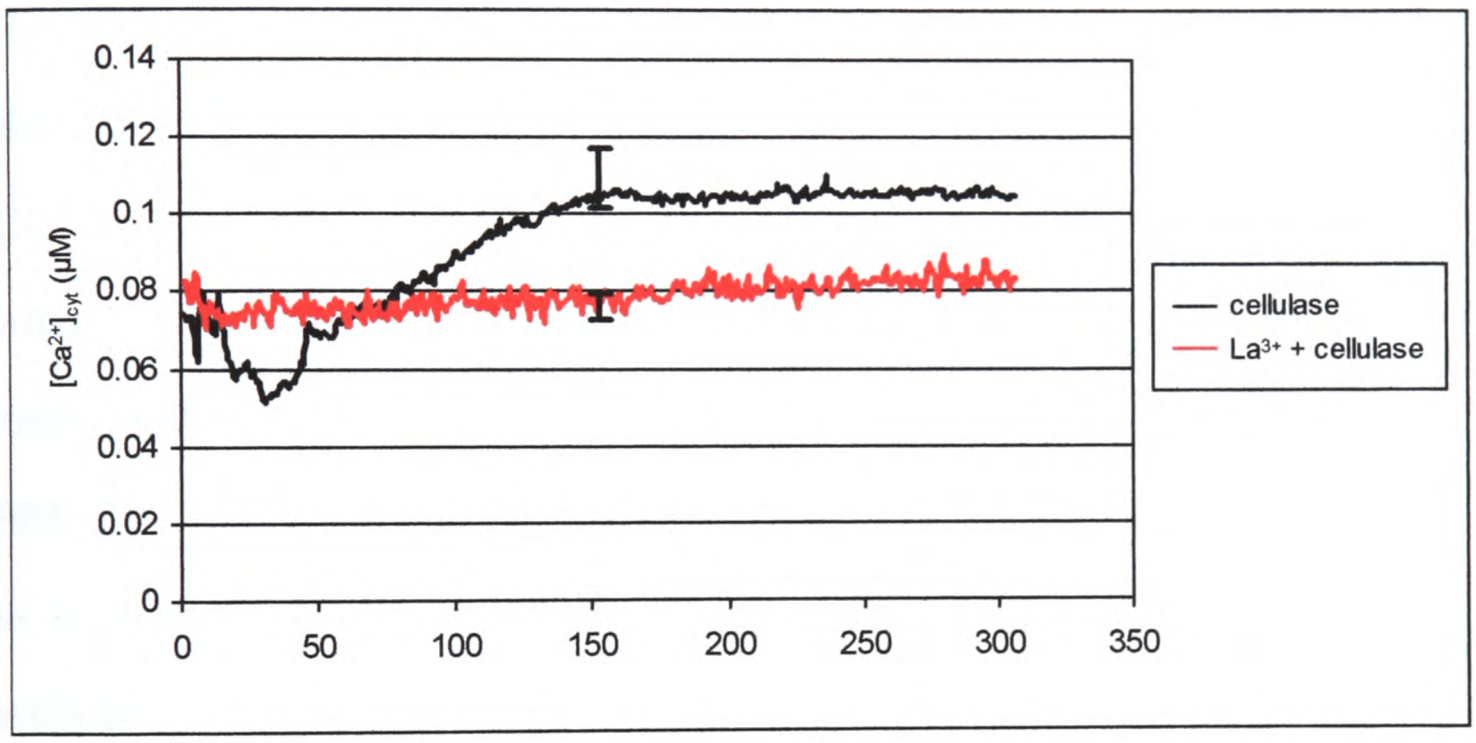

Figure 4.21: Increase in $[Ca^{2+}]_{cyt}$ in response to cellulase treatment
$[Ca^{2+}]_{cyt}$ was measured by luminometry as described in Methods. 7 day old reconstituted RLD1.1 seedlings were placed individually into plastic cuvettes containing 0.5 ml H_2O and left to rest for 5 min. At 5 s, cellulase solution was added (final concentration: 0.05 % (w/v)). At 300 s, remaining aequorin was discharged. Traces represent the mean of 3 individual seedlings with error bars indicating standard error at the time point where the $[Ca^{2+}]_{cyt}$ increase in response to cellulase treatment has reached a plateau.

As $LaCl_3$ inhibits the cellulase-triggered elevation in $[Ca^{2+}]_{cyt}$, the effect of this treatment upon *OX1* induction by cellulase was also investigated (Figure 4.22). This showed that incubation with $LaCl_3$ also prevented the rise in *OX1* levels.

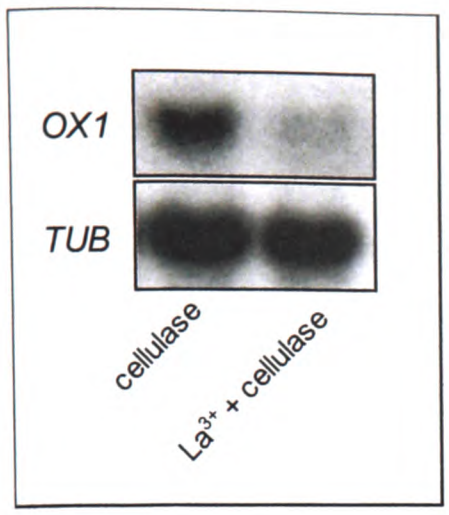

Figure 4.22: Inhibition of cellulase-triggered *OX1* induction by treatment with $LaCl_3$
Northern analysis was carried out as described in Methods. 7 day old Col-0 seedlings were transferred into H_2O and allowed to recover for 3 h before addition of $LaCl_3$ solution (final concentration: 0.2 mM). Control samples remained in H_2O. After 1 h incubation, samples were placed into fresh $LaCl_3$ and cellulase was added (final concentration: 0.01 % (w/v)). Samples were removed and frozen after 30 min incubation. Total RNA was extracted, electrophoresed and transferred to nylon membrane. *OX1* and *β-TUBULIN* probes were labelled and hybridised to the RNA on the membrane.

4.2.4. Analysis of the *OX1* promoter

Inspection of the *OX1* promoter revealed the presence of a number of elements with ACGT cores (Figure 4.23). One element (at position – 364 of the putative start ATG) corresponds to a palindromic C-box (TGACGTCA) found in Soybean and involved in binding bZIP transcription factors with homology to *A. thaliana HY5* (Cheong *et al.*, 1998). The same element (from position – 362) also matches parts of a sequence in the *A. thaliana PR-1* promoter (ACGTCA) shown to be essential for induction in response to treatment with a SA analog (Lebel *et al.*, 1998). In addition, the (T/C/G)(T/C/G)(A/T)GAC(C/T)T found to occur at high frequency in promoters of pathogen-inducible genes (Chen *et al.*, 2002) is identical to this region over the six central basepairs (from – 365). This sequence contains the well studied pathogen-inducible W-box (T)TGAC(C/T) (Yang *et al.*, 1999). (Du and Chen, 2000). A second ACGT motif is placed 12 bp upstream of the – 362 ACGT sequence; the same spacing is found for two ACGT motifs in the promoter of the light-responsive bZIP protein *Common plant regulatory factor1* (*CPRF1*) (Feldbrügge *et al.*, 1994) as well as the *ocs* element (Ellis *et al.*, 1993). Other elements in the *OX1* promoter include a G-box (CACGTG) (at position – 343), which is found in light-, ABA-, ethylene- and

JA-responsive gene promoters (Menkens *et al.*, 1995), and the motif CGACG (at position – 324), which has been shown to couple with a G-box related element in rice (Hwang *et al.*, 1998).

Induction properties of the (-385 - -317) region of the OX1 promoter (indicated by asteriks in Figure 4.23) was investigated by fusing it to the CaMV35 minimal promoter and the *GUS* reporter gene (see Appendix B.2). This region of the promoter contains the palindromic C-box and several W-box-like elements. However, cellulase treatment, wounding or infection with a virulent *P. parasitica* isolate did not induce staining in the cotyledons (data not shown) as is observed with the full length promoter (Figures 4.7 and 4.11). Faint staining was at times observed in the hypocotyl and root, independently of treatments. Hence, this 68 pb region of the *OX1* promoter is either not sufficient to confer stress inducibility or requires precise spacing with respect to the transcriptional initiation site.

CCGCCGCGTCTTCCAAGGCATTGA**ACGTC**CCTCCTCCACGCCTTCTA
GGTTCTTTCGCCT*CC**ACGT**AAA**ACGTCACCCCTGACGTCA**CATCC
TCTAGAACAC**CACGTG**TTTGTCTTAAACA**CGACG**AG*TAATTACACAT
TTGGTCAAACTCAAACCAACAAAACACTTTTTAAACAAGGCTAAATTG
GTCAAACGCATGGCAACGAATCTCAGGCGTTTTTTCGTTTTCTTTATTA
TTGACTTATTTTTATTTTTATTTTATTTTGCTTCTTTGAAATCTTCCCCG
GCAAGGCAAAGCAAACGAGTGGACGTTTTTGAAGATTCGTTAATTTTT
CTCTCTCTCTTTATAATATAAGAAGTCGCCTACTACGTAGAACCAAAA
GAGAGACAAAAATACACTTTCATTGCTGTCTTAACTCTAACGGAGT
TAACTAACGTCGACATT**ATG**

Figure 4.23: Identification of putative promoter elements in the *OX1* promoter
A 401 bp region 5' of the putative *OX1* start codon (ATG, in black) is shown. Putative promoter elements important in *OX1* expression are underlined. Asterisks indicate the promoter region analysed for stress-inducibility.

4.2.5. Characterisation of the *ox1* mutant

4.2.5.1. Comparison of gene induction in ox1 *and WS-2*

Kinase activation is a fast response following signal perception and does not require transcription of the kinase gene; however, a correlation between kinase activation and up-regulation of transcription of the kinase gene is often detected (Hirt, 1999). Therefore, in order to determine the role of the OX1 kinase in stress signal transduction, the *ox1* mutant was examined for differential gene induction in response to a number of stimuli that were able to induce increased transcript levels of *OX1* in the wild-type.

4.2.5.1.1 Gene induction in response to AOS treatment

As demonstrated in section 4.2.2.2.3 (*e.g.* Figure 4.4), *OX1* transcript levels increase in response to treatment with H_2O_2 and menadione. Thus, the antioxidant genes *GST1* and *APX1*, shown to be affected by these treatments in section 3.2.2.2.3 (*e.g.* Figure 3.24), were examined for differential induction in *ox1* and the WS-2 wild-type. The results indicate that *GST1* and *APX1* levels are not significantly changed in the *ox1* mutant (Figure 4.28).

To identify other H_2O_2-responsive genes that may be affected by the *ox1* mutation, microarray analysis was carried out on Affymetrix chips (NASC Affymetrix Facility, Nottingham). Four samples were thus analysed for expression levels: WS-2 and *ox1* control samples (in H_2O) and WS-2 and *ox1* treated samples (3 h in 10 mM H_2O_2). The analysed data is attached in Appendix C.

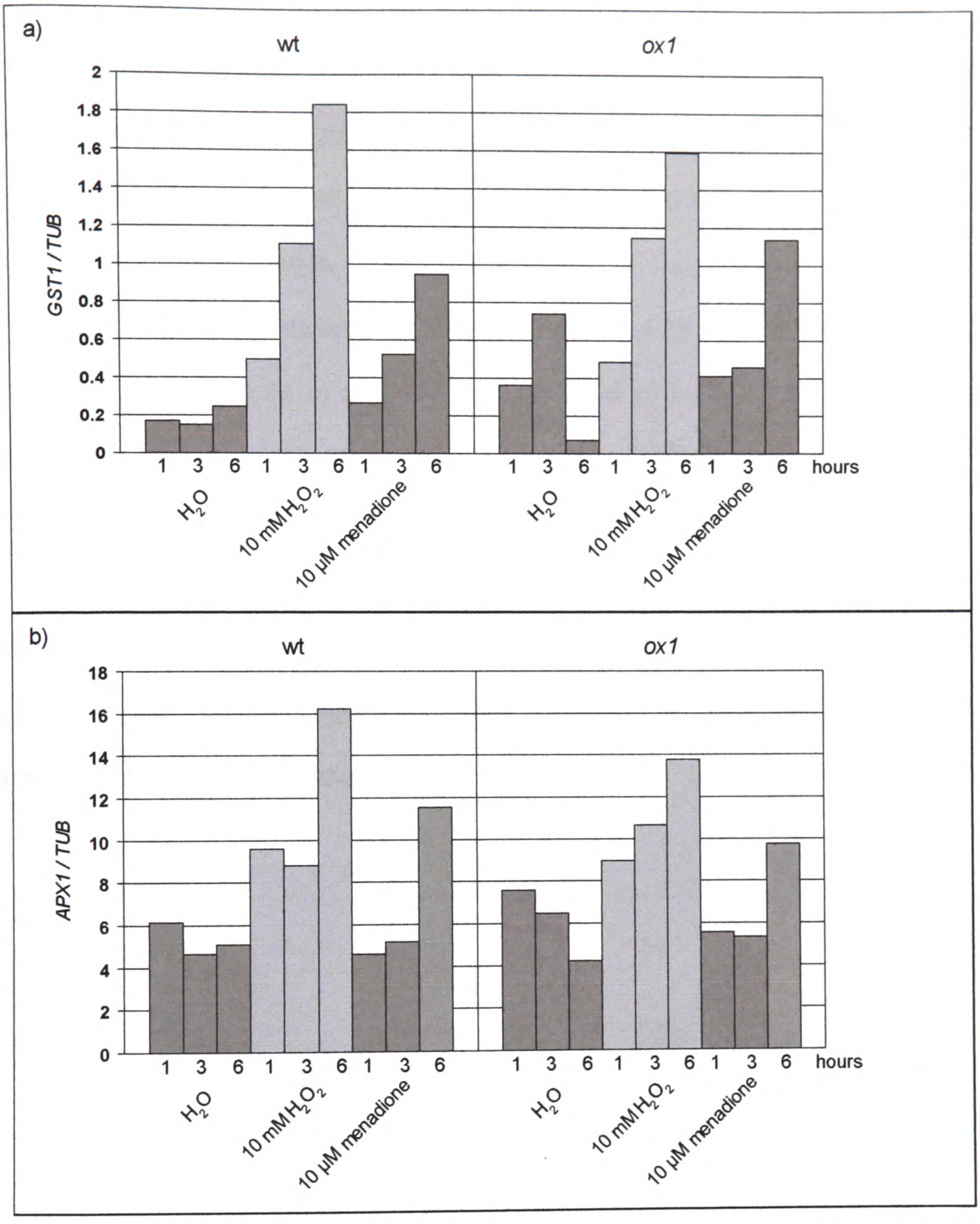

Figure 4.28: Antioxidant gene induction in response to H_2O_2- and menadione in the *ox1* mutant

Northern analysis and normalisation of gene induction was carried out as described in Methods. 7 day old WS-2 and *ox1* seedlings were transferred to H_2O and left to recover for 2 h. H_2O_2 (final concentration: 10 mM) or menadione (final concentration: 10 µM) were added as indicated. Samples were frozen after 1 h, 3 h and 6 h incubation. Total RNA was extracted, electrophoresed and transferred to nylon membrane. *GST1*, *APX1* and *β-TUBULIN* probes were labelled and hybridised to the RNA on the membrane. Bars represent antioxidant gene induction relative to *β-TUBULIN* mRNA levels.

4.2.5.1.2 Gene induction in response to cellulase treatment and wounding

The most significant increase in *OX1* transcript levels was observed in response to cellulase treatment (e.g. Figure 4.6). Cell wall digestion by this enzyme may mimic wounding, which was also shown to induce *OX1* (Figure 4.6). Thus, the *ox1* mutant was examined for changes in gene expression in response to these stresses. Wounding-induced increases in *GST1* (Figure 4.29 a), *ACX1* (*ACYL-CoA OXIDASE1*) (Figure 4.29 b) and *AOS* (Figure 4.29 c) levels were not significantly affected in *ox1*. *GST1* and *ACX1* have been shown to be induced independently of *COI1* (a gene coding for a component of the JA-signal transduction chain (Ellis *et al.*, 2002)) in response to wounding, whereas *AOS* gene induction was *COI1*-dependent (Reymond *et al.*, 2000). The data therefore suggest that OX1 is not involved in the signalling pathway linking wounding to induction of downstream genes, irrespective of JA dependency.

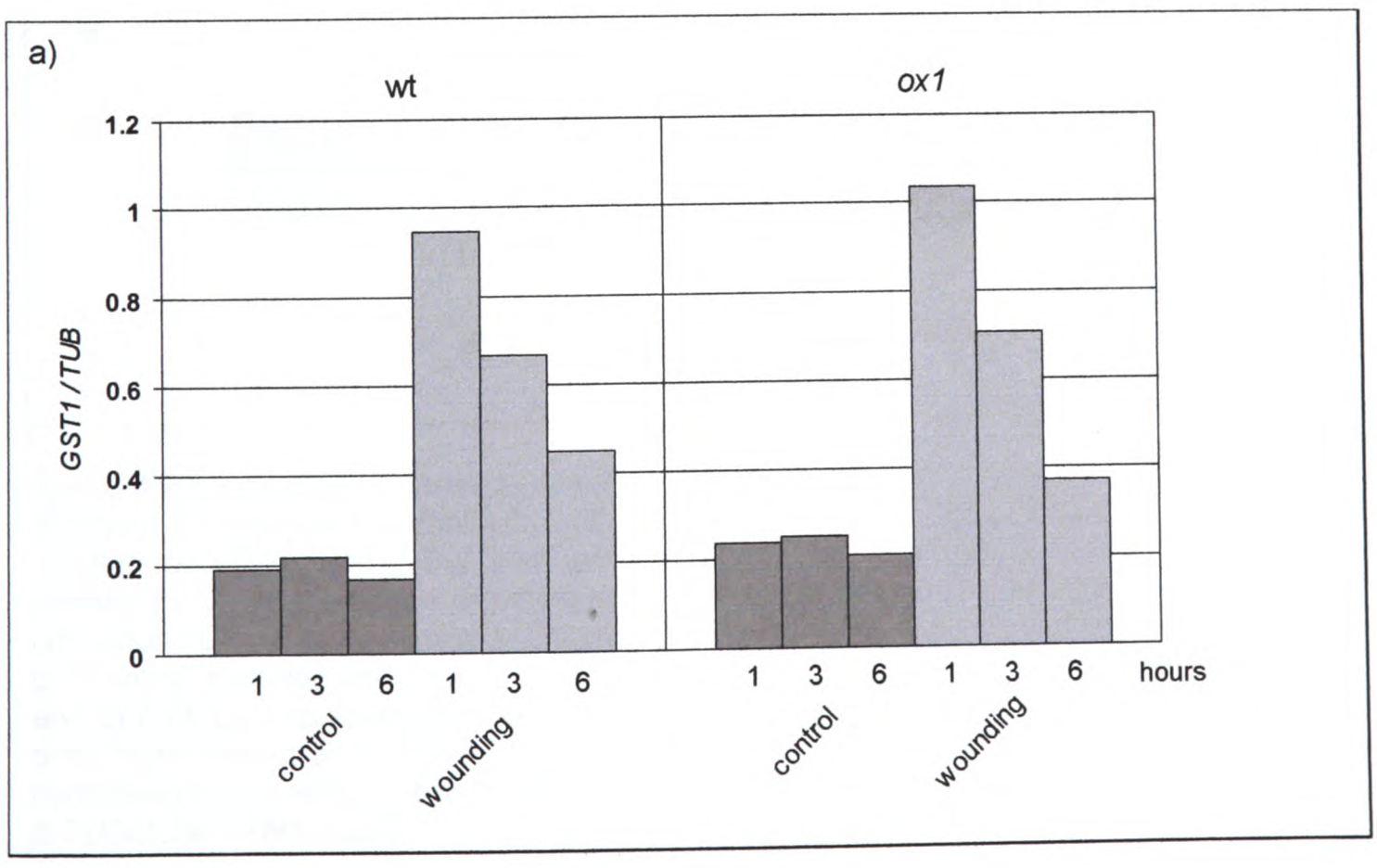

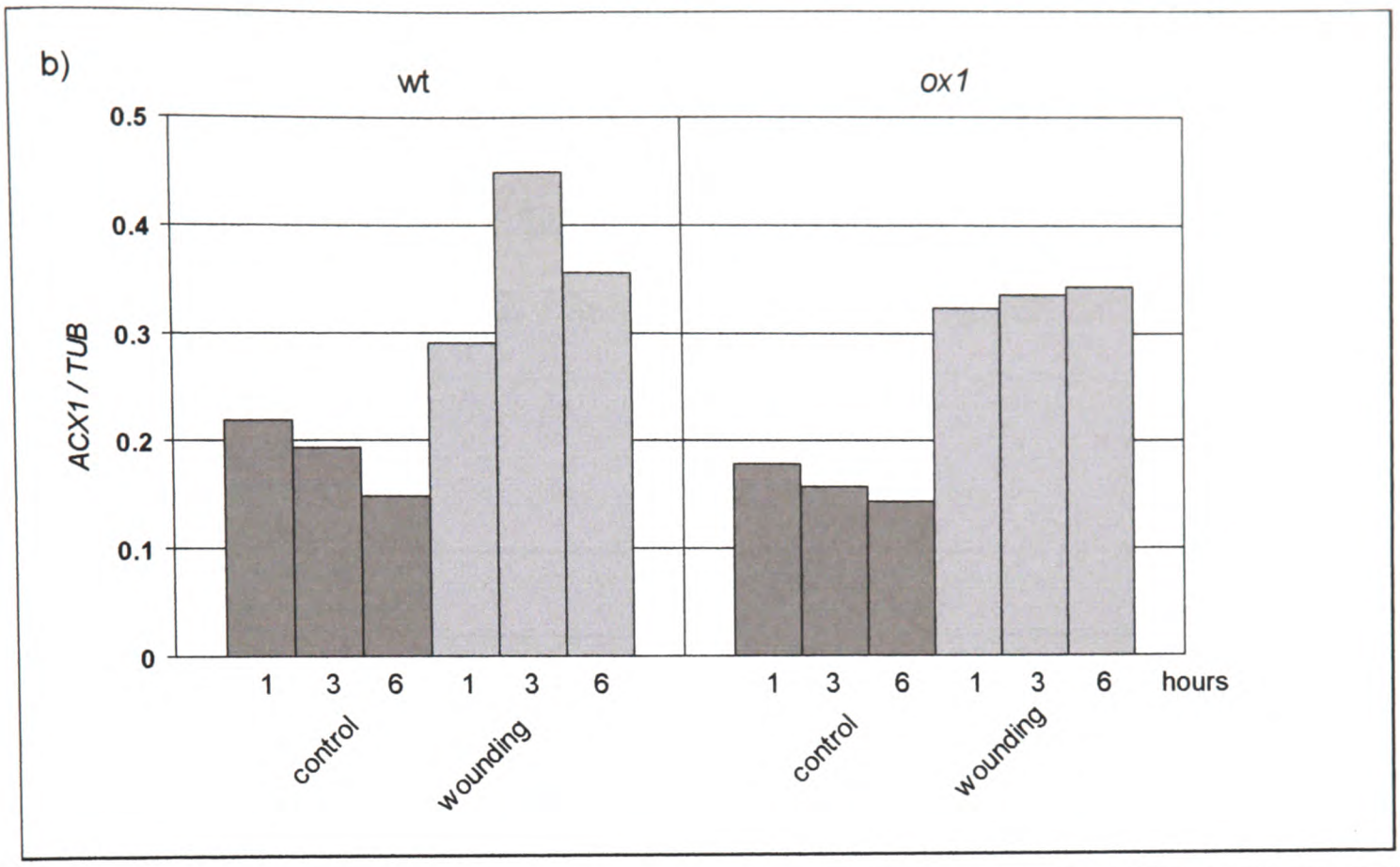

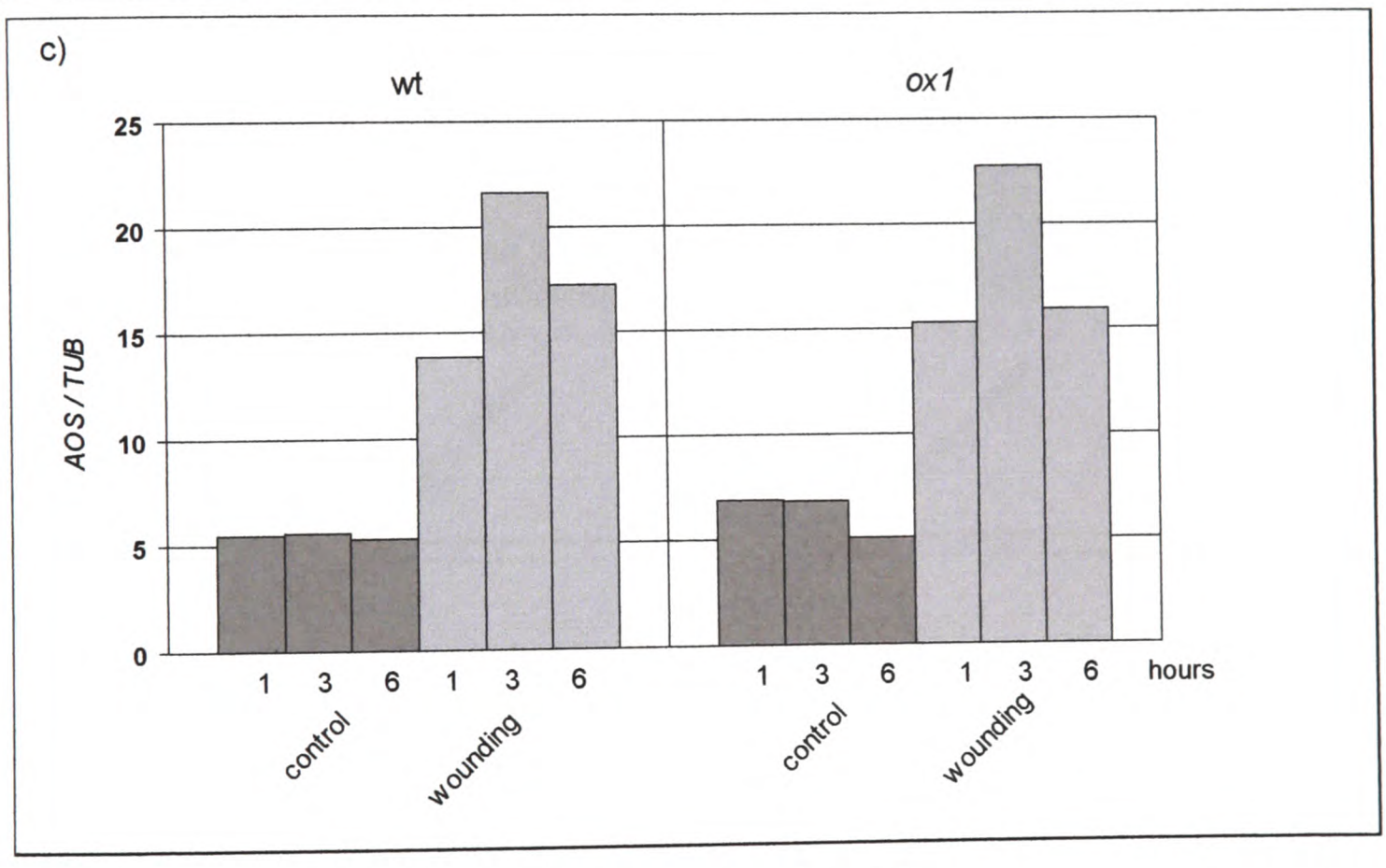

Figure 4.29: Induction of genes by wounding in *ox1* and WS-2
Northern analysis and normalisation of gene induction data was carried out as described in Methods. 6 day old WS-2 and *ox1* seedlings were transferred into H_2O and left to recover for 2.5 h. Seedlings were wounded with tweezers until approximately 25 % of the cotyledon surface was damaged. Control samples remained undamaged in H_2O. After 1, 3 or 6 hours, samples were frozen and total RNA was extracted. a) 10 µg / sample and b) and c) 6.25 µg / sample were electrophoresed on separate agarose gels and transferred onto nylon membrane. *GST1*, *ACX1*, *AOS* and *β-TUBULIN* probes were labelled and hybridised to the RNA on the membrane. Bars represent wound gene induction relative to *β-TUBULIN* mRNA levels.

Increases in *ERF6* (ethylene responsive element binding protein, see section 5.1) and *PDF1.2* transcript levels in response to cellulase treatment was also not significantly altered in *ox1* (Figure 4.30). *PDF1.2* is induced by treatment with ethylene (see section 4.2.3.3.2, Figure 4.14), suggesting that *ox1* is not impaired in ethylene signalling.

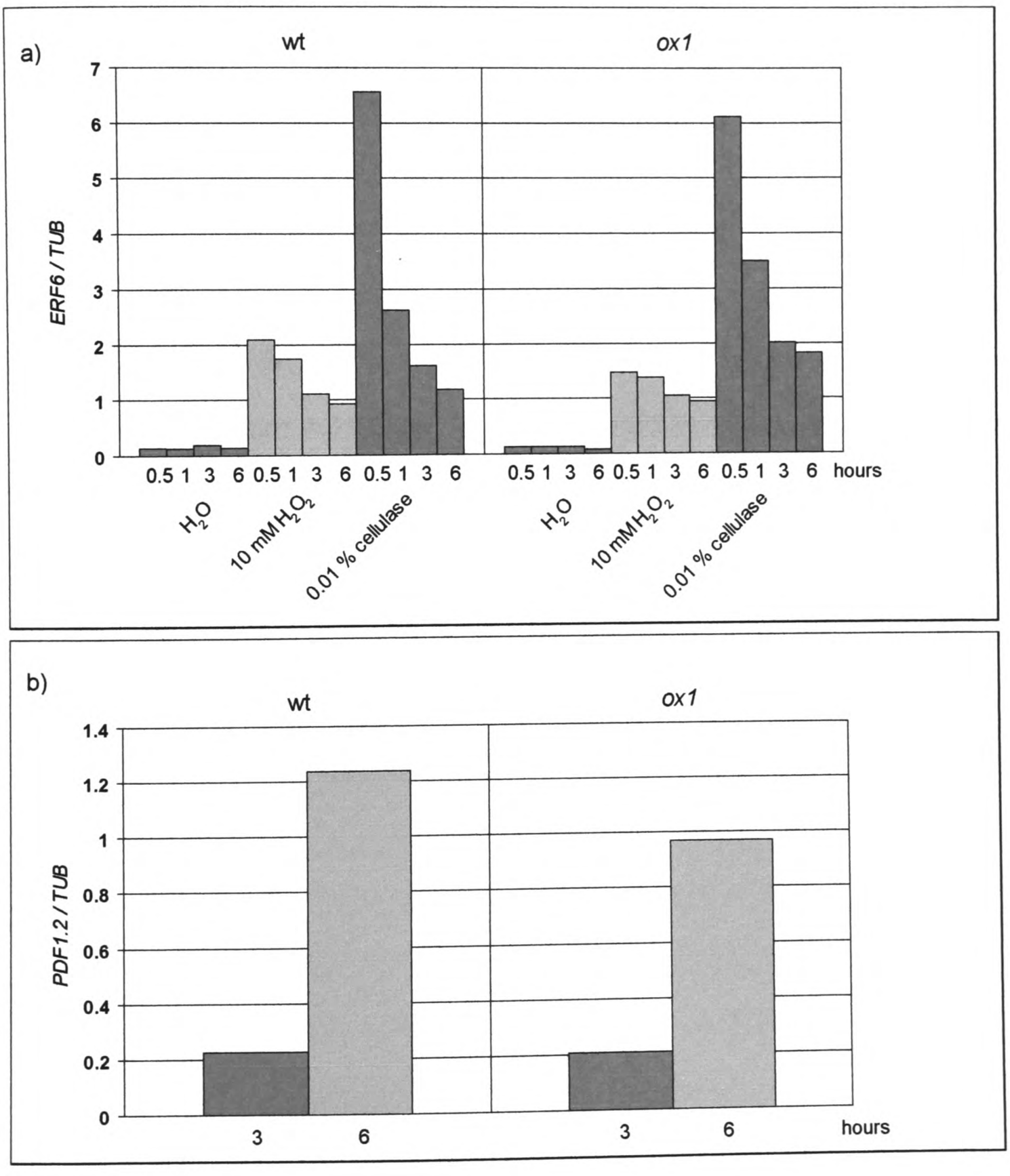

On the previous page:
Figure 4.30: Induction of genes by cellulase treatment in the *ox1* mutant
Northern analysis and normalisation of gene induction data was carried out as described in Methods. 7 day old WS-2 and *ox1* seedlings were transferred to H_2O and left to recover for 3 h. H_2O_2 (final concentration: 10 mM) or cellulase (final concentration: 0.1 % (w/v)) were added as indicated. Samples were frozen after 0.5 h, 1 h, 3 h and 6 h incubation and total RNA was extracted, electrophoresed and transferred onto nylon membrane. *AtERF6*, *PDF1.2* and *β-TUBULIN* probes were labelled and hybridised to the RNA on the membrane. In b), only the 3 h and 6 h time points for cellulase treatment are shown as expression of *PDF1.2* was undetectable in all other samples. Bars represent gene induction relative to *β-TUBULIN* mRNA levels

4.2.5.1.3 Gene induction in response to fungal infection

Growth of *P. parasitica* through shoot tissue triggered expression of the GUS reporter gene fused to the *OX1* promoter in cells along the fungal hyphae (Figure 4.11). Thus, transcript levels in pathogen-inducible genes were examined in WS-2 and *ox1* seedlings infected with the virulent Emco5 isolate. Expression of *PR-1 (PATHOGENESIS-RELATED PROTEIN1)* was reduced by approximately 50 % in the *ox1* mutant (Figure 4.31 a and b), whereas *ECS1* induction was even further decreased in *ox1* (Figure 4.31 a).

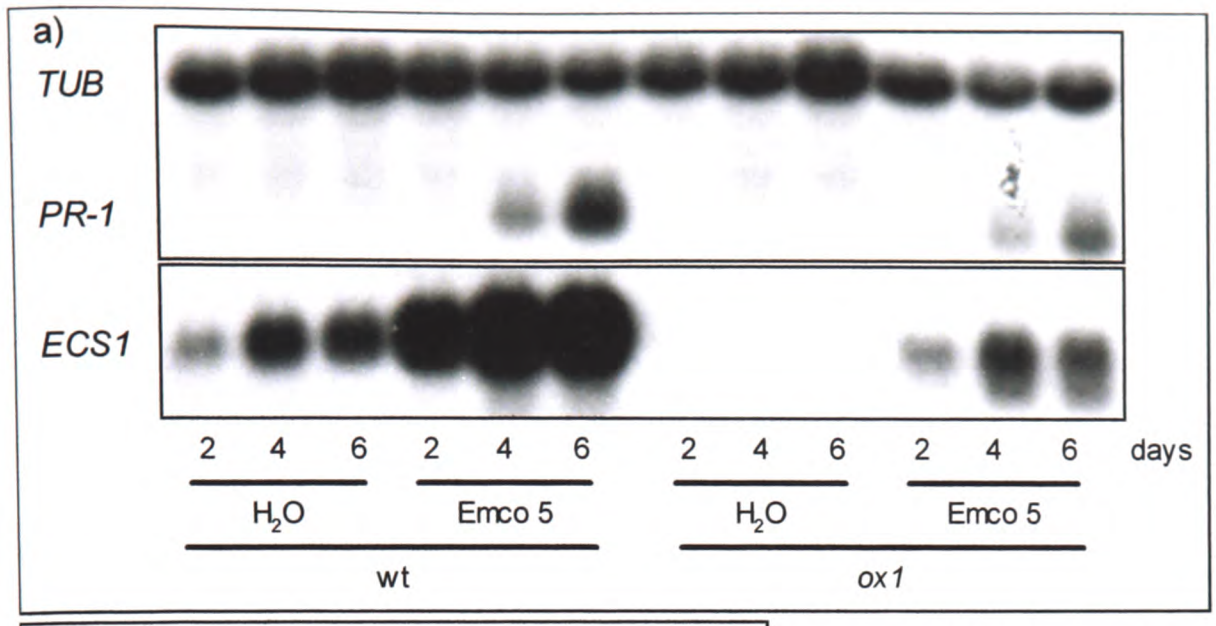

Figure 4.31: Gene induction by infection with virulent *P. parasitica* in the *ox1* mutant Northern analysis and normalisation of gene induction data was carried out as described in Methods. 10 day WS-2 and *ox1* old seedlings were sprayed with H_2O or a spore suspension of the virulent *P. parasitica* isolate Emco5. Samples were frozen after 2, 5 and 7 days and total RNA extracted, electrophoresed and tranferred onto nylon membrane. *β-TUBULIN*, *PR-1* and *ECS1* probes were labelled and hybridised to the RNA on the membrane. b) Bars represent induction of *PR-1* in the infected samples after 5 and 7 days relative to *β-TUBULIN* mRNA levels.

In the microarray experiment, *ECS1* and *THI2.2* were identified as a genes with lower transcript levels in *ox1* as compared to the wild-type WS-2 (see Appendix C, c). Neither of these genes was induced by H_2O_2 treatment. The microarray data was confirmed by RT-PCR (Figure 4.32 a) and Northern analysis (Figures 4.31 and 4.32 b). *ECS1* was induced by *P. parasitica* infection but to much lower levels in *ox1*. *THI2.2* has strong homology to *THI2.1* and very little unique sequence. The probe therefore cross-hybridised to the *THI2.1* transcript. Concomitantly, two bands are visible in the WS-2 samples whereas the lower band is absent in the *ox1* samples, confirming that *THI2.2* transcript levels are substantially reduced in the mutant (Figure 4.32 b).

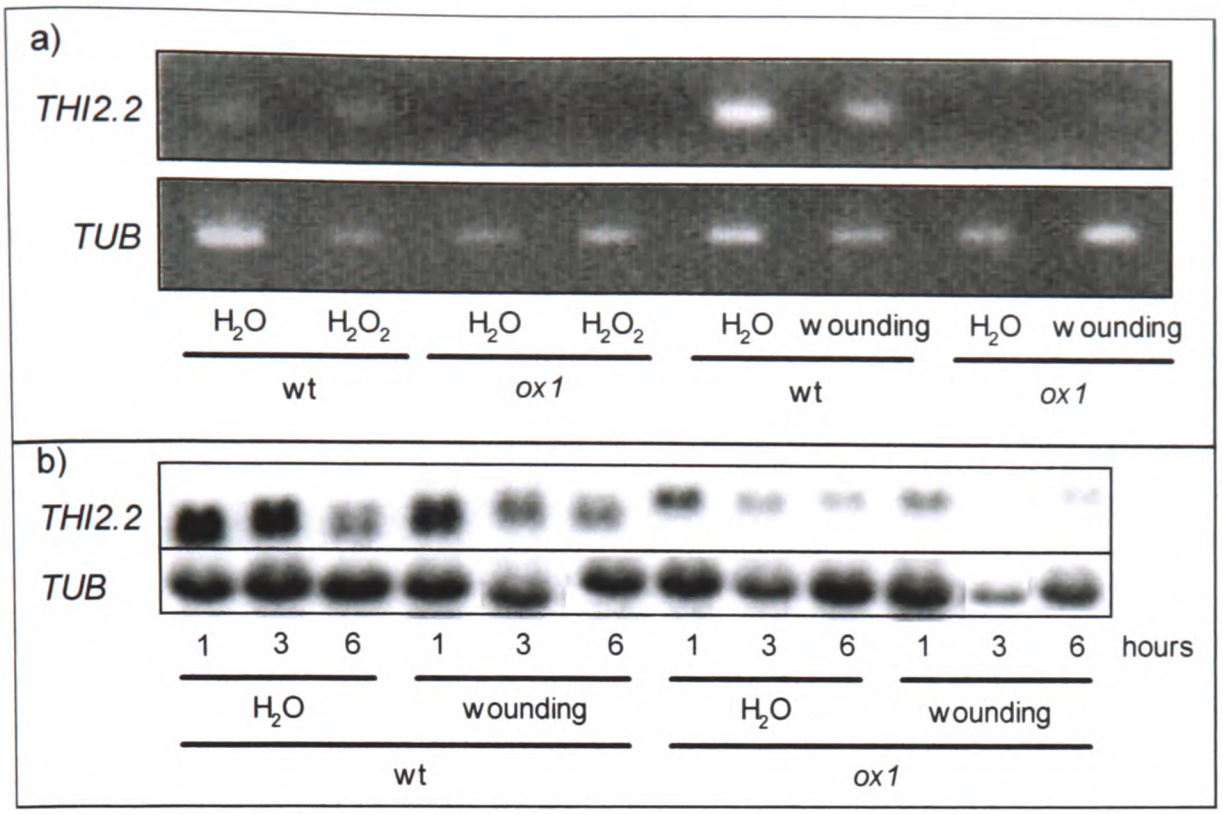

Figure 4.32: *THI2.2* levels in the *ox1* mutant
a) 7 day old WS-2 and *ox1* seedlings were transferred to H_2O for 3 h before either treatment with H_2O_2 (final concentration: 10 mM) or wounding with tweezers (~ 25 % cotyledon surface). After 3 h, samples were frozen and RNA extracted. cDNA was synthesised from 2.5 µg RNA and diluted 1:50. 10 µl of this dilution was used per PCR reaction, using heat-activated polymerase (Immolase, Bioline). 20 cycles (*THI2.2*) or 26 cycles (*TUB*) amplification were carried out. 10 µl per reaction was electrophoresed on an agarose gel and imaged under the UV camera.
b) Northern analysis was carried out as described in Methods. 6 day old WS-2 and *ox1* seedlings were transferred into H_2O and left to recover for 2.5 h. Seedlings were wounded with tweezers until approximately 25 % of the cotyledon surface was damaged. Control samples remained undamaged in H_2O. After 1, 3 or 6 hours, samples were frozen. Total RNA was extracted, electrophoresed and transferred to nylon membrane. *THIONIN2.2* and *β-TUBULIN* probes were labelled and hybridised to the RNA on the membrane.

Induction of the *ECS1* gene was tested in transformed Col-0 lines carrying an oestradiol inducible *OX1* constitutive mutant gene (see Appendix B.3). No difference in ECS1 induction was seen following incubation in oestradiol in lines that show increased *OX1* constitutive mutant levels (data not shown).

4.2.5.1.4. Gene induction in response to SA treatment

SA has been shown to function in defense response signalling pathways (see section 1.3.3.3.) and is implicated in induction of *PR-1* in response to pathogen infection (see section 4.3.2.2.2). To test whether OX1 functions upstream of SA

accumulation, gene induction in response to SA treatment was investigated. *ECS1* transcript levels increased in response to SA, but this increase is strongly reduced in the *ox1* mutant.

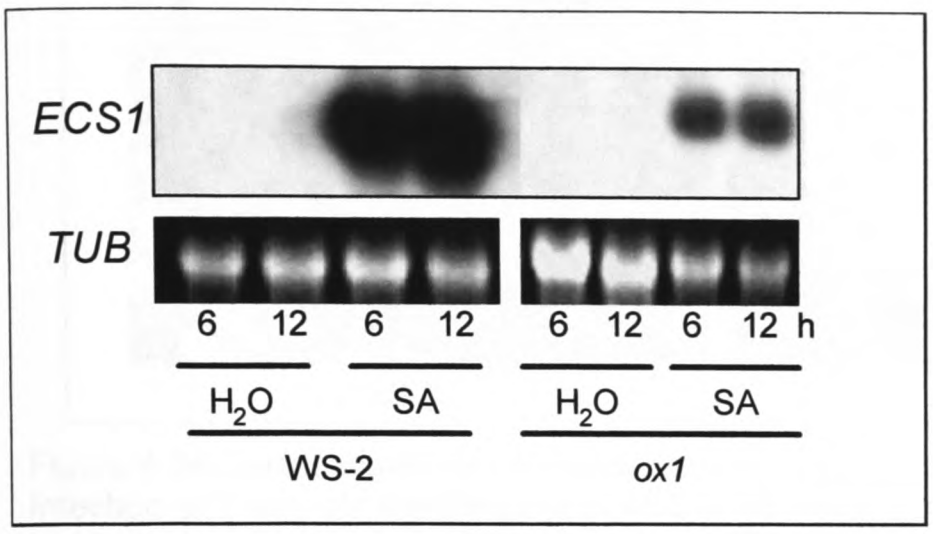

Figure 4.33: *ECS1* induction in response to SA in *ox1*
Northern analysis was carried out as described in Methods. 7 day old WS-2 and *ox1* seedlings were transferred into H_2O and left to recover for 3 h. SA (final concentration: 250 µM) was added as indicated. Samples were frozen after 6 h or 12 h incubation. Total RNA was extracted, electrophoresed and transferred to nylon membrane. *ECS1* probe was labelled and hybridised to the RNA on the membrane. The RNA stained with ethidium bromide is depicted as a loading control.

4.2.5.2. *Phenotypic analysis of the of the* ox1 *mutant*

4.2.5.2.1 Susceptibility of the *ox1* mutant to *Peronospora parasitica*

Transcript levels of several pathogen-inducible genes are reduced in *ox1*, including *ECS1* and *THI2.2* (Figures 4.31 and 4.32) as well as two RPP5-like proteins and epoxide hydrolase and caffeic acid O-methyltransferase (see Appendix C, section c). Thus, susceptibility of this mutant to *P. parasitica*, a biotrophic fungus (Koch and Slusarenko, 1990), was investigated. Both WS-2 and *ox1* were resistant to infection with the avirulent isolate Emoy2 (Holub *et al.*, 1994), displaying only short fungal hyphae at attempted penetration sites (data not shown). However, *ox1* exhibited considerable enhanced susceptibility to the virulent isolate Emco5 (Bittner-Eddy *et al.*, 1999). This was evident visually (Figure 4.34, Figure 4.35 a) and also through quantification of Emco 5 sporulation (Figure 4.36 b and c).

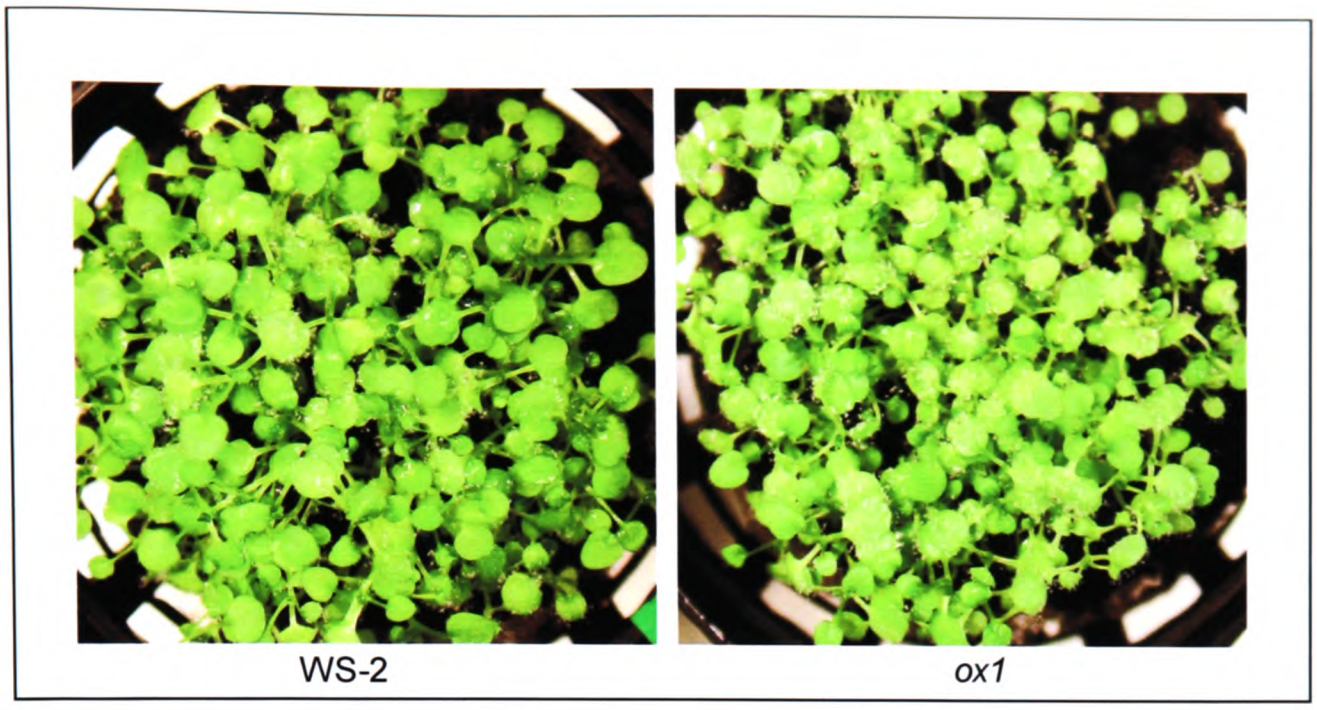

Figure 4.34: Susceptibility of *ox1* to the virulent *P. parasitica* isolate Emco5
Infection of 7 day old seedlings with an Emco5 spore suspension was carried out as described in Methods. Images represent seedlings 7 days post infection which had been located in the same box. Images were taken with a Nikon Coolpix 990 digital camera.

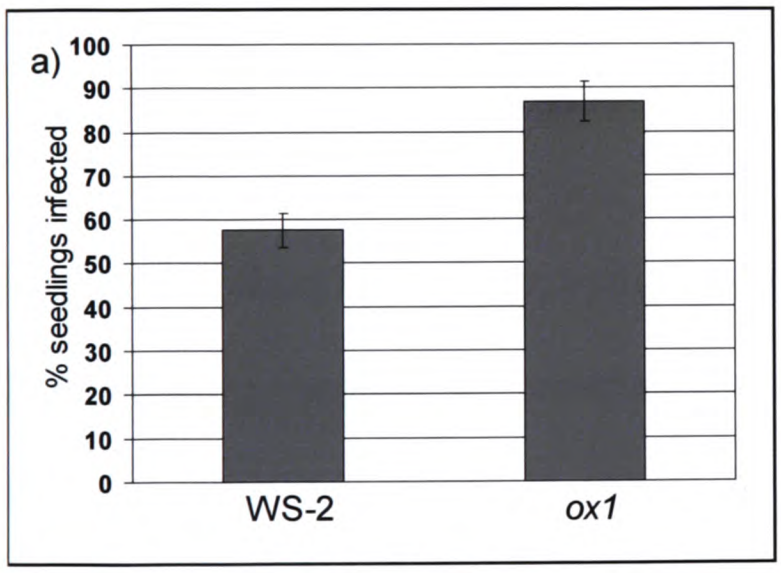

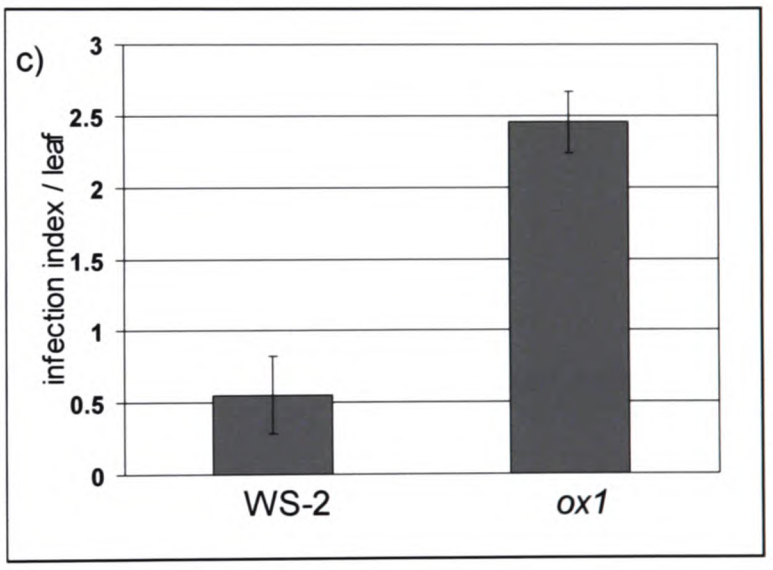

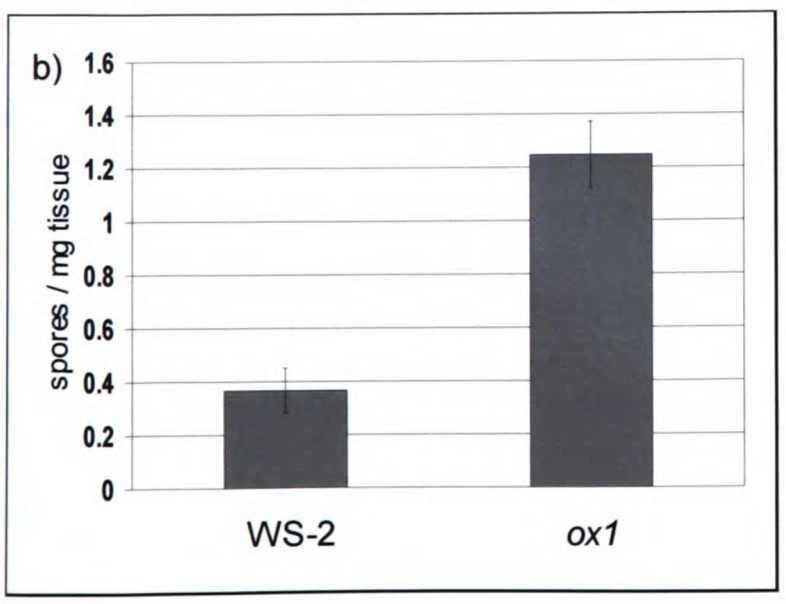

Previous page:
Figure 4.35: Susceptibility of *ox1* to infection with the virulent *P. parasitica* isolate Emco5
Seeds were stratified for 3 days in 0.15 % agar and spread out in a dilute suspension onto peat plugs. Seedlings were grown for a) 7 days, b) 9 days or c) 4 weeks at 21 °C, 16 h light, in transparent boxes with lids before spraying them with fungal spore suspension. a) 8 days post infection, all seedlings with sprorangiophores on each plug were counted (10 – 60 seedlings / plug). Bars express the percentage of infected seedlings per sample (plug), with error bars representing standard error for 4 samples. b) 6 days post infection, the level sporulation was assessed as described in Methods. 150 – 300 mg tissue (cotyledons and small leaves) from separate plugs were removed into Eppendorf tubes, weighed and 200 µl H_2O was added. After vortexing for 30 s, spores were counted on a haemocytometer. The mean of ten squares (each 0.1 mm^3 suspension) was recorded per sample and several samples were scored twice to ensure accuracy. The resultant count was divided by the weight of the tissue (mg). Error bars represent standard error of 8 samples. c) 6 days post infection, leaves were assessed for sporulation. Leaves with 75 – 100 %, 25 – 75 %, < 25 % and 0 % of their surface covered with sporangiophores were given a score of 4, 2.5,1 and 0, respectively. The added score per plant was divided by the number of leaves to yield the 'infection index'. Error bars represent standard error for 7 WS-2 and 9 *ox1* plants.
Student's t-tests indicated that infection levels of wild type and *ox1* were significantly different (a: p = 0.0003; b: p , 0.0001; c: p = 0.0005).

4.2.5.2.2 Root hair growth in the *ox1* mutant

GUS staining assays of seedlings transformed with the *OX1*promoter::*GUS* construct showed that *OX1* is constitutively expressed in roots and in particular in epidermal cells that formed root hair (Figure 4.36). Expression was not caused by wounding upon transfer from agar plates to solution as GUS expression was also observed in seedlings that were stained immediately, without time to allow for transcription to take place (data not shown). *ox1* seedlings grown on vertical agar plates were therefore examined for changes in root hair growth (Figure 4.37). Root hair appeared generally shorter and less robust than in the WS-2 wild type. The growth rate of the primary root was unaffected in the *ox1* mutant (data not shown).

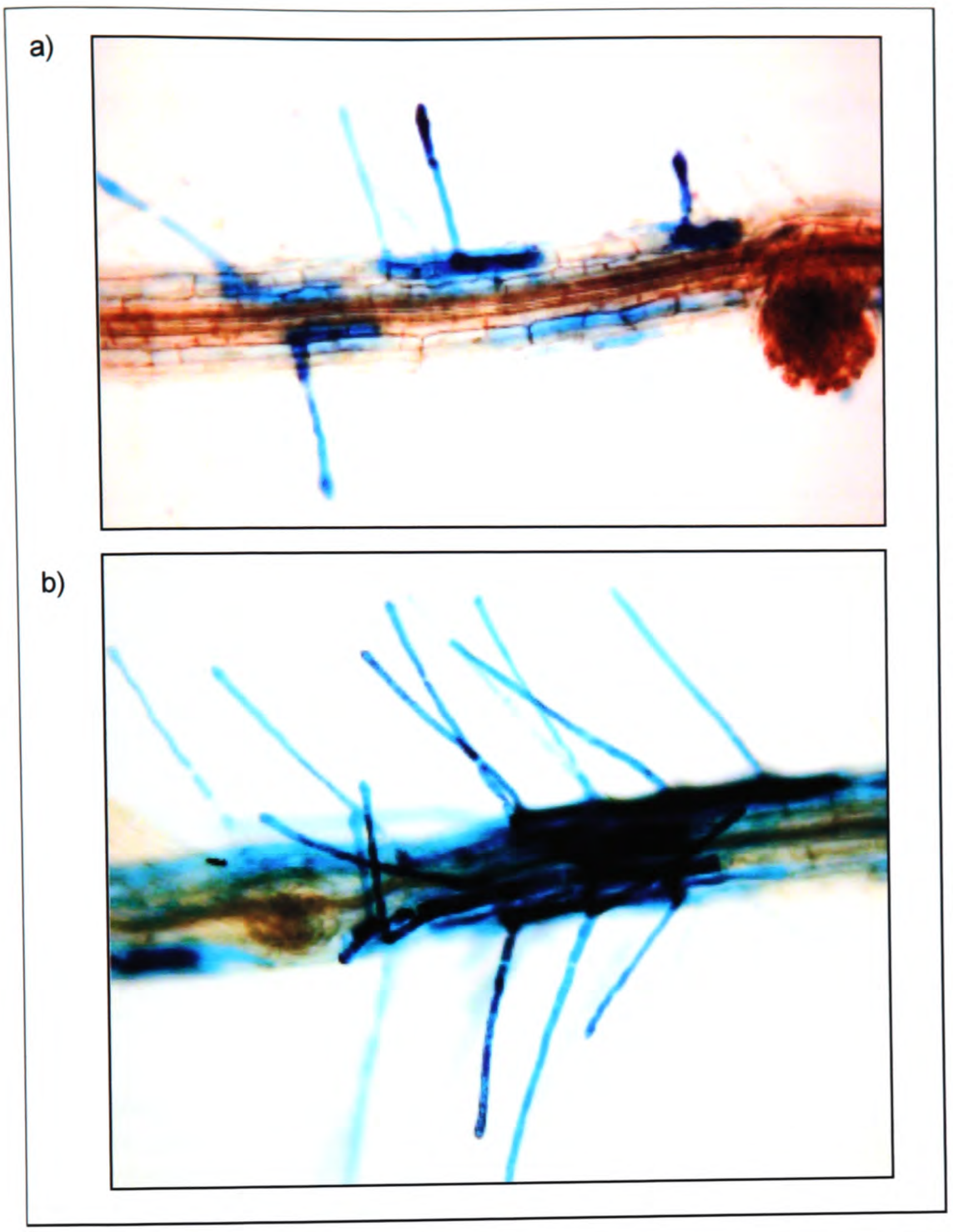

Figure 4.36: OX1 promoter activity in roots
In vivo GUS staining was performed as described in Methods. 7 day old Col-0 seedlings transformed with the *OX1* promoter::GUS construct were transferred to H_2O and left for 4 h before staining for GUS expression. Images were taken with a Nikon Coolpix 990 digital camera mounted on a Leica DM R microscope. 1000 x 4000 x magnification; with variation of an extra 2.8 x magnification (from no zoom to full zoom of the digital camera).

Figure 4.37: Root hair growth in the *ox1* mutant
Seedlings were grown on vertical MS agar plates (1.2 % agar) for 4 days before transferring single seedlings to fresh vertical plates. Growth was marked with pen every 24 h on the Petri dish. Images of the root section grown over a 24 h period (from 48 h to 72 h after transfer) were taken with a RS photometrix (A99M81020) camera mounted on a Leica MZ FL III microscope. Images represent root sections of the three seedlings (out of ten) with the longest root hairs.

4.2.5.2.3 Flowering time in the *ox1* mutant

When WS-2 and *ox1* seedlings were grown up to maturity in the greenhouse, it was noted that the *ox1* plants started bolting at an earlier time than the WS-2 wild type (Figure 4.38). This difference in initiation of flowering was not observed in other growth facilities.

Figure 4.38: Flowering time in the *ox1* mutant
5 day old seedlings were transferred from MS agar plates onto peat plugs and grown in the greenhouse, 24 °C, 16 h light / 8 h dark cycle (in June, also natural light) , arranged in alternating lines to ensure equal conditions for WS-2 and *ox1*. Depicted are 21 day old plants. Images were taken with a Nikon Coolpix 990 digital camera.

4.2.5.2.4 Changes in activation of signal transduction components in the *ox1* mutant

In collaboration with Dr Brian Ellis, University of Vancouver, activation of AtMPK3 and AtMPK6 in the *ox1* mutant in response to ozone treatment was investigated (Fig. 4.39) as these MAPKs have been implicated in signal transduction in response to H_2O_2 and treatment with H_2O_2-generating stresses (see sections 4.1.2 and 4.1.3). Activation of MAPKs requires the phosphorylation on threonine and

tyrosine residues which can be detected by phosphorylation-specific antibodies and is related to the activation state of the kinases. AtMPK3 and AtMPK6 displayed increased phosphorylation in response to ozone fumigation, but this increase was much reduced in the *ox1* mutant. Thus, OX1 is necessary for full activation of AtMPK3 and AtMPK6 in response to ozone fumgiation.

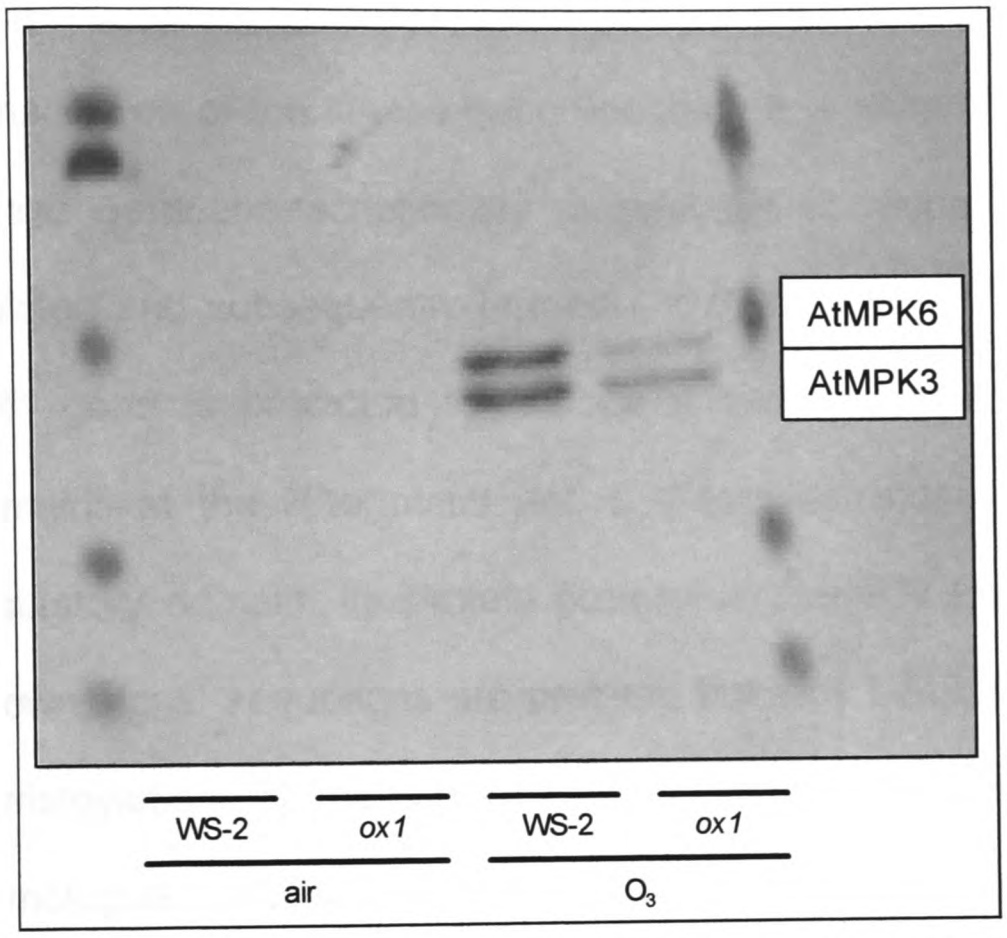

Figure 4.39: AtMPK3 and AtMPK6 activation in *ox1* in response to ozone
Plants were ozone-fumigated for 20mins at 500ppb. Protein was extracted and AtMPK3 and AtMPK6 immunoprecipitated with specific antibodies. The precipitated protein was run on a polyacrylamide gel and blotted onto membrane. Western blot analysis was carried out using anti-pERK1/2 antibodies (NEB, UK). A detailed description of the protocol can be found in Miles *et al*, 2002.

4.3. Discussion

4.3.1. Analysis of the *OX1* gene

Protein phosphorylation catalysed by protein kinases regulates biological processes in response to a wide range of stimuli. Hence, kinases involved in transducing the H_2O_2 signal were investigated by comparing relative transcript levels in response to H_2O_2 treatment, as a correlation between kinase activation and up-regulation of transcription of the kinase gene encoding it is often detected (Hirt, 1999). A single kinase gene, transcriptionally upregulated in response to H_2O_2 treatment, was isolated and subsequently termed *OXIDATIVE STRESS-INDUCIBLE1* (*OX1*). The *OX1* gene is predicted to encode a ser/thr kinase with the conserved kinase domains at the N-terminus and a C-terminal extension which may constitute a regulatory domain. Its protein product is probably localised in the cytosol, as no known signal sequences are present, but may be recruited to membranes through myristoylation at several putative myristoylation sites. *OX1* has one close homologue (*OX2*) which lacks the putative C-terminal regulatory domain; however, transcript levels of this gene were very low and were not induced by H_2O_2 (Figures 4.4 and 4.5), indicating that the OX2 protein is probably not involved in transducing the H_2O_2 signal.

OX1 belongs to the kinase gene family 4.2.6, including the *NON-PHOTOTROPHIC HYPOCOTYL* (*NPH*) kinases. In addition, the *OX1* promoter contains sequences with homology to light-regulated elements (see section 4.2.4). However, the *ox1* null-mutant is neither affected in perception of blue and red light during germination and early development, nor is it impaired in phototropism to blue light (data not shown). Other members of kinase gene family 4.2.6 are the *INCOMPLETE ROOT*

HAIR ELONGATION (*IRE*) kinases. A mutant with reduced *IRE* transcript levels had shorter root hairs (length approximately 60 % of wild-type length) but displayed otherwise normal root morphology (Oyama *et al.*, 2002). Similarly, root hair in the *ox1* mutant was shorter (Figure 4.37) while growth rate of the main root was unaffected (data not shown). Both genes (*IRE* and *OX1*) are expressed to particulary high levels in root hair-forming cells (Oyama *et al.*, 2002, Figure 4.36), indicating that the OX1 and IRE kinases may function in similar developmental processes (see also section 6.5.1).

4.3.1.1. Induction of OX1 *transcription by H_2O_2-generating stimuli*

Transcript levels of the *OX1* gene increased not only in response to treatment with H_2O_2 (Figures 4.4, 4.5, 4.8, 4.15 and 4.18) but also to treatment with menadione (Figure 4.4), wounding and cellulase (Figures 4.6, 4.7, 4.8, 4.13, 4.14, 4.16, 4.18, 4.19 and 4.22), salt, drought and cold (Figure 4.8), UV-B and flagellin (Figure 4.9), ABA (Figure 4.17) as well as in areas of fungal penetration (Figures 4.10, 4.11 and 4.12), all of which have been shown to cause generation of AOS (see section 1.2). Surprisingly, *OX1* was not induced during recovery from heat shock (Figure 4.8), even though AOS are generated during this phase (Vallelian-Bindschedler *et al.*, 1998). It may be that the heat shock administered was not sufficiently severe. Among the inducing treatments, cellulase had the strongest effect on *OX1* transcript levels (*e.g.* Figure 4.8). Cellulase degrades cellulose chains within the plant cell wall. However, the cellulase preparation used (cellulase 'Onozuka R-10' from *Trichoderma viride*, Yakult Honsha Co. Ltd, Japan) also contains hemicellulases and therefore degrades mannans, xylans, galactomannans, pectins and other

polysaccharides (http://www.serva.de/products/data/16419.02.shtm). Localised application of hemicellulase resulted in localised AOS generation (Mellersh *et al.*, 2002) and AOS generation was detected in response to treatment with commercial cellulase in tobacco leaves and in tobacco cell suspension cultures, but not if purified cellulase was applied (Harding *et al.*, 1997; Papadakis and Roubelakis-Angelakis, 1999). In addition, the observation that *GST1* is induced by wounding (Figure 4.29 a) but not cellulase (data not shown) indicates that these two treatments differ. Thus, treatment with 'unpurified' cellulase may trigger an elicitor response through the action of hemicellulases such as xylanase which has been shown to trigger defense responses in tobacco cells (Enkerli *et al.*, 1999). It remains to be verified if purified cellulase is able to trigger transcription of the *OX1* gene.

Enhanced induction of *OX1* in response to cellulase in DPI-treated seedlings is surprising if cellulase triggers an oxidative burst (Figure 4.19). However, this compound does not specifically act on NADPH oxidases but functions as a general flavoprotein antagonist that acts by drawing an electron away from the reduced flavin of its target protein (Trost *et al.*, 1997).Thus, DPI has been shown to inhibit redox enzymes in plant plasma membranes, including NADPH oxidases but also an NAD(P)H:quinone oxidoreductase (Trost *et al.*, 1997). Therefore, possible non-specific effects need to be considered when interpreting data involving DPI as a 'specific' inhibitor of the NADPH oxidases. In addition, oxidative bursts can also be generated by other enzymes such as cell wall associated peroxidases (see section 1.7.1) which are not inhibited by DPI.

Induction of the *OX1* gene in response to cellulase was inhibited by lanthanum (Figure 4.22), indicating that Ca^{2+} influx may be required for OX1 activation. In

agreement with this hypothesis, activation of SIPK in response to ozone fumigation (Samuel *et al.*, 2000) and of SIPK and WIPK in response to *R* gene interaction (Romeis *et al.*, 1999) has been shown to be abolished by pre-treatment with lanthanum. OX1 was demonstrated to be important for full activation of AtMPK3 and AtMPK6 (Figure 4.39, see also section 4.3.2.5.), the *A. thaliana* orthologues of WIPK and SIPK, thus placing it between the increase in $[Ca^{2+}]_{cyt}$ and MAPK activation in the signal transduction cascade.

4.3.1.2. OX1 *induction during infection with* P. parasitica *– is there more to it than just* H_2O_2*?*

The observation that *OX1* expression is not strongly increased in response to infection with an avirulent *P. parasitica* isolate suggests that *R*-gene recognition is not essential in this process. This is surprising as H_2O_2 has been shown to accumulate in incompatible reactions via a prolonged oxidative burst (Levine *et al.*, 1994) and *OX1* transcription is augmented by H_2O_2 (Figure 4.4). However, sufficiently high AOS levels may only be reached in cells directly attacked by the pathogen, explaining the restricted induction of *OX1*. Alternatively, changes in the cell wall, *e.g.* during fungal penetration, may be required in addition to H_2O_2 for full induction of *OX1*. This hypothesis is supported by the different levels of *OX1* induction observed for different stresses: cellulase, wounding and infection with virulent *P. parasitica* caused high expression of the GUS reporter gene at the sites of cell wall damage whereas H_2O_2 alone caused a much lower expression, detectable by Northern analysis but not with the *OX1promoter::GUS* reporter construct. Accordingly, wounding, which has been shown to trigger systemic

microbursts, induces *OX1* only at the wound site (Figure 4.7). OX1 activation may thus respond to H_2O_2 but full activation may require an additional cell wall signal. Alternatively, H_2O_2 generated in an oxidative burst may reach very high localised concentrations not reached by external addition of H_2O_2, accounting for the difference in expression levels observed.

4.3.1.3. OX1 may negatively influence its own promoter function

OX1 may negatively regulate transcription from its own promoter. This becomes apparent in the *ox1* null-mutant, where transcript levels of the truncated *OX1::T-DNA* are above those of the *OX1* transcript levels in the wild-type (Figures 4.17 and 4.18). Alternatively, the difference in relative transcript levels may indicate that the native *OX1* mRNA is subject to degradation whereas the *OX1::T-DNA* mRNA is not recognised by the degradation machinery and hence more stable. It is also possible that the *OX1* intron and 3' UTR, which are not included in the *OX1promoter::GUS* fusion construct, influence transcription of the *OX1* gene.

In order to investigate this observation further, the *OX1promoter::GUS* fusion construct could be introduced into the *ox1* mutant as well as an *OX1*-overexpressing line and GUS expression levels analysed after stress challenge. Enhanced and reduced accumulation of GUS would be expected, respectively, if OX1 exerted a negative influence on its promoter; whereas, GUS levels would be similar in all lines if increased *OX1::T-DNA* mRNA levels were due to increased RNA stability or transcription.

4.3.2. Downstream effects of OX1

In order to find gene induction mediated by OX1 in response to H_2O_2 treatment, transcript levels before and 3 h after H_2O_2 challenge were determined in a micorarray experiment, comparing gene induction in the WS-2 wild-type and the *ox1* null-mutant (Appendix C). Transcripts of the majority of genes were present at similar levels in wild-type and mutant, and genes that had previously been tested for H_2O_2 induction by Northern analysis were up-regulated as expected (*e.g. GST1, AtERF1*, *AtERF6*). Thus, even though each sample was only hybridised to one microarray chip, the similarity between gene transcript levels in the control and H_2O_2-treated samples of WS-2 and *ox1* seedlings indicates that data from the four samples are comparable.

4.3.2.1. Changes in gene induction triggered by H_2O_2 treatment

H_2O_2 treatment induced genes encoding heat shock proteins, glucosyltransferases, glutathione-*S*-transferases, electron transport proteins, transporters and various signalling molecules (Appendix C, a). Many of these genes were also shown to be up-regulated in H_2O_2-treated *A. thaliana* cell suspension cultures (Desikan *et al.*, 2001a). Among the repressed genes were extensins, peroxidases and aquaporins (Appendix C, b). The *OX1* gene exhibited the strongest transcriptional up-regulation among the induced kinase genes, and showed the expected increase in transcript levels in the *ox1* null-mutant relative to the wild-type (see section 4.3.1.3).

4.3.2.2. OX1-dependent changes in transcript levels

Several genes differed in their transcript levels in WS-2 compared to *ox1*, both in the control samples and after H_2O_2 treatment (Appendix C, c). These include a number of genes involved in pathogen defense and secondary metabolism, energy and electron transport as well as signal transduction. Interestingly, transcript levels of several genes with a putative role in the auxin signal cascade are reduced in *ox1*. (discussed in section 4.3.2.4).

Different levels of a number of pathogenesis-associated genes in wild-type and *ox1* were verified by Northern analysis and are discussed below.

Many differences in gene regulation between wild-type and *ox1* may remain to be identified, as only those genes which were induced by H_2O_2, or present at different levels in the control samples were detected in the microarray experiment. Thus, genes such as *PR-1* were not noticed as this gene is present at undetectably low levels in the control samples and is not induced by H_2O_2. Differential induction of this gene was only revealed upon analysis of transcript levels in *P. parasitica* infected plants (Figure 4.31).

4.3.2.2.1 *ECS1*

The *ECS1* gene has previously been shown to be induced in response to infection with an incompatible, but not a compatible, strain of *Xanthomonas campestris* (Aufsatz and Grimm, 1994) and ECS1 protein was detected in the cell wall in overexpressor lines (Aufsatz *et al.*, 1998). However, further analysis demonstrated that expression of this gene does not influence resistance to the bacterial pathogen (Aufsatz *et al.*, 1998). The results presented here indicate that *ECS1* transcript

levels increase in response to infection with a virulent isolate of *P. parasitica* (Figure 31) and also, but to a lesser degree, with an avirulent isolate (data not shown). Hence, induction of *ECS1* subsequent to *P. parasitica* infection is independent of the pathogen's virulence or may even be more strongly increased in compatible interactions. Its putative cell wall localisation may indicate that the ECS1 protein could be involved in events triggered by changes in the cell wall. However, wounding or H_2O_2 alone are insufficient to increase *ECS1* levels (tested at 3 and 24 h, data not shown). Hence, a pathogen-specific component may be involved in *ECS1* induction. Accordingly, SA treatment elevated *ECS1* transcript levels strongly (Figure 4.33), placing this gene downstream of SA accumulation. It would be interesting to see if *ECS1* transcripts accumulate in systemic tissue and are thus involved in SAR rather than resistance to a primary infection. A role in SAR could explain why modulating *ECS1* levels did not affect resistance to *X. campestris* in a primary infection (Aufsatz and Grimm, 1994). As demonstrated in Figure 4.31 a, *ECS1* induction in response to infection with a virulent *P. parasitica* isolate is very much reduced in the *ox1* mutant, indicating that OX1 is essential in this process.

4.3.2.2.2 *PR-1*

Pathogen infection generally results in the accumulation of a number of pathogenesis-related proteins (PR proteins), some of which have been shown to possess anti-microbial activity (Glazebrook *et al.*, 1997). The *PR-1* gene is induced in response to *P. syringae* inoculation by an SA-dependent pathway (Gaffney *et al.*, 1993) and is also induced subsequent to *P. parasitica* infection (Thomma *et al.*, 2001b). In the latter study, *PR-1* was induced more slowly, but to a higher level, in

response to infection with virulent as compared to avirulent *P. parasitica* isolates (accumulation detected after 72 h as opposed to 48 h) (Thomma *et al.*, 2001b). This observation contrasts with *PR-1* induction observed after inoculation with an avirulent or a virulent strain of *P. syringae*, where the incompatible interaction leads to much higher accumulation of *PR-1* transcripts (Thomma *et al.*, 2001b).

Figure 4.31 depicts *PR-1* induction in response to infection with virulent *P. parasitica* isolate Emco5, with significantly reduced transcript levels in the *ox1* mutant as compared to the WS-2 wild-type. However, the difference in transcript levels was much smaller than in for ECS1, indicating that *PR-1* can also be induced by OX1-independent pathways.

4.3.2.2.3 *THI2.2*

Thionins are cysteine-rich proteins which display toxic effects towards bacterial and fungal plant pathogens and may therefore play a role in plant defense (Fernandez del Caleya *et al.*, 1972; Terras *et al.*, 1993). In *A. thaliana*, induction of two thionin genes, *THI2.1* and *THI2.2*, in response to a variety of stimuli has been studied in more detail (Epple *et al.*, 1995). It was determined that *THI2.1* is transcriptionally up-regulated upon infection with a virulent fungal isolate and application of JA. *THI2.2* on the other hand was not induced by these treatments but transcript levels of this gene displayed circadian variation. In the present study, *THI2.2* transcripts were present in control samples and treated samples of wild-type seedlings but not in any of the *ox1* samples, whereas *THI2.1* was present in both wild-type and *ox1* (Figure 4.32). Neither of the genes was induced by wounding but high transcript levels of both genes in the early control and wounding samples (Figure 4.32 b) may indicate

that these genes are up-regulated in response to hypo-osmotic shock, experienced upon transfer from MS agar plates into H_2O. *THI2.2* transcript levels also did not increase in response to infection with virulent *P. parasitica* or SA treatment (data not shown), demonstrating that the regulation of this gene differs from that of *ECS1* and *PR-1*.

4.3.2.3. OX1 and SA

Reduced induction of *ECS1* and *PR-1* in the *ox1* mutant, both of which are SA-inducible genes, indicate that OX1 may function upstream of SA accumulation. To test this hypothesis, *ECS1* induction in response to SA application was investigated in *ox1* (Figure 4.33). Surprisingly, *ECS1* induction was still strongly reduced in the *ox1* mutant, suggesting that OX1 functions downstream of SA accumulation. It is possible that SA and OX1 operate in a positive feedback loop. Hence, SA treatment may cause H_2O_2 generation (Neuenschwander *et al.*, 1995; Shirasu *et al.*, 1997), thereby activating OX1 which in turn mediates further SA accumulation. However, in this scenario, *OX1* transcript levels would be expected to increase in response to SA, which was not the case (Figure 4.13). The relationship between SA and OX1 therefore needs to be investigated further. To this end, direct measurements of SA levels in wild-type and *ox1* seedlings are in process (in collaboration with Dr Luis Mur, University of Aberystwyth). As SA plays a role in the establishment of SAR (see section 1.3.3.3) as well as in basal resistance, it would also be interesting to investigate if SAR is reduced in *ox1*. However, *ox1* plants infected with virulent *P. parasitica* survive longer than *eds1* plants (data not shown), which cannot

accumulate SA and therefore fail to induce SAR (Parker *et al.*, 1996), indicating that SAR may not be abolished in the *ox1* mutant.

4.3.2.4. Auxin-regulated genes

Several genes associated with the response to the plant hormone auxin (*e.g. ARF1-BINDING PROTEIN-LIKE*, *UBIQUITIN-PROTEIN LIGASE 8* (*UBC8*)) were differentially expressed in wild-type and *ox1* seedlings as revealed in the microarray experiment (Appendix C, c). Application of H_2O_2 together with auxin inhibited transcriptional activation of auxin-responsive promoters in *A. thaliana* protoplasts, suggesting that H_2O_2 and auxin function in an antagonistic manner (Kovtun *et al.*, 2000). However, if OX1 transduces the H_2O_2 signal, the observed down-regulation of auxin signalling components in the *ox1* mutant indicate a positive role of H_2O_2 in auxin signalling.

Alternatively, it may not be auxin signalling that is affected but other processes regulated by ubiquitination. Recently, components of the ubiquitin-proteasome pathway have been implicated in regulation of disease resistance in *A. thaliana* (Austin *et al.*, 2002; Kim and Delaney, 2002) and barley (Azevedo *et al.*, 2002), in resistance-inducing (Austin *et al.*, 2002; Azevedo *et al.*, 2002), as well as resistance-repressing functions (Kim and Delaney, 2002). The proteasome pathway is also involved in the regulation of photomorphogenesis. In the absence of light, the positive regulator HY5 is targeted for proteasomal degradation in a process involving COP1 (Osterlund *et al.*, 2000). COP1 has been shown to interact with COP1-interacting protein 8 (CIP8) which in turn interacts strongly with UBC8 (Hardtke *et al.*, 2002). The *UBC8* gene was found to be down-regulated in *ox1*

(Appendix C, c), indicating that this pathway may be inhibited in the mutant. To clarify if OX1 plays a role in photomorphogenesis, the dark-grown phenotype of the *ox1* mutant could be analysed; *ox1* seedlings would be expected to display a light-adapted phenotype. Interestingly, an element in the *OX1* promoter corresponds to a palindromic C-box, found in Soybean and involved in binding bZIP transcription factors with homology to *A. thaliana HY5* (see section 4.1.1.4) (Cheong *et al.*, 1998). This would indicate that OX1 down-regulates its own expression by enhancing degradation of HY5 (unless HY5 also functions as a repressor!). Further analysis is required.

4.3.2.5. Reduced activation of AtMPK3 and AtMPK6 in the ox1 *mutant*

Activation of the MAPKs AtMPK3 and AtMPK6 and their orthologues in other plant species has been implicated in the signal transduction pathways in response to H_2O_2 application, wounding, pathogen attack and ozone fumigation (see sections 4.1.2 and 4.1.3). The role of OX1 in the ozone-triggered activation of these kinases was investigated by analysing the phosphorylation status of the MAPKs, an indicator of their activity (Figure 4.39). Both, AtMPK3 and AtMPK6, displayed increased phosphorylation in response to ozone fumigation, but this increase was reduced in the *ox1* mutant background. Thus, OX1 is required for full activation of AtMPK3 and AtMPK6. The inhibitory effect of the *ox1* mutation supplies indirect evidence that the OX1 protein has kinase activity. In tobacco, two defence genes encoding key enzymes in phytoalexin and salicylic acid biosynthesis pathways (*PAL* and *HMGR* (3-hydroxy-3-methylglutaryl CoA)) appear to be controlled by a MAPK cascade

including SIPK and WIPK (Yang *et al.*, 2001). It would be interesting to determine if *OX1* is required for full activation of the corresponding genes in *A. thaliana*.

4.3.3. Phenotypic effects of the *ox1* mutation

4.3.3.1. Enhanced susceptibility to a virulent isolate of P. parasitica

Localised induction of *OX1* in areas of fungal attack led to an investigation of the susceptibility of the *ox1* mutant. The virulent *P. parasitica* isolate Emco5 was able to sporulate to higher levels on the *ox1* mutant than on the wild-type (Figures 4.34 and 4.35), indicating that basal resistance is impaired. *R* gene mediated resistance was still intact as observed in the incompatible interaction with the avirulent isolate Emoy2 (data not shown). The enhanced susceptibility phenotype may stem from reduced transcription of pathogenesis-associated genes in the mutant (Figures 4.31 and 4.32, Appendix C, c) through disruption of SA signalling pathways (see section 1.3.3.3). The effect of the *ox1* mutation on basal resistance to necrotrophic fungi such as *Alternaria brassicicola* could be investigated, as the response to these fungi appears to involve JA and ethylene rather than SA (Thomma *et al.*, 1998). Hence, it could be clarified if OX1 functions specifically in a SA pathway, or if this kinase plays a more general role in pathogen resistance.

4.3.3.2. Reduced root hair elongation

Root hair elongation was reduced in the *ox1* mutant, independently of stress application. This phenotype relates to the constitutive expression of the *OX1promoter::GUS* construct, particularly in root hair cells. H_2O_2 has been shown to be involved in root hair growth (see section 6.5.1), and hair cell elongation requires

changes in the cell wall. As both these factors are important in *OX1* induction in response to stress stimuli (see section 4.3.1.2), OX1 may also regulate processes during root hair elongation. This hypothesis is further discussed in section 6.5.1.

4.3.3.3. The flowering phenotype

It was observed that the *ox1* mutant displayed an early flowering phenotype compared to the WS-2 wild-type under greenhouse conditions (Figure 4.38). The difference in bolting was approximately 4 days and was only seen when plants were grown in the greenhouse, but not in growth cabinets, suggesting that a component of natural daylight may influence the onset of flowering. Interestingly, *Flowering locus C* (*FLC*), was one of the genes down-regulated in the *ox1* mutant (Appendix C, c). This gene functions as a repressor of flowering (Michaels and Amasino, 2000) and low expression levels would therefore be expected to accelerate flowering time. Low expression of *FLC* in the microarray does not support a crucial role for natural daylight in the flowering phenotype as the RNA analysed in this experiment stemmed from growth cabinet-grown seedlings. Further analysis of flowering time in the *ox1* mutant under different light conditions is necessary. A possible connection between H_2O_2 signalling and the regulation of flowering is discussed in section 6.5.2.

On the basis of work presented in this thesis, a scheme for H_2O_2 signalling is proposed in Figure 4.40. Elements of this model will be discussed further in Chapter 6.

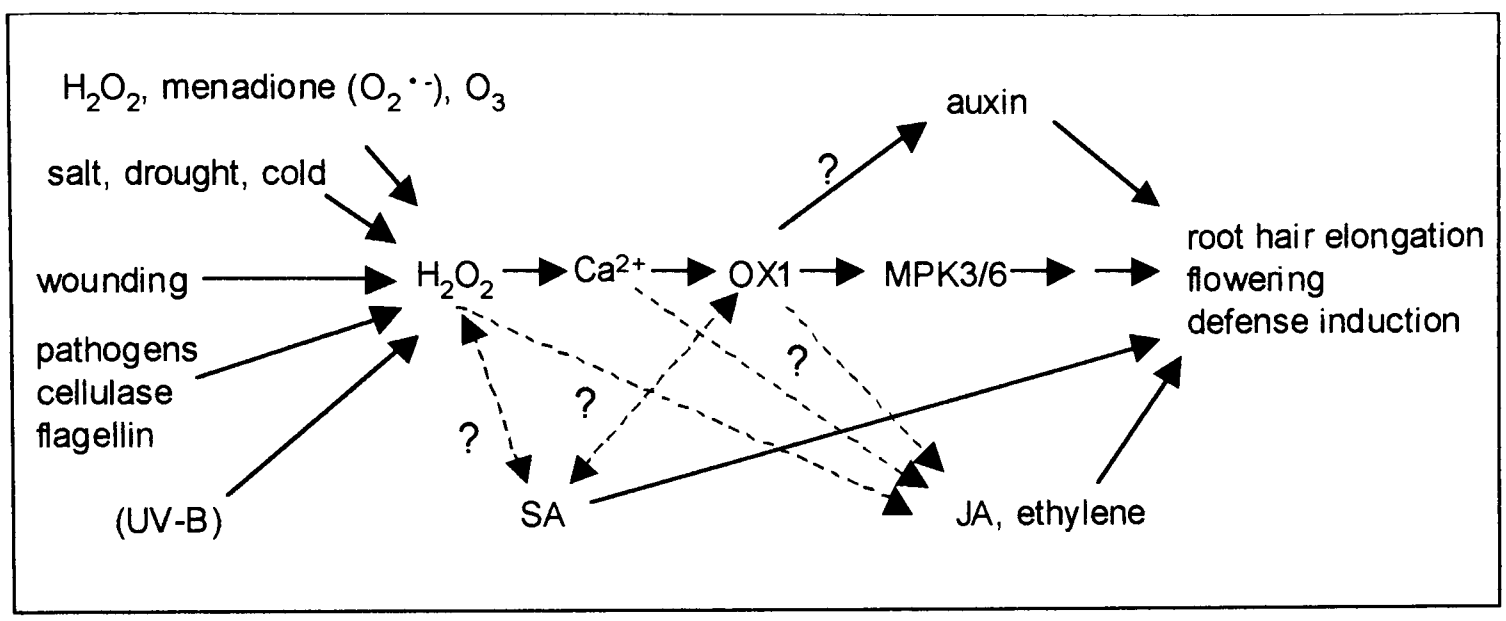

Figure 4.40: A model for H_2O_2 signal transduction
H_2O_2-triggered $[Ca^{2+}]_{cyt}$ elevations cause activation of the OX1 kinase. Subsequently, OX1 activates a MAPK cascade involving the MAPKs AtMPK3 and AtMPK6. Downstream effects of this signalling cascade include a variety of cellular processes such as induction of defence mechansims, root hair elongation and regulation of flowering time. The position of auxin and the stress-hormones JA and ethylene in this signal transduction chain is likely to be downstream of OX1. SA on the other hand may function in a positive feed-back loop with H_2O_2 and OX1.

5. Signalling pathways mediating *ERF* gene expression in response to oxidative stress

5.1. Introduction

5.1.1. The ERF family of transcription factors

The class of ethylene-responsive element binding factors (ERFs) belongs to the AP2 / EREBP family of transcription factors and comprises approximately 124 members in *A. thaliana* (Riechmann *et al.*, 2000). These proteins were first isolated from tobacco as factors binding the GCC box (GCCGCC) (Ohme-Takagi and Shinshi, 1995; Fujimoto *et al.*, 2000;), a short *cis*-acting element found in many ethylene-inducible and pathogensis-related (*PR*) genes (Ohme-Takagi and Shinshi, 1990). The ERFs contain a highly conserved DNA-binding domain consisting of 59 amino acids (Hao *et al.*, 1998), which interacts with the target DNA as a monomer (Allen *et al.*, 1998). *ERF* genes have been identified by sequence comparison in a range of species, including tobacco *ERF*s, tomato *Pti4/5/6* and *A. thaliana* ethylene responsive factor (*ERF1*, ethylene-responsive element binding protein (*AtEBP*), and *AtERF1 – 15*) (Buettner and Singh, 1997; Riechmann and Ratcliffe, 2000; Onate-Sánchez and Singh, 2002). This family contains both positive and negative regulators of transcription (Fujimoto *et al.*, 2000; Ohta *et al.*, 2000).

5.1.2. Regulation of *ERF* gene expression and ERF protein activity

Transcript levels of specific ERF genes are regulated by different environmental stresses (Chen *et al.*, 2002), implicating these transcription factors in responses to a range of conditions. A detailed study of expression patterns of the *A. thaliana* *AtERF1 – 5* (Fujimoto *et al.*, 2000) demonstrated that *AtERF1,2,4* and *5* levels were

increased 6 h after wounding. At that time point, *AtERF4* was also induced by cold, high salt concentration and drought stress whereas *AtERF5* expression was up-regulated by cold stress but not salt and drought stress. Also, *ERF1*, *AtERF1* and *AtERF2* were induced in response to *Pseudomonas syringae* infiltration and *Peronospora parasitica* infection (Chen *et al.*, 2002) and a tomato homolog of *A. thaliana ERF6* was induced within 30 min of challenge with fungal elicitor and wounding (Durrant *et al.*, 2000).

In addition to changes in transcript levels, ERFs also undergo post-translational modifications. For example, expression of the tomato *Pto- interacting4* (*Pti4)* gene is increased in response to infection with *Pseudomonas syringae* pv *tomato* (Thara *et al.*, 1999). Additionally, the Pti4 protein is phosphorylated by the *Pseudomonas* tomato resistance (Pto) kinase (*in vitro*) which enhances its GCC-box binding acitivity (Gu *et al.*, 2000). This mechanism may regulate the induction of defense-related genes *in vivo*.

5.1.3. Interaction of ERFs with other transcription factors

Communication between different transcription factors in defense-gene induction has also been demonstrated. *AtEBP* was shown to interact with the *octopine synthase* (*ocs*) element binding protein 4 (OBF4), a member of the bZIP factor family (Buettner and Singh, 1997). *ocs* elements are used by bacterial and viral pathogens (*e.g.* present in the cauliflower mosaic virus (CaMV) 35S promoter) to express genes in plants, but also regulate transcription of plant defense genes such as *GSTs* (Chen, 1996; Chen and Singh, 1999) and *PR-1* (Lebel *et al.*, 1998). As synergistic effects between the GCC-box and *ocs* elements (fused in an artificial

promoter) have been demonstrated, the results suggest that interaction between ERF and bZIP transcription factors may play a role in regulating gene expression during plant defense responses.

5.1.4. Role of ethylene in *ERF* gene induction

Ethylene has been implicated in ERF-mediated transcription through several observations. Firstly, tobacco ERFs were shown to bind the GCC box (Ohme-Takagi and Shinshi, 1990), previously identified as an essential promoter element for ethylene responsiveness in ethylene-inducible *PR*-genes (Ohme-Takagi and Shinshi, 1995). Secondly, *ERF1* overexpression in *A. thaliana* led to a partial triple response phenotype (indicating constitutive ethylene signalling) and activation of ethylene-inducible genes (Solano *et al.*, 1998). Thirdly, mRNA levels of *ERF* genes have been shown to increase in response to ethylene treatment, *e.g.* Arabidopsis *AtERF1*, *2*, *5* (Fujimoto *et al.*, 2000) and *14* (Onate-Sánchez and Singh, 2002) as well as *ERF1* (Solano *et al.*, 1998) and tobacco *ERF*s (Ohme-Takagi and Shinshi, 1995), (Kitajima *et al.*, 2000). However, in several cases, ERF activation and increases in *ERF* transcript levels have been shown to be ethylene-independent. For example, post-transcriptional regulation of ERFs through the ethylene signalling cascade is not always required (see section 5.1.2), as overexpression of *ERF1* in *A. thaliana* ethylene signalling mutant backgrounds (*e.g. ethylene-insensitive2* (*ein2*) and *ein3*) still led to a partial triple response phenotype (Solano *et al.*, 1998). Moreover, *AtERF* induction by wounding, cold and drought is independent of ethylene signalling pathways as responses to these stresses were similar in wild-type and *ein2* mutant backgrounds. By contrast, induction of *AtERF3* and *4* in

response to salt and drought stress was abolished in the *ein2* mutant (although the expression of these *AtERF*s is not induced by ethylene) (Fujimoto *et al.*, 2000). Similarly, *ERF1*, *AtERF1* and *AtERF2* induction in response to *P. syringae* infiltration was reduced in the *ein2* mutant (Chen *et al.*, 2002). Not all *ERF* genes appear to be ethylene-inducible; thus, *AtERF13* is not induced after 12 h or 24 h of treatment (Onate-Sánchez and Singh, 2002). Ethylene-triggered induction of *ERF1* and *AtERF14* was shown to be dependent on *EIN2*, indicating that changes in *ERF* expression levels indeed require the 'traditional' ethylene signal cascade (Onate-Sánchez and Singh, 2002). In summary, the data indicate that different ERF genes as well as different stresses vary in their dependence on the ethylene signal cascade: not all stresses require ethylene signalling for *ERF* induction, and not all *ERF* genes function downstream of the ethylene signalling pathway.

The aim of this study was to

- determine if there are differences between the induction patterns of different *ERF* genes in response to oxidative stress treatment
- test the hypothesis that oxidative stress-triggered *ERF* gene induction is independent of the ethylene signalling pathway
- investigate the dependence of H_2O_2-mediated *ERF* gene induction on increases in $[Ca^{2+}]_{cyt}$

5.2. Results

5.2.1. Differential display of cDNA fragments

7 day old RLD1 seedlings were incubated for various time periods in 10 mM H_2O_2. The cDNA produced from these samples was used for PCR amplification employing degenerate primers complementary to sequences conserved in protein phosphatases, class PP2C specifically. After size fractionation of the amplified fragments, gene induction was detected by comparing band intensities for H_2O_2 treatment with the water control. One fragment was present at a higher levels (Figure 5.1). This fragment was cloned into pUC18 and sequenced.

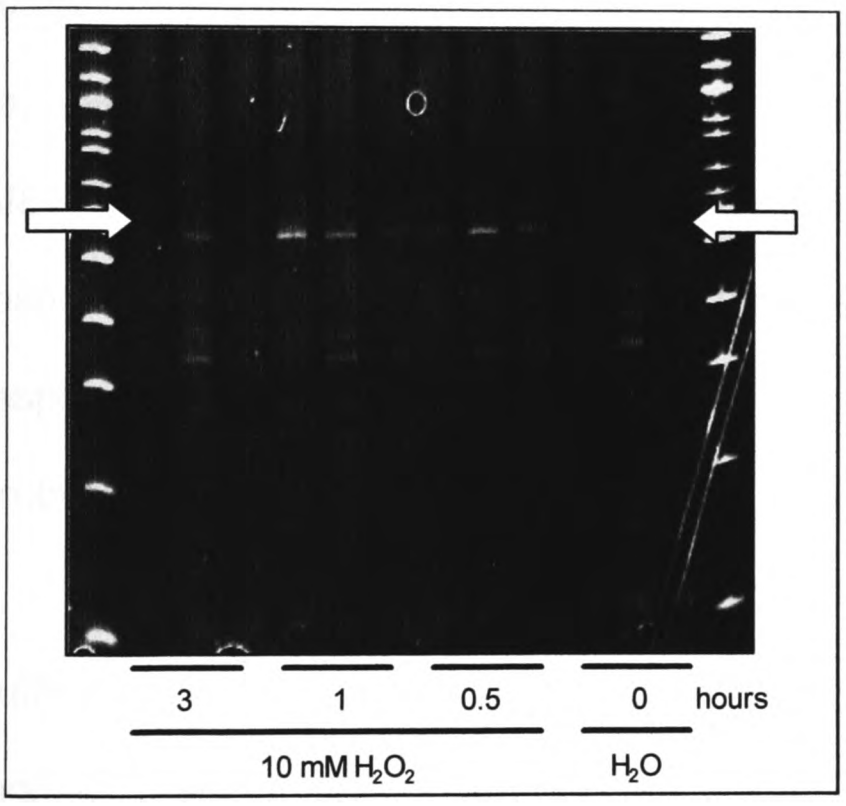

Figure 5.1: Differential display of cDNAs induced by 10 mM H_2O_2
7 day old RLD1 seedlings were transferred into H_2O and left to recover for 3 hours before addition of H_2O_2 (final concentration: 10 mM). Samples were incubated for 0.5, 1 or 3 h (each in triplicate) and frozen. RNA extraction, cDNA synthesis and PCR amplification of DNA with phosphatase specific primers was performed as described in Methods. 10 µL samples of PCR product were size fractionated on a 6.67 % TBE polyacrylamide gel, stained with SYBR Green and visualised on the UV-transilluminator. The white arrows indicate the position of the band which was excised and cloned band (size ~ 500 bp). Markers: 100 bp ladder.

5.2.2. Identification of induced genes

Plasmids isolated from 16 colonies had their cDNA inserts sequenced. Two sequences were recovered more than once and were thus identified by a BLAST search (Altschul *et al*, 1997): part of the *AtERF6* gene (At4g17490) was isolated 9 times whereas an unknown protein (At4g28080) was recovered 3 times. At4g28280

has similarity to a 150 kD protein from *Dictyostelium* and 15 ESTs are listed in the MIPS database. The protein has an N-terminal ATP/GTP binding site motif (P-loop) and a C-terminal carbohydrate kinase signature. None of the cloned fragments encoded a phosphatase; however, the degenerate primers showed complementarity to a region in the *AtERF6* gene, explaining why this sequence was amplified.

5.2.3. *ERF* genes are differentially induced by oxidative stress treatment

At the time this work was carried out, ten *AtERF* genes had been annotated in the NCBI database (subsequently, two more have been added). These genes show strong homology in regions coding for the protein DNA-binding domain but have variable 5'- and 3'- 'tails'. Primers were designed to amplify unique regions in *AtERF1*, *4*, *5* and *6* (At4g17500, At3g15210, At5g47230, At4g17490, At3g20310, respectively), cloned into pBlueScript (blunt-ended cloning) and gene induction in response to oxidative stress was analysed by Northern analysis using these as probes. In addition, RT-PCR was carried out using primers specific to *AtERF1*, *4*, *5*, *6*, *7* (At1g53170) and *10* (At1g03800) as the latter two genes did not have a sufficiently long unique region to use as a probe in Northern hybridisation. The data indicate that *AtERF1*, *4*, *5* and *6* are induced strongly in response to H_2O_2 (Figure 5.2, a and b, Figure 5.3). *AtERF1* and *4* have higher background transcript levels than *AtERF5* and *6*, and *AtERF4* in particular appears to be also induced by touch as transfer into H_2O_2 after the rest period induced this gene (Figure 5.2 b). *AtERF7* and *10* on the other hand did not appear to show any changes in transcript levels in response to H_2O_2 treatment (Figure 5.3).

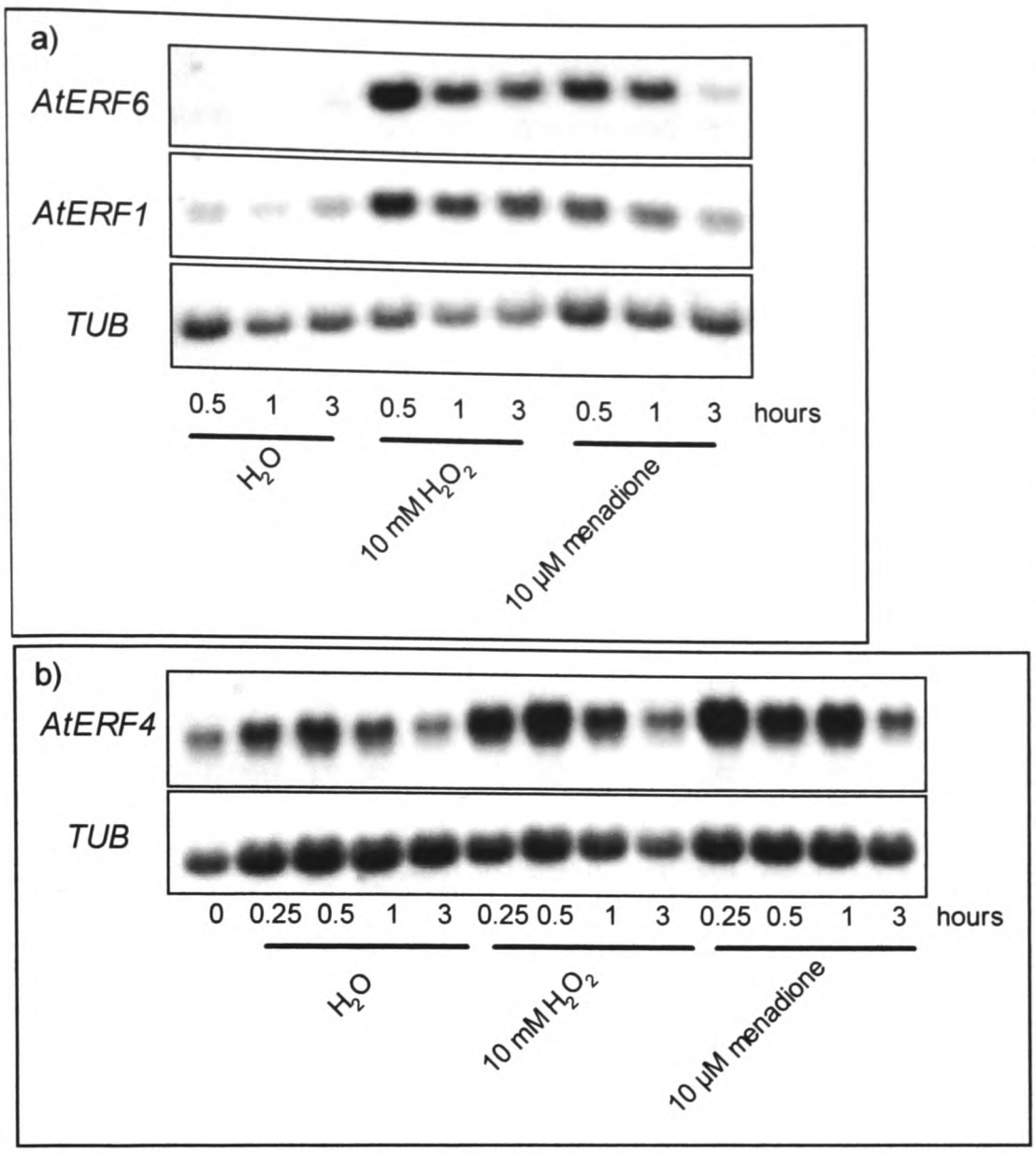

Figure 5.2: Induction of *AtERF* genes by oxidative stress
Northern analysis was carried out as described in Methods. 7 day old RLD1 seedlings were transferred into H_2O and left to recover for a) 2.5 h and b) 3 h before they were moved into fresh solutions of H_2O_2 (final concentration: 10 mM), menadione (final concentration: 10 µM) or H_2O. Samples were removed and frozen after 0.5 h, 1 h and 3 h and total RNA was extracted. *AtERF6*, *AtERF1*, *AtERF4* and *β-TUBULIN* probes were labelled and hybridised to the RNA on the membrane.

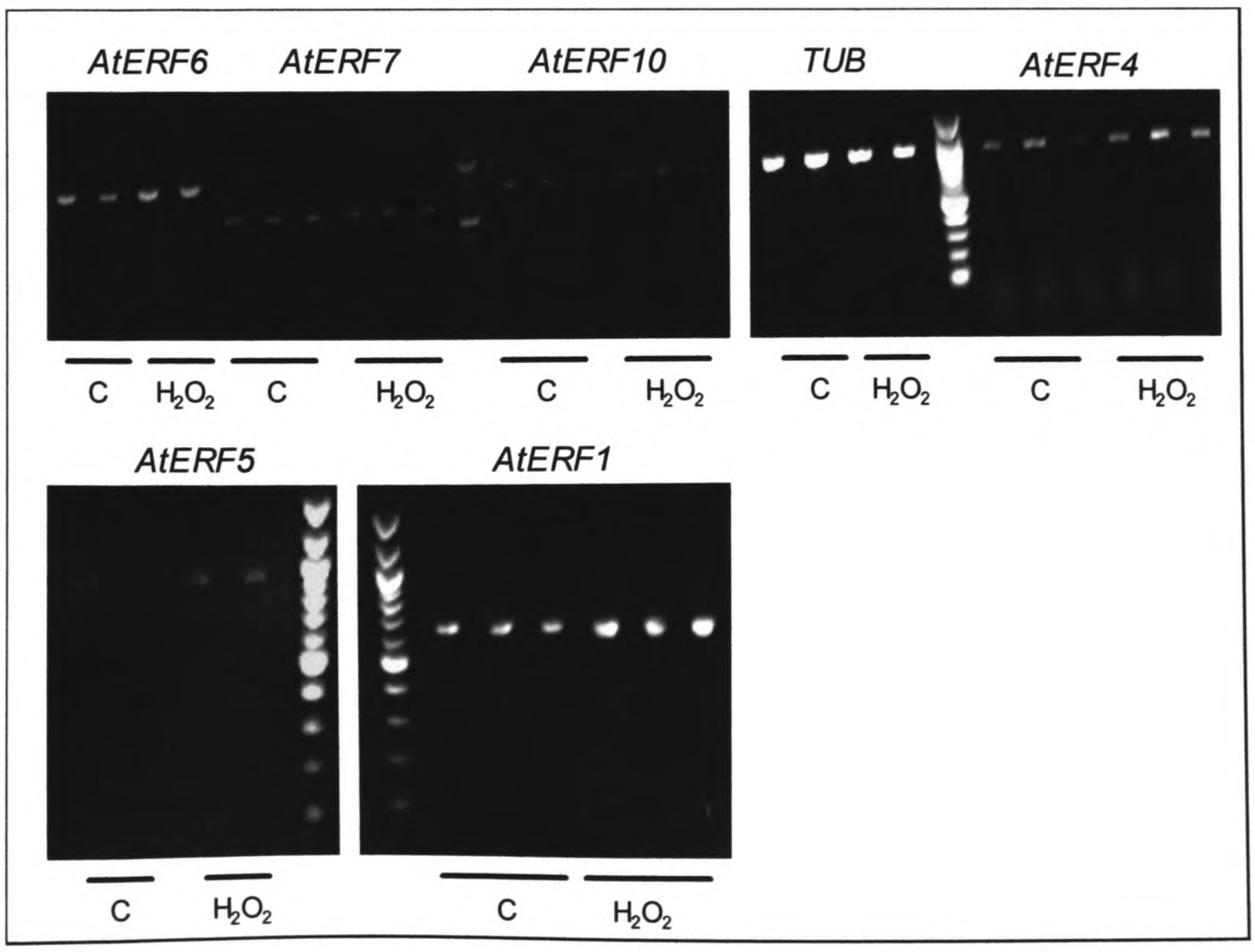

Previous page:
Figure 5.3: Induction of *AtERF* genes by H_2O_2
7 day old RLD1 seedlings were transferred into H_2O and left to recover for 3 h before addition of H_2O_2 (final concentration: 10 mM) or H_2O (control sample 'C'). Samples were frozen after 1 h incubation and RNA was extracted and treated with DNase. Two samples of cDNA were synthesised from 1 µg RNA and diluted 1:10. 9 µl of these dilutions were used per PCR reaction, using heat-activated polymerase (Immolase, Bioline, UK). Cycle number for each reaction: *TUB* and *AtERF5*: 25 cycles; *AtERF6* and *AtERF10*: 35 cycles; *AtERF1*, *AtERF4* and *AtERF7*: 28 cycles. *AtERF10*, *AtERF4* and *AtERF6* include two reactions with one of the cDNA preparations and one reaction with the other; all others include one reaction per cDNA preparation. 10 µl per reaction was electrophoresed on an agarose gel and imaged under the UV camera.

5.2.4. The role of ethylene in *ERF* induction

ERFs have been proposed to operate as a late component in the ethylene signal transduction chain, responsible for transcription of genes containing a GCC-box in their promoter (see section 5.1.1). According to this hypothesis, ethylene leads to increased levels of ERFs which subsequently exert their effects on downstream genes. The involvement of ethylene in *AtERF* gene induction was determined by treating seedlings with ACC, an ethylene biosynthesis precursor. This treatment induced *AtERF6* (Figure 5.4 a) and *AtERF5* (Figure 5.4 b) to low levels when compared with induction by H_2O_2 or cellulase. ACC was effective as a generator of ethylene, gauged by the fact that the *CHITINASEB* gene was induced (Figure 5.4 a). SA, a signalling molecule involved in resistance signalling (see section 1.3.3.3) did not induce *AtERF5*.

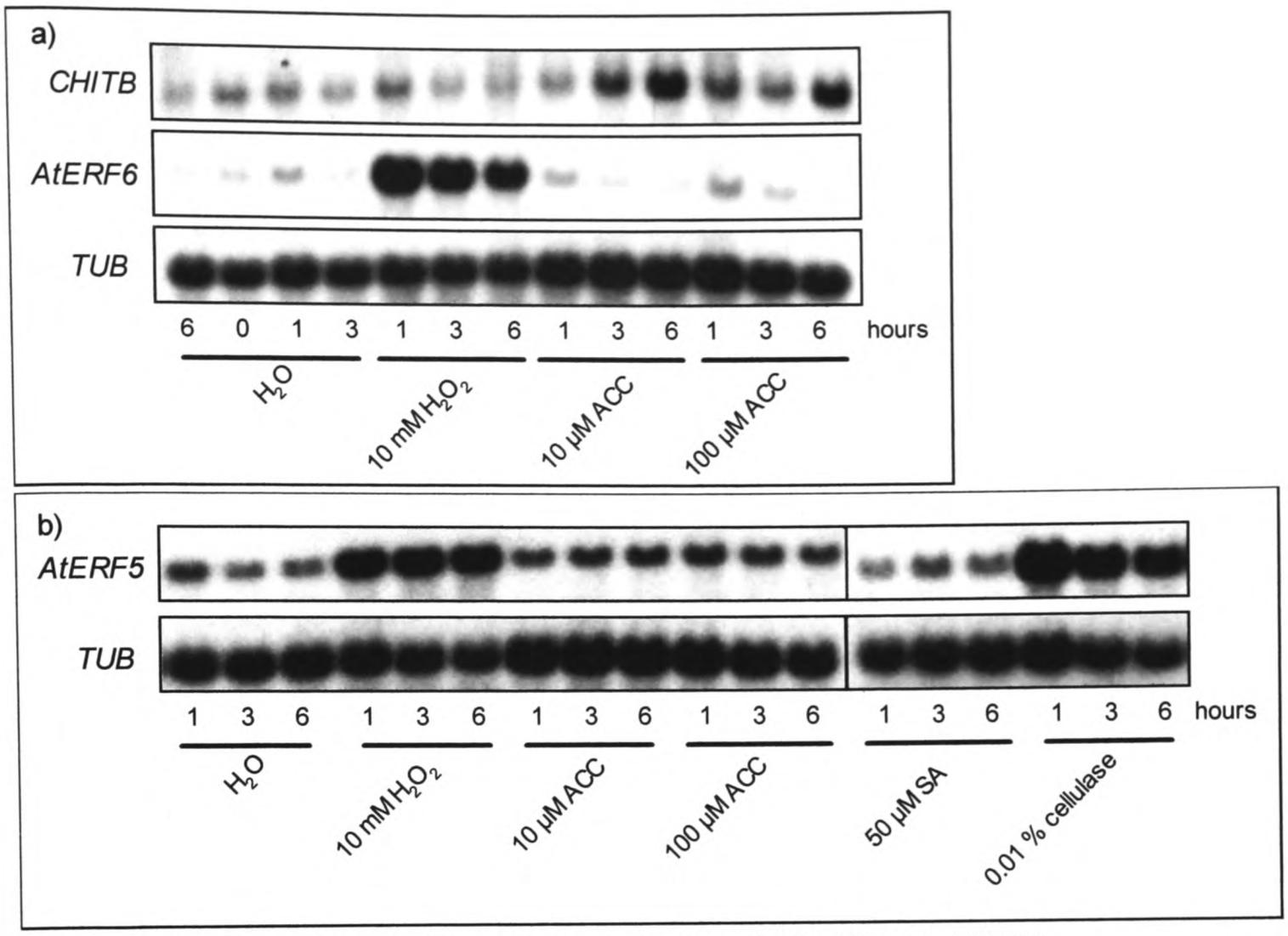

Figure 5.4: Involvement of ethylene in the induction of *AtERF5* and *AtERF6*
Northern analysis was carried out as described in Methods. 7 day old RLD seedlings were transferred to H_2O and left to recover for 3 h. H_2O_2 (final concentration: 10 mM), ACC (final concentrations: 10 µM and 100 µM), SA (final concentration: 50 µM) or cellulase (final concentration: 0.01 % (w/v) were added as indicated. Samples were frozen after 1 h, 3 h and 6 h incubation and total RNA was extracted. The H_2O, H_2O_2 and ACC samples were electrophoresed on a second gel and blotted separately (a). *CHITB*, *AtERF6*, *AtERF5* and *β-TUBULIN* probes were labelled and hybridised to the RNA on the membrane.

In order to test ethylene dependence further, the *etr1* and *ctr1* mutants (deficient and constitutive in ethylene signalling, respectively) were tested for *AtERF5* and *AtERF6* induction in response to H_2O_2 and cellulase (Figure 5.5). No clear pattern of dependence was discernible. [Note: In Figure 5.5 a, induction levels between the control samples and mutants cannot be compared as the seedlings have different ecotype backgrounds (RLD1 and Col-0).]

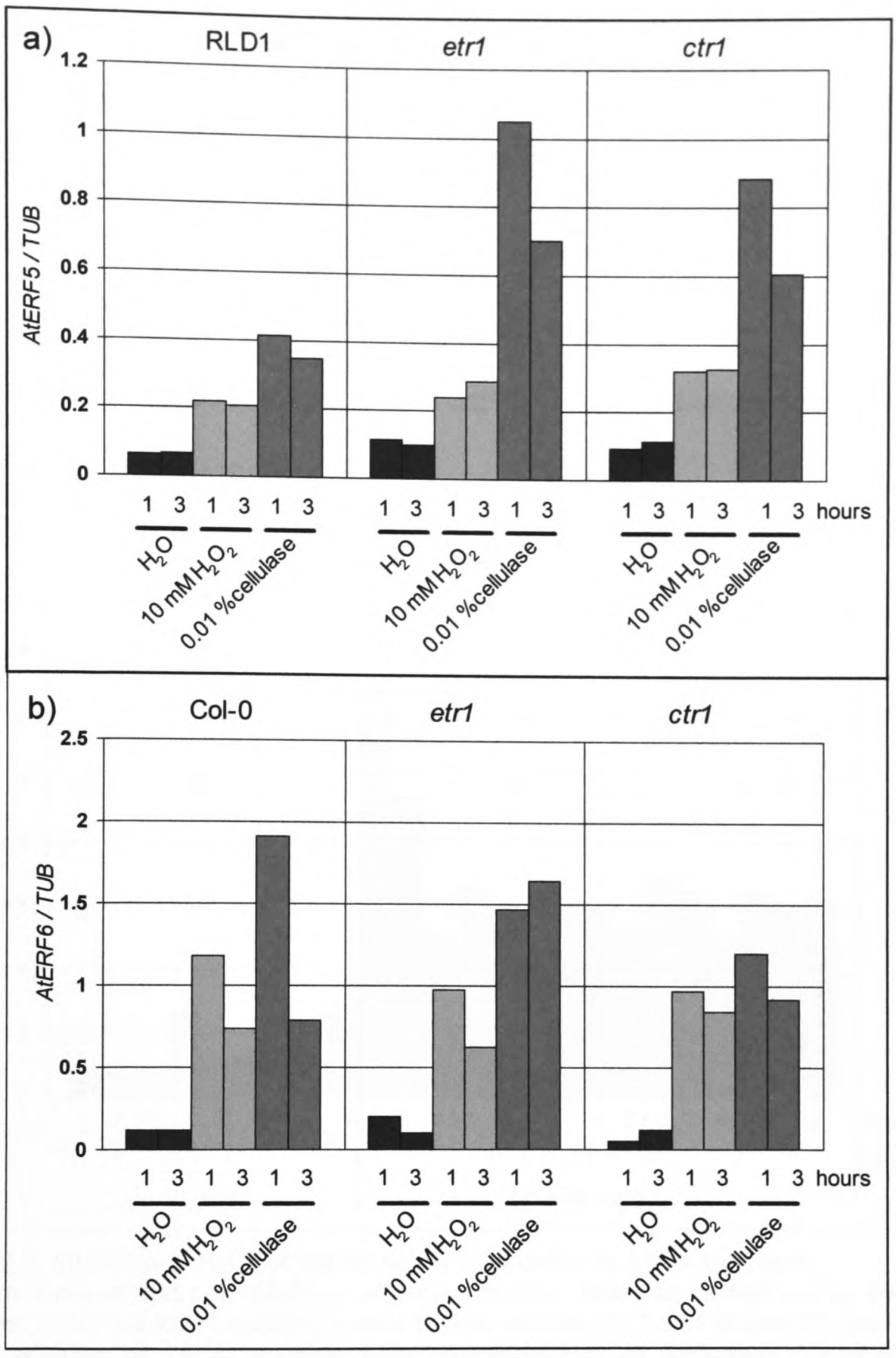

Figure 5.5: *AtERF* gene induction in the ethylene signalling mutants *etr1* and *ctr1*
Northern analysis and normalisation of gene induction data was carried out as described in Methods. 7 day old seedlings were transferred to H_2O and left to recover for a) 30 min and b) 3 h. H_2O_2 (final concentration: 10 mM) or cellulase (final concentration: 0.01 % (w/v)) were added as indicated. Samples were frozen after 1 h and 3 h incubation and total RNA was extracted, electrophoresed and transferred to nylon membrane. *AtERF5*, *AtERF6* and *β-TUBULIN* probes were labelled and hybridised to the RNA on the membrane. Bars represent *ERF* gene induction relative to *β-TUBULIN* mRNA levels

5.2.5. Dependence of *ERF* induction on calcium signalling

Challenging seedlings with H_2O_2 was shown to cause increases in $[Ca^{2+}]_{cyt}$ (section 3.2.1.1, *e.g.* Figure 3.1) which could be inhibited by treatment with the channel blocker $LaCl_3$ (Figures 3.14 and 3.15). The effect of inhibition of the H_2O_2-triggered $[Ca^{2+}]_{cyt}$ signature upon *AtERF6* induction was investigated. $LaCl_3$ treatment reduced *AtERF6* induction at all concentrations that had also been shown to inhibit the first $[Ca^{2+}]_{cyt}$ peak (Figure 5.6).

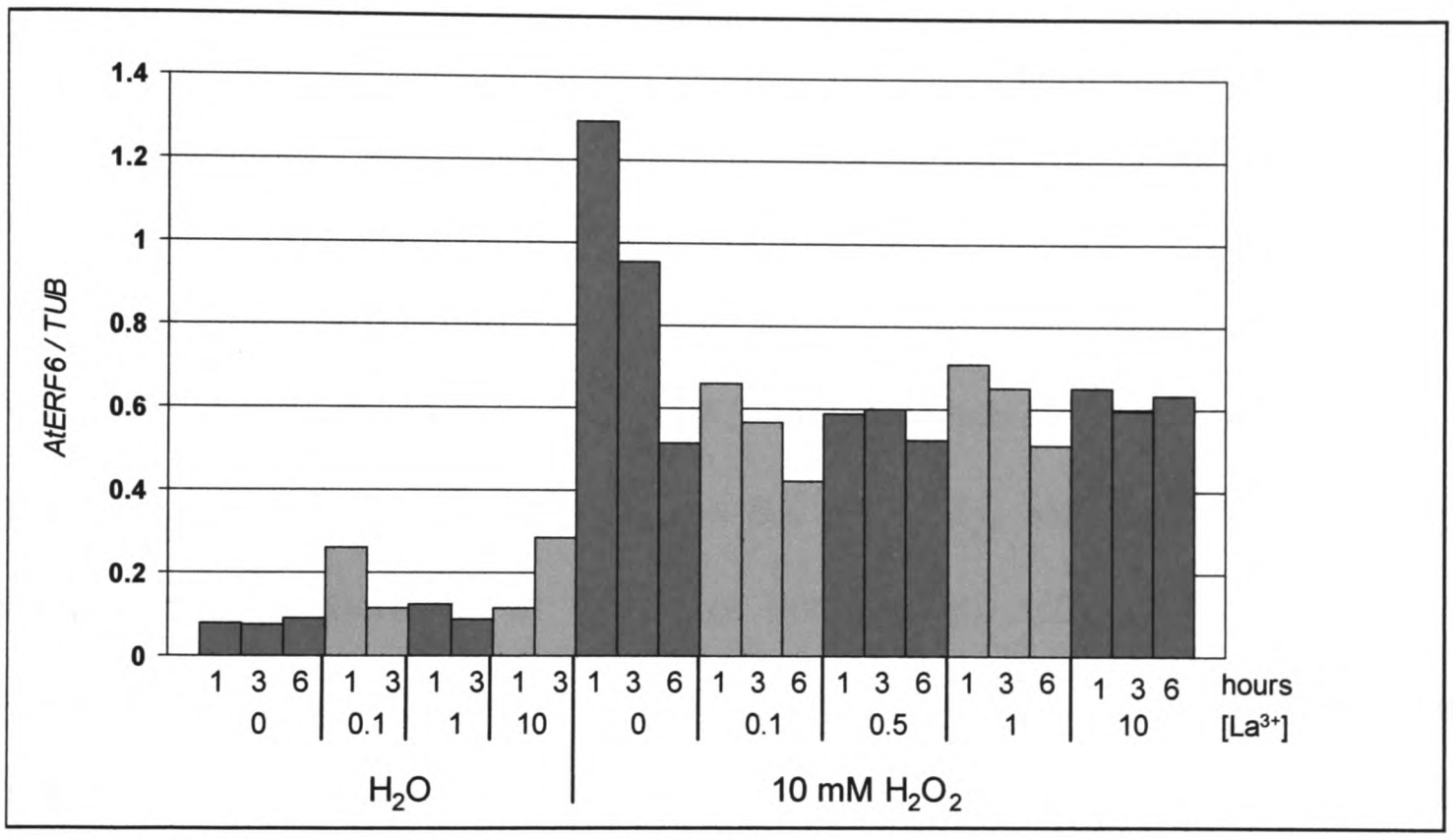

Figure 5.6: Inhibition of H_2O_2-triggered *AtERF6* induction by $LaCl_3$-treament
Northern analysis and normalisation of gene induction data was carried out as described in Methods. 7 day old RLD1 seedlings were transferred into H_2O and allowed to recover for 2 h before addition of $LaCl_3$ solution (final concentration as indicated). Control samples remained in H_2O. After 1 h incubation, samples were placed into fresh $LaCl_3$ and H_2O_2 was added where indicated (final concentrations $LaCl_3$: as before; H_2O_2: 10 mM). Samples were removed and frozen after 1 h, 3 h or 6 h. Total RNA was extracted, electrophoresed and transferred onto nylon membrane. *AtERF6* and *β-TUBULIN* probes were labelled and hybridised to the RNA on the membrane. Bars represent *ERF6* gene induction relative to *β-TUBULIN* mRNA levels.

5.3. Discussion

5.3.1. *ERF* genes are differentially regulated by AOS treatment

ERF proteins contain a highly conserved DNA-binding domain and may therefore share target promoter sequences, *e.g.* the GCC box (Ohme-Takagi and Shinshi, 1995). To achieve specificity in gene induction by different members of the ERF family, a particular stimulus may increase transcription of a subset of *ERF* genes only. In support of this hypothesis, AOS treatment induced *AtERF4*, *AtERF5* and *AtERF6*, but not *AtERF7* and *AtERF10* transcription (Figure 5.2 and 5.3). Accordingly, differences in the induction pattern of *AtERF* genes was demonstrated for other stresses, such as cold and drought (Fujimoto *et al.*, 2000). It is likely that specificity of AtERF protein actvation in response to a certain stimulus is also conferred by other mechanisms, *e.g.* post-translational modifications.

Interestingly, both *AtERF5* and *AtERF6* were transcriptionally up-regulated in response to cellulase treatment (Figures 5.4 and 5.5), with *AtERF5* displaying a more pronounced increase in transcript levels than *AtERF6* (Figure 5.5). As cellulase activity may mimic wounding stress (see section 4.3.1.1) , the observation that *AtERF5* is induced in response to wounding (Fujimoto *et al.*, 2000) supports the data presented here.

5.3.2. Ethylene signalling is not required for *AtERF5* and *AtERF6* induction in response to H_2O_2 treatment

ERFs have been proposed to operate as a late component in the ethylene signalling pathway (see section 5.1.4) (Ohme-Takagi and Shinshi, 1995; Solano *et al.*, 1998). However, recent evidence has indicated that several of these transcription factors

are up-regulated independently of ethylene, and that not all stresses require ethylene signal transduction pathways to trigger increases in *ERF* transcript levels (Fujimoto *et al.*, 2000; Onate-Sánchez and Singh, 2002). Accordingly, *AtERF5* and *AtERF6* were not induced by ACC treatment (Figure 5.4) and transcript accumulation of these genes in response to H_2O_2 or cellulase treatment was unaffected in the ethylene signalling mutant backgrounds *etr1* and *ctr1* (Figure 5.5). This corresponds to previous observations, which indicate that *AtERF5* induction in response to wounding is not altered in the *ein2* mutant background (Fujimoto *et al.*, 2000).

5.3.3. Induction of *AtERF6* by H_2O_2 is Ca^{2+}-dependent

Increases in $[Ca^{2+}]_{cyt}$ have been implicated in signal transduction in response to a wide range of stresses (Knight *et al.*, 1996; Knight *et al.*, 1998), including AOS treatment (Price *et al.*, 1994) (see section 3.2.1). However, a link between *AtERF* gene induction and Ca^{2+} signalling has not been investigated so far. In the present study, $[Ca^{2+}]_{cyt}$ elevations were shown to be necessary for activation of downstream responses upon H_2O_2 treatment (see section 3.2.2). Accordingly, lanthanum pre-treatment, which resulted in inhibition of the H_2O_2-triggered Ca^{2+}-signal (see section 3.2.1.5.1), decreased At*ERF6* induction by H_2O_2. Hence, similar to induction of *GST1* and *APX1* (see section 3.2.2.2.3), induction of *AtERF6* by H_2O_2 is dependent on Ca^{2+} signalling.

In summary, the presented work demonstrates that AOS treatment differentially induces genes encoding *AtERF* transcription factors. Induction occurs in an ethylene-independent but Ca^{2+}-dependent manner.

6. General Discussion and Future Work

6.1. Signal transduction in response to H_2O_2

H_2O_2 has been implicated in signal transduction mediating a variety of responses (reviewed in Neill *et al.*, 2002), including induction of protective mechanisms upon, high light irradiation (Karpinski *et al.*, 1999) and acclimation to chilling, salt and heat (Prasad *et al.*, 1994; Uchida *et al.*, 2002). In addition, active generation of H_2O_2 in oxidative bursts has been demonstrated as a response to a wide variety of stresses, *e.g.* pathogen attack (Doke, 1983; Levine *et al.*, 1994) and wounding (Doke, 1997; Orozco-Cadenas and Ryan, 1999). H_2O_2 accumulation appears to function as a signalling mechanism rather than 'self-imposed' oxidative stress, triggering the deployment of protective mechanisms (see sections 1.2 and 1.7.4.4).

Despite evidence pointing to a role for H_2O_2 signalling in response to such a broad range of stimuli, little is known about downstream components of the H_2O_2 signal transduction chain.

6.2. H_2O_2 and the Ca^{2+} response

Challenge of whole seedlings with H_2O_2 triggers a biphasic Ca^{2+} signature with the first peak located in the cotyledons and the second peak in the root (Figure 3.4). The short delay between H_2O_2 application and the first Ca^{2+} rise indicates that this Ca^{2+} influx may be one of the earliest responses to H_2O_2 perception. The $[Ca^{2+}]_{cyt}$ elevations can be inhibited by incubation with the Ca^{2+} channel blocker lanthanum (Figure 3.15) and are affected by the cellular redox buffer (Figure 3.20), suggesting

that changes in the cellular redox balance may trigger activation of plasma membrane Ca^{2+} channels, leading to Ca^{2+} influx.

6.2.1. Hyperpolarisation-activated Ca^{2+} channels - responsible for the H_2O_2-triggered Ca^{2+} signature?

The $[Ca^{2+}]_{cyt}$ elevations seen in response to H_2O_2 treatment may arise through activation of hyperpolarisation-activated Ca^{2+}-permeable channels. These channels play a critical role in ABA signal transduction and mediate Ca^{2+} influx across the plasma membrane in response to H_2O_2 treatment in *A. thaliana* guard cells (Pei *et al.*, 2000). However, the delay between H_2O_2 application and the $[Ca^{2+}]_{cyt}$ elevation (2.4 ± 0.8 min) and the duration of the $[Ca^{2+}]_{cyt}$ transient (2.8 ± 0.5 min) were longer compared to data presented in this thesis (Table 3.1). Treatment with 0.1 mM and 1 mM lanthanum strongly inhibited the H_2O_2-triggered $[Ca^{2+}]_{cyt}$ elevation (Pei *et al.*, 2000), similar to the effect seen on the first cotyledon-localised Ca^{2+} peak (Figure 3.14). In older plants, H_2O_2 challenge caused a second Ca^{2+} peak not only in the lower half of the main root but also in parts of the lateral roots distal from the main root (Figure 3.7). This pronounced $[Ca^{2+}]_{cyt}$ elevation in the lower third of the root and the lateral root tips in older plants coincides with the localisation of hyperpolarisation-activated channels which were detected in the root elongation zone (Kiegle *et al.*, 2000b) and the tips of actively growing root hairs (Very and Davies, 2000). Again, lanthanum was shown to block Ca^{2+} influx in both these studies and correspondingly reduced the root-localised $[Ca^{2+}]_{cyt}$ elevation in the data presented here (Figure 3.15).

6.2.2. Two mechanisms of early H_2O_2 signal transduction?

The different tissue locations of the biphasic Ca^{2+} signature triggered by H_2O_2 (Figure 3.4) as well as the isolation of Ca^{2+} signalling mutants that are impaired in only one of the Ca^{2+} rises (Figure 3.29) indicates that H_2O_2 is perceived by different mechanisms in shoot and root cells. The first $[Ca^{2+}]_{cyt}$ elevation in response to both, H_2O_2 and menadione ($^{\bullet}O_2^-$) was modulated by altering the cellular redox buffer, suggesting that this peak is the result of a change in the cellular redox balance on AOS treatment. The second peak was influenced by BSO, demonstrating a redox balance component; but its delayed kinetics (several minutes after stress application) and absence in the menadione-triggered Ca^{2+} signature indicate that other additional mechanisms are involved. However, as discussed above, both elevations may arise through activation of hyperpolarisation-activated plasma membrane Ca^{2+} channels; the reason for the late response in the root is therefore unclear. The delayed timing of this peak suggest that the Ca^{2+} signal is not an early response in this tissue but may be the result of cellular processes initiated by external H_2O_2 application. One such process could be generation of H_2O_2 by the plant itself in an oxidative burst, as is seen in response to ozone fumigation (Wohlgemut *et al.*, 2002). If NADPH oxidases are involved in this putative oxidative burst, pre-treatment with DPI may inhibit the second $[Ca^{2+}]_{cyt}$ elevation of the H_2O_2 response.

H_2O_2 and increased $[Ca^{2+}]_{cyt}$ have been implicated in root hair growth (see section 6.5.1); it would thus be interesting to examine the effect of BSO on the Ca^{2+} gradient within growing root hair and on the rate of root hair elongation.

6.2.3. AOS sensing – can the plant cell distinguish between different AOS?

$^{\bullet}O_2^-$ dismutates to H_2O_2 spontaneously or in a reaction catalysed by superoxide dismutase (see section 1.1.1). Thus, the observation that $^{\bullet}O_2^-$ and H_2O_2 do not trigger the same Ca^{2+} signatures is surprising (Figures 3.4 and 3.8). It is possible that dismutation of $^{\bullet}O_2^-$ to H_2O_2 proceeds more slowly than triggering of an $^{\bullet}O_2^-$-sensing mechanism, or that the sensor can only respond to $^{\bullet}O_2^-$ but not H_2O_2 (similar to SoxR in *E.coli*, (Demple, 1996), hence allowing the cell to distinguish between these two AOS. Alternatively, the difference in Ca^{2+} signatures may be explained by restricted localisation of menadione-mediated $^{\bullet}O_2^-$ generation, as $^{\bullet}O_2^-$ is charged and thus unable to cross membranes (Halliwell and Gutteridge, 1999). The site of $^{\bullet}O_2^-$ generation by menadione has not been established (Thor *et al.*, 1982), but is likely to coincide with the presence of an electron transport chain, *e.g.* in the mitochondria or chloroplasts. Dismutation to H_2O_2 in addition to diffusion out of a specific compartment may be slow compared to the reaction time with cellular components, thus confining the oxidative stress to a particular location. Hence, two hypotheses can be put forward: differences in the Ca^{2+} signatures for H_2O_2 and menadione ($^{\bullet}O_2^-$) either stem from separate sensing mechanisms for these AOS or are the result of AOS perception at different locations (here, external application of H_2O_2 vs intracellular/intracompartmental generation of $^{\bullet}O_2^-$). To resolve the issue, the Ca^{2+} response upon extracellular application of a $^{\bullet}O_2^-$-generating system needs to be investigated; appearance of a second Ca^{2+} peak would support the latter hypothesis. However, both mechanisms could enable the plant to distinguish between different stresses, as these can cause accumulation of different AOS (*e.g.* $^{\bullet}O_2^-$ or H_2O_2 via NADPH oxidase- or cell wall peroxidase-mediated oxidative bursts,

see section 1.7.1) in different compartments (*e.g.* at the plasma membrane or in mitochondria, see Coelho *et al.*, 2002). This would also allow distinction between 'genuine' oxidative stress and accumulation of different AOS through oxidative bursts where H_2O_2 functions as a signalling molecule rather than a stress agent.

6.3. Activation of kinases

6.3.1. OX1 – a general sensor of H_2O_2?

Transcript levels of the *OX1* gene increased not only in response to treatment with H_2O_2 but also in response to other stresses, all of which have been shown to cause generation of AOS (see section 1.2). Even though activation of kinases does not require transcription of the kinase gene itself, a correlation between kinase activation and up-regulation of transcription of the kinase gene encoding it has freqently been detected (Hirt, 1999), *e.g.* in the case of AtMPK3 in response to H_2O_2 treatment (Kovtun *et al.*, 2000; Desikan *et al.*, 2001b; also Appendix C, a). Thus, up-regulation of *OX1* transcription in response to AOS-generating stimuli suggests that activity of the OX1 kinase may be involved in transducing the AOS signal. As menadione and H_2O_2 were equally capable of inducing *OX1* transcription (Figure 4.4), and $^{\bullet}O_2^-$ generated by menadione dismutates to H_2O_2 (McKersie, 1996), it is assumed that H_2O_2 functions as the inducing stimulus. Accordingly, wounding and infection with virulent *P. parasitica* increased expression of the *OX1promoter::GUS* reporter construct in cell layers adjacent to the wounded/infected cells, indicating diffusion of a signalling molecule (Figures 4.7 and 4.11). H_2O_2 is relatively stable as well as being the only AOS capable of crossing membranes (Allan and Fluhr, 1997); and is therefore the most likely AOS to function in this process. To verify the identity

of H_2O_2 as a local signal, leaves could be infiltrated with catalase before stress application and *OX1* induction monitored.

Up-regulation of *OX1* transcription was inhibited by lanthanum treatment, indicating that activation of OX1 may also be regulated by Ca^{2+} and hence placing OX1 activation downstream of AOS-triggered $[Ca^{2+}]_{cyt}$ elevations (Figure 4.40). On the other hand, treatment with SA, JA and the ethylene precursor ACC did not have an effect on *OX1* transcript levels, indicating that these hormones may function downstream of OX1 or in OX1-independent pathways (Figure 4.40).

Several downstream effects of OX1 were identified, including induction of pathogenesis-associated genes and basal resistance to pathogen infection, root hair elongation and regulation of flowering time. These processes are diverse and may indicate that OX1 is a general sensor of H_2O_2, functioning downstream of H_2O_2 accumulation in various different processes. However, not all effects mediated by H_2O_2 involve OX1; thus, *ox1* mutants were neither hypersensitive to UV-B irradiation (Gareth Jenkins, University of Glasgow, personal communication) nor did they display increased wilting under water deficit conditions as expected for ABA signalling mutants (data not shown). Hence, other mechanisms may confer specificity upon OX1 activation. Alternatively, other pathways may be able to compensate for the *ox1* mutation in UV-B and ABA signalling, masking the involvement of OX1 in these processes.

6.3.2. Activation of AtMPK3 and AtMPK6

Activation of the MAPKs AtMPK3 and AtMPK6 and their orthologues in other plant species has been demonstrated in the signal transduction pathways in response to

H_2O_2 application, wounding, pathogen attack and ozone fumigation (see section 4.1). OX1 activity can putatively be placed upstream of AtMPK3 and AtMPK6 as activation of these MAPKs upon ozone fumigation was inhibited in the *ox1* mutant background. These results need to be confirmed and an effect of the *ox1* mutation on AtMPK3 and AtMPK6 activation in response to H_2O_2, cellulase and wounding remains to be demonstrated (currently pursued in collaboration with Brian Ellis, University of Vancouver).

In addition, lanthanum treatment inhibited *OX1* transcription (Figure 4.22) as well as activation of SIPK and WIPK (Romeis *et al.*, 1999; Samuel *et al.*, 2000), placing these kinases downstream of Ca^{2+}. Hence, OX1 may mediate H_2O_2-triggered activation of AtMPK3 and AtMPK6.

6.4. Overlap of gene regulation in response to H_2O_2, pathogen infection and wounding

Gene regulation revealed by microarray data presented here overlaps to a large extent with expression patterns in response to wounding, identified in a microarray experiment by Cheong *et al.*, 2002. Thus, most of the groups of genes discussed by the authors are also up-regulated in response to H_2O_2. Examples are *RLK*s (*e.g. RLK3*), calcium-binding signalling molecules, WRKYs, *ERF*s (*e.g. AtERF1*), *MYB*s (*e.g. MYB51*), pathogenesis-related genes, cytochrome 450s, *GST*s, secondary metabolism enzymes (*e.g.* cinnamyl-alcohol dehydrogenase *ELI3-2*), glucosyltransferases, transporters (*e.g. SUC1*), heat shock proteins (*e.g. HSP17.6-II, HSP70, HSP17.6A*) and JA- as well as ethylene- responsive genes (*e.g. ACC synthase AtACS-6*). However, expression of several peroxidases, extensins and

aquaporins was also enhanced in response to wounding (Cheong *et al.*, 2002) whereas these classes of genes were down-regulated in response to H_2O_2 (Appendix C, b). Some of the differences in induction patterns may be due to differences between the time points investigated: the wounding array examined transcript levels 30 min and 6 h after treatment, whereas the H_2O_2 array included only a 3 h time point. Other differences, such as the opposite effect the two treatments have on peroxidases, extensins and aquaporins, indicate that wounding activates additional signalling components. Accordingly, not all genes induced by H_2O_2 were inducible by other stresses; *e.g. GST1* is up-regulated by H_2O_2 and menadione (*e.g.* Figure 4.28 a) but not cellulase (data not shown). Overlap between wound- and pathogenesis-induced changes in transcript levels have also been observed (see section 1.6). In addition, Northern analysis of 14 genes shown to be induced by H_2O_2 revealed that these genes were also induced in response to a number of other stresses, such as wilting, UV irradiation and treatment with the bacterial elicitor harpin (Desikan *et al.*, 2001a). Hence, stresses inducing H_2O_2 generation overlap in their downstream effects, indicating that common signalling pathways may be employed.

6.4.1. Is there a common component of H_2O_2-generating stresses?

OX1 induction was particularly strong in response to stresses that not only caused H_2O_2 generation but also induced changes in the plant cell wall (see section 4.3.1.2). Touching, enzymatic digestion or wounding of the plant cell wall have all been shown to trigger oxidative bursts (see sections 1.7.5 and 1.8). In addition, H_2O_2 also accumulates during compatible interactions, if at lower levels than during

incompatible interactions (see section 1.7.2). The finding that initiation of an oxidative burst by the elicitor flagellin is dependent on the presence of its receptor FLS2 (Gomez-Gomez *et al.*, 1999) indicates that enhanced H_2O_2 generation during incompatible interactions may be the result of 'gene-for-gene'-mediated recognition events. This oxidative burst could be superimposed on basal H_2O_2 generation triggered by signals common to compatible and incompatible interactions. Mechanical stress and a change in the state of the cell wall could constitute such a universal signal. In support of this hypothesis, modulation of cell wall architecture by inhibiting cellulose synthesis enhanced resistance to infection with the biotrophic fungus *Erysiphe orontii* (Ellis *et al.*, 2002) (see section 1.8) and interference with cell wall – plasma membrane attachment sites decreased resistance (as well as H_2O_2 generation) to incompatible fungi (Mellersh and Heath, 2001; see section 1.9).

Hence, signals emanating from the cell wall may trigger a localised 'basal' oxidative burst whereas *R* gene interactions amplify this burst, leading to activation of the same defensive mechanisms but in a shorter time frame. Accordingly, mutations impairing *R* gene mediated resistance also affect basal resistance (*e.g. eds1*; Parker *et al.*, 1996), and transcription of essentially the same set of genes is up-regulated in incompatible and compatible interactions, however with different kinetics (Maleck *et al.*, 2001; see section 1.4.4). The finding that *OX1* is induced strongly in response to stimuli that affect the cell wall indicates that this kinase may play a particular role in the associated signalling mechanisms, possibly by a combination of H_2O_2 generation and a cell wall-specific component. This mechanism may be similar to the situation in mammalian T lymphocytes, where exposure to AOS or other inducers of oxidative stress did not bypass the requirement for

signalling cascades initiated by specific cell membrane receptors; however, AOS treatment was able to amplify signalling cascades after relatively weak receptor stimulation (Dröge, 2002).

As discussed in section 1.6, many signalling molecules are shared between pathogenesis and wounding, including the tobacco orthologues of AtMPK3 and AtMPK6 (see also section 4.1) and transcription factors that bind the W-box promoter element (Rushton *et al.*, 2002). This provides further evidence that OX1 may be involved in a general pathway sensing H_2O_2 and changes in the cell wall, as OX1 was shown to act upstream of these MAPKs (Figure 4.39). It would be interesting to investigate if AtMPK3 and AtMPK6 are activated to different levels by H_2O_2 application alone and by wounding or pathogenesis, where cell wall-factors and H_2O_2 generation coincide.

6.5. Involvement of OX1 in other signalling pathways

6.5.1. OX1 and root hair

The *OX1* gene is constitutively expressed in the root, particularly in root hair-forming cells (trichoblasts) (Figure 4.36), and root hair elongation is impaired in the *ox1* mutant (Figure 4.37). This phenotype is very similar to that of the *incomplete root hair elongation* (*ire*) mutant (Oyama *et al.*, 2002). The *IRE* genes fall into the same kinase gene family as *OX1* (family 2.4.6, see section) and the IRE protein was shown to extend the duration of tip growth (Oyama *et al.*, 2002). A similar role for OX1 in the regulation of root hair elongation remains to be investigated (*e.g.* by root hair length measurements in the *ox1* mutant in different zones of root hair development, see Oyama *et al.*, 2002). A role for OX1 in this process would tie in

with several other observations. **Firstly**, *OX1* transcription is induced by H_2O_2 (*e.g.* Figure 4.4) and the OX1 kinase may thus be activated by oxidative bursts. Root hair elongation has been shown to be induced by H_2O_2 in the *root hair defective2* (*rhd2*) mutant, which fails to enter the elongative growth phase, indicating that H_2O_2 generation is involved in this process (Dr Liam Dolan, personal communication). Accordingly, AOS production in *rhd2* roots is reduced compared to wild-type. The *RHD2* gene was recently cloned and shown to be identical to the NADPH oxidase *AtrbohC* gene (Liam Dolan, personal communication). **Secondly**, elongation growth in root hairs has been shown to be dependent on a $[Ca^{2+}]_{cyt}$ gradient, with high $[Ca^{2+}]_{cyt}$ at the root hair tip (Dolan, 2001). The *rhd2* mutant lacks this $[Ca^{2+}]_{cyt}$ gradient (Wymer *et al.*, 1997). External H_2O_2 increases $[Ca^{2+}]_{cyt}$ in root cells as seen in this study (Figure 3.4). Also, direct activation of the hyperpolarisation plasma membrane Ca^{2+}-channels by H_2O_2 treatment was demonstrated in root hair cells (Very and Davies, 2000; see section 6.2.1). These channels were inhibited by treatment with lanthanum. Accordingly, the H_2O_2-triggered $[Ca^{2+}]_{cyt}$ elevation in the root was reduced by lanthanum in this study (Figure 3.15), and lanthanum treatment also inhibited induction *OX1* (Figure 4.22). Hence, H_2O_2 generated in an oxidative burst may activate Ca^{2+} channels in the root hair plasma membrane which leads to activation of the OX1 kinase mediating subsequent root hair elongation. **Thirdly**, SIMK, the alfalfa ortholog of AtMPK6, was shown to play a role in root hair tip growth (Samaj *et al.*, 2002). SIMK is localised to the tips of growing root hairs where it co-localises with the actin network. Overexpression of constitutively active SIMK resulted in much longer root hairs whereas disruption of MAPK signalling by treatment with an MAPKK inhibitor inhibited root hair growth and disrupted the actin

cytoskeleton. However, treatment of the constitutively active SIMK overexpressor lines with the MAPKK inhibitor had a much smaller effect on hair elongation rate and did not remodel the cytoskeleton, indicating that SIMK activity is involved in cytoskeletal organisation required for root hair elongation. In this study, the *ox1* mutant was shown to be impaired in AtMPK6 activation in response to ozone fumigation, which is known to trigger an oxidative burst (Wohlgemut *et al.*, 2002). Hence, OX1 may connect H_2O_2 generation with activation of AtMPK6 in root hair elongation. It would be interesting to see if a constitutively active *ox1* mutant displays longer root hairs and if OX1 also co-localises to the actin cytoskeleton.

Fourthly, several genes involved in auxin signalling are down-regulated in *ox1* (Appendix C, c). Auxin has been shown to be required for normal root hair elongation (Pitts *et al.*, 1998). The *ox1* mutation may therefore affect root hair growth by disrupting auxin signalling.

6.5.2. Regulation of flowering time

Two common environmental signals that can affect flowering time are day-length and cold (via the vernalization pathway) (Michaels and Amasino, 2000). The *FLOWERING LOCUS C* (*FLC*) gene encodes a MADS-domain-containing transcription factor and is expressed to high levels in late-flowering, winter-annual *A. thaliana* ecotypes. Early-flowering ecotypes, such as WS-2, contain very low levels of FLC protein (Rouse *et al.*, 2002). After cold treatment, *FLC* transcript levels are down-regulated and remain low for the remainder of the plant's life. This vernalization pathway therefore promotes flowering by reducing the inhibitory effect of FLC (Michaels and Amasino, 2000). However, a recent study demonstrated that

components of other flowering pathways can also affect FLC expression (Rouse *et al.*, 2002).

It has been shown that the main control of FLC protein concentration is exerted at the level of transcription and/or transcript stability. Hence, reduced transcript levels of the floral inhibitor *FLC* in the *ox1* mutant (Appendix C, c) together with an early flowering phenotype (Figure 4.38) indicate that *OX1* may play a role in the vernalization pathway.

A few studies have demonstrated a role for oxidative stress/H_2O_2 in the regulation of flowering time. Thus, repression of APX activity was observed during the developmental transition to flowering and this is accompanied by increased levels of lipid peroxidation (possibly through H_2O_2-dependent activation of a lipoxygenase) (Zhenzhen *et al.*, 2000). Also, treatment with BSO at certain developmental stages promoted flowering, and this effect was abolished by GSH application (Ogawa *et al.*, 2001). Endogenous GSH levels were shown to be elevated in the late-flowering (*fca-1*) mutant, but were reduced by chilling treatment which also promoted flowering (Ogawa *et al.*, 2001). The *gigantea* (*gi*) mutant displays enhanced tolerance to oxidative stress treatment as well as a late-flowering phenotype (Kurepa *et al.*, 1998). The *GI* gene encodes a protein implicated in the phytochrome B signalling pathway (Huq *et al.*, 2000), suggesting that a disruption of red-light perception leads to an increase in the antioxidant capacity of the plant. If the developmental transition to flowering is triggered by increased endogenous AOS generation and a change in the cellular redox balance (as indicated in Ogawa *et al.*, 2001 and Zhenzhen *et al.*, 2000), the increased antioxidant capacity of the *gi* mutant may buffer these processes and thus delay flowering. It would be interesting to see

if *FLC* expression in late-flowering ecotypes is reduced by AOS treatment, providing a mechanism for the repressive effect of cold treatment on this gene.

According to the model presented above, the *ox1* mutant would be expected to have reduced antioxidant capacity, causing an early flowering phenotype. This would be the case if the mutant were deficient in oxidative stress signal transduction pathways. However, *GST1* and *APX1* induction upon H_2O_2 treatment (Figure 4.28) as well as H_2O_2 sensitivity (data not shown) were unaltered in *ox1*. The link between OX1, AOS levels and flowering time is therefore unclear.

To confirm a role of OX1 in the regulation of flowering, *OX1*-overexpressor lines could be tested for delayed flowering. In addition, expression of the *OX1promoter::GUS* construct in floral meristems could be investigated, as expression of *OX1* in this tissue would support a role of OX1 in flowering.

6.6. Future work

A number of experiments that could be carried out to place results presented in this thesis into a broader context have already been suggested in the relevant Discussion sections. This Future Work section will not repeat the suggestions made, but proposes further experiments concentrating on the OX1 protein, as no biochemical data has been obtained so far.

6.6.1. Protein levels

Changes in transcript levels may not be proportional to changes in the level of the encoded protein. Hence, OX1 protein levels should be determined in response to stress treatment by Western blot analysis.

Assessment of OX1 protein levels was attempted by using an antibody raised to a peptide sequence specific to OX1 (data not shown). The antibody recognised purified OX1 protein (overexpressed in *E. coli* and purified via a his-tag), but the signal was not sufficiently strong to detect any protein in plant extracts (data not shown). *A. thaliana* lines transformed with an *OX1promoter::OX1-YFP* fusion construct were analysed for protein expression using anti-GFP antibody; again, no protein was detected in plant extracts (data not shown). These attempts indicate that the OX1 protein may be present at very low levels, even after treatment that strongly increased *OX1* transcript levels, a factor that has to be taken into consideration when designing further experiments. The *OX1promtoer::OX1-YFP* construct also contains a c-myc-tag. Detection of the protein could be attempted with an anti-c-myc antibody, as it may bind very strongly to its epitope.

6.6.2. Cellular localisation

Signalling molecules which function within a signal transduction cascade have to reside in the same location in order to interact, and therefore either remain localised in signalling complexes or translocate upon stimulus perception to transduce the signal to the next component. The localisation of OX1 could be investigated by transforming *A. thaliana* with an *35S::OX1-YFP* fusion. Confocal microscopy should allow visualisation of the fluorescent protein. Hence, it could be determined whether OX1 is uniformly distributed within the cytosol or whether it is associated with other cellular components. Overexpression of the OX1– YFP fusion protein may lead to changes in cellular location; however, no protein was detected (by confocal imaging or Western blotting) when the *OX1-YFP* fusion gene was linked to the *OX1*

promoter (data not shown). Correct localisation of overexpressed OX1-YFP protein could be confirmed by transforming the *ox1* mutant with this construct; complementation of the *ox1* mutant phenotype would indicate that the OX1-YFP protein is able to interact with upstream as well as target molecules at the appropriate location.

It is possible that OX1 localises to membrane systems due to myristoylation on the putative myristoylation sites identified within the protein sequence (see section 4.2.2.1). Directed mutagenesis of these sites could alter OX1 localisation, as has been observed for two CDPKs (Martin and Busconi, 2000; Lu and Hrabak, 2002), and thus reduce activation of downstream effects. Thus, transformation of the *ox1* mutant with a mutagenised *OX1* construct (under the native promoter) should not be able to complement the *ox1* phenotype.

6.6.3. Kinase activity

OX1 was predicted to be a kinase on the basis of its sequence homology. However, kinase activity of the OX1 protein remains to be demonstrated. Kinase assays of the OX1 expressed in *E. coli* (with the artificial substrates myelin basic protein, histone and caseine) did not detect any phosphorylating activity (data not shown). However, a number of reasons could be responsible for this negative result: OX1 may need to associate with additional factors (*e.g.* activating proteins or Ca^{2+}) or may require post-translational modification (*e.g.* phosphorylation) by upstream kinases. To solve this problem, an *OX1*-epitope tag construct under the native or a constitutive promoter could be transformed into *A. thaliana* and the protein immunoprecipitated from plant extracts obtained before and after stress treatment. In this way,

modifications to OX1 can be made by other cellular components before precipitation and associated proteins should be pulled down with the OX1 protein. Thus, it could be determined a) if OX1 has kinase activity and b) which stress stimuli trigger OX1 activation *in vivo*.

6.6.4. Placing OX1 into a signalling network

6.6.4.1. Interacting proteins

Analysis of proteins interacting with OX1 could reveal further signalling components of the H_2O_2 signal transduction chain. The following two approaches are conceivable:

a) Immunoprecipitation of OX1 from plant extracts under native conditions followed by electrophoresis under denaturing conditions. Detection of additional proteins on the gel indicates that other proteins are associated with OX1, which could subsequently be identified by mass spectrometry. If plants expressing OX1 with an epitope tag are generated (for kinase assays, see above), this approach would be easy to carry out alongside.

b) A yeast-two hybrid screen, using OX1 as a bait. This method is often more sensitive than co-precipitation studies, can detect transient interactions and simplifies identification of interacting proteins as the cloned cDNAs encoding them become available (Causier and Davies, 2002).

Identification of interacting proteins by either method would place OX1 into a wider signalling context, possibly indicating additional pathways this kinase is involved in. The requirement of any interacting proteins in OX1-mediated signalling could be verified by analysing null mutants of possible candidates, *e.g.* for enhanced

susceptibility to pathogens. In addition, crossing lines overexpressing interacting proteins or expressing constitutively active mutant forms of interacting proteins into the *ox1* mutant background should indicate if these proteins act upstream or downstream of OX1 in the signal transduction chain.

6.6.4.2. Downstream targets of OX1

In order to identify downstream targets, a 'directed proteomics' approach has been initiated in collaboration with Dr Scott Peck, Sainsbury Laboratories, Norwich, UK. This involves pulse-labelling seedlings with radioactive orthophosphate followed by stress application and protein separation by two-dimensional gel electrophoresis (see Peck *et al.*, 2001). Subsequently, proteins phosphorylated in response to stress treatment can be identified by comparing the protein location on the gel with that of known proteins, or by mass spectrometry. It should be possible to determine if AtMPK3 and AtMPK6 are phosphorylated by OX1, and experiments with the *ox1* mutant could confirm that AtMPK3 and AtMPK6 activation is indeed reduced in response to stress treatment (see Figure 4.39).

6.6.5. Further analysis of the OX1 protein

Amino acid residues and domains with important functions within the OX1 protein could be identified with the help of the TILLING (Targeting Induced Local Lesions In Genomes) reverse genetic strategy (Colbert *et al.*, 2001) which involves screening of EMS-mutagenised populations for point mutations in the gene of interest. This is of particular interest for the C-terminal region, which does not show homology to any protein sequence in the NCBI database.

7. Bibliography

Allan, A. C., Fricker, M. D., Ward, J. L., Beale, M. H. and Trewavas, A. J. (1994). Two transduction pathways mediate rapid effects of abscisic acid in Commelina guard cells. *The Plant Cell* **6**, 1319 - 1328.

Allan, A. C. and Fluhr, R. (1997). Two distinct sources of elicited reactive oxygen species in tobacco epidermal cells. *The Plant Cell* **9**, 1559 - 1572.

Allen, G. J., Chu, S. P., Schumacher, K., Shimazaki, C. T., Vafeados, D., Kemper, A., Hawke, S. D., Tallmann, G., Tsien, R. Y., Harper, J. F. et al. (2000). Alteration of stimulus-specific guard cell calcium oscillations and stomatal closing *Arabidopsis det3* mutant. *Science* **289**, 2338 - 2342.

Allen, M. D., Yamasaki, K., Ohme-Takagi, M., Tateno, M. and Suzuki, M. (1998). A novel mode of DNA recognition by a ß-sheet revealed by the solution structure of the GCC-box binding domain in complex with DNA. *EMBO Journal* **17**, 5485 - 5496.

Alonso, J. M., Hirayama, T., Roman, G., Nourizadeh, S. and Ecker, J. R. (1999). EIN2, a bifunctional transducer of ethylene and stress responses in Arabidopsis. *Science* **284**, 2148 - 2152.

Altschul, S. F., Madden, T. L., Schäffer, A. A., Zhang, J., Zhang, Z., Miller, W., Lipman, D. J. (1974). Gapped BLAST and PSI-BLAST – a new generation of protein database search programs. *Nucleic Acids Res* **25**, 3389 - 3402.

Alvarez, M. E., Pennell, R. I., Meijer, P.-J., Ishikawa, A., Dixon, R. A. and Lamb, C. (1998). Reactive oxygen intermediates mediate a systemic signal network in the establishment of plant immunity. *Cell* **92**, 773 - 784.

Asai, T., Tena, G., Plotnikova, J., Willmann, M. R., Chiu, W. L., Gomez-Gomez, L., Boller, T., Ausubel, F. M. and Sheen, J. (2002). MAP kinase signalling cascade in Arabidopsis innate immunity. *Nature* **415**, 977-83.

Aufsatz, W. and Grimm, C. (1994). A new, pathogen-inducible gene of *Arabidopsis* is expressed in an ecotype-specific manner. *Plant Mol Biol* **25**, 229 - 239.

Aufsatz, W., Amry, D. and Grimm, C. (1998). The *ECS1* gene of *Arabidopsis* encodes a plant cell wall-associated protein and is potentially linked to a locus influencing resistance to *Xanthomonas campestris*. *Plant Mol Biol* **38**, 965 - 976.

Azevedo, C., Sadanandom, A., Kitagawa, K., Freialdenhoven, A., Shirasu, K. and Schulze-Lefert, P. (2002). The RAR1 interactor SGT1, an essential component of R gene-triggered disease resistance. *Science* **295**, 2073 - 2076.

Bai, C., Sen, P., Hofmann, K., Ma, L., Goebl, M., Harper, J. W. and Elledge, S. J. (1996). SKP1 connects cell cycle regulators to the ubiquitin proteolysis machinery through a novel motif, the F-box. *Cell* **86**, 263-274.

Banzet, N., Richaud, C., Deveaux, Y., Kazmaier, M., Gagnon, J. and Triantaphylidès, C. (1998). Accumulation of small heat shock proteins, including mitochondrial HSP22, induced by oxidative stress and adaptive responses in tomato cells. *Plant Journal* **13**, 519 - 527.

Benhamou, N., Chamberland, H. and Pauze, F. (1990). Implication of pectic components in cell surface interactions between tomato root cells and *Fusarium oxysproum* f. sp. *radicis-lycopersici*. *Plant Physiology* **92**, 995 - 1003.

Bergey, D. R., Orozco-Cardenas, M., de Moura, D. S. and Ryan, C. A. (1999). A wound- and systemin-inducible polygalacturonase in tomato leaves. *Proc Natl Acad Sci U S A* **96**, 1756-60.

Berrocal-Lobo, M., Molina, A. and Solano, R. (2002). Constitutive expression of ethylene-response-factor 1 in *Arabidopsis* confers resistance to several necrotrophic fungi. *Plant Journal* **29**, 23 - 32.

Bi, Y.-M., Kenton, P., Mur, L., Darby, R. and Draper, J. (1995). Hydrogen peroxide does not function donwstream of salicylic acid in the production of PR protein expression. *Plant Journal* **8**, 235-245.

Bittner-Eddy, P., Can, C., Gunn, N., Pinel, M., Tör, M., Crute, I. R., Holub, E. B. and Beynon, J. L. (1999). Genetic and physical mapping of the *RPP13* locus, in Arabidopsis, responsible for specific recognition of several *Peronospora parasitica* (Downy Mildew) isolates. *Mol Plant - Microbe Interactions* **12**, 792 - 802.

Blatt, M. R. (1999). Reassessing roles for Ca^{2+} in guard cell signalling. *Journal of Experimental Botany* **50**, 989 - 999.

Bleecker, A. B. and Kende, H. (2000). Ethylene: A gaseous signal molecule in plants. *Annual Review of Cell and Developmental Biology* **16**, 1 - 18.

Bögre, L., Ligterink, W., Meskiene, I., Baker, P., Heberle-Bors, E. and Hirt, H. (1997). Wounding induces the rapid and transient activation of a specific MAP kinase pathway. *The Plant Cell* **9**, 75 - 83.

Bolwell, P. G. and Wojtaszek, P. (1997). Mechanisms for the generation of reactive oxygen species in plant defense: a broad perspective. *Physiol Mol Plant Pathol* **51**, 347 - 366.

Bolwell, P. G., Davies, D. R., Gerrish, C., Auh, C.-K. and Murphy, T. M. (1998). Comparative biochemistry of the oxidative burst produced by rose and French bean cells reveals two distinct mechansims. *Plant Physiology* **116**, 1379 - 1385.

Bowler, C., Van Montagu, M. and Inzé, D. (1992). Superoxide dismutase and stress tolerance. *Annual Review of Plant Physiology and Plant Molecular Biology* **43**, 83 - 116.

Bradley, D. J., Kjellborn, P. and Lamb, C. J. (1992). Elicitor- and wound-induced oxidative cross-linking of a proline-rich plant cell wall protein: a novle, rapid defense response. *Cell* **70**.

Brisson, L. F., Tenhaken, R. and Lamb, C. (1994). Function of oxidative cross-linking of cell wall structural proteins in plant disease resistance. *The Plant Cell* **6**, 1703 - 1712.

Broekaert, W. F., Cammue, B. P. A., DeBolle, M. F. C., Thevissen, K., DeSamblanx, G. W. and Osborn, R. W. (1997). Antimicrobial peptides from plants. *Critical Reviews in Plant Sciences* **116**, 297 - 323.

Buck, V., Quinn, J., Soto Pino, T., Martin, H., Saldanha, J., Makino, K., Morgan, B. A. and Millar, J. B. (2001). Peroxide sensors for the fission yeast stress-activated mitogen-activated protein kinase pathway. *Mol Biol Cell* **12**, 407-19.

Buettner, M. and Singh, K. B. (1997). Arabidopsis thaliana ethylene-responsive element binding protein (AtEBP), an ethylene-inducible, GCC box DNA-binding protein interacts with an ocs element binding protein. *Proc Natl Acad Sci U S A* **94**, 5961 - 5966.

Bush, D. S. (1995). Calcium regulation in plant cells and its role in signalling. *Annual Review of Plant Physiology and Plant Molecular Biology* **46**, 95 - 122.

Canut, H., Carrasco, A., Galaud, J. P., Cassan, C., Bouyssou, H., Vita, N., Ferrara, P. and Pont-Lezica, R. (1998). High affinity RGD-binding sites at the plasma membrane of Arabidopsis thaliana links the cell wall. *Plant Journal* **16**, 63-71.

Cao, H., Bowling, S. A., Gordon, S. and Dong, X. (1994). Characterization of an *Arabidopsis* mutant that is nonresponsive to inducers of systemic acquired resistance. *The Plant Cell* **6**, 1583 - 1592.

Cardinale, F., Jonak, C., Ligterink, W., Niehaus, K., Boller, T. and Hirt, H. (2000). Differential activation of four specific MAPK pathways by distinct elicitors. *The Journal of Biological Chemistry* **275**, 36734 - 36740.

Cardinale, F., Meskiene, I., Ouaked, F. and Hirt, H. (2002). Convergence and divergence of stress induced mitogen-activated protein kinase signaling pathways at the level of two distinct mitogen-activated protein kinase kinases. *The Plant Cell* **14**, 703 - 711.

Causier, B. and Davies, B. (2002). Analysing protein-protein interactions with the yeast two-hybrid system. *Plant Mol Biol* **50**, 855 - 870.

Cessna, S. G., Chandra, S. and Low, P. S. (1998). Hypo-osmotic shock of tobacco cells stimulates Ca^{2+} fluxes deriving from external and the internal Ca^{2+} stores. *Journal of Biological Chemistry* **273**, 27286 - 27291.

Chamnongpol, S., Willekens, H., Moeder, W., Langebartels, C., Sandermann, H., VanMontagu, A., Inze, D. and VanCamp, W. (1998). Defense activation and enhanced pathogen tolerance induced by H_2O_2 in transgenic tobacco. *Proc Natl Acad Sci U S A* **95**, 5818-5823.

Chandra, S. and Low, P. S. (1995). Role of phosphorylation in elicitation of the oxidative burst in cultured soybean cells. *Proc Natl Acad Sci U S A* **92**, 4120 - 4123.

Chandra, S. and Low, P. S. (1997). Measurement of Ca^{2+} fluxes during elicitation of the oxidative burst in aequorin-transformed tobacco cells. *The Journal of Biological Chemistry* **272**, 28274 - 28280.

Chang, C. and Stadler, R. (2001). Ethylene hormone receptor action in *Arabidopsis*. *BioEssays* **23**, 619 - 627.

Chen, W., Provart, N. J., Glazebrook, J., Katagiri, F., Chang, H.-S., Eulgem, T., Mauch, F., Luan, S., Zou, G., Whitham, S. A. et al. (2002). Expression profile matrix of *Arabidopsis* transcription factor gene suggests their putative functions in response to environmental stresses. *The Plant Cell* **14**, 559 - 574.

Cheng, S.-H., Willmann, M. R., Chen, H.-C. and Sheen, J. (2002). Calcium signaling through protein kinases. The Arabidopsis calcium-dependent protein kinase gene family. *Plant Physiology* **129**, 469 - 485.

Chen, W., Chao, G., Singh, K. B. (1996). The promoter of a H_2O_2-inducible, Arabidopsis glutathione S-transferase gene contains closely linked OBF- and OBP1-binding sites. *Plant Journal* **10**, 955 - 966.

Chen, W. and Singh, K. B. (1999). The auxin, hydrogen peroxide and salicylic acid induced expression of the *Arabidopsis GST6* promoter is mediated in part by an ocs element. *Plant Journal* **19**, 667 - 677.

Cheong, Y. H., Cheol, M. Y., Park, J. M., Ryu, G. R., Goekjian, V. H., Nagao, R. T., Key, J. L., Cho, M. J. and Hong, J. C. (1998). STF1 is a novel TGACG-binding factor with a zinc-finger motif and a bZIP domain which heterodimerizes with GBF proteins. *Plant Journal* **15**, 199 - 209.

Cheong, Y. H., Chang, H.-S., Gupta, R., Wang, X. and Luan, S. (2002). Transcriptional profiling reveals novel interactions between wounding, pathogen, abiotic stress, and hormonal responses in Arabidopsis. *Plant Physiology* **129**, 661 - 677.

Cibulsky, S. M. and Sather, W. A. (1999). Block by ruthenium red of cloned neuronal voltage-gated calcium channels. *The Journal of Pharmacology and Experimental Therapeutics* **189**, 1447 - 1453.

Clapham, D. E. (1995). Calcium signaling. *Cell* **80**, 259 - 268.

Clayton, H., Knight, M. R., Knight, H., McAinsh, M. R. and Hetherington, A. M. (1999). Dissection of the ozone-induced calcium signature. *Plant Journal* **17**, 575 - 579.

Clough, S. J. and Bent, A. F. (1998). Floral dip: a simplified method for *Agrobacterium*-mediated transformation of *Arabidopsis thaliana*. *Plant Journal* **16**, 735 - 743.

Coelho, S. M., Taylor, A. R., Ryan, K. P., Sousa-Pinto, I., Brown, M. T. and Brownlee, C. (2002). Spatiotemporal patterning of reactive oxygen production and Ca^{2+} wave propagation in Fucus rhizoid cells. *The Plant Cell* **14**, 2369 - 2381.

Cohen, P. (1997). The search for physiological substrates of MAP and SAP kinases in mammalian cells. *Trends in Cell Biology* **7**, 353 - 361.

Colbert, T., Till, B. J., Tompa, R., Reynolds, S., Steine, M. N., Yeung, A. T., McCallum, C. M., Comai, L. and Henikoff, S. (2001). High-throughput screening for induced point mutations. *Plant Physiology* **126**, 480 - 484.

Conklin, P. L. and Last, R. L. (1995). Differential accumulation of antioxidant mRNAs in *Arabidopsis thaliana* exposed to ozone. *Plant Physiology* **109**, 203 - 212.

Constabel, C. P., Yip, L. and Ryan, C. A. (1998). Prosystemin from potato, black nightshade, and bell pepper: primary structure and biological activity of predicted systemin polypeptides. *Plant Mol Biol* **36**, 55-62.

Creelman, R. A. and Mullet, J. E. (1997). Biosynthesis and action of jasmonates in plants. *Annual Review of Plant Physiology and Plant Molecular Biology* **48**, 355-381.

Czernic, P., Visser, B., Sun, W., Savoure, A., Deslandes, L., Marco, Y., van Montagu, M. and Verbruggen, N. (1999). Characterization of an Arabidopsis thaliana receptor-like protein kinase gene activated by oxidative stress and pathogen attack. *Plant Journal* **18**, 321 - 327.

Dangl, J. L. and Jones, J. D. G. (2001). Plant pathogens and integrated defence responses to infection. *Nature* **411**, 826 - 833.

Dat, J. F., Inzé, D. and Van Breusegem, F. (2000). Catalase-deficient tobacco plants: tools for *in planta* studies on the role of hydrogen peroxide. *Redox Report* **6**, 37 - 42.

Deblaere, R., Bytebier, B., Degreve, H., Deboek, F., Shell, J., Van Montagu, M. and Leemans, J. (1985). Efficient octopine T_i plasmid-derived vectors for *Agrobacterium*-mediated gene-transfer to plants. *Nucleic Acids Res* **13**, 4777 - 4788.

Delaney, T. P., Uknes, S., Vernooij, B., Friedrich, L., Weymann, K., Negrotto, D., Gaffney, T., Gutrella, M., Kessmann, H., Ward, E. et al. (1994). A central role of salicylic-acid in plant-disease resistance. *Science* **266**, 1247 - 1250.

Delaunay, A., Isnard, A. D. and Toledano, M. B. (2000). H_2O_2 sensing through oxidation of the Yap1 transcription factor. *Embo J* **19**, 5157-66.

Delledonne, M., Zeier, J., Marocco, A. and Lamb, C. (2001). Signal interactions between nitric oxide and reactive oxygen intermediates in the plant hypersensitive disesase resistance response. *Proc Natl Acad Sci U S A* **98**, 13454 - 13459.

Demple, B. (1996). Redox signaling and gene control in the Escherichia coli soxRS oxidative stress regulon - a review. *Gene* **179**, 53 - 57.

Desikan, R., Hancock, J. T., Coffey, M. J. and Neill, S. J. (1996). Generation of active oxygen in elicited cells of Arabidopsis thaliana is mediated by a NADPH oxidase-like enzyme. *FEBS Letters* **382**, 213-217.

Desikan, R., Clarke, A., Hancock, J. T. and Neill, S. J. (1999). H_2O_2 activates a MAP kinase-like enzyme in Arabidopsis thaliana suspension cultures. *Journal of Experimental Botany* **50**, 1863-1866.

Desikan, R., Hancock, J. T., Ichimura, K., Shinozaki, K. and Neill, S. J. (2001a). Harpin induces activation of the Arabidopsis mitogen-activated protein kinases AtMPK4 and AtMPK6. *Plant Physiol* **126**, 1579-87.

Desikan, R., S, A. H.-M., Hancock, J. T. and Neill, S. J. (2001b). Regulation of the Arabidopsis transcriptome by oxidative stress. *Plant Physiol* **127**, 159-72.

Doares, S. H., Syrovets, T., Weiler, E. W. and Ryan, C. A. (1995). Oligogalacturonides and Chitosan Activate Plant Defensive Genes Through the Octadecanoid Pathway. *Proc Natl Acad Sci U S A* **92**, 4095-4098.

Doke, N. (1983). Involvement of superoxide anion generation in the hypersensitive response of potato-tuber tissues to infection with an incompatible race of *Phyotphtora infestans* and to the hyphal wall components. *Physiol Plant Pathol* **23**, 345 - 357

Doke, N. (1997). The oxidative burst: roles in signal transduction and plant stress. Cold Spring Harbor: Cold Spring Harbor Laboratory Press.

Dolan, L. (2001). How and where to build a root hair. *Curr Opin Plant Biol* **4**, 550-554.

Dolmetsch, R. E., Lewis, R. S., Goodnow, C. C. and Healy, J. I. (1997). Differential activation of transcription factors induced by Ca^{2+}-response amplitude and duration. *Nature* **386**, 855 - 858.

Draper, J. (1997). Salicylate, superoxide synthesis and cell suicide in plant defence. *Trends in Plant Science* **2**, 162 - 165.

Dröge, W. (2002). Free radicals in the physiological control of cell function. *Physiological Reviews* **82**, 47 - 95.

Droillard, M.-J., Boudsocq, M., Barbier-Brygoo, H. and Laurière, C. (2002). Different protein kinase families are activated by osmotic stresses in *Arabidopsis thaliana* cell suspensions. *FEBS Letters* **527**, 43 - 50.

Du, L. and Chen, Z. (2000). Identification of genes encoding receptor-like protein kinases as possible targets of pathogen- and salicylic acid-induced WRKY DNA-binding proteins in Arabidopsis. *Plant Journal* **24**, 837-847.

Ducibella, T., Huneau, D., Angelichio, E., Xu, Z., Schultz, R. M., Kopf, G. S., Fissore, R., Madoux, S. and Ozil, J.-P. (2002). Egg-to-embryo transition is driven by differential responses to Ca^{2+} oscillation number. *Developmental Biology* **250**, 280 - 291.

Durner, J., Shah, J. and Klessig, D. F. (1997). Salicylic acid and disease resistance in plants. *Trends in Plant Science* **2**, 266 - 274.

Durrant, W. E., Rowland, O., Piedras, P., Hammond-Kosack, K. E. and Jones, J. D. G. (2000). cDNA-AFLP reveals a striking overlap in race-specific resistance and wound response gene expression profiles. *The Plant Cell* **12**, 963 - 977.

Edwards, R., Dixon, D. P. and Walbot, V. (2000). Plant glutathione S-transferases: enzymes with multiple functions in sickness and in health. *Trends in Plant Science* **5**, 193-198.

Ellis, C. and Turner, J. G. (2001). The Arabidopsis mutant cev1 has constitutively active jasmonate and ethylene signal pathways and enhanced resistance to pathogens. *The Plant Cell* **13**, 1025 - 1033.

Ellis, C., Karafyllidis, I., Wasternack, C. and Turner, J. G. (2002). The Arabidopsis Mutant cev1 Links Cell Wall Signaling to Jasmonate and Ethylene Responses. *The Plant Cell* **14**, 1557-66.

Enkerli, J., Felix, G. and Boller, T. (1999). The enzymatic activity of fungal xylanase is not necessary for its elicitor activity. *Plant Physiology* **121**, 391 - 397.

Epple, P., Apel, K. and Bohlmann, H. (1995). An *Arabidopsis thaliana* thionin gene is inducible via a signal transduction pathway different from that for pathogenesis-related proteins. *Plant Physiology* **109**, 813 - 820.

Eulgem, T. R., Paul J.; Schmelzer, Elmon; Hahlbrock, Klaus; Somssich, Imre E. (1999). Early nuclear events in plant defence signalling: rapid gene activation by WRKY transcription factors. *The EMBO Journal* **18**, 4689 - 4699.

Fath, A., Bethke, P. C. and Jones, R. L. (2001). Enyzmes that scavenge reactive oxygen species are down-regulated prior to gibberellic acid-induced programmed cell death in barley aleurone. *Plant Physiology* **126**, 156 - 166.

Feldbrügge, M., Sprenger, M., Dinkelbach, M., Yazaki, K., Harter, K. and Weisshaar, B. (1994). Functional analysis of a light-responsive plant bZIP transcriptional regulator. *The Plant Cell* **6**, 1607 - 1621.

Fernandez del Caleya, R., Gonzalez-Pascual, B., Garcia-Olmedo, F. and Carbonero, P. (1972). Susceptibility of phytopathogenic bacteria to wheat purothionins in vitro. *Applied Microbiology* **23**, 998 - 1000.

Feys, B. J. F., Benedetti, C. E., Penfold, C. N. and Turner, J. G. (1994). Arabidopsis Mutants Selected For Resistance to the Phytotoxin Coronatine Are Male-Sterile, Insensitive to Methyl Jasmonate, and Resistant to a Bacterial Pathogen. *The Plant Cell* **6**, 751-759.

Finkel, T. (1998). Oxygen radicals and signaling. *Current Opinion in Cell Biology* **10**, 248 - 253.

Flohr, H. (1971). Current status of the gene-for-gene concept. *Annual Review of Phytopathology* **9**, 275 - 296.

Foyer, C. H., LopezDelgado, H., Dat, J. F. and Scott, I. M. (1997). Hydrogen peroxide- and glutathione-associated mechanisms of acclimatory stress tolerance and signalling. *Physiologia Plantarum* **100**, 241-254.

Fricker, M. D., Plieth, C., Knight, H., Blancaflor, E., Knight, M. R., White, N. S. and Gilroy, S. (1999). Fluorescence and luminescence techniques to probe ion activities in living plant cells. In *Fluorescent and Luminescent Probes for Biological Activity*, (ed. W. Mason), pp. 569 - 594. London: Academic Press.

Fujimoto, S. Y., Ohta, M., Usui, A., Shinshi, H. and Ohme-Takagi, M. (2000). Arabidopsis ethylene-responsive element binding factors act as transcriptional activators or repressors of GCC box-mediated gene expression. *The Plant Cell* **12**, 393 - 404.

Gaffney, T., Friedrich, L., Vernooij, B., Negrotto, D., Nye, G., Uknes, S., Ward, E., Kessmann, H. and Ryals, J. (1993). Requirement of salicylic acid for the induction of systemic acquired resistance. *Science* **261**, 754 - 756.

Giancotti, F. G. and Ruoslahti, E. (1999). Transduction - Integrin signaling. *Science* **285**, 1028-1032.

Glazebrook, J., Rogers, E. E. and Ausubel, F. M. (1997). Use of Arabidopsis for genetic dissection of plant defense responses. *Annual Review of Genetics* **31**, 547 - 569.

Goddard, H., Manison, N. F. H., Tomos, D. and Brownlee, C. (2000). Elemental propagation of calcium signals in response-specific patterns determined by environmental stimulus strength. *Proc Natl Acad Sci U S A* **97**, 1932 - 1937.

Gomez-Gomez, L., Felix, G. and Boller, T. (1999). A single locus determines sensitivity to bacterial flagellin in Arabidopsis thaliana. *Plant Journal* **18**, 277 - 284.

Grant, J., J., Yun, B.-W. and Loake, G. J. (2000). Oxidative burst and cognate redox signalling reported by luciferase imaging: identification of a signal network that functions independently of ethylene, SA and Me-JA but is dependent on MAPKK activity. *Plant Journal* **24**, 569 - 582.

Grant, J. J. and Loake, G. J. (2000a). Role of Reactive Oxygen Intermediates and Cognate Redox Signaling in Disease Resistance. *Plant Physiology* **124**, 21 - 29.

Grant, M., Brown, I., Adams, S., Knight, M., Ainslie, A. and Mansfield, J. (2000b). The RPM1 plant disease resistance gene facilitates a rapid and sustained increase in cytosolic calcium that is necessary for the oxidative burst and hypersensitive cell death. *Plant Journal* **23**, 441-450.

Griffith, O. W. and Meister, A. (1979). Potent and specific inhibition of glutathione synthesis by buthionine sulfoximine (S-n butyl homocysteine sulfoximine). *Journal of Biological Chemistry* **254**, 7558 - 7560.

Groom, Q. J., Torres, M. A., Fordham-Skelton, A. P., Hammond-Kosack, K. E., Robinson, N. J. and Jones, J. D. G. (1996). *rbohA*, a rice homolgue of the mammalian gp91^{phox} respiratory burst oxidase gene. *Plant Journal* **10**, 515 - 522.

Gross, P., Julius, C., Schmelzer, E. and Hahlbrock, K. (1993). Translocation of cytoplasm and nucleus to fungal penetration sites is associated with depolymerization of microtubules and defense gene activation in infected, cultured parsley cells. *The EMBO Journal* **12**, 1735 - 1744.

Gu, X. and Spitzer, N. (1995). Distinct aspects of neuronal differentiation encoded by frequency of spontaneous Ca^{2+} transients. *Nature* **375**, 784 - 787.

Gu, Y.-Q., Yang, C., Thara, V. K., Zhou, J. and Martin, G. B. (2000). *Pti4* is induced by ethylene and salicylic acid, and its product is phosphorylated by the Pto kinase. *The Plant Cell* **12**, 771 - 785.

Guan, L. M., Zhao, J. and Scandalios, J. G. (2000). Cis-elements and trans-factors that regulate expression of the maize Cat1 antioxidant gene in response to ABA and osmotic stress: H_2O_2 is the likely intermediary signaling molecule for the response. *Plant Journal* **22**, 87 - 95.

Gundlach, H., Muller, M. J., Kutchan, T. M. and Zenk, M. H. (1992). Jasmonic acid is a signal transducer in elicitor-induced plant cell cultures. *Proc Natl Acad Sci U S A* **89**, 2389-93.

Gupta, R., Huang, Y., Kieber, J. J. and Luan, S. (1998). Identification of a dual-specificity protein phosphatase that inactivates a MAP kinase from *Arabidopsis*. *Plant Journal* **16**, 581 - 589.

Gus-Mayer, S., Naton, B., Hahlbrock, K. and Schmelzer, E. (1998). Local mechanical stimulation induces components of the pathogen defense response in parsley. *Proc Natl Acad Sci U S A* **95**, 8398 - 8403.

Guyton, K. Z., Liu, Y., Gorospe, M., Xu, Q. and Holbrook, N. J. (1996). Activation of mitogen-activated protein kinase by H_2O_2. Role in cell survival following oxidant injury. *J Biol Chem* **271**, 4138-42.

Halliwell, B. and Gutteridge, J. M. C. (1999). Free radicals in biology and medicine. Oxford: Oxford University Press.

Hao, D., Ohme-Takagi, M. and Sarai, A. (1998). Unique mode of GCC box recognition by the DNA-binding domain of ethylene-responsive element-binding factor (ERF domain) in plants. *Journal of Biological Chemistry* **273**, 26857 - 26861.

Hanks, S. K. and Quinn, A. M. (1991). Protein kinase catalytic domain sequence database - identification of conserved features of primary structure and classification of family members. *Methods in Enzymology* **200**, 38 -62.

Hardie, D. G. (1999). Plant protein serine threonine kinases: Classification and functions. *Annual Review of Plant Physiology and Plant Molecular Biology* **50**, 97 - 131.

Hardie, D. G. (2000). Plant protein-serine/threonine kinases: classification into subfamilies and overview of function. In *Advances in Botanical Reserach: Plant Protein Kinases*, vol. 32 (ed. M. Kreis and J. C. Walker). London: Academic Press.

Harding, S. A., Oh, S.-H. and Roberts, D. M. (1997). Transgenic tobacco expressing a foreign calmodulin gene shows an enhanced production of active oxygen species. *The EMBO Journal* **16**, 1137 - 1144.

Hardingham, G. E., Chawla, S., Johnson, C. M. and Bading, H. (1997). Distinct functions of nuclear and cytoplasmic calcium in the control of gene expression. *Nature* **385**, 260 - 265.

Hardtke, C. S., Okamoto, H., Stoop-Myer, C. and Deng, X. W. (2002). Biochemical evidence for ubiquitin ligase activity of the *Arabidopsis* COP1 interacting protein 8 (CIP8). *The Plant Journal* **30**, 385 - 394.

Haring, M. A., Siderius, M., Jonak, C., Hirt, H., Walton, K. M. and Musgrave, A. (1995). Tyrosine phosphatase signalling in a lower plant: cell-cycle and oxidative stress-regulated expression of the Chlamydomonas eugametos VH-PTP13 gene. *The Plant Journal* **7**, 981-988.

Harmon, A. C., Gribskov, M., Gubrium, E. and Harper, J. F. (2001). The CDPK superfamily of protein kinases. *New Phytologist* **151**, 175 - 183.

Harper, J. F., Sussmann, M. R., Schaller, G. E., Putnam-Evans, C., Charbonneau, H. and Harmon, A. C. (1991). A calcium-dependent protein kinase with a regulatory domain similar to calmodulin. *Science* **252**, 951 - 954.

Heath, M. C. (1997). Signalling between pathogenic rust fungi and resistant or susceptible host plants. *Annals of Botany* **80**, 713-720.

Heath, M. C. (2000). Nonhost resistance and nonspecific plant defenses. *Current Opinion in Plant Biology* **3**, 315 - 319.

Henzier, T. and Steudle, E. (2000). Transport and metabolic degradation of hydrogen peroxide in *Chara corallina*: model calculations and measurements with thte pressure probe suggest transport of H_2O_2 across water channels. *Journal of Experimental Botany* **51**, 2053 - 2066.

Herrlich, P. and Bohmer, F. D. (2000). Redox regulation of signal transduction in mammalian cells. *Biochem Pharmacol* **59**, 35-41.

Hirt, H. (1999). Transcriptional upregulation of signaling pathways: more complex than anticipated? *Trends in Plant Science* **4**, 7 - 8.

Holub, E. B., Beynon, J. L. and Crute, I. R. (1994). Phenotypic and genotypic characterization of interactions between isolates of *Peronospora parasitica* and accessions of *Arabidopsis thaliana*. *Mol Plant - Microbe Interactions* **7**, 223 - 239.

Hrabak, E. M. (2000). Calcium-dependent protein kinases and their relatives. In *Advances in Botanical Research: Plant Protein Kinases*, vol. 32 (ed. M. Kreis and J. C. Walker), pp. 185 - 223. London: Academic Press.

Hua, J. and Meyerowitz, E. M. (1998). Ethylene responses are negatively regulated by a receptor gene family in *Arabidopsis*. *Cell* **94**, 261 – 271.

Huq, E., Tepperman, J. M. and Quail, P. H. (2000). GIGANTEA is a nuclear protein involved in phytochrome signaling in Arabidopsis. *Proc Natl Acad Sci U S A* **97**, 9789-94.

Hwang, Y.-S., Karrer, E. E., Thomas, B. R., Chen, L. and Rodriguez, R. L. (1998). Three *cis*-elements required for rice α-amylase *Amy3D* expression during sugar starvation. *Plant Mol Biol* **36**, 331 - 341.

Ichimura, K., Mizoguchi, T., Yoshida, R., Yuasa, T. and Shinozaki, K. (2000). Various abiotic stresses rapidly activate Arabidopsis MAP kinases ATMPK4 and ATMPK6. *Plant Journal* **24**, 655-65.

Ikura, M. (1996). Calcium binding and conformational response in EF-hand proteins. *Trends in Biochemical Sciences* **21**, 14 - 17.

Jabs, T., Tschope, M., Colling, C., Hahlbrock, K. and Scheel, D. (1997). Elicitor-stimulated ion fluxes and O_2^- from the oxidative burst are essential components in

triggering defense gene activation and phytoalexin synthesis in parsley. *Proc Natl Acad Sci U S A* **94**, 4800 - 4805.

Jaglo-Ottosen, J., Gilmour, S., Zarka, D., Schabenberger, O. and Thomashow, M. (1998). *Arabidopsis* CBF1 overexpressor induces cor genes and enhances freezing tolerance. *Science* **280**, 104 - 106.

Jefferson, R. A., Kavanagh, T., A. and Bevan, M. W. (1987). GUS fusions: ß-glucuronidase as a sensitive and versatile gene fusion marker in higher plants. *The EMBO Journal* **6**, 3901 - 3907.

Jonak, C., Ökrész, L., Bögre, L. and Hirt, H. (2002). Complexity, cross talk and integration of plant MAP kinase signalling. *Current Opinion in Plant Biology* **5**, 415 - 424.

Joo, J. H., Bae, Y. S. and Lee, J. S. (2001). Role of auxin-induced reactive oxygen species in root gravitropism. *Plant Physiology* **126**, 1055 - 1060.

Jouannic, S., Leprince, A.-S., Hamal, A., Picaud, A., Kreis, M. and Henry, Y. (2000). Plant mitogen-activated protein kinase signalling pathways in the limelight. In *Advances in Botanical Research*, vol. 32, pp. 299 - 354: Academic Press.

Karpinski, S., Reynolds, H., Karpinska, B., Winglse, G., Creissen, G. and Mullineaux, P. (1999). Systemic signaling and acclimation in response to excess excitation energy in *Arabidopsis*. *Science* **284**, 654 - 657.

Keller, T., Damude, H. G., Werner, D., Doerner, P., Dixon, R. A. and Lamb, C. (1998). A plant homolog of the neutrophil NADPH oxidase gp91*phox* subunit gene encodes a plasma membrane protein with Ca^{2+} binding motifs. *The Plant Cell* **10**, 255 - 266.

Keyse, S. M. (2000). Protein phosphatases and the regulation of mitogen-activated protein kinase signalling. *Current Opinion in Cell Biology* **12**, 186 - 192.

Kieber, J. J. (1997). The ethylene response pathway in Arabidopsis. *Annual Review of Plant Physiology and Plant Molecular Biology* **48**, 277 - 96.

Kiegle, E., Moore, C. A., Haseloff, J., Tester, M. A. and Knight, M. R. (2000a). Cell-type-specific calcium responses to drought, salt and cold in the Arabidopsis root. *Plant Journal* **23**, 267-278.

Kiegle, E., Gilliham, M., Haselhoff, J. and Tester, M. (2000b). Hyperpolarisation-activated calcium currents found only in cells from the elongation zone of *Arabidopsis* thaliana roots. *Plant Journal* **21**, 225 - 229.

Kim, H. S. and Delaney, T. P. (2002). Arabidopsis SON1 is an F-Box protein that regulates a novel induced defense response independent of both salicylic acid and systemic acquired resistance. *The Plant Cell* **14**, 1469 - 1482.

Kim, S. O., Merchant, K., Nudelman, R., Beyer, W. F., Keng, T., DeAngelo, J., Hausladen, A. and Stamler, J. S. (2002). OxyR: A molecular code for redox-related signaling. *Cell* **109**, 383 - 396.

Kitajima, S., Koyama, T., Ohme-Takagi, M., Shinshi, H. and Sato, F. (2000). Characterization of gene expression of NsERFs, transcription factors of basic PR genes from *Nicotiana sylvestris*. *Plant Cell Physiol.* **41**, 817 - 824.

Kliebenstein, D. J., Monde, R. A. and Last, R. L. (1998). Superoxide dismutase in Arabidopsis: an eclectic enzyme family with disparate regulation and protein localization. *Plant Physiology* **118**, 637-50.

Knight, M. R., Campbell, A. K., Smith, S. M. and Trewavas, A. J. (1991). Transgenic plant aequorin reports the effects of touch and cold-shock and elicitors on cytosolic calcium. *Nature* **352**, 524 - 526.

Knight, H., Trewavas, A. J. and Knight, M. R. (1996). Cold calcium signaling in Arabidopsis involves two cellular pools and a change in calcium signature after acclimation. *The Plant Cell* **8**, 489 - 503.

Knight, H., Brandt, S. and Knight, M. R. (1998). A history of stress alters drought calcium signalling pathways in Arabidopsis. *Plant Journal* **16**, 681 - 687.

Koch, E. and Slusarenko, a. (1990). *Arabidopsis* is susceptible to infection by a downy mildew fungus. *The Plant Cell* **2**, 437 - 445.

Kovtun, Y., Chiu, W.-L., Tena, G. and Sheen, J. (2000). Functional analysis of oxidative stress-activated mitogen-activated protein kinase cascade in plants. *Proc Natl Acad Sci U S A* **97**, 2940 - 2945.

Krysan, P. J., Young, J. C. and Sussmann, M. R. (1999). T-DNA as an insertional mutagen in Arabidopsis. *The Plant Cell* **11**, 2283 - 2290.

Kuchitsu, K., Kosaka, H., Shiga, T. and Shibuya, N. (1995). EPR evidence for generation of hydroxyl radical triggered by N-acetylchitooligosaccharide elicitor and a protein phosphatase inhibitor in suspension-cultured rice cells. *Protoplasma* **188**, 138 - 142.

Kunkel, B. N. and Brooks, D. M. (2002). Cross talk between signaling pathways in pathogen defense. *Current Opinion in Plant Biology* **5**, 325 - 331.

Kurepa, J., Smalle, J., Van Montagu, M. and Inze, D. (1998). Oxidative stress tolerance and longevity in Arabidopsis: the late-flowering mutant gigantea is tolerant to paraquat. *Plant Journal* **14**, 759-64.

Kyriakis, J. M. and Avruch, J. (2001). Mammalian mitogen-activated protein kinase signal transduction pathways activated by stress and inflammation. *8Physiol. Rev.* **18**, 807 – 869.

Lamb, C. and Dixon, R. A. (1997). The oxidative burst in plant disease resistance. *Annual Review of Plant Physiology and Plant Molecular Biology* **48**, 251 - 275.

Laval, V., Chabannes, M., Carriere, M., Canut, H., Barre, A., Rouge, P., Pont-Lezica, R. and Galaud, J. P. (1999). A family of Arabidopsis plasma membrane receptors presenting animal beta-integrin domains. *Biochimica et Biophysica Acta-Protein Structure and Molecular Enzymology* **1435**, 61-70.

Lebel, E., Heifetz, P., Thorne, L., Uknes, S., Ryals, J. and Ward, E. (1998). Functional analysis of regulatory sequences controlling *PR-1* gene expression in *Arabidopsis*. *Plant Journal* **16**, 223 - 233.

Lecourieux, D., Marzars, C., Pauly, N., Ranjeva, R. and Pugin, A. (2002). Analysis and effects of cytosolic free calcium increase in response to elicitors in *Nicotiana plumbaginifolia* cells. *The Plant Cell* **14**, 2627 - 2641.

Levine, A., Tenhaken, R., Dixon, R. and Lamb, C. (1994). H_2O_2 from the oxidative burst orchestrates the plant hypersensitive disease resistance response. *Cell* **79**, 583 - 593.

Levine, A., Pennell, R. I., Alvarez, M. E., Palmer, R. and Lamb, C. (1996). Calcium-mediated apoptosis in a plant hypersensitive disease resistance response. *Current Biology* **6**, 427 - 437.

Lewis, B. D. and Spalding, E. P. (1998). Nonselective block by La^{3+} of *Arabidopsis* ion channels involved in signal transduction. *The Journal of Membrane Biology* **162**, 81 - 90.

Li, W.-H., Llopis, J., Whitney, M., Zlornak, G. and Tsien, R. Y. (1998). Cell-permeant caged $InsP_3$ ester shows that Ca^{2+} spike frequency can optimize gene expression. *Nature* **392**, 936 - 941.

Liu, Y. G., Mitsukawa, N., Oosumi, T. and Whittier, R. F. (1995). Efficient isolation and mapping of *Arabidopsis thaliana* T-DNA insert junctions by thermal asymmetric interlaced PCR. *Plant Journal* **8**, 457 - 463.

Lu, S. X. and Hrabak, E. M. (2002). An Arabidopsis calcium-dependent protein kinase is associated with the endoplasmic reticulum. *Plant Physiology* **128**, 1008 - 1021.

Mackerness, S. A. H., John, C. F., Jordan, B. and Thomas, B. (2001). Early signaling components in ultraviolet-B responses: distinct roles for different reactive oxygen species and nitric oxide. *FEBS Letters* **489**, 237-242.

Madhani, H. D. and Fink, G. R. (1998). The riddle of MAP kinase signaling specificity. *Trends in Genetics* **14**, 151 - 155.

Maleck, K., Levine, A., Eulgem, T., Morgan, A., Schmid, J., Lawton, K. A., Dangl, J. L. and Dietrich, R. A. (2001). The transcriptome of *Arabidopsis thaliana* during systemic acquired resistance. *Nature Genetics* **26**, 403 - 410.

Malhó, R., Moutinho, A., Van der Luit, A. and Trewavas, A. J. (1998). Spatial characteristics of calcium signalling: the calcium wave as a basic unit in plant cell signalling. *Phil. Trans. R. Soc. Lond. B* **353**, 1463 - 1473.

Marrs, K. (1996). The functions and regulation of glutathione S-transferases in plants. *Annual Review of Plant Physiology and Plant Molecular Biology* **47**, 127 - 158.

Martin, M. L. and Busconi, L. (2000). Membrane localization of a rice calcium-dependent protein kinase (CDPK) is mediated by myristoylation and palmitoylation. *Plant Journal* **24**, 429 - 435.

May, M. and Leaver, C. J. (1993). Oxidative stimulation of glutathione synthesis in *Arabidopsis thaliana* suspension-cultures. *Plant Physiology* **103**, 621 - 627.

McAinsh, M. R., Clayton, H., Mansfield, T. A. and Hetherington, A. M. (1996). Changes in stomatal behaviour and guard cell cytosolic free calcium in response to oxidative stress. *Plant Physiology* **111**, 1031 - 1042.

McAinsh, M. R. and Hetherington, A. M. (1998). Encoding specificity in Ca^{2+} signalling systems. *Trends in Plant Science* **3**, 32 - 36.

McCormick, M. L., Denning, G. M., Reszka, K. J., Bilski, P., Buettners, G. R., Rasmussen, G. T., Railsback, M. A. and Britigan, B. E. (2000). Biological effects of menadione phytochemistry:effects of menadione on biological systmes may not involve classical oxidant production. *Biochem. J.* **350**, 797 - 804.

McKersie, B. D. (1996). http://www.agronomy.psu.edu/Courses/AGRO518/Oxygen.htm

McLusky, S. R., Bennett, M. H., Beale, M. H., Lewis, M. J., Gaskin, P. and Mansfield, J. W. (1999). Cell wall alterations and localized accumulation of feruloyl-3'-methoxytyramine in onion epidermis at sites of attempted penetration by *Botrytis allii* are associated with actin polarization, peroxidase activity and suppression of flavonoid biosynthesis. *Plant Journal* **17**, 523 - 534.

Meinhard, M. and Grill, E. (2001). Hydrogen peroxide is a regulator of ABI1, a protein phosphatase 2C from Arabidopsis. *FEBS Letters* **508**, 443 - 446.

Meinhard, M., Rodriguez, P. L. and Grill, E. (2002). The sensitivity of ABI2 to hydrogen peroxide links the abscisic acid-response regulator to redox signalling. *Planta* **214**, 775 - 782.

Mellersh, D. G. and Heath, M. C. (2001). Plasma membrane-cell wall adhesion is required for expression of plant defense responses during fungal penetration. *The Plant Cell* **13**, 413-424.

Mellersh, D. G., Foulds, I. V., Higgins, V. J. and Heath, M. C. (2002). H_2O_2 plays different roles in determining penetration failure in three diverse plant-fungal interactions. *Plant Journal* **29**, 257-268.

Menkens, A. E., Schindler, U. and Cashmore, A. R. (1995). The G-box: a ubiquitous regulatory DNA element in plants bound by the GBF family of bZIP proteins. *Trends in Biochemical Sciences* **20**, 509 - 510.

Michaels, S. D. and Amasino, R. M. (2000). Memories of winter: vernalization and the competence to flower. *Plant, Cell and Environment* **23**, 1145 - 1153.

Miles, G. P., Samuel, M. A. and Ellis, B. E. (2002). Suramin inhibits oxidative signalling in tobacco suspension-cultured cells. *Plant, Cell and Environment* **25**, 521 -527.

Mirabelli, F., Salis, A., Vairetti, M., Bellomo, G., Thor, H. and Orrenius, S. (1989). Cytoskeletal alterations in human platelets exposed to oxidative stress are mediated by oxidative and Ca^{2+}-dependent mechansims. *Arch Biochem Biophys* **270**, 478 - 488.

Mittler, R., Feng, X. and Cohen, M. (1998). Post-transcriptional suppression of cytosolic ascorbate peroxidase expression during pathogen-induced programmed cell death in tobacco. *The Plant Cell* **10**, 461 - 473.

Mittler, R. (2002). Oxidative stress, antioxidants and stress tolerance. *Trends in Plant Science* **7**, 405 - 410.

Miura, Y., Yoshioka, H. and Doke, N. (1995). An autophotographic determination of the active oxygen generation in potato tuber discs during hypersensitive response to fungal elicitor. *Plant Science* **105**, 45 - 52.

Moller, I. M. (2001). Plant mitochondria and oxidative stress: Electron transport, NADPH turnover, and metabolism of reactive oxygen species. *Annual Review of Plant Physiol and Plant Mol Biol* **52**, 561 - 591.

Moon, H., Lee, B., Choi, G., Shin, D., Prasad, D. T., Lee, O., Kwak, S.-S., Kim, D. H., Nam, J., Bahk, J. et al. (2003). NDP kinase 2 interacts with two oxidative stress-activated MAPKs to regulate cellular redox state and enhances multiple stress tolerance in transgenic plants. *Proc Natl Acad Sci U S A* **100**, 358 - 363.

Morita, S., Kaminaka, H., Masumura, T. and Tanaka, K. (1999). Induction of rice cytosolic ascorbate peroxidase mRNA by oxidative stress; the involvement of hydrogen peroxide in oxidative stress signalling. *Plant and Cell Physiology* **40**, 417 - 422.

Mustilli, A.-C., Merlot, S., Vavasseur, A., Fenzi, F. and Giraudat, J. (2002). Arabidopsis OST1 protein kinase mediates the regulation of stomatal aperture by abscisic acid and acts upstream of reactive oxygen species production. *The Plant Cell* **14**, 3089 - 3099.

Nagpal, P. and Quatrano, R. S. (1999). Isolation and characterization of a cDNA clone from Arabidopsis thaliana with partial sequence similarity to integrins. *Gene* **230**, 33-40.

Navrath, C. and Métraux, J.-P. (1999). Salicylic acid induction-deficient mutants of *Arabidopsis* express *PR-2* and *PR-5* and accumulate high levels of camalexin after pathogen inoculation. *The Plant Cell* **11**, 1393 - 1404.

Neill, S. J., Desikan, R. and Hancock, J. T. (2002). Hydrogen peroxide signalling. *Current Opinion in Plant Biology* **5**, 388 - 395.

Neuenschwander, U., Vernooij, B., Friedrich, L., Uknes, S., Kessmann, H. and Ryals, J. (1995). Is hydrogen peroxide a second messenger of salicylic acid in systemic acquired resistance? *Plant Journal* **8**, 227 - 233.

Nimchuck, Z., Rohmer, L., Chang, J. H. and Dangl, J. L. (2001). Knowing the dancer from the dance: *R*-gene products and their interactions with other proteins from host and pathogen. *Current Opinion in Plant Biology* **4**, 288 - 294.

Noctor, G. and Foyer, C. H. (1998). Ascorbate and glutathione: Keeping active oxygen under control. *Annual Review of Plant Physiology and Plant Molecular Biology* **49**, 249-279.

Nuehse, T. S., Peck, S. C., Hirt, H. and Boller, T. (2000). Microbial elicitors induce activation and dual phosphorylation of the Arabidopsis thaliana MAPK 6. *The Journal of Biological Chemistry* **11**, 7521 - 7526.

Nürnberger, T. and Brunner, F. (2002). Innate immunity in plants and animals: emerging parallels between the recognition of general elicitors and pathogen-associated molecular patterns. *Current Opinion in Plant Biology* **5**, 1 - 7.

Nürnberger, T. and Scheel, D. (2001). Signal transmission in the plant immune response. *Trends in Plant Science* **6**, 372 - 379.

Ogawa, K., Tasaka, Y., Mino, M., Tanaka, Y. and Iwabuchi, M. (2001). Association of glutathione with flowering in Arabidopsis thaliana. *Plant Cell Physiol* **42**, 524-30.

Ohme-Takagi, M. and Shinshi, H. (1990). Structure and expression of a tobacco ß-1,3-glucanase gene. *Plant Mol Biol* **15**, 941 - 946.

Ohme-Takagi, M. and Shinshi, H. (1995). Ethylene-inducible DNA binding proteins that interact with an ethylene-responsive element. *The Plant Cell* **7**, 173 - 183.

Ohta, M., Ohme-Takagi, M. and Shinshi, H. (2000). Three ethylene-responsive transcription factors in tobacco with distinct transactivation functions. *Plant Journal* **22**, 29 - 38.

Onate-Sánchez, L. and Singh, K. B. (2002). Identification of Arabidopsis ethylene-responsive element binding factors with distinct induction kinetics after pathogen infection. *Plant Physiology* **128**, 1313 - 1322.

O'Rourke, S. M., Herskowitz, I. and O'Shea, E. K. (2002). Yeast go the whole HOG for the hyperosmotic response. *Trends in Genetics* **18**, 405 - 412.

Orozco-Cadenas, M. and Ryan, C. A. (1999). Hydrogen peroxide is generated systemically in plant leaves by wounding and systemin via the octadecanoid pathway. *Proc Natl Acad Sci U S A* **96**, 6553 - 6557.

Orozco-Cardenas, M. L., Narvaez-Vasquez, J. and Ryan, C. A. (2001). Hydrogen peroxide acts as a second messenger fo the induction of defense genes in tomato plants in response to wounding, systemin, and methyl jasmonate. *The Plant Cell* **13**, 179 - 191.

Osterlund, M. T., Hardtke, C. S., Wei, N. and Deng, X. W. (2000). Targeted destabilization of HY5 during light-regulated development of *Arabidopsis*. *Nature* **405**, 462 - 466.

Overmyer, K., Tuominen, H., Kettunen, R., Betz, C., Langebartels, C., Sandermann, H. J. and Kangasjärvi, J. (2000). Ozone-sensitive Arabidopsis rcd1 mutant reveals opposite roles for ethylene and jasmonate signaling pathways in regulating superoxide-dependent cell death. *The Plant Cell* **12**, 1849 - 1862.

Oyama, T., Shimura, Y. and Okada, K. (2002). The *IRE* gene encodes a protein kinase homologue and modulates root hair growth in *Arabidopsis*. *Plant Journal* **30**, 289 - 299.

Papadakis, A. K. and Roubelakis-Angelakis, K. A. (1999). The generation of active oxygen species differs in tobacco and grapevine mesophyll protoplasts. *Plant Physiology* **121**, 197-205.

Parchmann, S., Gundlach, H. and Mueller, M. J. (1997). Induction of 12-oxo-phytodienoic acid in wounded plants and elicited plant cell cultures. *Plant Physiology* **115**, 1057-1064.

Parker, J. E., Holub, E. B., Frost, L. N., Falk, A. and Gunn, N. D. (1996). Characterization of *eds1*, a mutation in *Arabidiopsis* suppressing resistance to *Peronospora parasitica* specified by several different *RPP* genes. *The Plant Cell* **8**, 2033 - 2046.

Pasqualini, S., Batini, P., Ederli, L., Porceddu, A., Piccioni, C., De Marchis, F. and Antonielli, M. (2001). Effects of short-term ozone fumigation on tobacco plants:

response of the scavenging system and expression of the glutathione reductase. *Plant, Cell and Environment* **24**, 245-252.

Peck, S. C., Nuehse, T., S., Hess, D., Iglesias, A., Meins, F. and Boller, T. (2001). Directed proteomics identifies a plant-specific protein rapidly phophorylated in response to bacterial and fungal elicitors. *The Plant Cell* **13**, 1467 - 1475.

Pei, Z.-M., Murata, Y., Benning, G., Thomine, S., Klusener, B., Allen, G. J., Grill, E. and Schroeder, J. I. (2000). Calcium channels activated by hydrogen peroxide mediate abscisic acid signalling in guard cells. *Nature* **406**, 731 - 734.

Pell, E. J., Schlagnhaufer, C. D. and Arteca, R. N. (1997). Ozone-induced oxidative stress: mechanisms of action and reaction. *Physiologia Plantarum* **100**, 264 - 273.

Pellinen, R., Palva, T. and Kangasjarvi, J. (1999). Short communication: subcellular localization of ozone-induced hydrogen peroxide production in birch (Betula pendula) leaf cells. *Plant Journal* **20**, 349-56.

Peng, M. and Kuc, J. (1992). Peroxidase-generated hydrogen peroxide as a source of anti-fungal activity *in vitro* and on tobacco leaf disks. *Phytopathology* **82**, 696 - 699.

Petersen, M., Brodersen, P., Naested, H., Andreasson, E., Lindhart, U., Johansen, B., Nielsen, H. B., Lacy, M., Austin, M. J., Parker, J. E. et al. (2000). Arabidopsis map kinase 4 negatively regulates systemic acquired resistance. *Cell* **103**, 1111-20.

Piedras, P., Hammond-Kosack, K. E., Harrison, K. and Jones, J. D. G. (1998). Rapid, Cf-9- and Avr9-dependent production of active oxygen species in tobacco suspension cultures. *Molecular Plant - Microbe Interactions* **11**, 1155 - 1166.

Pieterse, C. M. J. and van Loon, L. C. (1999). Salicylic acid-independent plant defence pathways. *Trends in Plant Science* **4**, 52 - 58.

Pietrzak, M., Shillito, R. D., Hohn, T. and Potrykus, I. (1986). Expression in plants of two bacterial antibiotic-resistance genes after protoplast transformation with a new plant expression vector. *Nucleic Acids Res* **14**, 5857 - 5868.

Pitts, R. J., Cernac, A. and Estelle, M. (1998). Auxin and ethylene promote root hair elongation in *Arabidopsis*. *Plant Journal* **16**, 553 - 560.

Poovaiah, B. W. and Reddy, A. S. N. (1993). Calcium and Signal Transduction in Plants. *Critical Reviews in Plant Sciences* **12**, 185 - 211.

Prasad, T. K., Anderson, M. D., Martin, B. A. and Stewart, C. R. (1994). Evidence for chilling-induced oxidative stress in maize seedlings and a regulatory role for hydrogen peroxide. *The Plant Cell* **6**, 65 - 74.

Price, A. H., Taylor, A., Ripley, S. J., Griffiths, A., Trewavas, A. J. and Knight, M. R. (1994). Oxidative signals in tobacco increase cytosolic calcium. *The Plant Cell* **6**, 1301 - 1310.

Rajasekhar, V. K., Lamb, C. and Dixon, R. A. (1999). Early events in the signal pathway for the oxidative burst in soybean cells exposed to avirulent *Pseudomonas syringae* pv *glycinea*. *Plant Physiology* **120**, 1137 - 1146.

Rao, M. V., Gopinadhan, P. and Ormrod, D. P. (1996). Ultraviolet-B- and ozone-induced biochemical changes in antioxidant enzymes of *Arabidopsis thaliana*. *Plant Physiology* **110**, 135 - 136.

Rao, M. V., Koch, J. R. and Davis, K. R. (2000). Ozone: a tool for probing programmed cell death in plants. *Plant Molecular Biology* **44**, 345 - 358.

Ren, D., Yang, H. and Zhang, S. (2002). Cell death mediated by MAPK is associated with hydrogen peroxide production in *Arabidopsis*. *The Journal of Biological Chemistry* **277**, 559 - 565.

Reuber, T. L., Plotnikova, J. M., Dewdney, J., Roger, E. E., Wood, W. and Ausubel, F. M. (1998). Correlation of defense gene induction defects with powdery mildew susceptibility in *Arabidopsis* enhanced disease susceptibility mutants. *Plant Journal* **16**, 473 - 485.

Reymond, P. and Farmer, E. E. (1998). Jasmonate and salicylate as global signals for defense gene expression. *Current Opinion in Plant Biology* **1**, 404 - 411.

Reymond, P., Weber, H., Damond, M. and Farmer, E. E. (2000). Differential gene expression in response to mechanical wounding and insect feeding in *Arabidopsis*. *The Plant Cell* **12**, 707-20.

Riechmann, J. L., Heard, J., Martin, G., Reuber, L., Jiang, C., Keddie, J., Adam, L., Pineda, O., Ratcliffe, O., Samaha, R. et al. (2000). *Arabidopsis* transcription factors: Genome-wide comparative analysis among eukaryotes. *Science* **290**, 2105 - 2110.

Riechmann, J. L. and Ratcliffe, O. J. (2000). A genomic perspective on plant transcription factors. *Current Opinion in Plant Biology* **3**, 423 - 434.

Romeis, T., Piedras, P., Zhang, S. Q., Klessig, D. F., Hirt, H. and Jones, J. D. G. (1999). Rapid Avr9- and Cf-9-dependent activation of MAP kinases in tobacco cell cultures and leaves: Convergence of resistance gene, elicitor, wound, and salicylate responses. *The Plant Cell* **12**, 803 - 816.

Romeis, T., Piedras, P. and Jones, J. D. G. (2000). Resistance gene-dependent activation of a calcium-dependent protein kinase in the plant defense response. *The Plant Cell* **12**, 803 - 816.

Rouse, D. T., Sheldon, C. C., Bagnall, D. J., Peacock, J. W. and Dennis, E. S. (2002). FLC, a repressor of flowering, is regulated by genes in different inductive pathways. *Plant Journal* **29**, 183 - 191.

Rushton, P. J., Torres, J. T., Parniske, M., Wernert, P., Hahlbrock, K. and Somssich, I. E. (1996). Interaction of elicitor-induced DNA-binding proteins with elicitor response elements in the promoters of parsley *PR1* genes. *The EMBO Journal* **15**, 5690 - 5700.

Rushton, P. J., Reinstädler, A., Lipka, V., Lippok, B. and Somssich, I. E. (2002). Synthetic plant promoters containing defined regulatory elements provide novel insights into pathogen- and wound-induced signaling. *The Plant Cell* **14**, 749 - 762.

Ryan, C. A. (2000). The systemin signaling pathway: differential activation of plant defensive genes. *Biochim Biophys Acta* **1477**, 112-21.

Sagi, M. and Fluhr, R. (2001). Superoxide production by plant homologues of the $gp91^{phox}$ NADPH oxidase. Modulation of activity by calcium and by tobacco mosaic virus infection. *Plant Physiology* **126**, 1281 - 1290.

Samaj, J., Ovecka, M., Hlavacka, A., Lecourieux, F., Meskiene, I., Lichtscheidl, I., Lenart, P., Salaj, J., Volkmann, D., Bögre, L. et al. (2002). Involvement of the mitogen-activated protein kinase SIMK in regulation of root hair tip growth. *The EMBO Journal* **21**, 3296 - 3306.

Sambrook, J. and Russell, D. W. (2001). Molecular Cloning, A Laboratory Manual. Cold Spring Harbor, USA: Cold Spring Harbor Laboratory Press.

Samuel, M. A., Miles, G. P. and Ellis, B. E. (2000). Ozone treatment rapidly activates MAP kinase signalling in plants. *The Plant Journal* **22**, 367 - 376.

Samuel, M. A. and Ellis, B. E. (2002). Double jeopardy: both overexpression and suppression of a redox-activated plant mitogen-activated protein kinase render tobacco plants ozone sensitive. *The Plant Cell* **14**, 2059 - 2069.

Sanders, D., Brownlee, C. and Harper, J. F. (1999). Communicating **with** calcium. *The Plant Cell* **11**, 691 - 706.

Sanders, D., Pelloux, J., Brownlee, C. and Harper, J. F. (2002). Calcium at the crossroads of signalling. *The Plant Cell* **Supplement 2002**, S401 - S417.

Satterlee, J. S. and Sussman, M. R. (1998). Unusual membrane-associated protein kinases in higher plants. *The Journal of Membrane Biology* **164**, 205 - 213.

Schoonbroodt, S. and Piette, J. (2000). Oxidative stress interference with the nuclear factor-kappa B activation pathways. *Biochemical Pharmacology* **60**, 1075 - 1083.

Segal, A. W. and Abo, A. (1993). The biochemical basis of the NADPH oxidase of phagocytes. *Trends in Biochemical Sciences* **18**, 43 - 47.

Seo, S., Okamoto, M., Seto, H., Ishizuka, K., Sano, H. and Ohashi, Y. (1995). Tobacco MAP kinase: a possible mediator in wound signal transduction pathways. *Science* **270**, 1988-92.

Seo, S., Sano, H. and Ohashi, Y. (1999). Jasmonate-based wound signal transduction requires activation of WIPK, a tobacco mitogen-activated protein kinase. *The Plant Cell* **11**, 289-98.

Sharma, Y. K. and Davis, K. R. (1994). Ozone-induced expression of stress-related genes in *Arabidopsis thaliana*. *Plant Physiology* **105**, 1089 - 1096.

Sheen, J. (1996). Ca^{2+}-dependent protein kinases and stress signal transduction in plants. *Science* **274**, 1900 - 1902.

Shirasu, K., Nakajima, H., Rajasekhar, V. K., Dixon, R. A. and Lamb, C. (1997). Salicylic acid potentiates an agonist-dependent gain control that amplifies pathogen signals in the activation of defense mechansims. *The Plant Cell* **9**, 261 - 270.

Singh, K. B., Foley, R. C. and Onate-Sánchez, L. (2002). Transcription factors in plant defense and stress responses. *Current Opinion in Plant Biology* **5**, 430 - 436.

Smirnoff, N. (1995). Antioxidant systems and plant response to the environment. In *Environment and plant metabolism: flexibility and acclimation*, (ed. N. Smirnoff), pp. 217 - 243. Oxford: Bios Scientific.

Snedden, W. A. and Fromm, H. (2001). Calmodulin as a versatile calcium signal transducer in plants. *New Phytologist* **151**, 35 - 66.

Solano, R., Stepanova, A., Chao, Q. and Ecker, J. R. (1998). Nuclear events in ethylene signalling: a transcriptional cascade mediated by ETHYLENE-INSENSITIVE3 and ETHYLENE-RESPONSE-FACTOR1. *Genes & Development* **12**, 3703 - 3714.

Staswick, P. E., Su, W. and Howell, S. H. (1992). Methyl jasmonate inhibition of root growth and induction of a leaf protein are decreased in an Arabidopsis thaliana mutant. *Proc Natl Acad Sci U S A* **89**, 6837-40.

Storozhenko, S., De Pauw, P., Van Montagu, M., Inzé, D. and Kushnir, S. (1998). The heat-shock element is a functional component of the Arabidopsis APX1 gene promoter. *Plant Physiology* **118**, 1005 - 1014.

Sundarasan, M., Yu, Z., Ferrans, V., Irani, K. and Finkel, T. (1995). Requirement for generation of H_2O_2 for platelet-derived growth factor signal transduction. *Science* **270**, 296 - 299.

Surplus, S. L., Jordan, B. R., Murphy, A. M., Carr, J. P., Thomas, B. and Mackerness, S. A. H. (1998). Ultraviolet-B-induced responses in Arabidopsis thaliana: role of salicylic acid and reactive oxygen species in the regulation of transcripts encoding photosynthetic and acidic pathogenesis- related proteins. *Plant Cell and Environment* **21**, 685-694.

Suzuki, Y. J., Forman, H. J. and Sevanian, A. (1997). Oxidants as stimulators of signal transduction. *Free Radical Biology & Medicine* **22**, 269 - 285.

Sweetlove, L. J., Heazlewood, J. L., Herald, V., Holtzapffel, R., Day, D. A., Leaver, C. J. and Millar, A. H. (2002). The impact of oxidative stress on *Arabidopsis* mitochondria. *Plant Journal* **32**, 891 - 904.

Tenhaken, R., Levine, A., Brisson, L. F., Dixon, R. A. and Lamb, C. (1995). Function of the oxidative burst in hypersensitive disease resistance. *Proc Natl Acad Sci U S A* **92**, 4158 - 4163.

Terras, F. R. G., Schoofs, H. M. E., Thevissen, K., Osborn, R. W., Vanderleyden, J., Cammue, B. P. A. and Broekaert, W. F. (1993). Synergistic enhancement of the antifungal activity of wheat and barley thionins by radish and oilseed rape 2S albumins and by barley trypsin inhibitors. *Plant Physiology* **103**, 1311 - 1319.

Tester, M. and MacRobbie, E. A. C. (1990). Cytoplasmic calcium affects the gating of potassium channels in the plasma membrane of *Chara corallina*: a whole-cell study using calcium-channel effectors. *Planta* **180**, 569 - 581.

Thara, V. K., Tang, X., Gu, Y. Q., Martin, G. B. and Zhou, J.-M. (1999). Pseudomonas syringae pv tomato induces the expression of tomato EREBP-like genes Pti4 and Pti5 independent of ethylene, salicylate and jasmonate. *Plant Journal* **20**, 475 – 483.

Thomma, B., Eggermont, K., Penninckx, I., Mauch-Mani, B., Vogelsang, R., Cammue, B. P. A. and Broekaert, W. F. (1998). Separate jasmonate-dependent and salicylate-dependent defense- response pathways in Arabidopsis are essential for resistance to distinct microbial pathogens. *Proc Natl Acad Sci U S A* **95**, 15107-15111.

Thomma, B. P., Penninckx, I. A., Broekaert, W. F. and Cammue, B. P. (2001a). The complexity of disease signaling in Arabidopsis. *Curr Opin Immunol* **13**, 63-68.

Thomma, B. P. H. J., Tierens, K. F. M., Penninckx, I. A. M. A., Mauch-Mani, B., Broekaert, W. F. and Cammue, B. P. A. (2001b). Different micro-organisms differentially induce *Arabidopsis* disease response pathways. *Plant Physiol Biochem* **39**, 673 - 680.

Thor, H., Smith, M. T., Hartzell, P., Bellomo, G., Jewell, S. A. and Orrenius, S. (1982). The metabolism of menadione (2-methyl-1,4-naphthoquinone) by isolated hepatocytes. *The Journal of Biological Chemistry* **25**, 12419 - 12425.

Tiwari, B. S., Belenghi, B. and Levine, A. (2002). Oxidative stress increased respiration and generation of reactive oxygen species, resulting in ATP depletion, opening of mitochondrial permeability transition, and programmed cell death. *Plant Physiology* **128**, 1271 - 1281.

Toone, M. W. and Jones, N. (1998). Stress-activated signalling pathways in yeast. *Genes to Cells* **3**, 485 - 498.

Torres, M. A., Dangl, J. L. and Jones, J. D. (2002). *Arabidopsis* gp91phox homologues AtrbohD and AtrbohF are required for accumulation of reactive oxygen intermediates in the plant defense response. *Proc Natl Acad Sci U S A* **99**, 517-22.

Trost, P., Foscarini, S., Preger, V., Bonara, P., Vitale, L. and Pupillo, P. (1997). Dissecting the diphenylene iodonium-sensitive NAD(P)H:Quinone oxidoreductase of zucchini plasma membrane. *Plant Physiology* **114**, 737 - 746.

Tsien, R. Y. (1980). New calcium indicators and buffers with high selectivity against magnesium and protons: Design, synthesis and properties of prototype structures. *Biochemistry* **19**, 2396 - 2404.

Turner, J. G., Ellis, C. and Devoto, A. (2002). The jasmonate signal pathway. *The Plant Cell* **14**, S153-64.

Uchida, A., Jagendorf, A. T., Hibino, T., Takabe, T. and Takabe, T. (2002). Effects of hydrogen peroxide and nitric oxide on both salt and heat stress tolerance in rice. *Plant Science* **163**, 515 - 523.

Usami, S., Banno, H., Ito, Y., Nishihama, R. and Machida, Y. (1995). Cutting activates a 46-kilodalton protein kinase in plants. *Proc Natl Acad Sci U S A* **92**, 8660-4.

Vallelian-Bindschedler, L., Schweizer, P., Mosinger, E. and Metraux, J.-P. (1998). Heat induced resistance in barley to powdery mildew (*Blumeria graminins* f. sp. *hordei*) is associated with a burst of AOS. *Physiol Mol Plant Pathol* **52**, 185 - 199.

Vener, A., Ohad, I. and Anderson, B. (1998). Protein phosphorylation and redox sensing in chloroplast thylakoids. *Current Opinion in Plant Biology* **1**, 217 - 223.

Very, A.-A. and Davies, J. M. (2000). Hyperpolarization-activated calcium channels at the tip of Arabidopsis root hairs. *Proc Natl Acad Sci U S A* **97**, 9801 - 9806.

Vranová, E., Inzé, D. and Van Breusegem, F. (2002). Signal transduction during oxidative stress. *Journal of Experimental Botany* **53**, 1227 - 1236.

Wang, K. L.-C., Li, H. and Ecker, J. R. (2002). Ethylene biosynthesis and signaling networks. *The Plant Cell* **Supplement 2002**, S131 - S151.

Wohlgemut, H., Mittlestrass, K., Kschieschan, S., Bender, J., Weigel, H.-J., Overmyer, K., Kangasjärvi, J., Sandermann, H. J. and Langebartels, C. (2002). Activation of an oxidative burst is a general feature of sensitive plants exposed to the air pollutant ozone. *Plant, Cell and Environment* **25**, 717 - 726.

Wojtaszek, P. (1997). Oxidative burst: an early plant response to pathogen infection. *Biochemical Journal* **322**, 681 - 692.

Wu, G. S., Short, B. J., Lawrence, E. B., Levine, E. B., Fitzsimmons, K. C. and Shah, D. M. (1995). Disease resistance conferred by expression of a gene encoding H_2O_2-generating glucose oxidase in transgenic potato plants. *The Plant Cell* **7**, 1357 - 1368.

Wymer, C. L., Bibikova, t. N. and Gilroy, S. (1997). Cytoplasmic free calcium distributions during the evelopment of root hairs of *Arabidopsis thaliana*. *Plant Journal* **12**, 427 - 439.

Xie, D. X., Feys, B. F., James, S., Nieto-Rostro, M. and Turner, J. G. (1998). COI1: an Arabidopsis gene required for jasmonate-regulated defense and fertility. *Science* **280**, 1091-1094.

Xu, H. and Heath, M. C. (1998). Role of calcium in signal transduction during the hypersensitive response caused by basidiospore-derived infection of the cowpea rust fungus. *The Plant Cell* **10**, 585-598.

Yahraus, T., Chandra, S., Legendre, L. and Low, P. S. (1995). Evidence for a mechanically induced oxidative burst. *Plant Physiology* **109**, 1259 - 1266.

Yang, P., Chen, C., Wang, Z., Fan, B. and Chen, Z. (1999). A pathogen- and salicylic acid-induced WRKY DNA-binding activity recognizes the elicitor response element of the tobacco class I chitinase gene promoter. *Plant Journal* **18**, 141 - 149.

Yang, K. Y., Liu, Y. and Zhang, S. Q. (2001). Activation of a mitogen-activated protein kinase pathway is involved in disease resistance in tobacco. *Proc Natl Acad Sci U S A* **98**, 741 - 746.

Yu, D., Chen, C. and Chen, Z. (2001). Evidence for an important role in WRKY DNA binding proteins in the regulation of NPR1 gene expression. *The Plant Cell* **13**, 1527 - 1540.

Yuasa, T., Ichimura, K., Mizoguchi, T. and Shinozaki, K. (2001). Oxidative stress activates ATMPK6, an Arabidopsis homologue of MAP kinase. *Plant Cell Physiol* **42**, 1012-6.

Zhang, S. and Klessig, D. F. (1998a). The tobacco wounding-activated mitogen-activated protein kinase is encoded by SIPK. *Proc Natl Acad Sci U S A* **95**, 7225 - 7230.

Zhang, S. Q. and Klessig, D. F. (1998b). Resistance gene *N*-mediated de novo synthesis and activation of a tobacco mitogen-activated protein kinase by tobacco mosaic virus infection. *Proc Natl Acad Sci U S A* **95**, 7433 - 7438.

Zhang, S. Q., Du, H. and Klessig, D. F. (1998). Activation of the tobacco SIP kinase by both a cell wall-derived carbohydrate elicitor and purified proteinaceous elicitins from *Phytophthora* spp. *The Plant Cell* **10**, 435 - 449.

Zhang, S. Q. and Liu, Y. (2001). Activation of salicylic acid-induced protein kinase, a mitogen-activated protein kinase, induces multiple defense responses in tobacco. *The Plant Cell* **13**, 1877 – 1889.

Zheng, M. and Storz, G. (2000). Redox sensing by prokaryotic transcription factors. ***Biochemical Pharmacology*** **59**, 1 - 6.

Zhenzhen, Y., Rodriguez, R., Tran, A., Hoang, H., de los Santos, D., Brown, S. and Vellanoweth, R. L. (2000). The developmental transition to flowering represses ascorbate peroxidase activity and induces enzymatic lipid peroxidation in leaf tissue in *Arabidopsis thaliana*. *Plant Science* **158**, 115 – 127.

Zhong, H. H. and McClung, C. R. (1996). The circadian clock gates expression of two *Arabidopsis* catalase genes to distinct and opposite circadian phases. *Molecular & General Genetics* **251**, 196 – 203.

Zhou, N., Tootle, T. L., Tsui, F., Klessig, D. F. and Glazebrook, J. (1998). *PAD4* functions upstream from salicylic acid to control defense responses in *Arabidopsis*. *The Plant Cell* **10**, 1021 - 1030.

Zimmermann, S., Nurnberger, T., Frachisse, J.-M., Wirtz, W., Guern, J., Hedrich, R. and Scheel, D. (1997). Receptor-mediated activation of a plant Ca^{2+}-permeable ion channel involved in pathogen defense. *Proc Natl Acad Sci U S A* **94**, 2751 - 2755.

Zuo, J., Niu, Q. W. and Chua, N. H. (2000). Technical advance: An estrogen receptor-based transactivator XVE mediates highly inducible gene expression in transgenic plants. *Plant Journal* **24**, 265-73.

Appendix A:

Isolation of a "knock-out" *Arabidopsis* mutant line for *OX1*

In order to directly monitor the effect of a deficiency in *OX1*, several collections of "knock-out" populations were screened for a null mutation in this gene. In *A. thaliana*, insertional mutagenesis is a means of disrupting gene function and is based on the insertion of foreign DNA into the gene of interest. This involves the use of either transposable elements or T-DNA which are sufficiently large (5 to 25 kb) to render the gene they insert into non-functional (Krysan *et al.*, 1999). The foreign DNA can then be used as a marker for subsequent identification of the mutation. Screening of the SALK T-DNA insertion lines (by BLAST search) and SLAT transposon insertion lines by hybridisation of *OX1* probe to SLAT line PCR product filters did not show any insertions in the *OX1* gene (data not shown). However, lines with an insertion close to or within the *OX1* coding region were identified in the Wisconsin knock-out facility population, made up of 60,480 individual lines at the time.

A.1 Screening the Wisconsin knock-out collection for insertions in *OX1*

In round 1 of this screen, two reactions for each of the 30 DNA super pools (containing 2025 lines) were performed by the Wisconsin facility using primers either 2150 bp 5' or 1160 bp 3' of *OX1* against a left border T-DNA primer (Figure A.1). To detect the presence of PCR product in any of the super pools, the DNA was electrophoresed on agarose gels, Southern blotted and hybridised with *OX1* probe (Figure A.2). DNA from the six pools with a signal was amplified by PCR and mapped by sequencing and a BLAST search (Altschul *et al.*, 1974). Two of the

insertions were ~ 1500 bp and ~ 1200 bp upstream of the predicted start codon whereas three insertions were located ~ 1000 bp, ~ 3000 bp and ~ 3800 bp downstream of the predicted stop codon. One insertion (super pool 1) had occurred within the coding sequence, 93 bp downstream of the predicted ATG, thus disrupting the gene between the first and second conserved kinase domains (see Figure 4.3).

In round 2 of the screen, PCR reactions for each of the nine DNA pools (containing 225 lines) in super pool 1 was performed at the Knock-out facility. Electrophoresis on an agarose gel showed that a single band of the expected size was present in pool 3. Identity of this band was confirmed by direct sequencing of the PCR product in both directions.

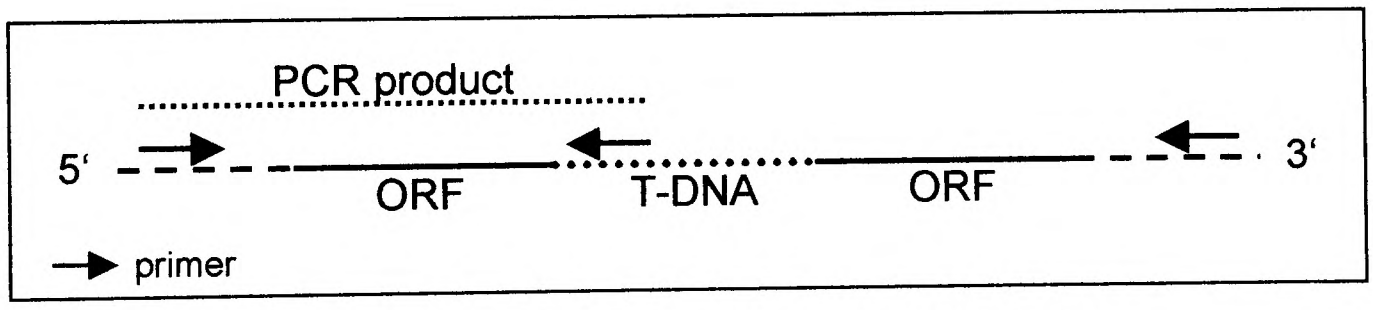

Figure A.1: Identification of a T-DNA knock-out line by PCR screening
PCR product using gene specific primers and a primer within the left border of the T-DNA reveals the presence of an insertion within the gene of interest.

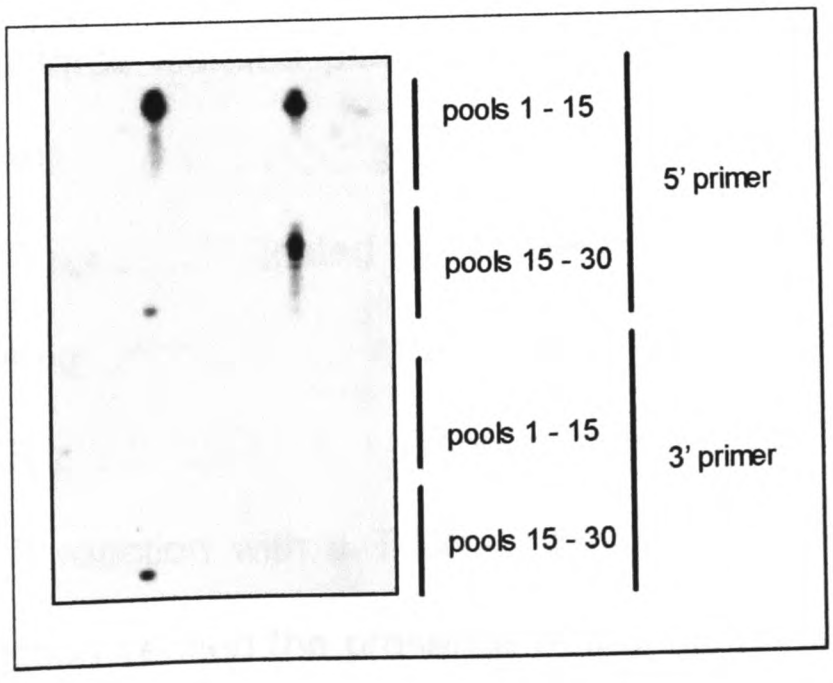

Figure A.2: Detection of a superpool containing an insertion in or near *OX1*
Southern analysis from PCR product was carried out as described in Methods. ^{32}P-labelled *OX1* probe was used to detect PCR product containing all or part of the *OX1* gene. Six pools were identified and analysed further.

A.2 Identification of plants containing the T-DNA insertion

Each DNA pool consists of 25 seed pools with 9 parent plants each. Seedlings for each seed pool were grown up on agar plates, genomic DNA extracted and used as template for PCR reactions with T-DNA and *OX1* specific primers. A single band in seed pool 51 of the expected size was obtained (data not shown). Plants from this seed pool were grown up in rows of 8 or 9 plants each and genomic DNA isolated from cotyledons which was subsequently used as template for the diagnostic PCR reaction. Rows 7 and 9 contained a single band of the expected size (data not shown). Finally, leaves from single plants were harvested for DNA extraction, the PCR reactions were carried out and plants 7-3, 9-2 and 9-3 identified as containing the T-DNA insertion (Figure A.3).

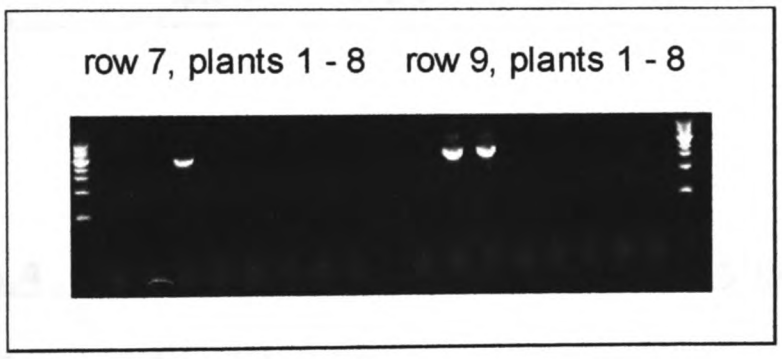

Figure A.3: Isolation of single plants containing a T-DNA insertion in *OX1*
Genomic DNA was extracted by a simple DNA prep from flower heads as described in Methods. PCR was performed with the T-DNA left border primer and the primer 3' of the *OX1* gene. Product indicates presence of a T-DNA insertion in this region.

A.3 Determination of homo- or heterozygosity for the isolated plants

The three isolated plants were tested for homo- or heterozygosity of the T-DNA insertion by PCR using primers on either side of the T-DNA insertion site. Lack of PCR product indicated that a insertion is present, as amplification across the T-DNA was not possible under the PCR conditions used (1 min extension at 72 °C). A small PCR product (560 bp) indicated that the T-DNA insertion is absent. As a control, a PCR reaction with a T-DNA internal primer was run alongside; product from this reaction verified the presence of the insertion. It was thus determined that lines 7-3

and 9-2 were homozygous for the T-DNA insertion whereas line 9-3 was heterozygous (Figure A.4). Homozygosity of bulked seed of line 9-2 was later confirmed in this manner.

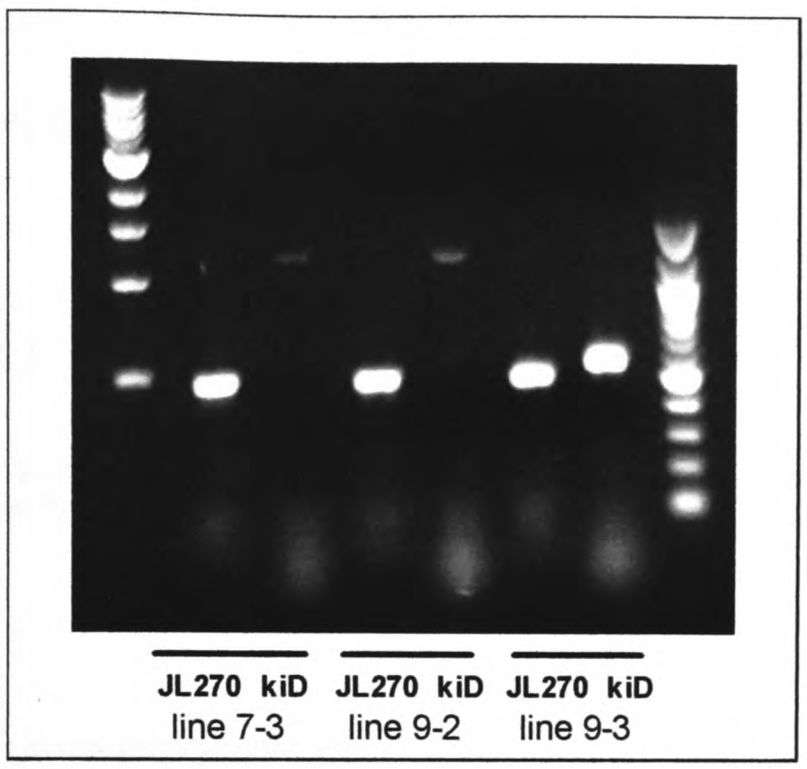

Figure A.4: Determination of homo- or heterozygosity for the *OX1* T-DNA insertion PCR with genomic DNA template was performed using a primer downstream of the T-DNA insertion and either a primer within the T-DNA (JL270) or upstream of the T-DNA insertion (kiD). The generation of a 560 bp fragment in the kiD reaction of line 9-3 indicates that it is heterozygous whereas lines 7-3 and 9-2 are homozygous.

A.4 The knock-out lines contain a single T-DNA insertion

The number of T-DNA insertions in the *ox1* null-mutant was determined by TAIL-PCR (Thermal Assymmetric InterLaced PCR, data not shown), using primers complementary to sequences in the T-DNA left border with three different non-specific primers (see Liu *et al* , 1995). The PCR program carried out yielded a single product for two of the three non-specific primers (the third primer did not amplify any sequences). The single product obtained with the non-specific primers was sequenced and shown to encode *OX1* downstream of the T-DNA sequence in both cases. Thus, only a single T-DNA insertion is present in the *ox1* null-mutant.

The protein product generated from the *OX1* promoter comprises the truncated OX1 N-terminus (31 amino acids) and 49 amino acids encoded by the right border of the T-DNA insertion (Figure A.5), as inferred from the known insertion site and the published right border sequence (www.biotech.wisc.edu). Due to its small size, the novel protein is unlikely to cause the *ox1* mutant phenotype (see section 4.2.5). This will be verified by complementation analysis (see below).

m l e g d e k q s r a l d f n r l e v l s l l g r g a k g v v W E N L A L P N L I A L
Q H I P L S P A G V I A K R P A P I A L P N S C A P E W R M R P Q L R A F *

Figure A.5: Truncated OX1 sequence (lower case) and T-DNA right border sequence (upper case) to the first in-frame stop codon (inferred from insertion point of T-DNA)

Future experiments

To verify that the *ox1* phenotype (see section 4.2.5) is due to a knockout mutation, the *OX1* gene will be complemented by transforming *ox1* with a 3500 bp genomic sequence containing *OX1* (work in progress). If the lack of OX1 activity is responsible for the observed *ox1* phenotype, transformed lines will show wild type characteristics (*e.g.* high *ECS1* transcript levels; normal root hair formation). In addition, the nature of the mutation could be investigated by genetic analysis through backcrossing of the *ox1* mutant with wild-type plants. If the mutation is recessive, the resulting F_1 should show a wild-type phenotype. A 3:1 segregation of wild-type plants relative to the mutant phenotype in the F_2 generation would confirm that the mutation is due to a recessive mutation at a single locus. Furthermore, co-segregation would confirm that the mutant phenotype is at least linked to the T-DNA insertion.

Appendix B: *OX1* constructs

Plants were transformed with *A. tumefaciens* carrying either the pBin19 (Bevan, 1984) or the pER8 (Zuo *et al.*, 2000) binary vectors. These vectors include a kanamycin resistance gene (pBin19) or spectinomycin and streptomycin resistance genes (pER8) (bacterial selectable markers), an origin of replication for *E.coli* cells and for *A. tumefaciens* cells, the left and right T-DNA borders spanning either the *LacZ* gene with a multiple cloning site (blue-white selection) and a kanamycin resistance gene (pBin19) or an oestrogen receptor-based chemical-inducible system and a hygromycin resistance gene (plant selectable marker) (pER8).

B.1 *OX1promoter::GUS* reporter gene fusion construct

A 1610 bp fragment starting 1608 bp upstream of the *OX1* gene start codon and including the first 2 bp of the *OX1* coding sequence was amplified by PCR (Pyrobest polymerase enzyme, TaKaRa, Japan) from Col-0 genomic DNA (120 ng template / reaction) with primers containing a BamHI and a PstI restriction site (5' and 3' primer, respectively). The purified fragment as well as the pDH51 plasmid (Pietrzak *et al.*, 1986) containing a *GUS* construct (ampicillin resistant, obtained from Dr. Joy Boyce, University of Oxford) was restricted with BamHI and PstI. After another purification, a ligation was carried out and the resulting *OX1promoter::GUS*-pdh51 plasmid transformed into *E. coli* cells. The plasmid was isolated from 3ml of overnight culture inoculated from a single colony and sequenced to verify the identity of the insert. The *OX1 promoter::GUS* insert including a CaMV transcription terminator was excised by restriction with BamHI and KpnI and purified. The binary vector pBin19 (kanamycin resistant) was also restricted with BamHI and KpnI and

ligated with the purified insert. The resulting *OX1promoter::GUS*-bin19 plasmid (see Figure B.1) was transformed into *E.coli*. After blue-white selection on kanamycin/X-gal/IPTG LB plates, an overnight culture was inoculated from a single white colony and the plasmid isolated the following day from 5 ml of culture. Presence of the insert was confirmed by restriction analysis and the plasmid transformed into *A. tumefaciens*. Col-0 plants were transformed with a culture obtained from a single *A. tumefaciens* colony. The plasmid was re-isolated from this culture, re-transformed into *E.coli*, isolated and sequenced to verify identity of the insert. Plants were grown up to maturity, seed was collected and transformants were selected for kanamycin resistance. Further experiments are described in Chapter 4.

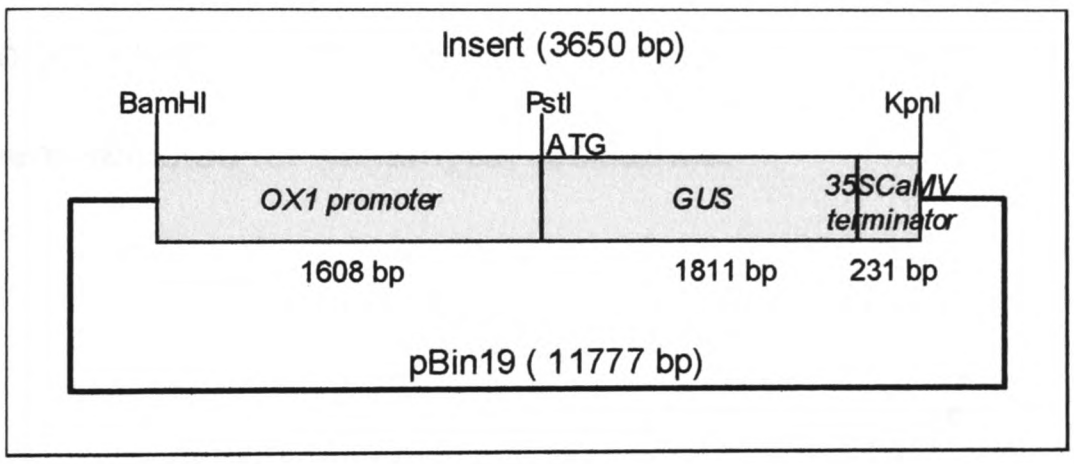

Figure B.1: The *OX1promoter::GUS* construct in binary vector pBin19
The *OX1promoter::GUS* construct (3650 bp) was cloned into pBin19 as described in the text.

B.2 *OX1 promoter (-385 to -317)::GUS* reporter gene fusion construct

A primer including the (-385 to –317) region from the putative start ATG and the -70 to –50 region of the 35S minimal promoter as well as a HindIII restriction site was designed. This primer together with a reverse primer downstream of (and ending in) the pBin19 EcoRI polylinker site was used to amplify the *(-385 - -317) OX1promoter::(-70) 35S minimal promoter::GUS* reporter gene fragment by PCR

using the pBin121 plasmid (Jefferson *et al.*, 1987) as a template (Pyrobest enzyme, TaKaRa, Japan; 300 ng template) (Figure b.2). The pBin121 vector is a pBin19 derivative containing a *GUS* gene as well as a NOS transcription terminator inserted into the multiple cloning site of pBIN19 within the T-DNA borders (Jefferson *et al.*, 1987). The purified fragment as well as pBin19 were restricted with HindIII and EcoRI, purified and ligated. The resulting plasmid was transformed into *E. coli*, re-isolated from 5 ml overnight culture inoculated from a single colony and analysed for presence of the insert by restriction analysis. The insert obtained was ligated into bluescript (HindIII and EcoRI sites), transformed into *E.coli* and entirely sequenced twice. The pBin19 plasmid containing the insert was transformed into *A. tumefaciens.* Col-0 plants were transformed with a culture obtained from a single colony. Plants were grown up to maturity, seed was collected and transformants were selected for kanamycin resistance.

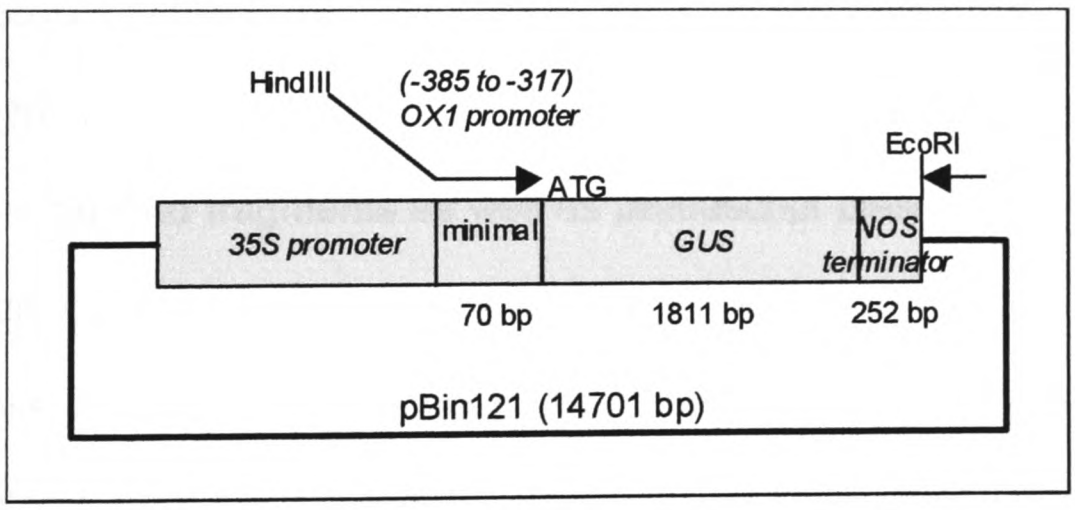

Figure B.2:
PCR of the *(-385 - -317) OX1promoter::35S minimal promoter::GUS* reporter gene fragment from pBin121 template
Arrows represent PCR primers.

B.3 *OX1* constitutive mutant and antisense constructs

B.3.1 Cloning and transformation

In order to generate *A. thaliana* lines inducibly expressing a **constitutively active** form of OX1, a 998 bp fragment including the *OX1* start codon and 9 bp downstream of the 12th conserved kinase domain (see Figure 4.3) was amplified by PCR (Pyrobest, TaKaRa, Japan) with primers containing a SalI and SpeI restriction site (5' and 3' primers, respectively) from cDNA (1 h treatment of RLD1 seedlings with 10 mM H_2O_2; 1:10 dilution, 10 µl per reaction). The 5' primer for the *OX1* constitutive mutant contained a TIC (translation initiation) site (ATAACA) to allow translation of the mRNA into the truncated OX1 protein. However, a stop codon was not present, causing addition of an extra 36 amino acids, encoded by the pER8 plasmid, onto the truncated OX1 protein.

An **antisense** construct of the same 998 bp fragment was obtained by PCR with the above primers containing reversed restriction sites, *i.e.* SpeI and SalI, 5' and 3', respectively.

The purified fragments as well as pBluescript plasmid were restricted with SpeI and SalI, purified again and ligated. The resulting plasmids were transformed into *E. coli* cells. Plasmids were isolated from 3 ml of overnight culture inoculated from a single colony and sequenced to verify the identity of the insert. The complete *OX1* constitutive mutant insert was sequenced twice to check for mutations introduced during PCR. Regions with differences to the Col-0 database were checked by sequencing RLD1 genomic DNA. The antisense construct was sequenced from both ends to verify its identity.

The inserts were excised by digestion with SpeI and SalI whereas the binary vector pER8 was digested with SpeI and XhoI (latter yielding a SalI compatible site). After purification, a ligation was carried out and the resulting plasmid transformed into *E.coli* cells. The plasmid was isolated from 5 ml of an overnight culture inoculated from a single colony. Presence of the inserts was confirmed by restriction analysis and the plasmid transformed into *A. tumefaciens*. Col-0 plants were transformed with a culture obtained from a single *A. tumefaciens* colony. The plasmids were re-isolated from this culture, re-transformed into *E.coli*, isolated and sequenced to verify identity of the insert. Plants were grown up to maturity, seed was collected and transformants were selected for hygromycin resistance.

B.3.2 Analysis of transformed *A. thaliana* lines

The lines transformed with the inducible pER8 constructs were tested for changes in mRNA levels following incubation in oestradiol. The constitutive mutant exhibited strong induction in response to 0.2 μM oestradiol in lines A and H and weak induction in lines D and F (Figure B.3). 27 transformants of the antisense construct lines were tested for decreases in *OX1* transcript levels in response to cellulase treatment (by using a probe complementary to the 3' tail of the *OX1* gene not included in the antisense construct), and increases in *OX1* antisense transcript levels (by using a probe complementary to the NOS terminator and polyadenylation signal sequences contained in the pER8 vector). None of the lines showed the expected decrease in *OX1* transcript levels despite low induction of *OX1* antisense levels visible in lines 34 and 39 (Figure B.4). 15 lines out of the examined 27 lines were grown on hygromycin plates and all exhibited resistance. These 15 lines were

induced in 2 μM oestradiol to check if a higher concentration was needed for induction; this was not the case.

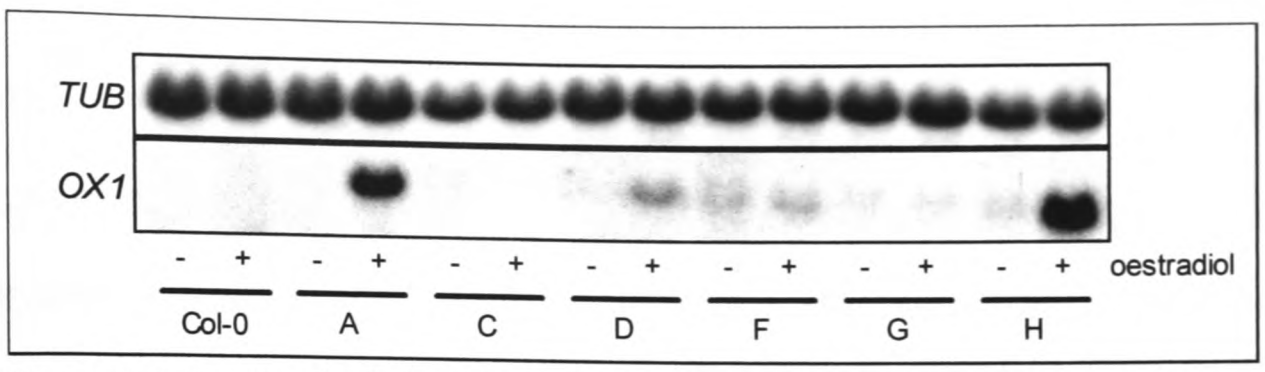

Figure B.3: Testing for inducible *OX1* constitutive mutant lines
Northern analysis was carried out as described in Methods. 7 day old seedlings transformed with an inducible *OX1* constitutive mutant construct were transferred into 1 x MS liquid medium. Oestradiol (Sigma, UK) (final concentration: 0.2 μM, 0.01 % DMSO) was added for induction to just above the 35S promoter level (Zuo *et al.*, 2000) and samples left in a growth cabinet. DMSO only (final concentration: 0.01 %) was added to the control samples (- oestradiol) in separate well plates. After 30 h incubation, seedlings were frozen and total RNA was extracted, electrophoresed and transferred to nylon membrane. *OX1* and β-*TUBULIN* probes were labelled and hybridised to the RNA on the membrane.

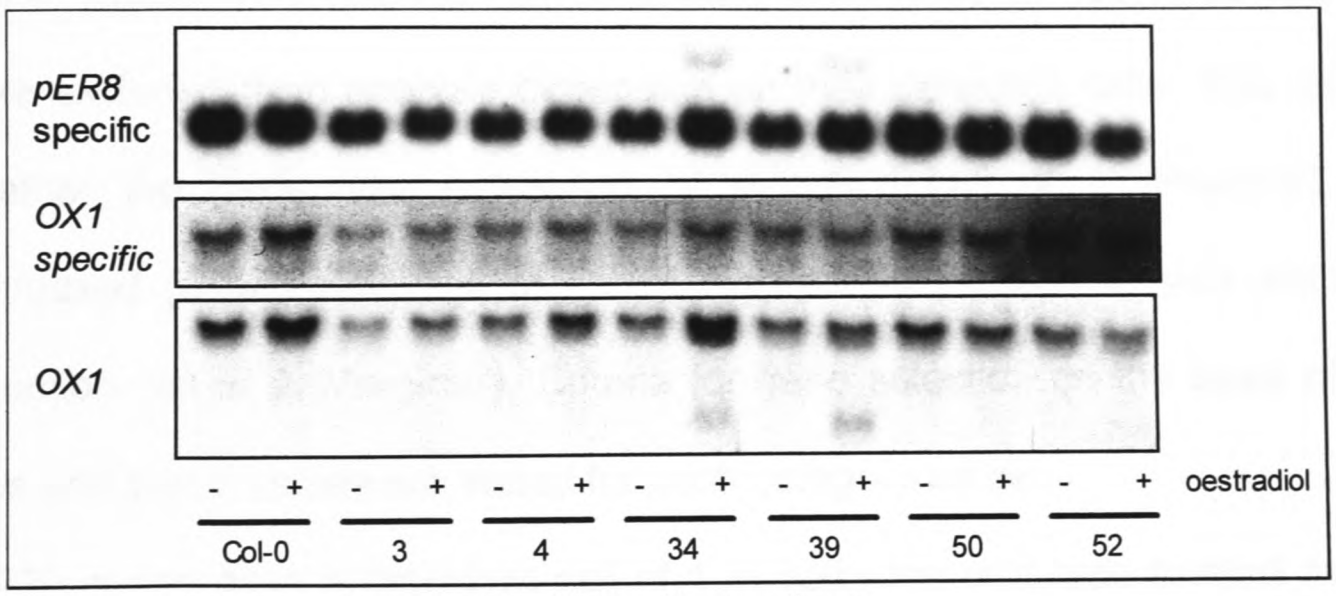

Figure B.4: Testing for inducible *OX1* antisense lines
Northern analysis was carried out as described in Methods. 7 day old seedlings transformed with an inducible *OX1* antisense construct were transferred into 1 x MS liquid medium. Oestradiol (Sigma, UK) (final concentration: 0.2 μM, 0.01 % DMSO) was added for induction to just above the 35S promoter level (Zuo *et al.*, 2000) and samples left for 48 h in the growth cabinet. DMSO only (0.01 %) was added to the control samples (- oestradiol) in separate well plates. Seedlings were placed for 1 h into cellulase solution (final concentration: 0.1 %) containing oestradiol or DMSO and frozen after this period. The pER8 specific probe (224 bp) is complementary to the 3' UTR polyA addition sequence (from pea Rubisco small chain 3a) present on the insert. The *OX1* specific probe is complementary to 285 bp outside the antisensed region.

Appendix C:

Microarray analysis of gene induction in the *ox1* mutant in response to H_2O_2 treatment

7 day old WS-2 wild-type and *ox1* seedlings were transferred into H_2O, left to recover for 3 h and treated for 3 h in H_2O_2 (final concentration: 10 mM). RNA was extracted, dessicated and sent to the NASC Affymetrix Facility (Nottingham, UK). 15 µg of biotin-labelled, fragmented cRNA, obtained from the four RNA samples, were hybridised to Affymetrix ATH1 Arabidopsis genome arrays. The top 5% and bottom 5% of signal intensities were excluded and the mean was calculated. The original signal values were scaled such that the mean was made equal to 100 (all carried out by the Affymetrix Facility).

Signal values were analysed by calculating their ratios as described below. Genes were excluded from analysis depending on their detection calls. This value states whether the gene was expressed (a detection call of 1, 'Present'), was not expressed (a detection call of –1, 'Absent') or if expression was ambiguous (a detection call of 0 'Marginal'). Criteria for gene selection on the basis of detection calls and signal values are stated for each category below.

11229 genes gave a detection call of 1 in both, the wild type treated and the wild type control sample. Of these genes, 5.60 % increased in response to H_2O_2-treatment whereas 2.24 % decreased (cut-off: 2 fold induction or repression). Similarly, 12023 genes gave a detection call of 1 in both, the *ox1* treated and *ox1* control sample, 5.11 % of which increased and 2.96 % decreased in response to H_2O_2 treatment.

Appendix C, a: Gene induction by H_2O_2 treatment

Signal ratios (increase in transcript levels) were calculated by adding signal values of the WS-2 and *ox1* treated samples for each spot and dividing this by the added signal values of the control samples. Genes sorted into categories are listed in descending order of fold induction. Spots were only included if both induced sample values had detection calls of 1. All genes with a known function or strong similarity to known genes are listed down to a fold induction of 2.5.

a) Gene induction by H_2O_2-treatment

gene code	gene name / function / similarity	fold induction	10 mM H_2O_2 wt	10 mM H_2O_2 *ox1*	control wt	control *ox1*
Heat shock proteins						
At1g74310	heat shock protein 101	464.3	1318.6	1420.8	4.3	1.6
At1g59860	heat shock protein, put. Hsp20	357.8	1540.0	2288.1	7.9	2.8
At1g52560	small heat stress protein (AtHsp26.5)	228.9	190.6	267.1	0.6	1.4
At5g12030	heat shock protein 17.6A	210.8	2141.6	3085.9	13.7	11.1
At4g25200	AtHSP23.6-mito	199.6	146.4	372.6	1.5	1.1
At5g12020	heat shock protein 17.6-II	193.7	1450.3	1629.8	14.2	1.7
At2g29500	putative small heat shock protein	167.7	1845.7	2078.9	9.2	14.2
At4g27670	heat shock protein 21	157.3	150.6	258.5	1.1	1.5
At2g26150	putative heat shock transcription factor	110.5	71.1	94.6	0.6	0.9
At3g46230	heat shock protein 17	110.0	1345.6	1779.3	19.2	9.2
At1g53540	17.6 kDa heat shock protein (AA 1-156)	97.7	1565.1	2127.8	19.6	18.2
At1g71000	similarity to DnaJ	81.9	105.6	90.9	0.7	1.7
At1g54050	Hsp-like	62.3	1939.7	2230.8	38.8	28.1
At1g16030	similarity to Hsp70	47.8	2707.2	1962.8	34.1	63.6
At3g12580	Hsp70	39.4	2237.4	1831.4	56.7	46.7
At5g52640	Hsp90a or Hsp81-1	34.8	1922.2	1914.6	54.2	56.0
At5g37670	Hsp20-like	24.9	248.4	280.5	8.1	13.1
At5g51440	mitochondrial heat shock 22 kd protein-like	24.6	306.5	310.2	15.2	9.9
At2g20560	putative heat shock protein	22.6	378.1	394.0	23.1	11.1
At5g59720	heat shock protein 18	22.0	86.4	96.6	3.6	4.7
At2g32120	70kD heat shock protein	11.2	632.2	671.6	52.6	63.6
At3g09440	heat-shock protein (At-hsc70-3)	8.1	1742.9	1166.6	183.4	177.1
At5g09590	heat shock protein 70 (Hsc70-5)	4.6	203.8	291.8	56.9	50.6
Glucosyl transferases						
At2g15480	putative glucosyltransferase	121.0	469.8	437.6	5.2	2.3
At2g36750	putative glucosyl transferase	57.4	36.6	60.9	0.8	0.9
At1g05560	UDP-glucose transferase (UGT75B2)	32.5	273.3	312.4	9.0	9.0
At4g34135	glucosyltransferase like protein	27.2	757.4	1066.0	39.1	27.9
At1g05680	putative indole-3-acetate beta-glucosyltransferase	19.3	283.8	296.3	11.2	18.9
At1g22400	putative UDP-glucose glucosyltransferase	8.3	477.7	746.5	54.1	93.3
At2g36790	putative glucosyl transferase	8.0	121.7	156.2	18.8	16.0
At4g01070	putative flavonol glucosyltransferase	5.6	273.2	191.0	41.1	41.5
At3g21560	UDP-glucose:indole-3-acetate beta-D-glucosyltransferase, pu	5.6	223.6	170.1	43.2	27.5
At4g15550	UDP-glucose:indole-3-acetate beta-D-glucosyltransferase	4.3	399.9	392.9	87.3	97.9
At4g15490	indole-3-acetate beta-glucosyltransferase like protein	4.1	329.9	216.9	63.6	70.0
Protective enzymes						
Glutathione S-transferases						
At1g17170	putative glutathione transferase	79.3	1551.1	2126.5	19.8	26.6
At1g17180	putative glutathione transferase	31.5	340.9	241.2	6.5	12.0
At2g29420	putative glutathione S-transferase	16.8	1700.5	1690.3	112.5	89.9
At2g29490	putative glutathione S-transferase	15.3	165.0	135.5	16.8	2.8
At2g29460	glutathione transferase , auxin-inducible	8.6	46.9	62.8	11.0	1.8
At1g69930	putative glutathione transferase	8.3	74.7	46.1	12.4	2.1
At2g47730	glutathione S-transferase (GST6)	4.2	4337.7	4830.2	1101.2	1094.2
At1g02930	glutathione S-transferase (ERD11)	3.9	2422.9	2352.7	573.0	639.8
At2g29450	glutathione S-transferase (GST1)	3.9	525.0	571.2	140.6	140.6
At1g78380	glutathione S-transferase like protein	3.4	4194.3	4791.2	1442.6	1227.6
Others						
At3g09640	putative ascorbate peroxidase	14.2	31.7	46.2	2.9	2.6
At5g20850	Rad51-like protein, DNA repair	11.2	44.9	40.1	3.5	4.1
At1g75270	GSH-dependent dehydroascorbate reductase 1, putative	8.4	1015.7	859.2	129.7	94.7
At4g11600	phospholipid hydroperoxide glutathione peroxidase	5.1	1944.2	2349.4	331.3	514.9
At5g03630	monodehydroascorbate reductase (NADH) - like protein	2.9	704.3	731.3	238.3	258.0

Primary metabolism						
Enzymes						
At4g21990	PRH26 protein, PAPS reductase homolog	33.7	1183.6	1265.5	34.6	38.0
At4g21323	subtilisin-like serine protease	15.1	56.6	56.9	3.5	4.0
At1g55920	serine acetyltransferase	12.3	1977.9	1888.8	170.5	145.0
At4g04610	5'-adenylylsulfate reductase	11.1	229.7	299.0	16.9	30.8
At4g13180	short-chain alcohol dehydrogenase like protein	9.8	554.5	549.8	59.8	52.5
At1g32940	putative subtilisin-like protease	9.4	97.6	104.1	16.2	5.2
At5g51830	fructokinase 1	8.7	521.2	381.3	49.2	54.4
At5g14760	L-aspartate oxidase -like protein	6.2	192.0	185.0	32.7	28.4
At1g02850	Similar to beta-glucosidases	4.8	577.4	631.4	115.6	134.0
At4g34710	arginine decarboxylase (spe2)	4.7	3503.5	3313.3	743.5	693.2
At1g55850	putative cellulose synthase catalytic subunit	4.7	584.0	635.0	143.8	117.0
At2g47180	putative galactinol synthase	4.4	469.5	676.1	144.5	117.0
At1g62180	putative adenosine-5'-phosphosulfate reductase	3.8	418.4	309.4	102.7	89.3
At5g44070	phytochelatin synthase	3.6	528.0	635.7	188.1	136.1
At2g37770	putative alcohol dehydrogenase	3.5	103.0	120.6	35.9	28.7
At2g37760	putative alcohol dehydrogenase	3.2	384.7	404.4	130.0	114.6
At2g19450	diacylglycerol O-acyltransferase (DAGAT)	3.2	346.8	375.8	116.6	107.8
At1g48850	chorismate synthase, putative	3.0	245.4	208.1	82.9	69.8
At3g22890	ATP sulfurylase, putative	2.9	809.8	689.1	267.8	240.5
At3g23920	beta-amylase, putative	2.8	514.3	595.9	170.0	223.0
At5g04590	sulphite reductase	2.5	725.7	585.8	262.4	258.7
Others						
At4g22530	putative protein, embryonic abundant protein-like	21.1	112.3	101.3	9.0	1.1
At2g41380	putative embryo-abundant protein	19.6	655.3	819.3	52.5	22.6
At5g64310	arabinogalactan-protein AGP1	9.2	732.4	663.7	90.5	61.8
At1g55450	embryonic abundant protein-like like	4.3	1070.7	903.8	226.4	233.7

Electron transport						
At4g37370	cytochrome P450 - like protein	16.4	246.3	276.2	18.1	13.8
At3g28740	cytochrome P450, putative	14.7	1363.3	1305.5	107.4	74.7
At5g57220	cytochrome P450	14.1	176.4	159.5	21.6	2.3
At5g17000	quinone oxidoreductase - like protein	7.8	47.2	50.2	6.5	6.0
At5g25450	ubiquinol--cytochrome-c reductase-like protein	7.9	512.6	798.9	89.1	77.1
At5g16970	quinone oxidoreductase -like protein	7.5	1929.0	1888.0	265.3	242.3
At1g64950	cytochrome P450, putative	7.3	43.6	46.9	4.6	7.8
At1g75280	putative NADPH oxidoreductase	6.7	1339.9	1198.9	204.6	171.6
At4g10040	cytochrome c	6.6	229.7	290.7	41.6	37.0
At3g22370	alternative oxidase 1a precursor	6.1	721.2	737.4	134.3	103.7
At3g14660	putative cytochrome P450	4.2	394.0	318.7	90.4	79.1
At4g24570	putative mitochondrial uncoupling protein	4.0	118.6	174.8	34.0	39.9
At4g05390	ferredoxin-NADP+ reductase like protein	3.2	188.7	168.9	57.3	52.9
At3g14690	putative cytochrome P450	2.8	723.5	753.2	276.6	253.1
At4g30210	NADPH-ferrihemoprotein reductase (ATR2)	2.7	602.7	588.2	200.5	240.2
At2g34500	putative cytochrome P450	2.6	269.4	306.5	108.4	113.5

Secondary metabolism						
At1g09500	putative cinnamyl alcohol dehydrogenase	37.3	61.2	58.2	2.4	0.8
At5g61160	anthocyanin 5-aromatic acyltransferase - like protein	21.0	29.6	31.4	1.5	1.4
At4g37990	cinnamyl-alcohol dehydrogenase ELI3-2	5.3	161.6	195.3	36.2	30.9
At5g07870	N-hydroxycinnamoyl/benzoyltransferase - like protein	4.9	141.6	179.9	34.5	31.1
At1g72680	putative cinnamyl-alcohol dehydrogenase	4.2	527.0	403.8	142.9	79.1
At5g19440	cinnamyl-alcohol dehydrogenase - like protein	4.1	821.6	779.0	210.6	181.7
At2g33590	putative cinnamoyl-CoA reductase	3.4	347.1	313.4	110.3	81.7
At5g07860	N-hydroxycinnamoyl/benzoyltransferase - like protein	3.2	295.2	337.8	97.0	99.5

Pathogen defense						
At3g05360	putative disease resistance protein	29.7	70.4	69.0	3.3	1.4
At1g72900	similar to disease resistance protein	8.8	285.2	284.4	37.3	27.2
At1g72920	disease resistance protein -like protein	8.0	32.6	36.8	8.1	0.6
At4g36010	thaumatin-like predicted GPI-anchored protein	7.4	204.1	228.9	41.4	17.1
At1g72930	similar to downy mildew resistance protein RPP5	6.4	195.6	212.9	35.7	27.8
At3g04010	putative beta-1,3-glucanase	6.5	282.9	545.9	61.7	65.5
At4g20830	reticuline oxidase -like protein (alkaloid biosynthesis)	3.6	333.6	397.4	92.4	109.9
At5g06860	polygalacturonase inhibiting protein 1; PGIP1	3.6	1385.6	1061.0	356.1	321.1
At1g76600	TMV response-related gene product-like (Nicotiana)	3.2	1078.9	1266.2	363.9	371.1
At3g55840	nematode resistance protein-like protein	3.1	92.1	97.3	29.1	32.7
At1g09970	leucine-rich repeat receptor-like kinase	2.9	540.6	354.0	158.2	149.0
At2g34930	putative disease resistance protein	2.9	109.1	171.2	42.9	53.5
At2g38870	putative protease inhibitor	2.9	482.7	435.1	178.7	139.8
Transporters						
At4g35180	amino acid permease, aa transporter	6.9	95.7	96.8	22.2	5.8
At5g13750	transporter-like protein	6.8	406.6	331.7	56.1	53.0
At5g17860	potassium-dependent sodium-calcium exchanger - like protein	6.6	655.0	550.4	95.4	88.5
At1g64780	ammonium transporter ATM1;2	5.9	73.9	64.1	14.8	8.6
At1g61800	similar to glucose-6-phosphate/phosphate-translocator	5.6	84.9	105.8	20.8	13.5
At3g59140	ABC transporter-like protein	4.8	163.1	165.2	42.3	25.4
At2g23150	putative metal ion transporter (NRAMP), nramp3	4.3	622.7	714.2	143.0	166.2
At2g34660	MRP-like ABC transporter	4.2	198.1	246.7	55.3	51.6
At1g71880	sucrose transport protein SUC1	4.0	969.4	572.1	154.2	231.4
At5g13490	adenosine nucleotide translocator	3.9	439.6	553.2	127.4	125.9
At2g38290	putative ammonium transporter	3.9	240.9	269.1	61.9	69.1
At5g26340	hexose transporter - like protein	3.0	591.6	386.6	170.6	156.1
At3g51895	sulfate transporter ATST1	2.6	47.7	39.6	15.1	18.1
At5g14570	high affinity nitrate transporter - like protein	2.6	351.5	309.7	136.4	120.3
Signal transduction						
Calcium						
At5g49480	NaCl-inducible Ca2+-binding protein-like; calmodulin-like, ACP1	16.8	1305.9	1619.0	80.4	93.7
At5g42380	calmodulin-lie protein	8.1	20.3	21.1	0.5	4.6
At3g63380	Ca2+-transporting ATPase -like protein	8.0	383.9	249.8	42.9	36.1
At3g50770	calmodulin-like protein	5.2	502.5	575.2	112.1	96.1
At5g39670	calcium-binding protein - like	5.1	143.1	143.0	31.9	23.7
At1g27770	envelope Ca2+-ATPase, P-type	3.8	254.9	215.2	80.7	42.3
At2g41410	calmodulin-like protein	3.8	1179.9	698.5	264.8	229.7
At1g76650	putative calmodulin	3.1	120.4	190.5	42.6	56.1
At2g41090	calcium binding protein (CaBP-22)	2.6	300.3	262.6	114.3	102.4
Ethylene						
At3g24500	ethylene-responsive transcriptional coactivator, putative	15.6	801.7	1279.2	72.5	61.1
At4g11280	ACC synthase (AtACS-6)	6.9	286.8	343.7	52.2	39.4
At4g17490	ERF6	13.4	189.9	142.9	15.3	9.5
At4g17500	ERF1	2.8	240.6	236.6	81.3	87.8
At3g23230	Nicotiana EREBP-3-like protein	3.0	45.0	34.4	15.5	10.7
Jasmonate						
At1g76690	12-oxophytodienoate reductase (OPR2)	36.5	3137.8	3671.0	84.0	102.7

Kinases						
At3g16530	putative lectin	11.2	2653.5	2480.5	253.2	206.8
At4g02410	protein kinase-like	7.1	104.7	105.4	24.7	4.7
At4g23190	RLK3	7.1	56.0	54.0	11.7	3.9
At1g66880	wall-associated kinase, putative	5.6	37.1	45.5	10.8	4.0
At5g25930	receptor-like protein kinase - like	4.4	224.7	243.0	51.7	54.8
At4g28350	lectin receptor-like ser/thr kinase lecRK1	4.3	32.6	59.5	10.1	11.5
At5g66850	MAPK3	3.5	87.8	71.1	23.2	22.6
At4g25390	receptor kinase-like protein, similar to RLK3	3.3	118.0	127.8	45.1	30.3
At1g73500	putative MAPK, ATMKK5- like	3.3	155.5	133.4	42.1	44.8
At1g70740	putative protein kinase	3.0	127.4	111.2	38.4	42.4
At2g33580	putative protein kinase, RLK-like	2.6	50.4	70.2	20.2	25.7
At5g58350	MAP kinase	2.1	549.4	434.0	219.9	239.5
Phosphatases						
At4g17615	calcineurin B-like protein 1 (CBL1)	8.0	137.5	237.1	16.9	30.1
At4g31860	protein phosphatase 2C - like protein	4.7	441.0	337.7	90.9	74.9
At2g33700	putative protein phosphatase 2C	3.5	163.1	121.4	47.3	34.3
At2g30020	putative protein phosphatase 2C	3.5	57.3	78.7	16.7	22.4
At3g62260	PP2C,serine/threonine protein phosphatase	3.3	89.0	115.2	30.5	31.5
At4g23570	phosphatase like protein	3.4	287.6	309.1	93.3	83.6
Transcription factors						
At5g05410	DREB2A	14.1	634.8	649.7	54.4	36.6
At1g62300	transcription factor WRKY6	9.6	316.3	354.2	25.1	45.0
At3g56400	WRKY3-like	8.9	206.2	223.8	26.4	21.7
At1g27730	putative salt-tolerance zinc finger protein	8.1	923.8	1081.0	99.6	146.7
At1g80840	similar to WRKY4	8.1	464.2	514.1	63.8	56.7
At1g22810	TINY-like transcription factor	7.6	123.9	89.9	16.5	11.8
At2g38470	putative WRKY-type DNA binding protein	5.3	736.9	761.3	141.6	139.6
At2g40350	AP2 domain transcription factor	4.9	97.3	135.0	27.7	19.6
At2g26950	putative MYB family transcription factor	4.4	7.3	11.0	2.5	1.7
At4g31800	WRKY18	4.3	140.9	259.7	53.5	39.5
At2g46400	putative WRKY-type DNA binding protein	4.3	102.3	114.9	25.6	25.1
At1g18570	myb-related transcription factor MYB51	2.7	136.4	114.3	46.0	45.6
Others						
At4g38550	Phospholipase like protein	4.0	331.1	229.9	68.0	73.3
At5g20910	ABI3-interacting protein 2	3.5	156.7	255.8	56.4	61.7
At1g28600	lipase, putative	2.6	242.6	197.7	75.4	91.1
At3g21700	putative SGP1 monomeric G-protein	2.6	93.6	78.6	35.0	31.6
At2g30550	putative lipase	2.6	142.0	101.2	52.2	42.0

Appendix C, b: Gene repression by H_2O_2 treatment

Signal ratios (decrease in transcript levels) were calculated by adding signal values of the WS-2 and *ox1* control samples for each spot and dividing this by the added signal values of the treated samples. Genes sorted into categories are listed in descending order of fold repression. Spots were only included if both control sample values had detection calls of 1. All genes with a known function or strong similarity to known genes are listed down to a fold repression of 2.5.

b) Gene repression by H_2O_2-treatment

gene code	gene name / function / similarity	fold repression	10 mM H_2O_2 wt	10 mM H_2O_2 *ox1*	control wt	control *ox1*
extensins and cell wall enzymes						
At5g35190	extensin -like protein	86.7	1.2	0.6	62.0	94.1
At4g25820	putative xyloglucan endo-1,4-beta-D-glucanase	17.6	0.6	10.4	93.1	100.2
At4g02270	hypothetical protein similar to extensin-like protein	10.6	52.4	35.1	475.6	451.9
At4g12550	auxin-induced protein AIR1, putative cell wall-plasma membrane disconnecting CLCT protein (AIR1A)	7.9	134.9	146.0	1002.9	1223.3
At1g02810	pectinesterase family	5.0	2.5	15.0	43.5	44.0
At5g04960	pectinesterase	4.2	8.1	21.9	57.3	67.4
At1g62660	putative beta-fructosidase	3.8	206.0	190.0	976.6	543.6
At5g06640	putative protein, extensin homolog	3.7	84.7	60.4	234.8	297.8
At2g41850	polygalacturonase like protein	3.7	23.3	16.8	100.4	46.5
At5g46900	extA (extensin)	3.5	32.0	66.8	119.5	223.0
At1g26250	hypothetical protein, extensin-like	3.3	27.6	23.7	71.1	96.5
At3g54590	extensin precursor -like protein	3.1	149.5	91.6	310.0	439.1
At4g23820	putative polygalacturonase	3.1	180.4	137.2	532.2	436.7
At4g08410	extensin-like protein	2.6	56.6	71.6	149.3	184.3
peroxidases						
At4g26010	peroxidase like protein	17.4	14.3	14.9	214.7	292.0
At1g05250	putative peroxidase ATP12a	12.4	34.4	20.8	292.3	390.7
At5g17820	peroxidase ATP13a	8.8	25.6	26.6	233.2	227.5
At1g30870	peroxidase ATP5a	8.8	22.2	4.1	128.1	103.7
At5g38930	germin - like protein	8.4	11.5	9.4	86.1	89.6
At5g15180	prx10 peroxidase - like protein	7.2	8.2	18.6	83.9	108.9
At3g01190	putative peroxidase	6.9	27.4	24.0	184.1	169.4
At4g30170	peroxidase ATP8a	4.4	102.0	80.4	438.5	373.1
At5g19890	peroxidase ATP N	4.2	22.5	28.3	118.9	95.7
At5g64100	peroxidase ATP3a (emb|CAA67340.1)	3.4	629.8	411.7	1819.2	1691.9
At2g37130	putative peroxidase ATP2a	3.2	142.7	117.1	396.0	424.6
At2g35380	putative peroxidase	2.9	18.3	11.4	55.1	30.5
At5g42180	peroxidase	2.7	55.3	47.4	111.2	161.4
At5g66390	peroxidase (emb|CAA66964.1)	2.6	44.1	39.6	109.8	109.4
At2g38390	peroxidase	2.5	144.7	81.2	271.0	301.2
aquaporins						
At5g47450	membrane channel protein-like; aquaporin	5.3	115.4	165.7	676.5	804.2
At4g17340	membrane channel protein-like; aquaporin	5.2	295.0	225.0	1198.8	1526.5
At5g60660	mipC protein - like (aquaporin)	4.2	32.7	34.8	132.1	149.7
At1g17810	aquaporin	3.6	31.7	78.5	115.0	283.4
myrosinases						
At3g16440	myrosinase-binding protein-like protein	40.5	3.1	1.6	125.4	64.9
At1g47600	putative myrosinase precursor, putative	6.8	50.0	35.6	252.4	327.8
At1g52060	myrosinase-binding protein-like like	5.5	18.0	20.7	85.6	126.1
At1g52050	myrosinase-binding protein-like protein	5.3	23.4	20.2	94.5	137.9
At1g52070	myrosinase-binding protein-like like	5.2	17.2	12.5	75.8	78.9

Signal transduction						
Kinases						
At2g41970	putative protein kinase	3.6	5.8	16.8	38.2	43.5
At2g28960	putative receptor-like protein kinase	3.2	8.4	7.5	21.5	28.7
At2g23030	putative protein kinase	2.8	40.4	25.8	89.3	95.2
At5g63650	serine/threonine-protein kinase, ASK1	2.7	57.2	44.9	160.5	113.0
At5g59260	receptor-like protein kinase	2.6	12.4	14.2	32.5	36.7
Transcription factors						
At2g35270	putative AT-hook DNA-binding protein	3.0	28.6	21.8	82.0	70.8
At1g72200	RING-H2 zinc finger protein ATL3, putative	2.8	23.5	18.7	53.6	62.6
At1g29280	WRKY transcription factor 65 (WRKY65)	2.7	94.2	84.8	248.2	241.3
At5g22890	putative zinc finger protein	2.7	15.4	16.6	47.5	40.0
At1g62990	homeodomain transcription factor KNAT6 (KNAT6)	2.7	17.6	23.7	50.3	61.3
At3g01420	feebly like protein	2.7	73.5	82.6	222.6	198.4

Others						
At3g62680	proline-rich protein	39.9	5.9	4.4	205.9	205.5
At4g37070	patatin-like protein	38.0	1.1	0.5	36.5	24.3
At4g19690	Fe(II) transport protein	15.0	9.2	6.7	94.7	143.8
At1g06120	delta 9 desaturase, putative	14.7	9.3	3.3	84.6	101.1
At4g19680	putative Fe(II) transport protein	12.3	8.4	1.2	58.6	59.7
At5g60950	phytochelatin synthetase-like	10.8	6.0	4.2	60.3	50.1
At4g35350	cysteine proteinase - like protein	10.3	4.1	0.5	29.6	17.6
At3g23190	similar to HR lesion-inducing protein	7.0	10.6	10.4	70.1	76.1
At1g73270	putative serine carboxypeptidase	6.0	4.3	2.5	15.9	25.1
At1g66280	beta-glucosidase, putative	6.0	133.6	189.1	822.6	1110.3
At5g63600	ACC oxidase like protein	5.8	41.2	75.1	373.8	304.0
At1g73260	putative trypsin inhibitor	5.6	508.7	416.8	2525.8	2633.1
At4g16260	beta-1,3-glucanase class I precursor	5.3	18.4	9.7	70.3	79.9
At5g59090	cucumisin precursor - like	4.8	29.0	31.7	131.8	158.9
At5g65020	annexin	4.8	26.9	49.7	179.9	184.3
At2g23620	putative acetone-cyanohydrin lyase	4.7	48.9	31.9	180.5	202.1
At2g01530	probable major latex protein	4.2	199.1	195.4	843.7	809.0
At5g54370	root cap protein 2-like protein	4.1	13.9	11.5	44.1	60.7
At5g44380	berberine bridge enzyme-like protein	4.1	96.5	44.2	347.4	226.9
At1g01750	actin depolymerizing factor, putative	4.0	16.8	8.5	54.3	47.8
At4g13580	similar to disease resistance response protein	4.0	43.2	44.4	168.4	183.1
At1g32450	peptide transporter PTR2-B, putative	3.9	82.4	86.1	345.2	318.5
At1g21100	O-methyltransferase, putative	3.9	34.6	50.6	166.0	168.4
At4g37220	cold acclimation protein homolog	3.8	274.6	254.1	908.6	1095.4
At5g09530	periaxin-like protein	3.7	37.1	40.8	150.2	138.7
At3g14940	phosphoenolpyruvate carboxylase (PPC)	3.7	46.6	35.0	167.9	132.0
At1g54970	hypothetical protein, proline-rich protein 1	3.6	34.7	24.7	102.1	113.2
At4g26530	fructose-bisphosphate aldolase - like protein	3.6	148.8	230.3	722.2	634.7
At4g23700	putative Na+/H+-exchanging protein	3.5	68.0	68.6	222.7	254.4
At4g25790	putative pathogenesis-related protein	3.5	13.3	15.6	49.0	50.9
At1g17190	putative glutathione transferase	3.5	23.6	36.8	87.5	121.1
At4g12510	pEARLI 1-like protein	3.4	91.8	70.4	239.8	318.0
At1g80830	metal ion transporter	3.4	104.1	55.8	319.2	229.0
At3g16690	MtN3-like protein, cytochrome c oxidoreductase-like	3.4	56.2	56.4	194.9	189.8
At5g50200	putative component of high affinity nitrate transporter	3.3	161.1	164.2	530.0	553.3
At3g58810	zinc transporter -like protein	3.3	9.2	11.9	30.6	39.0
At1g70850	similar to major latex like protein from Prunus	3.2	141.7	116.3	464.8	368.9
At4g40090	arabinogalactan-protein (AGP3)	3.2	36.7	21.4	80.6	104.6
At5g56540	arabinogalactan-protein AGP14	3.2	31.6	33.6	107.7	98.5
At1g48930	putative glucanase	3.1	21.8	18.6	59.0	64.8

At2g38400	putative beta-alanine-pyruvate aminotransferase	3.0	320.3	300.0	918.9	970.2
At2g28630	putative fatty acid elongase	3.0	56.5	72.0	171.6	214.1
At5g59520	putative zinc transporter ZIP2 - like	3.0	73.0	48.0	175.8	186.8
At5g49730	FRO2-like protein; NADPH oxidase-like	3.0	144.4	159.8	463.9	436.8
At4g19030	nodulin-26 like protein	2.9	20.5	20.2	50.4	68.9
At1g77210	probable monosaccharide transport protein T14N5.7	2.9	267.0	206.3	728.7	650.9
At1g04040	vegetative storage protein-like	2.9	139.8	171.2	484.9	419.9
At1g53680	glutathione transferase, putative	2.9	12.8	17.1	50.0	36.3
At1g26820	ribonuclease RNS3	2.9	21.6	13.0	48.3	51.1
At4g20110	vacuolar sorting receptor-like protein	2.8	40.7	41.6	127.7	100.6
At2g43610	putative endochitinase	2.7	77.4	60.6	181.5	197.2
At1g22440	similar to alcohol dehydrogenase	2.7	42.7	60.0	141.5	139.7
At1g50560	cytochrome P450, putative	2.7	20.4	14.1	40.7	53.5
At3g16460	putative jasmonate inducible protein	2.7	395.1	396.0	1039.0	1115.3
At2g28670	putative disease resistance response protein	2.7	85.8	122.4	270.6	288.4
At3g54040	photoassimilate-responsive protein PAR-1b -like protein	2.6	61.5	41.8	143.3	129.8
At5g06330	harpin-induced protein-like	2.6	33.9	42.1	90.0	109.6
At5g22500	acyl CoA reductase-protein	2.6	239.2	144.0	649.0	354.8
At5g43370	inorganic phosphate transporter	2.6	192.1	87.6	449.5	282.7
At5g45670	GDSL-motif lipase/hydrolase-like protein	2.6	31.7	36.2	101.2	75.9
At1g48750	putative lipid transfer protein	2.5	139.7	153.0	321.8	420.4
At4g13660	isoflavone reductase-like protein	2.5	83.2	94.1	235.0	210.1

Appendix C, c: Differential gene induction in wt and *ox1* – increased levels in WS-2

Signal ratios were calculated in two ways.

1) Higher gene induction in WS-2 irrespective of H_2O_2 treatment

Signal ratios were calculated for each spot by adding signal values of both WS-2 samples and dividing them by the added signal values of *ox1*. Genes were only included if signal values for both WS-2 samples were at least twice as large as the *ox1* values, and had detection calls of 1. All genes fulfilling these criteria were grouped into categories and are listed in descending order of signal ratios down to 2.0, with the gene codes underlined.

2) Increase in gene induction in the treated WS-2 sample but not in other samples

Signal ratios were calculated for each spot by dividing the signal value for the WS-2 treated sample with the signal value of treated *ox1* sample. Genes were only included if the treated WS-2 sample showed at least two-fold induction compared to the *ox1* treated sample and the WS-2 and *ox1* control samples, and if the detection call was 1. All genes fulfilling these criteria were grouped into categories and are listed in descending order of signal ratios down to 2.0, with the gene codes in italics.

c) Differential gene induction in wt and *ox1* - increased levels in WS-2

gene code	gene name / function / similarity	fold induction	10 mM H_2O_2 wt	10 mM H_2O_2 *ox1*	control wt	control *ox1*
At3g25250	**OX1**	8.7	50.1	296.4	2.2	37.5
Pathogen defense and secondary metabolism						
At1g31580	pathogen-inducible protein CXc750 precursor	6.1	556.0	118.9	417.0	41.6
At1g66100	THI2.2	5.8	171.2	38.2	276.6	38.9
At4g16860	disease resistance RPP5 like protein	5.6	8.6	2.8	8.7	0.3
At2g26740	epoxide hydrolase (ATsEH)	3.7	255.5	77.2	301.3	73.9
At2g23590	putative acetone-cyanohydrin lyase	3.5	154.7	56.3	223.1	51.4
At1g21130	caffeic acid O-methyltransferase	2.7	486.9	173.2	420.7	162.6
At1g19540	2'-hydroxyisoflavone reductase, putative	2.6	186.8	83.1	255.9	87.8
At3g16450	putative lectin, jasmonate inducible protein	2.4	86.5	29.6	91.9	43.8
At1g56510	putative disease-resistance protein	2.1	84.8	21.5	51.6	42.0
At1g65390	putative disease resistance protein	4.6	88.4	19.3	33.4	15.2
At4g16990	disease resistance RPP5 like protein (fragment)	3.3	163.3	50.1	60.0	66.9
At1g58842	viral resistance protein, putative, 5 partial	3.0	99.0	32.8	44.9	31.5
At1g66090	disease-resistance protein like	2.9	58.8	20.6	17.3	18.9
Energy and electron transport						
At5g61320	cytochrome P450 - like protein	2.9	14.8	4.0	13.8	5.8
At5g05750	DnaJ-like protein	2.8	101.1	32.1	114.7	44.2
psaA	PSI P700 apoprotein A1	7.7	2603.8	336.5	426.2	342.3
At5g16980	quinone oxidoreductase -like protein	6.2	282.9	45.7	25.7	9.7
psbD	PSII D2 protein	2.7	1531.4	570.0	669.4	579.9
At4g10250	heat shock protein 22.0	2.2	321.8	148.6	25.3	31.2
At5g17760	AAA-type ATPase-like protein, BCS1-protein	2.1	87.6	40.9	12.3	21.7
ndhH	NADH dehydrogenase 49KDa protein	2.1	91.3	30.3	43.2	33.2
Signal transduction						
At1g16260	putative wall-associated kinase	4.2	104.7	21.5	67.9	19.9
At2g46450	putative cyclic nucleotide-regulated ion channel protein	3.5	72.1	16.2	41.3	16.5
At5g18470	protein with protein kinase signature	2.5	76.1	28.0	53.8	23.8
At1g11280	serine/threonine kinase, putative, S-receptor like	2.5	142.5	34.0	78.2	55.0
At1g08420	protein serine/threonine phosphatase alpha, putative	3.2	54.2	16.8	11.0	23.7
At1g09020	putative activator subunit of SNF1-related protein kinase SNF4	3.2	73.9	23.0	24.1	32.5
At1g30270	calcineurin interacting protein kinase AtCIPK23	2.2	139.1	64.2	48.0	63.0
At4g35310	calmodulin-domain protein kinase CDPK isoform 5 (CPK5)	2.0	245.4	121.0	106.2	118.7
Putative transcription factors						
At1g20693	protein with HMG box	2.9	846.2	282.4	952.9	342.5
At4g02540	putative protein, CHP-rich zinc finger protein-like	2.7	110.9	32.2	89.8	41.3
At1g43160	AP2 domain containing protein RAP2.6	2.2	61.6	29.2	80.8	36.4
At1g22500	Similar to zinc finger protein	2.0	295.2	139.4	228.0	121.3
Auxin / ubiquitin						
At5g41700	ubiquitin-conjugating enzyme E2-17 kD 8 (ubiquitin-protein ligase 8)	4.3	1161.5	299.8	1501.2	322.0
At5g13360	auxin reponsive - like protein	3.6	153.2	50.2	42.2	18.6
At5g62010	ARF1-binding protein	2.5	453.7	189.2	181.9	211.7
At3g20630	de-ubiquitinase, putative, 3' partial	2.9	64.3	25.8	21.9	27.7
Flowering						
At5g10140	MADS box protein FLOWERING LOCUS F (FLF)	2.4	86.8	38.5	91.1	34.4
At5g57360	FKF1-like protein 2, circadian clock	2.6	147.6	57.5	69.6	74.3

Others						
At1g24793	carbohydrate esterase family 11	8.3	547.7	67.4	522.8	61.2
At1g73490	similar to poly(A)-binding protein	3.8	143.5	38.1	135.3	36.2
At1g73330	Soybean trypsin inhibitor (Kunitz) protease family; drought-induced protein Dr4	2.8	149.1	76.2	319.2	91.0
At5g65390	arabinogalactan protein AGP7	2.6	182.8	81.7	363.5	132.1
At1g16390	putative transport protein (hexose)	2.3	84.2	43.2	129.8	51.3
At1g06080	delta 9 desaturase	2.1	127.3	48.9	208.1	107.7
At5g17870	plastid-specific ribosomal protein 6 precursor - like	2.1	904.7	562.4	1296.4	467.0
At5g07010	steroid sulfotransferase-like protein	2.0	484.9	198.5	352.7	210.2
At1g62570	similar to glutamate synthase and dimethylaniline monooxygenase (N-oxide-forming)-like protein	2.0	125.3	28.2	67.6	69.4
At5g43370	inorganic phosphate transporter	1.7	192.1	87.6	449.5	282.7
At4g16143	Importin alpha-like protein	4.0	356.9	90.3	98.4	99.3
At1g22360	UDP-glucose glucosyltransferase	3.9	133.6	34.6	67.3	37.8
At3g22440	hydroxyproline-rich glycoprotein	2.9	396.2	135.9	141.2	156.6
At1g80410	putative N-terminal acetyltransferase	2.9	137.3	46.6	67.4	55.0
At1g27850	transposon protein, putative	2.7	110.9	41.6	54.9	66.3
At2g15490	putative glucosyltransferase	2.3	50.7	22.0	1.2	0.8
At5g53480	importin beta	2.0	182.1	90.7	64.4	79.7

Unknown proteins						
At5g05060		47.6	69.1	1.6	102.1	2.0
At1g23960		12.6	225.8	24.9	229.9	11.4
At2g04800		12.2	42.5	6.2	52.7	1.6
At1g24996		5.9	260.0	35.9	168.3	36.7
At5g43580		4.2	158.2	51.5	361.8	71.3
At5g12990		4.2	21.0	2.5	11.1	5.1
At1g58270		4.1	109.5	23.1	174.8	46.4
At2g44200		3.3	23.7	11.3	21.1	2.3
At1g21770		2.7	225.2	88.4	269.3	95.4
At1g27540		2.7	412.4	157.7	398.8	146.1
At5g51620		2.7	13.4	5.2	22.4	8.3
At3g47250		2.6	37.2	11.5	27.4	13.2
At5g16220		2.5	97.3	36.9	104.0	43.3
At5g17510		2.5	33.0	12.3	22.7	10.0
At1g67865		2.5	39.5	12.1	26.0	14.3
At1g23950		2.4	114.4	52.9	128.0	48.1
At2g45830		2.3	39.7	13.7	38.2	20.4
At5g46960		2.3	8.4	5.6	11.9	3.4
At1g63090		2.2	129.1	52.6	80.6	41.8
At5g11580		2.2	141.3	57.1	145.4	72.1
At5g22580		2.1	85.5	39.2	103.1	49.1
At2g17400		4.5	42.8	9.5	13.2	18.2
At5g24700		3.9	247.3	63.3	75.6	85.8
At3g46780		3.4	541.5	158.1	224.5	240.0
At2g11260		2.7	63.1	23.6	17.4	17.4
At1g76970		2.5	87.8	35.4	31.7	31.9
At4g34150		2.5	950.9	383.8	203.0	234.0
At4g01870		2.4	3973.8	1635.9	442.8	157.9
At1g72060		2.4	311.1	129.5	134.1	75.3
At5g13030		2.4	150.3	63.6	64.3	71.2
At5g55120		2.1	114.8	53.9	41.1	55.0
At5g50270		2.1	56.6	26.6	20.6	19.9
At1g44414		2.1	56.6	27.3	12.9	10.4
At3g02040		2.1	179.4	87.0	47.0	52.3

Appendix C, d: Differential gene induction in wt and *ox1* – increased levels in *ox1*

Signal ratios were calculated for each section.

- *'Higher gene levels in ox1 irrespective of H_2O_2'*

Signal values of both *ox1* samples were added and then divided by the added signal values of WS-2 samples. Genes were only included if signal values for both *ox1* samples were at least twice as large as the WS-2 values and had detection calls of 1. All genes fulfilling these criteria are listed in descending order of signal ratios down to 2.0.

- *'Gene induction in ox1 but not WS-2'*

The signal value of the treated *ox1* sample was divided by the value of the treated WS-2 sample. Genes were only included if the treated *ox1* sample showed at least two-fold induction compared to the WS-2 treated sample and the *ox1* and WS-2 control samples, and if the detection call was 1. All genes fulfilling these criteria are listed in descending order of signal ratios down to 2.0.

- *'Gene repression in WS-2 but not ox1'*

The signal value of the treated *ox1* sample was divided by the value of the treated WS-2 sample. Genes were only included if the treated WS-2 sample showed at least two-fold repression compared to the *ox1* treated sample and the *ox1* and WS-2 control samples, and if the detection calls of all non-repressed samples was 1. Genes fulfilling these criteria are listed in descending order of signal ratios down to 2.0.

d) Differential gene induction in wt and *ox1* - increased levels in *ox1*

Higher gene levels in *ox1* irrespective of H_2O_2						
At1g20490	hypothetical protein	3	13.7	49.6	19.9	51.4
At1g57660	60S RIBOSOMAL PROTEIN L21	2.6	135.8	683.5	427.7	782.1

Gene induction in *ox1* but not WS-2						
At1g66570	putative sucrose proton transporter	3.1	58.1	180.2	6.1	17
At4g25200	AtHSP23.6-mito	2.5	146.4	372.6	1.5	1.1
At4g08320	putative protein (fragment)	2.3	42.3	98.7	41.4	45.5
At2g30000	unknown protein	2.2	186.3	419.1	111.9	136.7
At3g28850	hypothetical protein	2.2	25.1	56.2	20.8	21.7
At1g29050	unknown protein	2.1	77.5	165.1	72.1	70.7
At3g11340	putative glucosyl transferase	2.1	130.1	267.8	39.9	63.8

Gene repression in WS-2 but not *ox1*						
At1g33810	GDSL-motif lipase/hydrolase-like like	4.8	114.4	549.8	446.4	578.5
At4g07950	putative DNA-directed RNA polymerase subunit	4.8	34.6	167.8	129.2	112.6
At5g05670	signal recognition particle receptor beta subunit-like protei	3.4	18.5	62	61.2	55.2
At5g09830	unknown protein	3	42.7	128.7	101.8	139.2
At4g29735	unknown protein	3	206.8	615.9	561.6	593.8
At4g36800	ubiquitin-protein ligase like protein, similar to RCE1 (RUB1-conjugating enzyme)	2.9	68.7	197.1	171.3	193.1
At3g51610	unknown protein	2.8	78.5	221.5	259.2	263.3
At1g23850	unknown protein	2.2	37.7	82.5	87.4	107.7
At5g14920	GIBBERELLIN-REGULATED PROTEIN 1 PRECURSOR,	2.1	440.3	904.5	1374.2	1605.8

'If we knew what it was we were doing, it would not be called research, would it?'

Albert Einstein